Springer Series in Advanced Manufacturing

Sanjay Mavinkere Rangappa
Munish Kumar Gupta
Suchart Siengchin
Qinghua Song *Editors*

Additive and Subtractive Manufacturing of Composites

Springer

Springer Series in Advanced Manufacturing

The **Springer Series in Advanced Manufacturing** includes advanced textbooks, research monographs, edited works and conference proceedings covering all major subjects in the field of advanced manufacturing.
The following is a non-exclusive list of subjects relevant to the series:

1. Manufacturing processes and operations (material processing; assembly; test and inspection; packaging and shipping).
2. Manufacturing product and process design (product design; product data management; product development; manufacturing system planning).
3. Enterprise management (product life cycle management; production planning and control; quality management).

Emphasis will be placed on novel material of topical interest (for example, books on nanomanufacturing) as well as new treatments of more traditional areas.

As advanced manufacturing usually involves extensive use of information and communication technology (ICT), books dealing with advanced ICT tools for advanced manufacturing are also of interest to the Series.

Springer and Professor Pham welcome book ideas from authors. Potential authors who wish to submit a book proposal should contact Anthony Doyle, Executive Editor, Springer, e-mail: anthony.doyle@springer.com.

More information about this series at http://www.springer.com/series/7113

Sanjay Mavinkere Rangappa ·
Munish Kumar Gupta · Suchart Siengchin ·
Qinghua Song
Editors

Additive and Subtractive Manufacturing of Composites

Springer

Editors
Sanjay Mavinkere Rangappa
Natural Composites Research Group Lab
Department of Materials and Production Engineering
The Sirindhorn International Thai-German Graduate School of Engineering (TGGS)
King Mongkut's University of Technology North Bangkok (KMUTNB)
Bangkok, Thailand

Suchart Siengchin
Natural Composites Research Group Lab
Department of Materials and Production Engineering
The Sirindhorn International Thai-German Graduate School of Engineering (TGGS)
King Mongkut's University of Technology North Bangkok (KMUTNB)
Bangkok, Thailand

Munish Kumar Gupta
Key Laboratory of High Efficiency and Clean Mechanical Manufacture
Ministry of Education
School of Mechanical Engineering
Shandong University
Jinan, China

Qinghua Song
Key Laboratory of High Efficiency and Clean Mechanical Manufacture
Ministry of Education
School of Mechanical Engineering
Shandong University
Jinan, China

This research was funded by Thailand Science Research and Innovation Fund, and King Mongkut's University of Technology North Bangkok with Contract no. KMUTNB-MHESI-64-16.1.

ISSN 1860-5168 ISSN 2196-1735 (electronic)
Springer Series in Advanced Manufacturing
ISBN 978-981-16-3183-2 ISBN 978-981-16-3184-9 (eBook)
https://doi.org/10.1007/978-981-16-3184-9

Editors are honoured to dedicate this book to their parents.

Preface

Composites are unique class of materials having extensive applications in various fields or modern manufacturing sectors like automobile, aerospace, defence and electronics. The major reason of these applications is that the composite consists of at least two constituents that are not products of solidification; however, the constituents are incorporated from an external source into the matrix. Hence, better mechanical properties as well as thermal properties are obtained compared with other materials during its application in different sectors. Based upon the processing and material used, the composites are divided into three major segments, namely (1) metal matrix composites (MMCS), ceramics composites (CMCS) and polymer matrix composites (PMCS), respectively.

Nowadays, the different methods in terms of additive and subtractive manufacturing are adopted to manufacture the composites into desired shape. Additive manufacturing is a layer-by-layer technology in which the complex shape component is easily fabricated with the short interval of time. The various types of additive manufacturing process used to fabricate the composites are fused deposition modeling, selective laser sintering/melting, stereolithography, poly-jet printing, etc. On the other hand, in subtractive manufacturing, special processes are used to remove the excessive material from the work piece. The various types of conventional and non-conventional subtractive manufacturing processes are turning, milling, drilling, grinding, electric discharge machining, ultrasonic machining, laser machining, electrochemical machining, etc. However, during the manufacturing of composites, various challenges need to be faced like poor surface integrity, mechanical properties, tribological properties, etc. Therefore, this book covers all the aspects during additive and subtractive manufacturing of composites.

We are thankful to all the authors for their chapter. We also thank the publisher for their guidance and support.

Bangkok, Thailand — Sanjay Mavinkere Rangappa
Jinan, China — Munish Kumar Gupta
Bangkok, Thailand — Suchart Siengchin
Jinan, China — Qinghua Song

Contents

Editors and Contributors

About the Editors

Dr. Sanjay Mavinkere Rangappa is currently working as Research Scientist and also Advisor within the office of the President for University Promotion and Development towards International Goals at King Mongkut's University of Technology North Bangkok, Bangkok, Thailand. He has received the B.E. (Mechanical Engineering) in the year 2010, M.Tech. (Computational Analysis in Mechanical Sciences) in the year 2013, Ph.D. (Faculty of Mechanical Engineering Science) from Visvesvaraya Technological University, Belagavi, India, in the year 2017, and Postdoctorate from King Mongkut's University of Technology North Bangkok, Thailand, in the year 2019. He is Life Member of Indian Society for Technical Education (ISTE) and Associate Member of Institute of Engineers (India). He acts as a board member of various international journals in the fields of materials science and composites. He is a reviewer for more than 85 international journals (for *Nature*, Elsevier, Springer, Sage, Taylor & Francis, Wiley, *American Society for Testing and Materials*, *American Society of Agricultural and Biological Engineers*, IOP, Hindawi, NC State University USA, *ASM International*, Emerald Group, Bentham Science Publishers, Universiti Putra, Malaysia) and also reviewer for book proposals and international conferences. He has published more than 125 articles in high-quality international peer-reviewed journals, five editorial corners, 35 chapters, one book, 15 books as an editor and also presented research papers at national/international conferences. In addition, he has filed one Thailand Patent and three Indian Patents. His current research areas include natural fiber composites, polymer composites and advanced material technology. He is a recipient of the DAAD Academic Exchange—PPP Programme (Project-related Personnel Exchange) between Thailand and Germany to Institute of Composite Materials, University of Kaiserslautern, Germany. He has received a Top Peer Reviewer 2019 Award, Global Peer Review Awards, powered by Publons, Web of Science Group. KMUTNB selected him for the 'Outstanding Young Researcher Award 2020'. He was recognized by Stanford University's list of the world's top 2% of the Most-Cited Scientists in Single Year Citation Impact 2019.
https://scholar.google.com/citations?user=al91CasAAAAJ&hl=en

Dr. Munish Kumar Gupta is working as Postdoc Research Fellow in the School of Mechanical Engineering, Shandong University, China. He obtained Ph.D. in Mechanical Engineering from National Institute of Technology, India, in 2018. He is a reviewer for more than 20 international journals (for Elsevier, Springer, Sage, Taylor & Francis, Wiley). In addition, he has published more than 90 articles in high-quality international peer-reviewed journals, six chapters, one book (editor) and also presented research papers at national/international conferences. His area of interest is sustainable manufacturing, machining, welding, rapid prototyping, etc.
https://scholar.google.co.in/citations?user=kL0oahMAAAAJ&hl=en

Prof. Dr.-Ing. habil. Suchart Siengchin is President of King Mongkut's University of Technology North Bangkok. He has received his Dipl.-Ing. in Mechanical Engineering from University of Applied Sciences Giessen/Friedberg, Hessen, Germany, in 1999, M.Sc. in Polymer Technology from University of Applied Sciences Aalen, Baden-Wuerttemberg, Germany, in 2002, M.Sc. in Material Science at the Erlangen-Nürnberg University, Bayern, Germany, in 2004, Doctor of Philosophy in Engineering (Dr.-Ing.) from Institute for Composite Materials, University of Kaiserslautern, Rheinland-Pfalz, Germany, in 2008, and Postdoctoral Research from Kaiserslautern University and School of Materials Engineering, Purdue University, USA. In 2016, he received the habilitation at the Chemnitz University in Sachen, Germany. He worked as Lecturer for Production and Material Engineering Department at The Sirindhorn International Thai-German Graduate School of Engineering (TGGS), KMUTNB. He has been full Professor at KMUTNB and became President of KMUTNB. He won the Outstanding Researcher Award in 2010, 2012 and 2013 at KMUTNB. His research interests are in polymer processing and composite material. He is Editor-in-Chief of: *KMUTNB International Journal of Applied Science and Technology*and the author of more than 250 peer-reviewed journal articles. He has participated with presentations in more than 39 international and national conferences with respect to materials science and engineering topics. He has recognized and ranked among the world's top 2% scientists listed by prestigious Stanford University.
https://scholar.google.com/citations?user=BNZEC7cAAAAJ&hl=en

Prof. Dr. Qinghua Song is working as Professor at the School of Mechanical Engineering, Shandong University, China. He obtained Ph.D. in Mechanical Engineering from Shandong University, China, in 2009. He is a reviewer for more than 20 international journals (for Elsevier, Springer, Sage, Taylor & Francis, Wiley). In addition, he has published more than 100 articles in high-quality international peer-reviewed journals, two chapters, one book (editor) and also presented research papers at national/international conferences. His areas of interest are high-performance manufacturing, micro-machining, etc.
https://scholar.google.com/citations?user=JoTc7sUAAAAJ&hl=en

Contributors

Jasgurpreet Singh Chohan Department of Mechanical Engineering, Chandigarh University, Mohali, India

Yashas Gowda Thyavihalli Girijappa Natural Composites Research Group Lab, Department of Materials and Production Engineering, The Sirindhorn International Thai-German Graduate School of Engineering (TGGS), King Mongkut's University of Technology North Bangkok (KMUTNB), Bangkok, Thailand

Munish Kumar Gupta Key Laboratory of High Efficiency and Clean Mechanical Manufacture, Ministry of Education, School of Mechanical Engineering, Shandong University, Jinan, China

Sristi Gupta Department of Civil Engineering, IIT Jammu, Jammu, India

Bhargav Reddy Isanaka Department of Civil Engineering, IIT Jammu, Jammu, India

Praveenkumara Jagadeesh Department of Mechanical Engineering, University Visvesvaraya College of Engineering, Bangalore University, Bangalore, India

Nirmal S. Kalsi Department of Mechanical Engineering, Beant College of Engineering & Technology, Gurdaspur, Punjab, India

Daljit Kaur Department of Physics, DAV University, Jalandahar, India

Brij Kishor Department of Materials Science and Engineering, National Institute of Technology, Hamirpur (H.P.), India

Jatinder Kumar Department of Research Innovation and Consultancy, IKG Punjab Technical University, Kapurthala, Punjab, India

Sachin Kumar MOE Key Lab for Liquid-Solid Structure Evolution and Materials Processing, Institute of Materials Joining, Shandong University, Jinan, People's Republic of China

Vineet Kumar Department of Civil Engineering, IIT Jammu, Jammu, India

Vinod Kushvaha Department of Civil Engineering, IIT Jammu, Jammu, India

Danil Yu. Pimenov Department of Automated Mechanical Engineering, South Ural State University, Chelyabinsk, Russia

Madhu Puttegowda Department of Mechanical Engineering, Malnad College of Engineering, Hassan, Visvesvaraya Technological University, Belagavi, Karnataka, India;
Natural Composites Research Group Lab, Department of Materials and Production Engineering, The Sirindhorn International Thai-German Graduate School of Engineering (TGGS), King Mongkut's University of Technology North Bangkok (KMUTNB), Bangkok, Thailand

Sanjay Mavinkere Rangappa Natural Composites Research Group Lab, Department of Materials and Production Engineering, The Sirindhorn International Thai-German Graduate School of Engineering (TGGS), King Mongkut's University of Technology North Bangkok (KMUTNB), Bangkok, Thailand

Anish Sachdeva Department of Industrial and Production Engineering, Dr B R Ambedkar National Institute of Technology, Jalandhar, Punjab, India

Konstantinos Salonitis Manufacturing Department, School of Aerospace, Transport and Manufacturing, Cranfield University, Cranfield, Bedfordshire, UK

Shoaib Sarfraz Manufacturing Department, School of Aerospace, Transport and Manufacturing, Cranfield University, Cranfield, Bedfordshire, UK

Aanchna Sharma Department of Civil Engineering, IIT Jammu, Jammu, India

Shubham Sharma Department of Mechanical Engineering, IK Gujral Punjab Technical University, Kapurthala, India;
Department of Mechanical Engineering, IKG Punjab Technical University, Kapurthala, Punjab, India

Vishal Sharma Department of Mechanical Engineering, DAV University, Jalandahar, India

Vishal S. Sharma School of Mechanical, Industrial and Aeronautical Engineering, University of the Witwatersrand, Johannesburg, South Africa

Essam Shehab Mechanical and Aerospace Engineering Department, School of Engineering and Digital Sciences, Nazarbayev University, Nur-Sultan, Kazakhstan

Suchart Siengchin Natural Composites Research Group Lab, Department of Materials and Production Engineering, The Sirindhorn International Thai-German Graduate School of Engineering (TGGS), King Mongkut's University of Technology North Bangkok (KMUTNB), Bangkok, Thailand

Dilbag Singh Department of Mechanical Engineering, Beant College of Engineering & Technology, Gurdaspur, Punjab, India

Gurpreet Singh Department of Mechanical Engineering, Chandigarh University, Mohali, India

Sharanjit Singh Department of Mechanical Engineering, DAV University, Jalandahar, India

Sukhdeep Singh Department of Mechanical Engineering, Chandigarh University, Mohali, India

Siddharth Srivastava Department of Civil Engineering, IIT Jammu, Jammu, India

Wojciech Suder Manufacturing Department, School of Aerospace, Transport and Manufacturing, Cranfield University, Cranfield, Bedfordshire, UK

Italo Tomaz SEAM Research Centre, Waterford Institute of Technology, Waterford, Ireland;
Instituto Federal Fluminense—Laboratory of Materials Testing (LEMat), Cabo Frio, RJ, Brazil

A Comprehensive Review on Composite Materials, Applications and Future Challenges of Friction Welding

Sukhdeep Singh, Jasgurpreet Singh Chohan, Gurpreet Singh, and Shubham Sharma

1 Introduction to Friction Welding (FW)

Since ancient times, it was known fact that metal when heated near to melting point can be easily moulded and fused with another metal component. But as civilization stepped forward towards industrialization, the need was felt to replace the traditional welding techniques to advanced welding processes which can deliver desired mechanical and metallurgical characteristics in weldments [47]. Even during the Bronze age, lap joints were made using tiny circular boxes through pressure welding. Welding is a traditional manufacturing technique in which materials are joined with each other, either metals or non-metals through utilization of force, heat or both. The heat can be generated through electric current, combustion, and chemical reaction of friction. The heat is applied to faces of both materials which are intended to be joined and force is applied (in many instances). As the high temperature reaches near the melting point of weldments, they are fused together which results in a strong joint after cooling [73]. The temperature at the joint is the major factor in all the welding processes but the other factors such as dimensions, impurities, metallurgy and other environmental conditions also influence the quality of the joint. There are various types of welding processes and their subcategories as shown in Fig. 1.

Attempts have been made to develop relationships between process parameters of friction welding and mechanical properties of weldments through numerous experimental, modelling and optimization studies [52]. The hardness, strength, wear behaviour and microstructure of welded joints have been extensively studied by researchers in recent past [27].

S. Singh · J. S. Chohan · G. Singh
Department of Mechanical Engineering, Chandigarh University, Mohali, India

S. Sharma (✉)
Department of Mechanical Engineering, IK Gujral Punjab Technical University, Kapurthala 144603, India

S. Mavinkere Rangappa et al. (eds.), *Additive and Subtractive Manufacturing of Composites*, Springer Series in Advanced Manufacturing,
https://doi.org/10.1007/978-981-16-3184-9_1

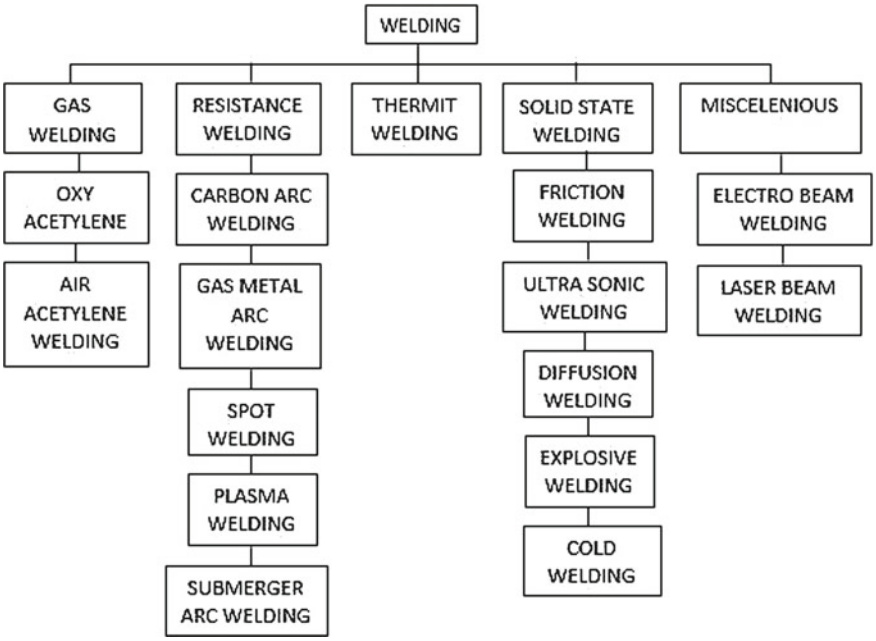

Fig. 1 Welding complete classification and its sub-types

In Solid State Welding, the friction welding as sub category, that is accomplished by the heat generated between two symmetrical and cylindrical parts rotating against each other. In this process the material should be parallel to each other as uniform rotation at an angle is not possible [42, 65]. These metals are pushed against each other by using force which creates friction and finally results in heat generation. Softening of metal occurs due to this friction as intense heat is achieved during the rotary process [45, 71]. The complete setup and schematic of friction welding is described in Fig. 2.

In this process, fusion of materials and plasticization occurs at the friction point also called a weld zone or area [41]. After the whole process is accomplished i.e., relative movement and axial pressure, then the extra materials are removed and a good bond is after solidification of the object.

There are generally three sections (Fig. 3) that are Unaffected Zones (UZF), Partially Deformed Zone (PDZ) and Plasticised Zone (PZ) as described by [14]. The FW is further divided in various types such as Linear Friction Welding (LFW), Inertia Friction Welding (IFW), Spin Welding (SW), Rotary Welding (RW), Friction Stud Welding (FSW), Friction Stir Welding (FSW), Friction Surfacing Welding (FSW) [62]. Basic fundamentals of friction welding are described as motion of material under high pressure which introduces heat between them, reaching plasticised temperature (solid but acts as plastic) without changing its state to liquid, this whole process gives an oxidized free joint and cleans to surface. As soon as it reaches the

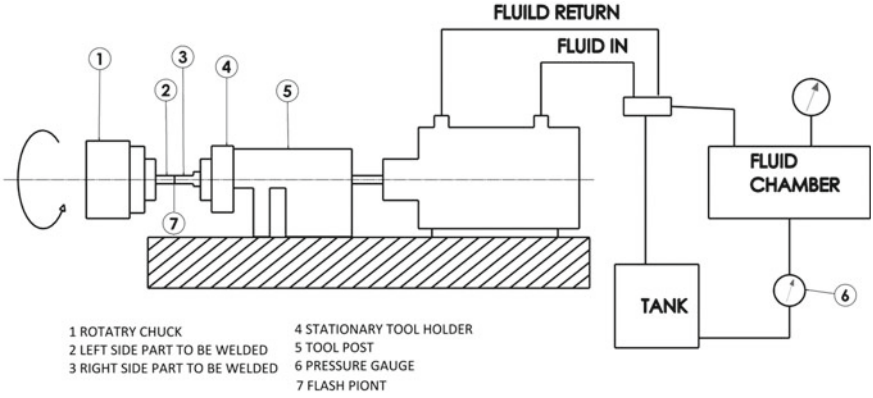

Fig. 2 Description for friction welding system

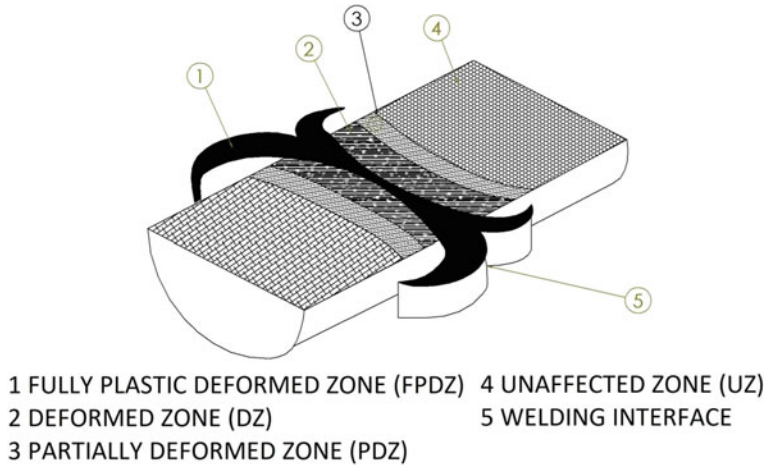

Fig. 3 Position of Unaffected Zone (UZF), Partially Deformed Zone (PDZ) and Plasticised Zone (PZ) on materials

plasticised temperature it becomes soft and then an external load is applied while rotating or linear motion is going on. This process is successful in joining the complex materials and structures that were previously thought to be difficult to join, that's why the complicated structure is made in parts and after that joined via friction welding i.e., truck differential, turbine shaft and propeller [6]. Table 1 displays the details of different materials, methodologies and key findings during fiction welding studies.

Table 1 Detailed literature survey of experimental studies using friction welding

No.	Material/methodologies	Details of experiments	Parameters of experiment	Testing techniques and equipment	Results/findings
1	Carbon steel SAE 1020, Aluminium oxide Al_2O_3, Aluminium 6160/Friction welding [23]	Powder Metallurgy process is used for Aluminium, by cold pressed at 10 MPa and hot pressed to 5 MPa at 500 °C	Rotary speed—2500 rpm, Forging pressure—5 MPa, Friction pressure—10 MPa, Forging time—4 s and time—8 s	Optical microscopy, energy dispersive X-ray spectroscopy (EDAX), Microhardness Profile, Shear Strengths by MFL Universal Test Equipment, Scanning Electron Microscopy (SEM)	Al_2O_3 is homogeneous with small grain size and uniform distribution, Fracture formed due to the metal oxide and Shear strength was inversely proportional to oxide and reinforced particle size
2	St–A1 and A1–Cu/Friction welding [78]	Electric motor of 10 kW with 3500 rpm was used, cleaning of sample with acetone to remove any dirt or grease	Rotary speed—[2000, 2500, 2800]. rpm, Applied load—[5–12.74, 6.37–17.83, 7.64–22.93]. kg, Time—[4.7, 10]. s	SEM, Optical microscopy, Microhardness Profile, Tensile Strength, Vickers hardness tester	**Steel-Aluminium welds** Thick intermetallic layer reduces Tensile value. Oxide film and contaminants reduce the quality of joints. Force, Speed and Time affects the joints and weld properties **Aluminium-copper welds** Intermetallic layer causes Fracture affecting tensile properties. Speed, load and time have a low impact on the strength of joints

(continued)

Table 1 (continued)

No.	Material/methodologies	Details of experiments	Parameters of experiment	Testing techniques and equipment	Results/findings
3	Copper C44300, Aluminium AA7075-T651/Friction welding [57]	Two cylindrical pipes of same dimension, Half of them threaded and other are not, all threaded have different pitch	Rotary speed—[545, 730, 950, 1320]. rpm, Forging length—[0.25, 0.5, 0.75, 1.00]. mm, Thread pitch—[0, 0.5, 1, 1.5]. mm	Vickers hardness tester, Compression test, Microstructural analysis, SEM IMAGE, Energy-dispersive X-ray	Friction Welding of thread tube to plate, threaded tube gives more compressive strength than unthreaded tube. EDX and SEM analysis has proved the results, 950 rpm gives Optimum joint strength and hardness
4	Virgin PE pipe/Friction welding [19]	A hollow pipe made from Mannesmann process; Intermediate ring used for joining pipes	Rotary speed—500 rpm, Forging forces—420 kN, Time—280 s	Dynamometer), X-ray diffraction (XRD), Optical Microscopy (OM)	FW is ten times more efficient than that of traditional butt welding of pipe in terms of electricity and time
5	API 5L X65 steel/Friction welding [48]	Intermediate ring of same material was used for friction welding the seamless pipe were used from the Mannesmann process	Rotary speed—500 rpm, Forging force—420 kN, Time—280 s	Optical microscopy, Vickers microhardness, X-ray diffractometer	The ring is subject to compressive stress and thermochemical effect, microhardness is less at HAZ, Corser microstructure formed due to FW which may leads to slower cool down, there is increased in micro hardness, FW provides enhanced homogeneous mixture of residual stress

(continued)

Table 1 (continued)

No.	Material/methodologies	Details of experiments	Parameters of experiment	Testing techniques and equipment	Results/findings
6	AA7075-SiC/Friction welding [68]	Alloy is prepared from Ingot AA7075 and Si. It is machined to remove oxidation and get smooth surface	Rotary speed—[1200, 1500, 1800]. rpm, Friction pressure—[50, 75, 100]. MPa, Burn-off length—[1, 2, 3]. mm, Upset pressure—[150, 200, 250]. MPa	Vickers Microhardness, Tensile Test, Genetic Algorithm, Scanning Electron Microscope	Optimized process parameter is Speed = 1491.54 rpm, Upset pressure = 209.26 MPa, Friction pressure = 98.94 MPa, Burn off length = 1.5 mm gives Ultimate tensile strength = 244.2866 MPa and Hardness = 148.2392. Microstructure analysis shows hard material inversely proportional to ductile ability
7	High-speed steel HS 6-5-2-5, Carbon steel for tempering C60/Friction welding [59]	Friction welding with 2400 rpm, Angular velocity 1.2 m/s, Welding time 3–18 s, Friction pressure 70, 80, 90 MPa, Forging pressure 0–120 MPa	Rotary speed—2400 rpm, Friction pressure—[70, 80, 90]. MPa, Angular velocity—1.2 m/s, Forging pressure—[0–210]. MPa, Time—[3–18]. s	Vickers Microhardness, Tensile Test, Scanning Electron Microscope	Forging pressure is suitable between 2.5 and 4 s, hardening of face occurs on HS steel, friction time has not much effect on the width of the joint

(continued)

Table 1 (continued)

No.	Material/methodologies	Details of experiments	Parameters of experiment	Testing techniques and equipment	Results/findings
8	Medium carbon steel 1045, 316L stainless steel/Friction welding [28]	Friction welding on lathe with maintaining temperature 780–800 °C	Rotary speed—560 rpm, Angular velocity 1.2 m/s, Time—38 s, Friction pressure 75–155 MPa, Forging time—2 s	K Type thermocouple, microscope and a scanning electron microscopy, hardness and tensile tests, Energy Dispersive X-ray Spectroscopy	Flashing 1045 MCS was more due to Chromium present in SS elevated its hardness and thermal conductivity, increase in hardness at the welded joint, sample 1 gives 513 MPa tensile, 21% elongation and 90% efficiency of joint, forging pressure is proportional to hardness and tensile strength
9	FeAl40 ODS alloy/Friction welding [26]	Continuous drive rotary friction welding machine	Rotary speed—1000 rpm, Friction force—28 kN, Forge force—70 kN, Burn-off length—5 mm	Metallographic technique, transmission electron microscopy, microscope, high resolution electron microscopy	Changes in base alloy was the oxide particle and recrystallization observed along the weld line, big clumps of 0.2–1 mm were also noted
10	UNS S32205 chromium-nickel-molybdenum-nitrogen stainless steel/Friction welding [55]	Pipe of 12.7 mm thick and 10 mm diameter and intermediate ring was used to join due to temperature difference	Displacement—10 mm, Forging force—200 kN, Displacement rate—0.1 mm/s, Forging force rate—7.5 kN/s	Electron Backscatter diffraction (EBSD), type K thermocouple, impact tests, fracture surface analyses, scanning electron microscope (SEM)	Slight change in grain size of both the metals, whereas austenite crystals were completely reformed which has direct effect on toughness simultaneously. flash formation causes cracks which leads to fracture

(continued)

Table 1 (continued)

No.	Material/methodologies	Details of experiments	Parameters of experiment	Testing techniques and equipment	Results/findings
11	AI–SiC metal and AI–Mg–Si alloys matrix composite/Friction welding [46]	Metals were casted by vertical direct cool billets with extrusion of 800 tons press	Rotary speed—3000 rpm, Friction force—30 MPa, Forge force—[50, 75, 100]. kN, Burn-off length—[1, 2.1, 3.3, 3.8, 6.8]. mm	Thermocouple, Hot-torsion testing, optical microscope, electron back scattering pattern (EBSP), Transmission electron microscope (TEM), Vickers hardness test (5 kg load)	Mathematical derived results are in tolerance with the physical experiment, Plasticized region is observed at the outer side of the weld line, variation in Axial values affects flow of material due to force applied while welding, Strain in the metal decreases within the region during welding
12	ABS and Nylon 6/Friction welding [67]	Dissimilar polymer/plastic materials that is reinforcement with Fe and Al separately	Rotary speed—[500, 775, 1200]. rpm, Time—[4, 6, 8]. S, Feed rate—[0.045, 0.090, 0.180]. mm/rev	Optical micrograph, Optical micrograph, Minitab software	Hardness value—79.0, from 775 rpm, 0.045 rev/mm and 6 s time Tensile strength—0.5375 kg/mm^2, from 1200 rpm, 0.045 rev/mm and 8 s time, %age porosity—7.16%, from 1200 rpm, 0.090 rev/mm and 4 s time
13	AISI 304 SS/Friction welding [63]	Rods of 16 mm diameter and 130- and 50-mm length with hot extrusion process. emery papers used on Faces to polished, and acetone to clean	Rotary speed—1125 rpm, Friction time—[3, 5, 8]. S, Friction pressure—[1.5, 2]. MPa, Upset time—[5, 7, 3]. s	Transition Electron Microscope (TEM), Tensile test, Vickers's, Impact test, scanning electron microscope (SEM)	Joint strength inversely proportional friction time and hardness. Ductile Surface was observed without any dimples. Impact strength has no variation in result

(continued)

Table 1 (continued)

No.	Material/methodologies	Details of experiments	Parameters of experiment	Testing techniques and equipment	Results/findings
14	Ti–6Al–4 V/Friction welding [16]	Bar of 50 mm diameter is friction welded with hydraulically controlled drive capable of giving 40 kN axial load	Rotary speed—[1500, 3000, 4500]. rpm, Friction pressure—[136, 272]. MPa, Forging pressure—408 MPa, Burn-off length—2 mm	Ultimate tensile strength (UTS), Vickers microhardness	Best tensile results from low pressure and rotating speed, transformation region width depends upon the applied pressure. i.e. 1500 rpm with 136 MPa gives best results whereas 4500 rpm and 272 MPa gives poor results
15	6082-T6 aluminium alloy and pure copper/Friction welding [50]	Cylindrical rod of 120 mm length and 20 mm Diameter is used and flash is removing via lathe machine	Rotary speed—1500 rpm, Friction pressure—110 MPa, Forging pressure—[80–160]. MPa, Forging time—4 S, Friction time—[1–4]. s	Optical metallography technique, X-ray diffraction (XRD), scanning electron microscope (SEM), V-notch impact	Optimized parameters of experiment are forging pressure and time 160 MPa and 4 s respectively. Higher tensile strength is achieved that is 198 MPa with 3.8% elongation. Strain hardening causes increased hardness at weld zones. Structure failure is ductile type with dimples presence

(continued)

Table 1 (continued)

No.	Material/methodologies	Details of experiments	Parameters of experiment	Testing techniques and equipment	Results/findings
16	UNS S32205/Friction welding [4, 5]	Sample of 10 × 10 were cleaned with acetone and electro-etching performed by 10% oxalic acid for 30 s at 9 V	Rotary speed—[1000–2000]. rpm, Friction pressure—[45–125]. MPa, Upset pressure—[140–200]. MPa, Burn off length—[2.5–4.5]. mm	Tensile test, Vickers microhardness test, MATLAB, Mathematical equation	Speed, upset pressure and Friction pressure are directly proportional to hardness and tensile strength, whereas burn off length is inversely proportional. Upset forces and rotary speed have direct impact on tensile strength and hardness
17	AISI 304L and 4340 steel/Friction welding [54]	Rod of 12 mm diameter and after cleaning it is micro polished using 0.3 μm Al_2O_3 powder	Rotary speed—[1500–2500]. rpm, Friction pressure—40 MPa, Forging pressure—60 MPa, Forging time—10 s, Friction time—5 s	Scanning electron microscopy (SEM), tensile test, X-ray diffraction (XRD)	Microstructure change in the region deformed zone and fully plasticized zone. To obtain strong tensile strength we need high speed for a short time. quality and strength of weld depends upon fusion process occurred at the weld zone

(continued)

Table 1 (continued)

No.	Material/methodologies	Details of experiments	Parameters of experiment	Testing techniques and equipment	Results/findings
18	SAF 2507/Friction stir welding [60]	Sample of 300 × 100 × 2 mm was used and the tool was given 3° angle from normal of plate liquid cooled tool was used to prevent oxidation	Rotary speed—[50–250]. rpm, Force—14 kN, Length—270 mm	X-ray diffraction (XRD), K-type thermocouple, e X-ray spectroscopy (EDS), optical microscopy (OM), scanning electron microscopy (SEM), Vickers hardness	Almost all the speed parameters give a solid joint except 250 mm/min. Tinny equal sided grain were observed that are decreased with the increased rpm and less heat input. Sigma face is absent at interface due to rapid cooling. Weld speed is directly proportional to the hardness and tensile strength
19	AA6092/17.5 SiCp-T6/Friction stir welding [1]	Sample of 150 × 60 × 6 mm is used was used and the tool was given 2° angle	Rotary speed—[1000, 1500, 2000]. rpm, Tool Pin Dia.—6 mm, Force—14 kN, Length—100 mm	Macroscope, scanning electron microscopy (SEM), Vickers microhardness, ultimate tensile strength (UTS), Energy Dispersive Spectroscopy (EDS)	All speed parameters give defect free weld with uniform particle distribution, alignment of grains is vertical at weld zone. But hardness varies along the weld line. Lower rpm gives good results with less destruction. Brittleness occurs at high speed

(continued)

Table 1 (continued)

No.	Material/methodologies	Details of experiments	Parameters of experiment	Testing techniques and equipment	Results/findings
20	Al/SiC/Al_2O_3/Friction welding [2]	Friction welding machine of 20 ton with servo motor of 20 HP was used for experiment	Rotary speed—[2000, 2250, 2500]. rpm, Friction pressure—[40, 50, 60]. MPa, Upset pressure—[100, 120, 145]. MPa, Burn-off length—[1, 2, 3]. s	Tensile strength (TS), Vickers hardness, field emission scanning electron microscope (FESEM), X-ray spectroscopy (EDX), micrograph, macroscopic visual analysis	Strain and plastic deformation at the weld zone increased hardness. Optimum parameters for this experiment are 60 MPa frictional pressure, 120 MPa upset pressure, 1 mm burn off length and 2250 rotatory speed. Equal size flash, aligned matrix and uplifted the characteristics quality and S/N ratio

2 Applications of Friction Welding

Although this technology is new in the industry but many industries rely on this technology for their parts which are discussed in this section.

2.1 Aerospace Industries

The requirement for accurate and clean joints for aerospace industries are achieved from friction welding because they produce tough and smooth joints while welding the materials, Aerospace has utilized the solid-state contact-based welding procedures inside the previous decade such as Rotary Friction welding (RFW) which is performed on two types of machines i.e., Continuous Friction Welding (CFW), Inertia Friction Welding (IFW) [56]. A Friction based welding has an ability to self-clean the rough surface of material as it comes in contact because when the load applied, it compresses the plasticised material at the weld zone to outwards in a ring shape, which removes any surface impurities or oxides that existed earlier, making it pointless to utilize protecting gas or any other accessories during welding. Inertial welding is used in aerospace industries more frequently among the past times, particularly in joining titanium alloys, nickel-based super alloys and steel air motor barrel shaped segments, is known for giving parts of clean and high-quality joints, contrasted and the utilization of fusion welding [15]. FSW is preferred to combine titanium alloys and aluminium alloys parts for the aerospace industry due to their sophisticated design that makes it difficult to approach joints that are to be welded. As these processes are so efficient that no defects were found during the microscopic inspection and X-ray scanning [34].

2.2 Manufacturing Industry

Butt welds that are made in bars or cylinders can be welded to plates or one another. One of the parts is commonly round in shape, friction welding is also used in joining different shapes but with some limitations like square bar can be welded. There are various sizes that can be used for friction weld from tiny diameter wire that are utilized in the hardware business with length of 150 mm approx., for example in the engine business [51]. Models like drive shafts, axles and valves that have a large combination of heat-opposing heads are to be welded to that of a lesser expensive one. We can weld bar stock to the plate that has to be a delivery dish. Most alloys as well as metals, exceptions like cast iron that cannot be friction welded. Fragile zone doesn't exist in friction welding of Divergent metals, which frequently happens with circular arc welding, for example we can weld steel to aluminium or vice-versa [43].

2.3 Marine Industries

As we know, the sea water is salty and very corrosive in nature. That's why we use a propeller shaft of aluminium 5083, that metal is very effectively and efficiently welded on the shaft with the help of RFW. As it is difficult to make propellers and shafts all together, so they are prepared separately and assembled using RFW, where crystalline structure is less weak at Heat Affected Zone (HAZ) and result in better strength at weld point than any other traditional joining method [13]. Welding in air and welding underwater is a very different process. Underwater welding requires high speed during welding because water decreases temperature quickly during welding and makes welding difficult. This high speed causes reduction in grain sizes and increment in microhardness at the interface. Elongation is twice at interface and tensile is almost near to original metal [30].

3 Comparative Analysis of FW with the Traditional Welding Processes

As we know that traditional methods were not cost effective nor eco-friendly, so nowadays industries are switching to friction welding than that of arc welding, gas welding etc. as we know that they also need some extra accessories like filler metal, gas, and their necessary parts but on the other hand friction welding don't require such additional things, and on top of it the welded joint are much cleaner and stronger than other methods. On top of it metals characteristics are not changed, mixed or affected in this technique [58]. FW is elaborated and distinguished in different parameters is compared in Table 2.

3.1 Arc Welding Versus Friction Welding

Arc Welding is an old method of joining objects generally metals, has many demerits than that of frictional welding such as it requires welding rod that is compatible with the welding material from a wide variety of metals, welded surface is not clean as compared to friction welding, the welded area of metal via arc welding give heterogeneous mixture was observed whereas homogeneous mixer was evaluated in friction welding at a microscopic level. That was authenticated in the results of the tensile test. Friction welding parts can withstand a large amount of pressure at the welded area Materials Research [66]. Friction welding overcomes arc welding by following points discussed:

1. Quality of weld is better than the traditional method.
2. The bending occurs after cooling in arc welding is very less with less power consumption of friction welding.

Table 2 Friction welding comparison with other types of welding [74]

Basic property	Fmriction welding	Electron beam welding	Electrical resistance welding	Electrical arc welding
Weld type material	Almost any	Metals only	Conductive only	Conductive only
Compatibility cross section to welded joint	Complete	Surface only	Surface only	Surface only
Welding geometry	Limited (mostly circular)	Any	Any	Any
Preparation of parts	Shafts, pipes, propeller etc.	Metal parts	Metal parts	Metal parts
Time taken	Low	Long	Quick	Moderate
Additive of materials	N.A	Powder or wire	N.A	Electrode
Process control	Mechanical rotary or linear motion	Servo motor control via computer	Push pedal by worker	Worker
Running cost	Cheaper	Very costly	Costly	Costly

3. It needs no shielding gas or additional metal, and it doesn't create any gas or fumes.
4. Lifespan of setup of friction welding is longer as it requires less maintenance, with very silent operation.
5. Almost each type of composites, metals and non-metals can be welded except few materials.
6. Strength of the welded area is similar to the base metal [31].

3.2 Tungsten Inert Gas (TIG) Welding Versus Friction Welding

Though, both of the processes are capable of joining the aluminium alloys. TIG is unable to perform without filler material due to the presence of iron impurities in high volume, as these impurities will lead to fracture due to temperature range. Even though there is a large difference in the test results of both, FSW performs better in terms of tensile strength, hardness at either base, HAZ, TMAZ etc. FSW produces greater ductility and strength, on the other hand TIG WELDING produces high levels of hardness in the HAZ and literally depends upon the variation of current applied to the work piece [24]. FSW process gives crystal growth like tree shape at microscopic level due to recrystallization process occurring. Although TIG has no such shape because rapid cooling by air occurs after the welding process. The observation of the welded material at a microscopic level showed the presence of

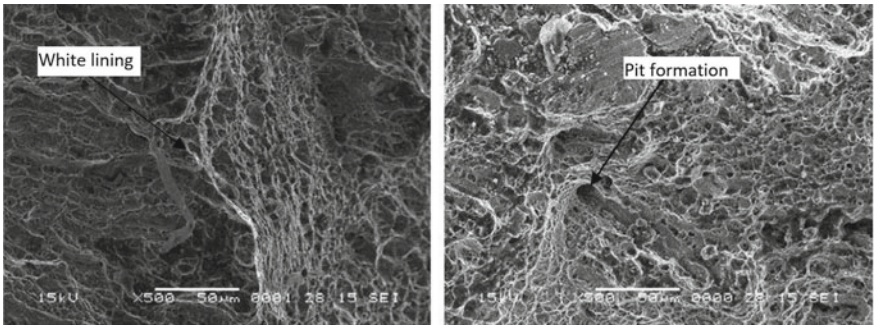

Fig. 4 Fracture on metal surface via scanning electron microscope (SEM) of AISI 304

micro fractured gain by tensile test as shown in Fig. 4. There can be clearly visible divergence in structure, proportion of spots than other [69].

TIG process applied without the filler material will produce cracks on aluminium alloy due to the presence of iron in aluminium, FSW joints are proven to give better results in terms of strength and ductility than TIG welding joints [64]. Medium speed is preferred for good results as higher will increase the hardness and lower will not give optimum joining due to less heat generated [36].

3.3 Friction Welding Versus Metal Inert Gas Welding (MIG)

MIG is a very popular type of welding since the 90s and dominated arc welding due to its convenient structure but not superior than friction welding in welding circular shaft, hollow pipe and welding of composites. As it requires filler wire and shielding gas (Argon) which increases cost whereas no such requirement in friction welding due to its simplicity. As, aluminium weld by MIG causes hardness due to rapid cooling and chances of fatigue of aluminium is much more frequent than that of friction welding. As we can see after weld images in Fig. 5 the friction welded area is dense whereas porous in TIG and MIG [49, 70].

4 Friction Welding Materials and Methods

In the universe, there is a wide range of metals and non-metals exist, they are welded to each other or similar as per need of manufacturing. but not all processes or techniques are there that can weld all the metals, so friction welding is preferred over the traditional welding method because it has the capability to weld almost all the materials that are used in industries. Intermediate layers of metal are used during

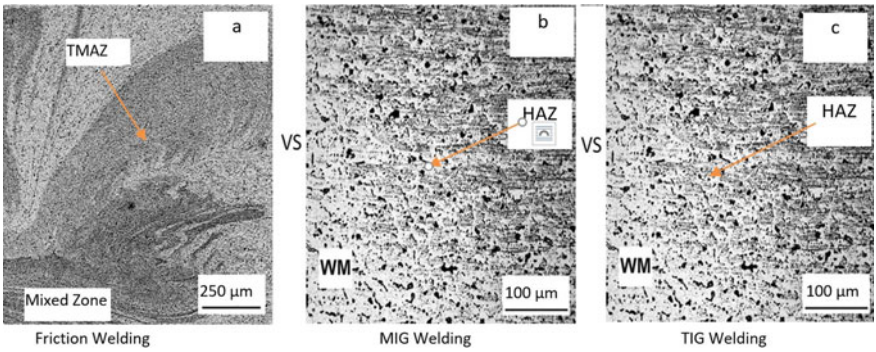

Fig. 5 Experimental image after friction welding of 5086-H32 aluminium alloy, MIG welding and TIG welding at welded zone

friction welding on those metals with high melting temperature difference between them [7].

4.1 Steel and Its Alloys Welding

Friction welding is a better and more cost-efficient method in terms of joining Stainless Steel with steel or its alloys than that of any other welding process. As, it produces less hardness and more toughness to bear stress and strain during working. Burn off length also has an effect on the toughness and hardness at the weld zone, as we increase the burn-off length it will increase hardness and decrease toughness and will help in removal of oxidized layers on faces of each other. But excessive burning of length produces brittle fracture due to increased hardness and develops intermetallic compounds and carbides near weld zones [11]. Thought different composites of steel have different optimized parameter value, such as 105 MPa Friction Pressure, 180 MPa Upsetting Pressure, 2000 rpm Rotary Speed, 3.9 mm burn-off length are the optimized values for FW of UNS S32205, which gives 827.17 MPa and 325.61 Hv as Hardness and Tensile strength respectively observed from the result [4].

4.2 Copper and Copper Alloys

Friction welding between copper and low carbon steel (LCS) at 30 MPa friction pressure, 2.4 s friction time gives low fracture joint and 40% efficient joint, but 80% can be achieved by using 180 MPa forging pressure.

Friction time is directly proportional to the efficiency of the joint [29]. In FSW 1250 rpm with 61 mm/min parameters gives no defect at interface, but reduction in grain size at the weld zone. Softening region developed at the interface, and reduction

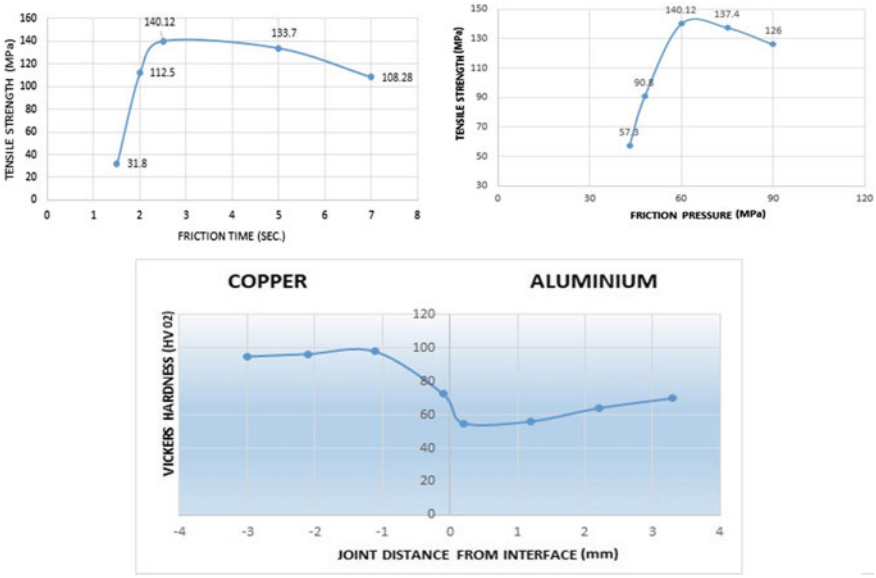

Fig. 6 Al–Cu friction welding graphical representation of friction pressure to tensile strength, tensile strength to friction time and hardness to distance from interface

in size of grain as compared with original metal. Hardness was larger at the centre and gradually reduced the hardness of the base material. Comparing base material, the tensile strength reduced to 87% [35].

Intermetallic layer formed at the interface due to the brittle nature of copper and 6061 aluminium alloy, that's why we use an intermediate layer of material to join them successfully with 136–760 HV of hardness from base to interface [61] as shown in Fig. 6. The temperature of welding reached to 580 °C that greater than Al–Cu alloys [53].

4.3 Aluminium and Aluminium Alloys

Friction welding is the best procedure for welding dissimilar metals i.e., aluminium & aluminium alloys etc. We obtained good Tensile strength and micro hardness from aluminium and its composites. Though the ductility of material was reduced but it was reasonable, whereas, chemical properties of composites have compromised the properties of weld if we use Fe as alloy of aluminium [12]. There are various parameters values in friction of different materials to get desired values of strength, hardness etc. that certainly affect the joint strength of the structure. The perspective of aluminium with iron welding process will give rise to intermetallic phases due to melting temperature variation between metals that leads to brittle weld joints [9].

4.4 Tungsten and Titanium Welding

As we know that tungsten is harder than titanium that's the major effect of heat or we can say plasticised temp of titanium meats faster than tungsten and the heat affected zone is majorly on titanium side. Generally, 750 rpm is used to obtain defect free joints rather than 1500 rpm because of large variation in melting temperature of both metals, so the weld joints are brittle and prone to breakage on drop. Interlayer metal i.e., copper is used to eliminate micro cracks formed during welding process [8]. The predicted heat distribution in the simulating model is similar to the experimental model performed physically i.e., length shortening value predicted was 2.8 mm and in actual it was 2.5 mm. Similarly, in terms of temperature it was 1340 °C in both the results. Variation in friction coefficient of model due to high temperature during welding which results in change in thermal field [37].

4.5 Titanium and Iron Welding

As there is a huge melting temperature difference between iron and titanium, as titanium is used for cutting iron or steel, it is inapplicable task of welding them due to the appearance of intermetallic phases after welding. Due to these intermetallic phases, there is no guarantee that complete welding across the cross-sectional area is successful, as these phases generate higher value of hardness among the metal and cracks in the weld zone are produced [40]. We can get good tensile value at high friction pressure and upsetting pressure but with poor bending test and fracture at the weld zone, due to intermetallic layer and titanium a brittle substrate. Surface roughness is inversely proportional tensile strength and directly proportional to residual strain obtained during welding process. To obtain good results low temperature around 550 °C but strictly not above 700 °C is required with short holding time [18].

4.6 Nylon 6 and ABS Reinforced Fe

Researchers used 40% of iron powder as additives in ABS and PA6 polymer matrix, so as to perform the friction welding process and get good bond strength between them, as reinforcing Fe brings their melting point closer to each other that helps in bonding. In their pure state polymers are impossible to yield good results as a very little tensile force can break the bond easily. This feed rate plays an important role. For better joint strength, we need slow feed rate, high rpm and adequate time [33].

5 Process Parameters of Friction Welding

As we know the parameters are very crucial part of any experiment, same is in friction welding it consists of various parameters i.e., speed, applied force, friction time etc. as in Fig. 7.

Friction Welding Experiments performed with some parameters taken in aspect are speed, feed with range of 700–1350 rpm, 75–115 mm/min. We get different values with different steps as written in Table 3 as described by Yilbas et al. [77]. The outcomes describe that hardness and tensile strength increases when speed is 1350 rpm with feed 115 mm/min as found by Hussain and Pasha [25].

5.1 Speed

Speed is the most important and phenomenal factor in the friction welding and its categories such as tensile strength and hardness i.e., Strength and hardness increases gradually with rise in speed as shown in Fig. 8. So, the speed has an impact on all the

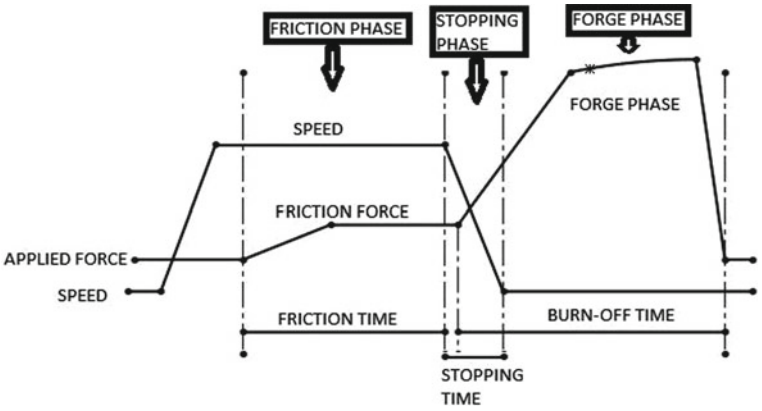

Fig. 7 Stages of friction

Table 3 Hardness and tensile strength measurements at conditions

No.	Speed (rpm)	Feed (mm/min)	Tensile strength (MPa)	Vickers hardness (HV)
1	700	75	160	85
2	900	90	166	88.5
3	1150	108	171	88.9
4	1350	115	172	90.2
Parent metal values			250	93.5

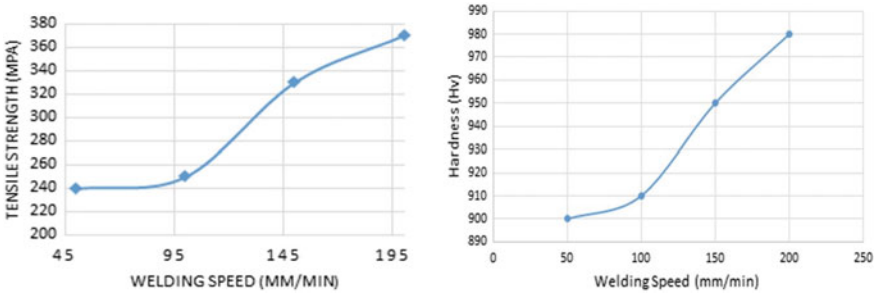

Fig. 8 Graphical relation of welding speed of SAF 2205 with respect to **a** hardness and **b** tensile strength

factor on the welded material, but it is inversely proportional to speed because there is elevation in temperature at the contact point which leads to plasticization of metal and the strength will tends to decrease at that area, even at the microscopic level the impact of speed is visible [39].

Aluminium alloy showed different results at different speeds at the Stir Zone (SZ) i.e., as speed increases it decreases the grain size and width of material as shown in Fig. 9 as found by Kumar and Kailas [32]. Residual stress is symmetrical in Bobbin Tool Friction Stir Welding (BTFSW) and it is maximum at centre and decreased to normal as we move to base metal. Similarly, Hardness is symmetrical at the weld zone and lowest at Heat Affected Zone (HAZ). 70% efficiency of the joint is observed at the test results [76]. Welding Aluminium with Aluminium Yttria Stabilized Zirconia (YSZ) composite gives strong joints at 630 rpm, on the other hand in pure aluminium bending strength is better at 2500 rpm, however, and results may vary after joining the metal due to internal flaws induced by thermal stresses. Though fracture may occur due to high temperature caused by high-speed rotation [72].

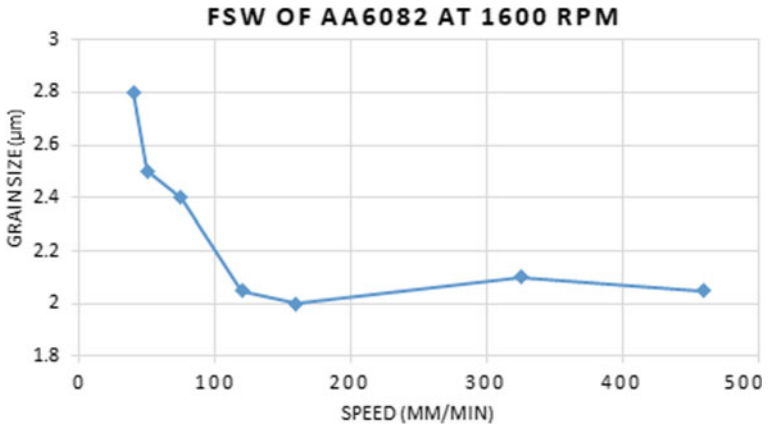

Fig. 9 Graphical relation of speed impact on grain size of AA6082 [32]

5.2 Friction Force

It is the force applied during the rotary process which makes friction more effective but hardness. Joint strength relies on particle bond quality at the weld zone, pure metal will have good bond as compared to composites, as impurity percentage mixing also has an impact on the strength of bond, as it basically depends upon the lattice size of both the materials. This helps in fabricating the metal matrix composites as per material [79]. Friction pressure is directly proportional to tensile strength, but excessive pressure than certain limit will also decline the strength i.e., welding between SS410 and INCONEL 718 at 190 MPa of friction pressure that is optimum value for tensile strength. Fracture observed on interfaces was a mixture of dimple and quasi-cleavage fracture. Dynamic recrystallization at the interface causes increased hardness value [10, 75].

5.3 Axial Pressure or Torque

Welded joint's bond strength majorly depends upon the axial pressure exerted during the experiment. As there is any change in axial pressure, it will reflect in the properties i.e., 135 MPa of axial pressure gives the highest tensile strength of 432 MPa because fusion of alloys with steel, but excessive pressure will cause ductile failure as shown in Fig. 10, but torsional strength will increase because it will transfer extra mass due to heavy axial pressure. Bond strength has direct relation with temperature, that is directly proportional element diffusion [21].

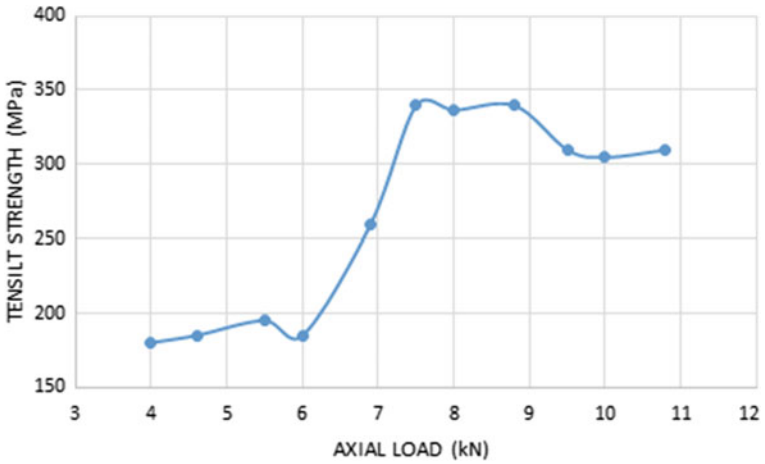

Fig. 10 Graphical relation of axial load and tensile strength with fracture point

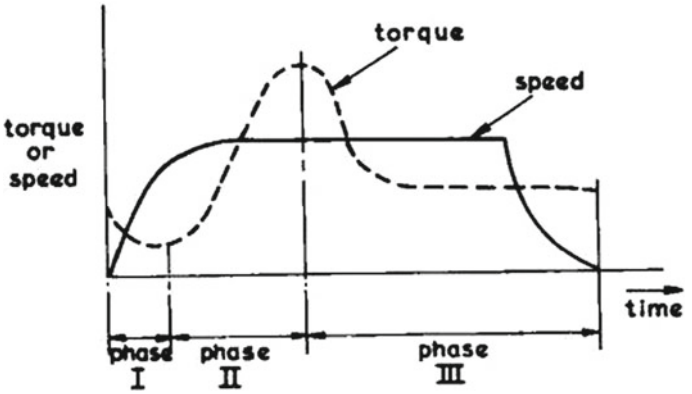

Fig. 11 Constant axial load with respect to time

As each parameter has their own impact on the outcome result, similarly change or variation in axial pressure is reflected on friction welds. 120 MPa axial pressure gives the optimum tensile strength and impact toughness, but due to brittleness the sample doesn't pass the basic requirements [32]. But, unfortunately the hardness of the specimen reached maximum value due to high temperature caused by high axial pressure. It has three faces with respect to time as shown in Fig. 11, torque firstly decreases [3] and then becomes constant before reaching peak during experiment [22].

5.4 Welding Time

Weld time is an important factor in friction welding as the welding time had major impact on hardness and burn off length, but tensile strength and bending strength are not affected during welding. If tempered or quenched material is used with friction timing of 14 and 15 s gives lower toughness value. Whereas more time is needed for such material to get reliable value, but excessive time duration will cause overheating of microstructure grains which will affect toughness values [17]. In experiment with parameters from 0.5 to 4 s time for welding, 3 s gives best results that are very fine material structure that is near to base metal, same as in case of HAZ regarding tempered hardening of metal. Time is directly proportional to length shortening [38].

Generally, Low fatigue strength of joints develops due to high speed, less force and less time duration. Friction time is inversely proportional to fatigue limits and tensile strength [20]. In the experiment it was observed that if at a certain speed we obtain tensile strength and fatigue limit values, these values can be increased just by giving more time with the same parameters. So, speed, time, pressure and force are the main parameters for better joint strength results as shown in Fig. 12 that shows relation of load with time in AISI 304 and AISI 1021 welding process [44].

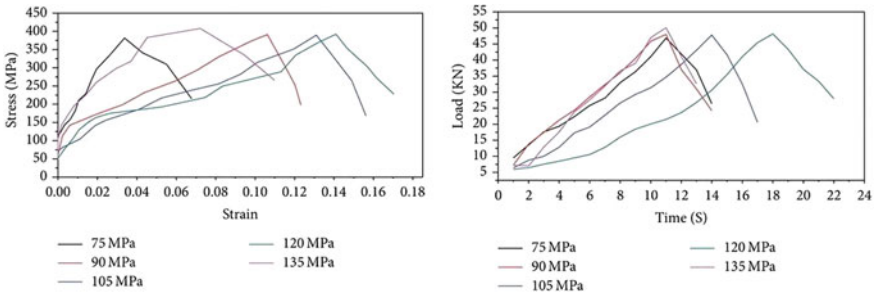

Fig. 12 Relation of load and time, stress and strain of AISI 304 and AISI 1021 steels

The data has been collected for the Clarivate Analytics portal which indicate that total 3453 articles have been published in refereed journals. It can be noticed from Fig. 13 that the research in friction welding has been increasing since 2011. Moreover, China leads in the world while reporting the research based on friction welding followed by India and Iran.

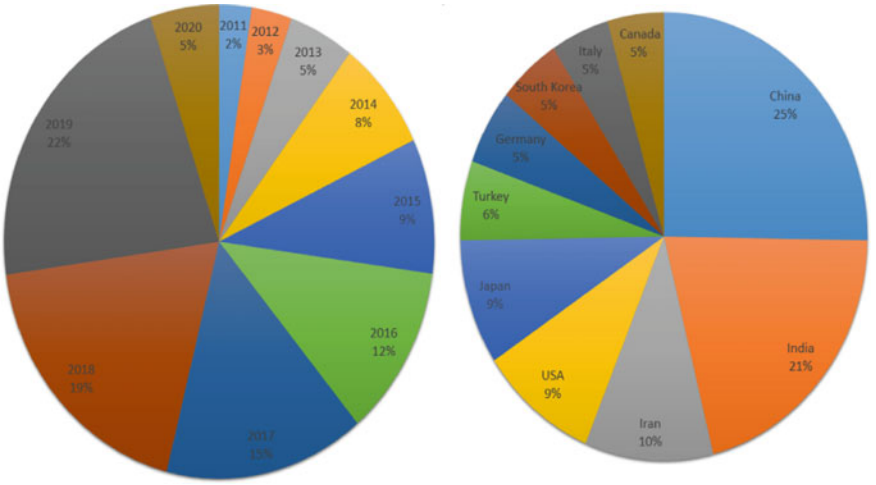

Fig. 13 Statistical data of published articles since last ten years **a** year wise **b** country wise

6 Conclusions

From critical literature review the following conclusions can be drawn:

From literature review it was observed that FW is generally performed at the speed range of 1000–4500 rpm and pressure at 40–60 MPa for metallic materials on the other hand this range was found to be 500–1200 rpm for plastic components. This technique can be performed on almost all metals and composites.

- During friction welding of Carbon steel SAE 1020, Aluminium oxide and Aluminium 6160 it was observed that fracture occurred due to the metal oxide and shear strength was inversely proportional to oxide as well as reinforced particle size.
- Friction welding of thread tube to plate, threaded tube gives more compressive strength than unthreaded tube.
- FW is ten times more efficient than that of traditional butt welding of pipe in terms of electrical power consumption and time. Utilizing this technique there was enhanced homogeneous mixture of residual stress reported. Further friction time has not much effect on the width of the other hand forging pressure is proportional to hardness and tensile strength.
- Variation of grain size has directly affected the toughness and flash formation hence further causes cracks and consequently leads to fracture.
- During friction welding of AISI 304 S.S component examined by using Transition Electron Microscope (TEM), Tensile test, Vickers's, Impact test and scanning electron microscope (SEM) resulted that the Joint strength was inversely proportional friction time and hardness.
- Friction welding of titanium alloy of 50 mm diameter with hydraulically controlled drive capable of giving 40 kN axial load resulted in the best tensile results were observed at low pressure and rotating speed, in addition to this transformation region width depends upon the applied pressure. During experimentation best results were observed that 1500 rpm and 136 MPa
- FW of Aluminium alloy and pure copper having 20 mm diameter and 120 mm length work piece examined by optical metallography technique, X-ray diffraction (XRD), scanning electron microscope (SEM) and V-notch impact revealed that optimum forging pressure and time was observed at 160 MPa and 4 s. Strain hardening was the main cause of increased hardness at weld zones. Further Structure failure was of ductile type having dimples in addition to this it was found that intermetallic joints failure occurs where the tensile strength was less.
- Performance analysis of UNS S32205 Friction Welding revealed that Speed, upset pressure and Friction pressure are directly proportional to hardness and tensile strength, whereas burn off length is inversely proportional, furthermore Upset forces and rotary speed has direct impact on tensile strength and hardness.
- Fusion process affects the quality and strength of weld within weld zone and for obtaining strong tensile strength there is a requirement of high speed within a short time interval.

- This type of welding can be performed along with traditional welding processes having several benefits over conventional types in context with environment, economical and performance aspects. FW has wide applications in industries like aerospace, marine, fabrication of shaft, rod, pipes, in addition to this square bar can also be welded using this technique. As far as material point is concerned this welding technique can applied to Steel and its Alloys, Copper and Copper Alloys, Aluminium and Aluminium Alloys, Tungsten and Titanium, Titanium and iron welding as well as non-metallic materials like Nylon 6 and ABS Reinforced Fe.
- The process parameters that affect the performance of FW are speed, friction pressure or axial force, welding time etc. The bond strength directly depends upon the axial force applied; welding time has major influence on hardness and burn off length without altering the tensile strength and bending strength. Further friction time relates inversely proportional to the fatigue limits and tensile strength.
- A Friction based welding has an ability to self-clean the rough surface of material as it comes in contact because when the load applied, it compresses the plasticized material at the weld zone to outwards in a ring shape, which removes any surface impurities or oxides that existed earlier, making it pointless to utilize protecting gas or any other accessories during welding.
- Inertial welding is used in aerospace industries more frequently among the past times, particularly in joining titanium alloys, nickel-based super alloys and steel air motor barrel shaped segments, is known for giving parts of clean and high-quality joints, contrasted and the utilization of fusion welding.

7 Future Challenges

- The studies have been performed to optimize various input parameters to achieve desired results during the friction welding process. Since, there are conflicting solutions when the number of response parameters are more than one, there is a need for multi-objective optimization studies.
- Thus, hybrid welding processes can be developed where FW can be combined with other processes which increase the possibility of achieving better output characteristics.
- Simulation and modelling of FW process parameters for different materials, alloys and composites is yet to be studied. This would help to predict and achieve the desired response in terms of mechanical strength and microstructure before initiating actual process.
- The process capability, environmental degradation of FW process, economical aspects and possibility of joining of materials with variable melting point is yet to be explored.

References

1. Acharya U, Roy BS, Saha SC (2020) Effect of tool rotational speed on the particle distribution in friction stir welding of AA6092/17.5 SiCp-T6 composite plates and its consequences on the mechanical property of the joint. Defence Technol 16(2). https://doi.org/10.1016/j.dt.2019.08.017
2. Adalarasan R, Sundaram AS (2015) Parameter design in friction welding of Al/SiC/Al_2O_3 composite using grey theory based principal component analysis (GT-PCA). J Braz Soc Mech Sci Eng 37(5). https://doi.org/10.1007/s40430-014-0294-0
3. Ahmed N (2005) New developments in advanced welding. In: New Developments in Advanced Welding. https://doi.org/10.1533/9781845690892
4. Ajith PM, Barik BK, Sathiya P, Aravindan S (2015a) Multiobjective optimization of friction welding of UNS S32205 duplex stainless steel. Defence Technol 11(2). https://doi.org/10.1016/j.dt.2015.03.001
5. Ajith PM, Husain TMAFSAL, Sathiya P, Aravindan S (2015b) Multi-objective optimization of continuous drive friction welding process parameters using response surface methodology with intelligent optimization algorithm. J Iron Steel Res Int 22(10). https://doi.org/10.1016/S1006-706X(15)30096-0
6. Alves EP, Neto FP, An CY, da Silva EC (2012) Experimental determination of temperature during rotary friction welding of AA1050 aluminum with AISI 304 stainless steel. J Aerosp Technol Manage 4(1). https://doi.org/10.5028/jatm.2012.04013211
7. Ambroziak A, Korzeniowski M, Kustroń P (2007) Friction welding of dissimilar metal joints with intermediate layers. J Achievement Mater Manuf Eng 21(2)
8. Ambroziak A (2010) Friction welding of titanium-tungsten pseudoalloy joints. J Alloys Compd 506(2). https://doi.org/10.1016/j.jallcom.2010.07.062
9. Ambroziak A, Korzeniowski M, Kustroń P, Winnicki M, Sokołowski P, Harapińska E (2014) Friction welding of aluminium and aluminium alloys with steel. Adv Mater Sci Eng 2014.https://doi.org/10.1155/2014/981653
10. Anitha P, Majumder MC, Saravanan V, Rajakumar S (2018) Effects of friction pressure and friction time on the mechanical and microstructure properties of friction welded IN718 and SS410 dissimilar joints. J Adv Microsc Res 13(2). https://doi.org/10.1166/jamr.2018.1381
11. Arivazhagan N, Singh S, Prakash S, Reddy GM (2011) Investigation on AISI 304 austenitic stainless steel to AISI 4140 low alloy steel dissimilar joints by gas tungsten arc, electron beam and friction welding. Mater Des 32(5). https://doi.org/10.1016/j.matdes.2011.01.037
12. Ashok Kumar CN, Deivanathan R (2012) Effect of aluminium alloy and mild steel on the productivity in sheet metal forming processes. Appl Mech Mater 234.https://doi.org/10.4028/www.scientific.net/AMM.234.64
13. Biswas P, Mandal NR (2009) Experimental study on friction stir welding of marine grade aluminum alloy. J Ship Prod 25(1). https://doi.org/10.5957/jsp.2009.25.1.21
14. Caligulu U, Acik M, Balalan Z, Kati N (2015) The effects of process parameters for joining of AISI 1010-Cu alloys by friction welded. Int J Steel Struct 15(4). https://doi.org/10.1007/s13296-015-1213-7
15. Chaturvedi MC (2011) Welding and joining of aerospace materials. In: Welding and joining of aerospace materials. https://doi.org/10.1533/9780857095169
16. da Silva AAM, Meyer A, dos Santos JF, Kwietniewski CEF, Strohaecker TR (2004) Mechanical and metallurgical properties of friction-welded TiC particulate reinforced Ti-6Al-4V. Compos Sci Technol 64(10–11). https://doi.org/10.1016/j.compscitech.2003.10.017
17. Faes K, Dhooge A, De Baets P, Afschrift P (2009) New friction welding process for pipeline girth welds-welding time optimisation. Int J Adv Manuf Technol 43(9–10). https://doi.org/10.1007/s00170-008-1775-z
18. Fuji A, North TH, Ameyama K, Futamata M (1992) Improving tensile strength and bend ductility of titanium/AlSI 304L stainless steel friction welds. Mater Sci Technol (United Kingdom) 8(3). https://doi.org/10.1179/mst.1992.8.3.219

19. Hamade RF, Andari TR, Ammouri AH, Jawahir IS (2019) Rotary friction welding versus fusion butt welding of plastic pipes—feasibility and energy perspective. Procedia Manuf 33. https://doi.org/10.1016/j.promfg.2019.04.087
20. Handa A, Chawla V (2014) An investigation on the effect of axial pressures on the mechanical properties of friction welded dissimilar steels. Adv Mech Eng 2014.https://doi.org/10.1155/2014/639378
21. Handa A, Chawla V (2016) Experimental evaluation of mechanical properties of friction welded dissimilar steels under varying axial pressures. Strojnicky Cas 66(1). https://doi.org/10.1515/scjme-2016-0008
22. Haribabu S, Cheepu M, Tammineni L, Gurasala NK, Devuri V, Kantumuchu VC (2019) Dissimilar friction welding of AISI 304 austenitic stainless steel and AISI D3 tool steel: mechanical properties and microstructural characterization. In: Lecture Notes in Mechanical Engineering.https://doi.org/10.1007/978-981-13-1780-4_27
23. Hascalik A, Orhan N (2007) Effect of particle size on the friction welding of Al_2O_3 reinforced 6160 Al alloy composite and SAE 1020 steel. Mater Des 28(1). https://doi.org/10.1016/j.matdes.2005.06.001
24. He ZB, Peng YY, Yin ZM, Lei XF (2011) Comparison of FSW and TIG welded joints in Al-Mg-Mn-Sc-Zr alloy plates. Trans Nonferrous Metals Soc China (English Edition) 21(8). https://doi.org/10.1016/S1003-6326(11)60915-1
25. Hussain A, Pasha S (2010) Evaluation of parameters of friction stir welding for aluminum AA6351 alloy. Int J Eng Sci Technol 2(10)
26. Inkson BJ, Threadgill PL (1998) Friction welding of FeAl40 Grade 3 ODS alloy. Mater Sci Eng A 258(1–2). https://doi.org/10.1016/s0921-5093(98)00950-2
27. Srivastava AK, Sharma A (2017) Advances in joining and welding technologies for automotive and electronic applications. Am J Mater Eng Technol 5(1). https://doi.org/10.12691/materials-5-1-2
28. Khidhir GI, Baban SA (2019) Efficiency of dissimilar friction welded 1045 medium carbon steel and 316L austenitic stainless steel joints. J Mater Res Technol 8(2). https://doi.org/10.1016/j.jmrt.2019.01.010
29. Kimura M, Kusaka M, Kaizu K, Fuji A (2009) Effect of friction welding condition on joining phenomena and tensile strength of friction welded joint between pure copper and low carbon steel. J Solid Mech Mater Eng 3(2). https://doi.org/10.1299/jmmp.3.187
30. Kishta EE, Darras B (2016) Experimental investigation of underwater friction-stir welding of 5083 marine-grade aluminum alloy. Proc Inst Mech Eng Part B: J Eng Manuf 230(3). https://doi.org/10.1177/0954405414555560
31. Kozyrev NA, Usol'tsev AA, Shevchenko RA, Kryu-Kov RE, Shishkin PE (2017) Modern welding methods of the rails of new generation. Izv Ferrous Metall 60(10). https://doi.org/10.17073/0368-0797-2017-10-785-791
32. Kumar K, Kailas SV (2008) On the role of axial load and the effect of interface position on the tensile strength of a friction stir welded aluminium alloy. Mater Des 29(4). https://doi.org/10.1016/j.matdes.2007.01.012
33. Kumar R, Singh R, Ahuja IPS, Amendola A, Penna R (2018) Friction welding for the manufacturing of PA6 and ABS structures reinforced with Fe particles. Compos Part B: Eng 132. https://doi.org/10.1016/j.compositesb.2017.08.018
34. Lee HS (2017) Application of solid state welding and superplastic forming to aerospace vehicles. SAE Technical Papers, 2017-September. https://doi.org/10.4271/2017-01-2148
35. Lee WB, Jung SB (2004) The joint properties of copper by friction stir welding. Mater Lett 58(6). https://doi.org/10.1016/j.matlet.2003.08.014
36. Lei X, Deng Y, Yin Z, Xu G (2014) Tungsten inert gas and friction stir welding characteristics of 4-mm-thick 2219-T87 plates at room temperature and −196 °C. J Mater Eng Perform 23(6). https://doi.org/10.1007/s11665-014-1013-9
37. Leśniewski J, Ambroziak A (2015) Modelling the friction welding of titanium and tungsten pseudoalloy. Arch Civ Mech Eng 15(1). https://doi.org/10.1016/j.acme.2014.06.008

38. Li WY, Ma TJ, Yang SQ, Xu QZ, Zhang Y, Li JL, Liao HL (2008) Effect of friction time on flash shape and axial shortening of linear friction welded 45 steel. Mater Lett 62(2). https://doi.org/10.1016/j.matlet.2007.05.037
39. Li X, Li J, Jin F, Xiong J, Zhang F (2018) Effect of rotation speed on friction behavior of rotary friction welding of AA6061-T6 aluminum alloy. Weld World 62(5). https://doi.org/10.1007/s40194-018-0601-y
40. Liao J, Yamamoto N, Liu H, Nakata K (2010) Microstructure at friction stir lap joint interface of pure titanium and steel. Mater Lett 64(21). https://doi.org/10.1016/j.matlet.2010.07.049
41. Lin CB, Mu CK, Wu WW, Hung CH (1999) Effect of joint design and volume fraction on friction welding properties of A360/SiC (p) composites. Weld J (Miami, Fla) 78(3)
42. Maalekian M (2007) Friction welding—critical assessment of literature. Sci Technol Weld Joining 12(8). https://doi.org/10.1179/174329307X249333
43. Manufacturing Engineer's Reference Book (1993) Manufacturing engineer's reference book. https://doi.org/10.1016/c2009-0-24956-7
44. Mercan S, Aydin S, Özdemir N (2015) Effect of welding parameters on the fatigue properties of dissimilar AISI 2205-AISI 1020 joined by friction welding. Int J Fatigue 81. https://doi.org/10.1016/j.ijfatigue.2015.07.023
45. Meshram SD, Mohandas T, Reddy GM (2007) Friction welding of dissimilar pure metals. J Mater Process Technol 184(1–3). https://doi.org/10.1016/j.jmatprotec.2006.11.123
46. Midling OT, Grong (1994) A process model for friction welding of AlMgSi alloys and AlSiC metal matrix composites-I. Haz temperature and strain rate distribution. Acta Metall Mater 42(5):1595–1609. https://doi.org/10.1016/0956-7151(94)90369-7
47. Miller Welds (2016) The history of welding. Miller Welds 3
48. De Moraes CAP, Chludzinski M, Nunes RM, Lemos GVB, Reguly A (2019) Residual stress evaluation in API 5L X65 girth welded pipes joined by friction welding and gas tungsten arc welding. J Mater Res Technol 8(1). https://doi.org/10.1016/j.jmrt.2018.07.009
49. Moreira PMGP, de Figueiredo MAV, de Castro PMST (2007) Fatigue behaviour of FSW and MIG weldments for two aluminium alloys. Theor Appl Fract Mech 48(2). https://doi.org/10.1016/j.tafmec.2007.06.001
50. Muralimohan CH, Haribabu S, Reddy YH, Muthupandi V, Sivaprasad K (2014) Evaluation of microstructures and mechanical properties of dissimilar materials by friction welding. Procedia Mater Sci 5. https://doi.org/10.1016/j.mspro.2014.07.404
51. Nicholas ED (2003) Friction processing technologies. Weld World 47(11–12). https://doi.org/10.1007/BF03266402
52. Norrish J (2006) Advanced welding processes. Adv Weld Process. https://doi.org/10.1533/9781845691707
53. Ouyang J, Yarrapareddy E, Kovacevic R (2006) Microstructural evolution in the friction stir welded 6061 aluminum alloy (T6-temper condition) to copper. J Mater Process Technol 172(1). https://doi.org/10.1016/j.jmatprotec.2005.09.013
54. Özdemir N, Sarsilmaz F, Hasçalik A (2007) Effect of rotational speed on the interface properties of friction-welded AISI 304L to 4340 steel. Mater Des 28(1). https://doi.org/10.1016/j.matdes.2005.06.011
55. Pissanti DR, Scheid A, Kanan LF, Dalpiaz G, Kwietniewski CEF (2019) Pipeline girth friction welding of the UNS S32205 duplex stainless steel. Mater Des 162. https://doi.org/10.1016/j.matdes.2018.11.046
56. Prater T (2014) Friction stir welding of metal matrix composites for use in aerospace structures. Acta Astronaut 93 https://doi.org/10.1016/j.actaastro.2013.07.023
57. Radhakrishnan E, Kumaraswamidhas LA, Palanikumar K, Muruganandam D (2019) Strength and hardness studies of C44300 tube to AA7075-T651 tube plate threaded and unthreaded dissimilar joints fabricated by friction welding process. J Mater Res Technol 8(4). https://doi.org/10.1016/j.jmrt.2019.06.008
58. Rao N, Midhani DGM (2016) Paper on comparision of conventional welding methods with solid-state welding techniques. Int Res J Eng Technol

59. Ratković N, Arsić D, Lazić V, Nikolić RR, Hadzima B (2016) Micro-structure in the joint friction plane in friction welding of dissimilar steels. Procedia Eng 149.https://doi.org/10.1016/j.proeng.2016.06.686
60. Saeid T, Abdollah-zadeh A, Assadi H, Malek Ghaini F (2008) Effect of friction stir welding speed on the microstructure and mechanical properties of a duplex stainless steel. Mater Sci Eng A 496(1–2). https://doi.org/10.1016/j.msea.2008.05.025
61. Sahin M (2010) Joining of aluminium and copper materials with friction welding. Int J Adv Manuf Technol 49(5–8). https://doi.org/10.1007/s00170-009-2443-7
62. Sami Yilbas B, Sahin AZ (2014) Friction welding: thermal and metallurgical characteristics 123. SpringerBriefs Appl Sci Technol 9783642546068 https://doi.org/10.1007/978-3-642-54607-5
63. Sathiya P, Aravindan S, Haq AN (2005) Mechanical and metallurgical properties of friction welded AISI 304 austenitic stainless steel. Int J Adv Manuf Technol 26(5–6). https://doi.org/10.1007/s00170-004-2018-6
64. Sathiya P, Aravindan S, Haq AN, Paneerselvam K (2009) Optimization of friction welding parameters using evolutionary computational techniques. J Mater Process Technol 209(5). https://doi.org/10.1016/j.jmatprotec.2008.06.030
65. Satyanarayana VV, Reddy GM, Mohandas T (2005) Dissimilar metal friction welding of austenitic-ferritic stainless steels. J Mater Process Technol 160(2). https://doi.org/10.1016/j.jmatprotec.2004.05.017
66. Sbalchiero JA, Martinazzi D, Lemos GVB, Reguly A, Ramos FD (2018) Replacement of gas metal arc welding by friction welding for joining tubes in the hydraulic cylinders industry. Mater Res 21(4). https://doi.org/10.1590/1980-5373-mr-2018-0015
67. Singh R, Kumar R, Feo L, Fraternali F (2016) Friction welding of dissimilar plastic/polymer materials with metal powder reinforcement for engineering applications. Compos Part B: Eng 101. https://doi.org/10.1016/j.compositesb.2016.06.082
68. Sreenivasan KS, Satish Kumar S, Katiravan J (2019) Genetic algorithm based optimization of friction welding process parameters on AA7075-SiC composite. Eng Sci Technol Int J 22(4). https://doi.org/10.1016/j.jestch.2019.02.010
69. Subbaiah K, Geetha M, Sridhar N, Koteswara Rao SR (2013) Comparison of tungsten inert gas and friction stir welding of AA 5083-H321 aluminum alloy plates. In: ASM Proceedings of the international conference: trends in welding research
70. Taban E, Kaluc E (2007) Comparison between microstructure characteristics and joint performance of 5086-H32 aluminium alloy welded by MIG, TIG and friction stir welding processes. Kovove Mater 45(5)
71. Thomas WM, Nicholas ED (1997) Friction stir welding for the transportation industries. Mater Des 18(4–6). https://doi.org/10.1016/s0261-3069(97)00062-9
72. Uday MB, Ahmad Fauzi MN, Zuhailawati H, Ismail AB (2011) Effect of welding speed on mechanical strength of friction welded joint of YSZ-alumina composite and 6061 aluminum alloy. Mater Sci Eng A 528(13–14). https://doi.org/10.1016/j.msea.2011.02.091
73. Uday MB, Fauzi MNA, Zuhailawati H, Ismail AB (2010) Advances in friction welding process: a review. Sci Technol Weld Joining 15(7). https://doi.org/10.1179/136217110X12785889550064
74. Uzkut M, Ünlü B, Yilmaz S, Akdağ M (2010) Friction welding and its applications in today's world. In: Sarajevo: international symposium on sustainable development
75. Wanjara P, Jahazi M (2005) Linear friction welding of Ti-6Al-4V: processing, microstructure, and mechanical-property inter-relationships. Metall Mater Trans A Phys Metall Mater Sci 36(8). https://doi.org/10.1007/s11661-005-0335-5

76. Wen Q, Li W, Patel V, Gao Y, Vairis A (2020) Investigation on the effects of welding speed on Bobbin tool friction stir welding of 2219 aluminum alloy. Metals Mater Int 26(12). https://doi.org/10.1007/s12540-019-00450-9
77. Yilbas BS, Sahin AZ, Coban A, Abdul Aleem BJ (1995) Investigation into the properties of friction-welded aluminium bars. J Mater Process Tech 54(1–4). https://doi.org/10.1016/0924-0136(95)01923-5
78. Yilbaş BS, Şahin AZ, Kahraman N, Al-Garni AZ (1995) Friction welding of StAl and AlCu materials. J Mater Process Tech 49(3–4):431–443. https://doi.org/10.1016/0924-0136(94)01349-6
79. Zhang XP, Quan GF, Wei W (1999) Preliminary investigation on joining performance of SiCp-reinforced aluminum metal matrix composite (Al/SiCp-MMC) by vacuum brazing. Compos Part A Appl Sci Manuf 30(6). https://doi.org/10.1016/S1359-835X(98)00186-9

Influence of Reinforcement Contents and Turning Parameters on the Machining Behaviour of Al/SiC/Cr Hybrid Aluminium Matrix Composites

Jatinder Kumar, Dilbag Singh, Nirmal S. Kalsi, and Shubham Sharma

1 Introduction

The materials used for aerospace, transportation, and underwater applications should have the properties like low weight, high wear, and corrosion resistances, high impact strength etc. These properties are not exhibited by existing monolithic materials/alloys or ceramics [4]. To overcome these shortcomings, the already existed monolithic material is being substituted by composite material. The composite materials are developed to combine favorable properties of different materials. Because of the superior qualities, the replacement of conventional monolithic materials and their alloys with composites, extend their applications in automobile, defense, marine, sports and recreation industries [20, 22].

In metal matrix composite (MMC) is the combination of two or more materials, in which one is a matrix and other is reinforcement in which the matrix used is generally a lighter metal, which supports the reinforced particles within the composites. The metals used as the matrix in MMCs are light metals like aluminium, titanium, magnesium, zinc and their alloys [3, 16]. However, copper, nickel, lead, iron, tungsten are also used as the matrix in some particular applications [4, 17, 28]. Also, the cobalt and Co–Ni alloys are used as a matrix material in the areas, where the materials are subjected to high temperature [4, 28].

J. Kumar
Department of Research Innovation and Consultancy, IKG Punjab Technical University, Kapurthala, Punjab 144603, India

D. Singh · N. S. Kalsi
Department of Mechanical Engineering, Beant College of Engineering & Technology, Gurdaspur, Punjab 143521, India

S. Sharma (✉)
Department of Mechanical Engineering, IKG Punjab Technical University, Jalandhar-Kapurthala Road, Kapurthala, Punjab 144603, India

S. Mavinkere Rangappa et al. (eds.), *Additive and Subtractive Manufacturing of Composites*, Springer Series in Advanced Manufacturing,
https://doi.org/10.1007/978-981-16-3184-9_2

The reinforcement, when added in matrix, improves its several properties (like hardness, strength etc.) and prevents its deformation. This material has its own particular microstructure, morphology, chemistry, physical and mechanical properties, cost and shapes and on the behalf of these characteristics, reinforcement is selected for particular matrix [4].

The single ceramic reinforced composites, sometime exhibit some negative effects also. These effects include the reduction in machinability, fracture toughness, wear resistance etc. in some specific weight reduction applications like cylinder blocks and liners, pistons, connecting rods, brake drums etc. [24]. These types of difficulties can be eliminated by using aluminium matrix based hybrid MMCs. The composites having three or more constituent particles present in it is known as hybrid metal matrix composites (HMMC). In such type of composite materials, at least two reinforced materials are used. The HMMCs possess higher strength/weight ratio, higher toughness, less sensitive to temperature changes, improved wettability as well as machinability etc. Due to this reason, HMMCs possess many applications in the field of aerospace and automobile components [18].

Out of the available matrix materials, aluminium is generally used as matrix material because of lower costs, easy availability, lower density, higher strength/weight ratio, highly resistant to corrosion and lower processing temperature requirement [4, 6]. In last one-two decades, the use of Al/SiC composites has been increased rapidly, particularly for automotive, recreation and aerospace applications as Aluminium exhibits lower density, lower coefficient of thermal expansion, higher strength/weight ratio, higher wear resistance etc.

The introduction of SiC enhances wear resistance, hardness value and tensile strength, but with the higher percentage of SiC, the machinability (ductility) and toughness resistance of the MMCs reduces [1, 19]. However, machinability of such materials can be improved by using additional reinforcement (like Graphite) along with SiC [26].

Among the available fabrication process, liquid state stirs casting is simplest one, and most effectively used in the fabrication of aluminium matrix composites. In this technique, the reinforcement(s) (ceramics, agro wastes or industrial wastes) is/are mixed with liquid matrix metal and stirred mechanically under controlled condition [4].

Grey relation analysis is an effective tool to solve multi performance parameters in many applications. Yih-Fong and Fu-Chen [13] optimized turning of tool steel to obtain the best set of input conditions for optimal vales of surface roughness and dimensional accuracy. GRA also successfully applied by the researchers in the optimization of various input conditions such as optimization of electric discharge machining process [9], chemical polishing [5, 8], for evaluation of tool conditions in turning, drilling [23].

In this experimental study, an attempt has been made to introduce chromium particles with SiC in the grain structure of Al–Si alloy and to evaluate its affect on the machining behaviour of novel composites. The composites are fabricated through conventional stir casting. The turning on standard samples, as prescribed by Taguchi's L27 array, has been conducted using conventional Lathe machine and the

machining performance in form of material removal rate, surface roughness and tool wear rate is evaluated. The Taguchi analysis followed by grey relation analysis has been performed and multiple responses optimization has been discussed to improve the machining integrity of novel composites.

2 Materials and Method

Al–Si alloy based composites, reinforced with 10 wt% SiC and (0–3 wt%) Cr, are formulated through stir casting method. The stir casting setup used for composite formulation is shown in Fig. 1.

The Al–Si alloy cleaned using acetone, weighed and cut in desire amount, charged in electric furnace and melted at 730 ± 20 °C for around 90 min under the argon gas environment. SiC (10 wt%) and Cr (0–3 wt% in steps of 1.5) are preheated to 600 ± 5 °C before introducing in the melt to remove any moisture contents. The slurry is then stirred continuously with electric motor integrated graphite rotor an average speed of 400 rpm for 8–10 min. 1 wt% of magnesium is also mixed in the slurry to enhance the wettability among the ingredients [12, 21]. the semi-solid mixture is then poured in steel mould and allowed to solidify. The specimens used for experimentation are having dimensions Φ 30 mm × 100 mm.

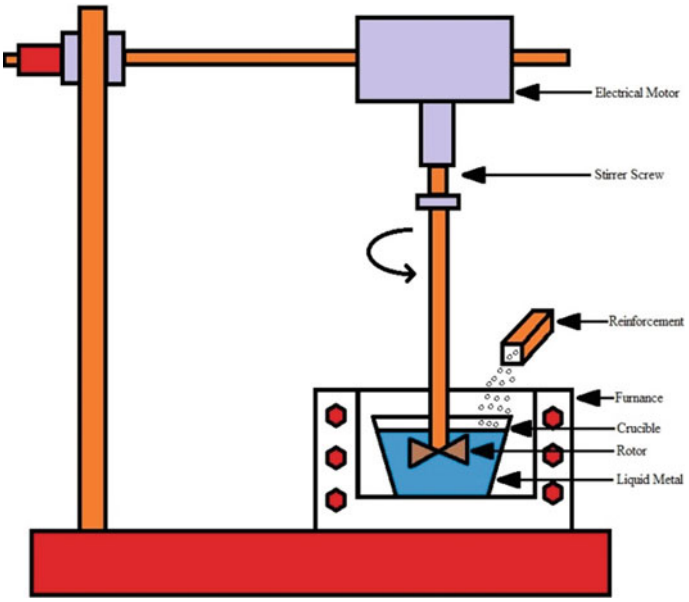

Fig. 1 Illustration of stir casting process

Table 1 Input and response parameters

S. No.	Input parameters	Symbol	Variations	Responses	Symbol
1	Cutting speed	A	60, 90, 120 (m/min)	Surface roughness (μm)	Ra
2	Feed rate	B	0.10, 0.14, 0.18 (mm/rev)	Material removal rate (mm^3/min)	MRR
3	Depth of cut	C	0.45, 0.60, 0.75 (mm)	Tool wear rate (mg/min)	TWR
4	Coating thickness	D	5, 8, 14 (μm)		
5	Weight % of Cr.	E	0, 1.5, 3 (wt%)		

The tools, chosen for this study, are multiple coated (with a varying coating thickness of TiN/Al_2O_3/TiCN/TiN), carbide inserts with an ISO designation CNMG120408-SU.

The design of experiments used for turning is Taguchi method. This method is effectively used in the optimization of multiple input parameters in many applications. A Taguchi coupled grey relation analysis is also carried out to optimize the multiple response parameters. As a result of the literature survey, five input parameters viz. cutting speed, feed rate, depth of cut, tool coating thickness and weight percentage of chromium are selected. Three output parameters include material removal rate, surface roughness and tool wear rate. A conventional HMT LB-17 lathe centre having 7.5 kW power is and for turning each run is performed on 30 mm sample length under dry condition.

Table 1 shows the input parameters with their levels and response parameters. Standard orthogonal Array L27 (3ˆ5) is selected for turning. A rough cut is carried out to remove the rust and irregular surface.

A Japan-made Mitutoyo roughness tester (J:400 Model) is used (sampling speed-0.25 mm/s) to measure Ra value at three different lsocations and their average is calculated. Before and after each run, the diameter of the specimen and weight of the carbide insert is measured using standard measuring devices. The time consumed in each run is recorded using a stopwatch. The MRR in the form of total volume removed per minute and TWR in the form of weight loss per minute is calculated. The experimental set up of input parameters and experimental outcomes corresponding to their signal to noise ratios are shown in Table 2. The S/N ratio analysis is carried out corresponding to all responses to analyze the experimental data. It is desired that the machining surface should have maximum surface finishing and material removal rate along with minimum tool wear.

Table 2 Conditions of controllable input parameters and experimental results

S. No.	A (m/min)	B (mm/rev)	C (mm)	D (μm)	E (wt%)	Ra (μm)	S/N ratio	MRR (mm^3/min)	S/N ratio	TWR (mg/min)	S/N ratio
1	60	0.1	0.5	5	0	0.92	0.72424	2552.07	68.1379	0.14121	17.0027
2	60	0.1	0.7	8	1.5	1.41	−2.98438	4289.67	72.6485	0.23242	12.6745
3	60	0.1	0.9	14	3	1.62	−4.19030	6037.00	75.6164	0.43542	7.2218
4	60	0.14	0.5	8	1.5	0.79	2.04746	3610.34	71.1510	0.34321	9.2888
5	60	0.14	0.7	14	3	1.02	−0.17200	6334.46	76.0342	0.58164	4.7069
6	60	0.14	0.9	5	0	0.85	1.41162	9288.91	79.3593	0.35243	9.0585
7	60	0.18	0.5	14	3	0.70	3.09804	4617.26	73.2877	0.71823	2.8747
8	60	0.18	0.7	5	0	0.68	3.34982	8817.88	78.9073	0.57923	4.7430
9	60	0.18	0.9	8	1.5	0.79	2.04746	12,451.82	81.9047	0.73493	2.6751
10	90	0.1	0.5	8	3	0.94	0.53744	3543.33	70.9882	0.41321	7.6766
11	90	0.1	0.7	14	0	0.76	2.38373	6008.55	75.5754	0.26143	11.6529
12	90	0.1	0.9	5	1.5	1.23	−1.79810	8466.82	78.5544	0.54256	5.3110
13	90	0.14	0.5	14	0	0.49	6.19608	5151.47	74.2386	0.36842	8.6731
14	90	0.14	0.7	5	1.5	0.76	2.38373	8907.47	78.9951	0.68342	3.3062
15	90	0.14	0.9	8	3	0.90	0.91515	12,673.56	82.0580	0.99664	0.0292
16	90	0.18	0.5	5	1.5	0.57	4.88250	6660.34	76.4699	0.81565	1.7699
17	90	0.18	0.7	8	3	0.67	3.47850	12,466.66	81.9150	1.16664	−1.3387
18	90	0.18	0.9	14	0	0.51	5.84860	16,627.55	84.4166	0.67881	3.3650
19	115	0.1	0.5	14	1.5	0.61	4.29340	4688.06	73.4199	0.56450	4.9667
20	115	0.1	0.7	5	3	0.88	1.11035	7558.15	77.5683	1.11843	−0.9722
21	115	0.1	0.9	8	0	0.64	3.87640	10,885.03	80.7366	0.65101	3.7282

(continued)

Table 2 (continued)

S. No.	A (m/min)	B (mm/rev)	C (mm)	D (μm)	E (wt%)	Ra (μm)	S/N ratio	MRR (mm^3/min)	S/N ratio	TWR (mg/min)	S/N ratio
22	115	0.14	0.5	5	3	0.55	5.19275	6391.64	76.1122	1.21212	−1.6709
23	115	0.14	0.7	8	0	0.44	7.13095	11,453.99	81.1791	0.77843	2.1756
24	115	0.14	0.9	14	1.5	0.56	5.03624	16,092.95	84.1327	1.13343	−1.0879
25	115	0.18	0.5	8	0	0.34	9.37042	8743.62	78.8338	0.91420	0.7792
26	115	0.18	0.7	14	1.5	0.43	7.33063	15,671.84	83.9024	1.29334	−2.2343
27	115	0.18	0.9	5	3	0.53	5.51448	20,167.93	86.0932	1.96943	−5.8868

3 Results and Discussion

It is desired that the machining surface should have the maximum surface finishing and material removal rate along with minimum tool wear. The objective of this study is to maximize the material removal rate and minimize surface roughness and tool wear rate.

3.1 Taguchi Analysis

So as per the terminology of Taguchi method, "larger is better" type response has been employed for material removal rate and "lower is the better" type response has been employed for surface roughness and tool wear rate. The mathematical equations used for these types of responses are shown in Eqs. 1 and 2.

For larger is better (Maximize):

$$\frac{S}{N} = -10 \log \frac{1}{n} \sum_{i=1}^{n} \frac{1}{Y_i^2} \tag{1}$$

For smaller is better (Minimize):

$$\frac{S}{N} = -10 \log \frac{1}{n} \sum_{i=1}^{n} Y_i^2 \tag{2}$$

where Y_i is the individual measured response parameters and n indicates the number of trials replicated. The signal to noise ratio should be high for an optimal solution.

The signal to noise ratios for material removal rate, surface roughness and tool wear rate at different levels of input parameters is calculated and plotted as shown in Figs. 2, 3 and 4.

The influence of speed, feed, DoC, coating thickness and per cent weightage of Cr on the material removal rate, surface roughness and tool wear rate can be explored as per the trend of curves. From figures, it is observed that larger cutting speed and feed results in an increase in material removal rate and surface quality, but with the loss of tool life. It is also considered that the presence of Cr contents causes deterioration of surface quality and reduces tool life. Also, the increase in coating thickness produces a positive effect on the surface quality as well as tool life.

ANOVA for all output parameters is shown in Tables 3, 4 and 5, which are indicating the significant parameters for the corresponding response.

The confirmation experiments, as per sets of best conditions obtained from Taguchi's analysis, are conducted for all responses individually and presented in Table 6.

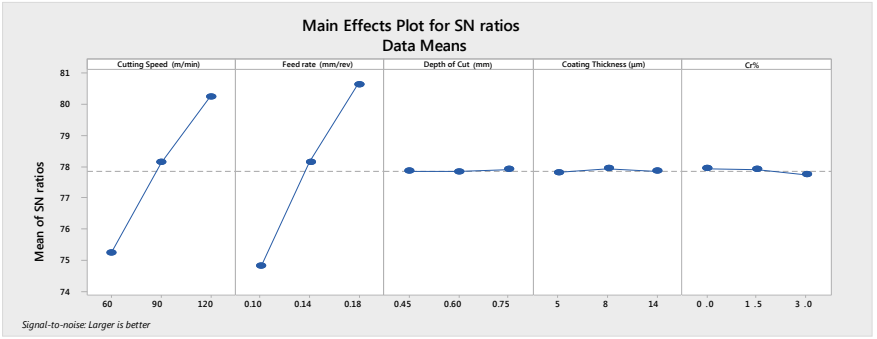

Fig. 2 Main effects plot for material removal rate

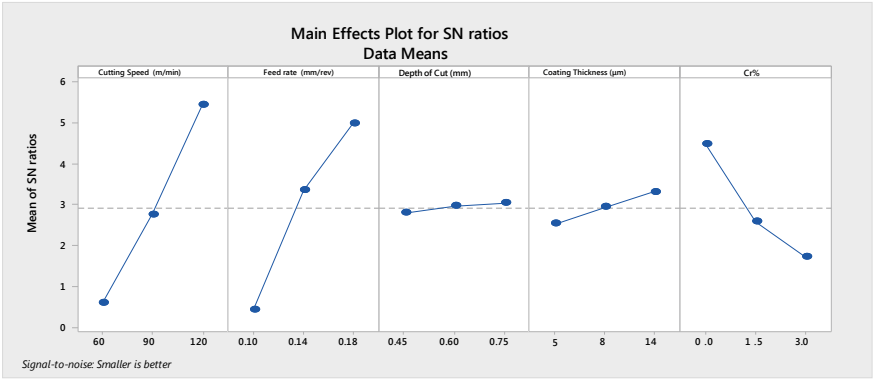

Fig. 3 Main effects plot for surface roughness

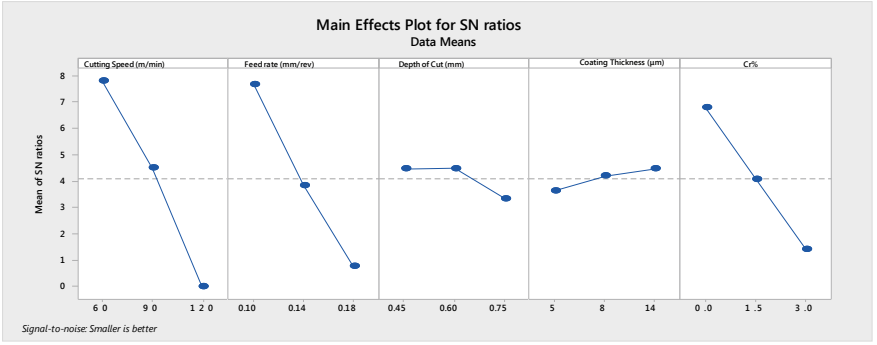

Fig. 4 Main effects plot for tool wear rate

Table 3 ANOVA table for material removal rate

Source	DF	Adj SS	Adj MS	F-value	P-value
Cutting speed (m/min)*	1	105,869,681	105,869,681	7.96	0.010
Feed rate (mm/rev)*	1	151,358,077	151,358,077	11.39	0.003
Depth of cut (mm)	1	2,584,909	2,584,909	0.19	0.664
Coating thickness (μm)	1	307,592	307,592	0.02	0.881
Cr%	1	3782	3782	0.00	0.987
Error	21	279,169,750	13,293,798		
Total	26	539,293,790			

*Significant factors

Table 4 ANOVA table for surface roughness

Source	DF	Adj SS	Adj MS	F-value	P-value
Cutting speed (m/min)*	1	0.80222	0.802222	42.20	0.000
Feed rate (mm/rev)*	1	0.79801	0.798006	41.97	0.000
Depth of cut (mm)	1	0.03556	0.035556	1.87	0.186
Coating thickness (μm)	1	0.00447	0.004471	0.24	0.633
Cr%*	1	0.26402	0.264022	13.89	0.001
Error	21	0.39924	0.019012		
Total	26	2.30352			

*Significant factors

Table 5 ANOVA table for tool wear rate

Source	DF	Adj SS	Adj MS	F-value	P-value
Cutting speed (m/min)*	1	1.69045	1.69045	71.09	0.000
Feed rate (mm/rev)*	1	1.13014	1.13014	47.53	0.000
Depth of cut (mm)	1	0.00179	0.00179	0.08	0.787
Coating thickness (μm)	1	0.08633	0.08633	3.63	0.071
Cr%*	1	0.83920	0.83920	35.29	0.000
Error	21	0.49935	0.02378		
Total	26	4.24726			

*Significant factors

Table 6 Taguchi's optimized input parameters for MRR, Ra and TWR

S. No.	Best setting of input parameters	Output parameters	Optimized values
1	$A_3B_3C_3D_2E_1$	MRR	20792.45 mm^3/min
2	$A_3B_3C_3D_3E_1$	Ra	0.32 (μm)
3	$A_1B_1C_2D_3E_1$	TWR	0.13953 (mg/min)

3.2 Grey Relation Analysis

In Taguchi analysis, a different set of conditions for input parameters are obtained for each response and it is complicated to choose the common set of input parameters for optimal values of all response characteristics. Under such circumstances, the multiple response optimizations may be the best solution. The grey relational analysis is one of the best techniques to solve these types of problems [12]. In recent 3–4 decades,this method is extensively used for solving the complex inter-relationships among the multiple output parameters. The steps involved, normalizing the results of experiments between 0 and 1 using Eqs. 3 and 4, deviating the sequence as per Eq. 5, calculating the grey relation coefficient (GRC) from normalized data (Eq. 6), calculating overall grey relation grades (GRG) with the help of Eq. 7 and converting the multi-response parameters into the optimization of single GRG [12, 25]. Normalized experimental results corresponding to large-is-better can be obtained as

$$Y_{ij} = \frac{x_{ij} - \min x_{ij}}{\max x_{ij} - \min x_{ij}} \tag{3}$$

Normalized experimental results corresponding to small-is-better can be obtained as

$$Y_{ij} = \frac{\max x_{ij} - x_{ij}}{\max x_{ij} - \min y_{ij}} \tag{4}$$

The normalized results can be deviated by calculating the difference between the absolute values of $\max Y_{ij}$ and Y_{ij}. Thus the deviated sequence values (Δ_{ij}) can be obtained as

$$\Delta_{ij} = \left|\max Y_{ij} - Y_{ij}\right| \tag{5}$$

The grey relation coefficient (ξ_{ij}) can be calculated as follows

$$\xi_{ij} = \frac{\min \Delta_{ij} - \Psi \max \Delta_{ij}}{\Delta_{ij} - \Psi \max \Delta_{ij}} \tag{6}$$

where Ψ is the distinguished coefficient and it varies as $0 \leq \Psi \leq 1$. It is usually kept as 0.5.

Grey relation grades (γ) can be obtained as:

$$\gamma = \frac{1}{n} \sum \xi_{ij} \tag{7}$$

where n represents number of output parameters and ξ represents GRC. The analysis is performed; results are calculated and represented in Table 7.

Table 7 Calculated normalized data, grey relation coefficients and grey relation grades

Run no.	Normalization (Y)			Deviation sequences (Δ)			Grey relation coefficients (ξ)			Grey reslation grades (γ)	Rank
	Ra	MRR	TWR	Ra	MRR	TWR	Ra	MRR	TWR		
1	0.547	0.000	1.000	0.453	1.000	0.000	0.525	0.333	1.000	0.61931	9
2	0.164	0.099	0.950	0.836	0.901	0.050	0.374	0.357	0.909	0.54678	19
3	0.000	0.198	0.839	1.000	0.802	0.161	0.333	0.384	0.757	0.49127	26
4	0.648	0.060	0.890	0.352	0.940	0.110	0.587	0.347	0.819	0.58447	13
5	0.469	0.215	0.759	0.531	0.785	0.241	0.485	0.389	0.675	0.51624	24
6	0.602	0.382	0.884	0.398	0.618	0.116	0.557	0.447	0.812	0.60541	10
7	0.719	0.117	0.684	0.281	0.883	0.316	0.640	0.362	0.613	0.53821	21
8	0.734	0.356	0.760	0.266	0.644	0.240	0.653	0.437	0.676	0.58869	12
9	0.648	0.562	0.675	0.352	0.438	0.325	0.587	0.533	0.606	0.57548	15
10	0.531	0.056	0.851	0.469	0.944	0.149	0.516	0.346	0.771	0.54438	20
11	0.672	0.196	0.934	0.328	0.804	0.066	0.604	0.383	0.884	0.62368	8
12	0.305	0.336	0.780	0.695	0.664	0.220	0.418	0.429	0.695	0.51422	25
13	0.883	0.148	0.876	0.117	0.852	0.124	0.810	0.370	0.801	0.66025	4
14	0.672	0.361	0.703	0.328	0.639	0.297	0.604	0.439	0.628	0.55678	17
15	0.563	0.575	0.532	0.438	0.425	0.468	0.533	0.540	0.517	0.53007	23
16	0.820	0.233	0.631	0.180	0.767	0.369	0.736	0.395	0.575	0.56859	16
17	0.742	0.563	0.439	0.258	0.437	0.561	0.660	0.534	0.471	0.55487	18
18	0.867	0.799	0.706	0.133	0.201	0.294	0.790	0.713	0.630	0.71103	1
19	0.789	0.121	0.768	0.211	0.879	0.232	0.703	0.363	0.683	0.58315	14
20	0.578	0.284	0.465	0.422	0.716	0.535	0.542	0.411	0.483	0.47898	27

(continued)

Table 7 (continued)

Run no.	Normalization (Y)			Deviation sequences (Δ)			Grey relation coefficients (ξ)			Grey reslation grades (γ)	Rank
	Ra	MRR	TWR	Ra	MRR	TWR	Ra	MRR	TWR		
21	0.766	0.473	0.721	0.234	0.527	0.279	0.681	0.487	0.642	0.60323	11
22	0.836	0.218	0.414	0.164	0.782	0.586	0.753	0.390	0.461	0.53448	22
23	0.922	0.505	0.651	0.078	0.495	0.349	0.865	0.503	0.589	0.65226	6
24	0.828	0.769	0.457	0.172	0.231	0.543	0.744	0.684	0.480	0.63580	7
25	1.000	0.351	0.577	0.000	0.649	0.423	1.000	0.435	0.542	0.65905	5
26	0.930	0.745	0.370	0.070	0.255	0.630	0.877	0.662	0.442	0.66039	3
27	0.852	1.000	0.000	0.148	0.000	1.000	0.771	1.000	0.333	0.70147	2

Table 8 Analysis of variance for grey relation grades

Source	DF	Adj SS	Adj MS	F-value	P-value	% Contribution
Cutting speed (m/min)*	1	0.010900	0.010900	8.43	0.008	10.96
Feed rate (mm/rev)*	1	0.016976	0.016976	13.13	0.002	17.07
Depth of cut (mm)	1	0.002212	0.002212	1.71	0.205	2.22
Coating thickness (μm)	1	0.003670	0.003670	2.84	0.107	3.69
Wt% of Chromium*	1	0.038544	0.038544	29.82	0.000	38.76
Error	21	0.027147	0.001293			27.30
Total	26	0.099449				

S = 0.0359546, R-sq = 72.70%, R-sq(adj) = 66.20%
*Significant parameter

Now, from the orthogonal design of experiments, the influence of input parameters on grey relation grades GRG can be obtained with an objective of large -is-better type response. The ANOVA analysis for grey relation grades is shown in Table 8. It is also noted that the significant parameters for maximized GRG are cutting speed, feed rate and weightage of chromium contents.

The significant level for each input parameter can be estimated to obtain the optimal value of GRG from Table 9. Also as per delta value, all input parameters may be ranked. The GRG graph for the level of input parameters for turning is shown in Fig. 5. The main objective of this analysis is to obtain a large value of GRG, which means better are, the response parameters.

ANOVA Table illustrates that Feed rate; cutting speed and weight percentage of Cr contents are significant parameters which are influencing the material removal rate, tool wear rate and surface quality of the composites. Also, Cr.% contributes most significantly in the optimization of response characteristics, followed by feed rate and cutting speed, however, least contribution of the depth of cut and coating thickness is obtained.

Table 9 Response table for grey relation grades

Level	Cuttin speed (m/min)	Feed rate (mm/rev)	Depth of cut (mm)	Coating thickness (μm)	Cr.%
1	0.5629	0.5561109	0.5904883	0.5742146	**0.6358794***
2	0.584875	0.5861959	**0.6010348***	0.5833993	0.5806285
3	**0.612091***	**0.6175311***	0.5683148	**0.602224***	0.54333
Delta	0.0492	0.0614202	0.03272	0.0280094	0.0925493
Rank	3	2	4	5	1

*Significant Level

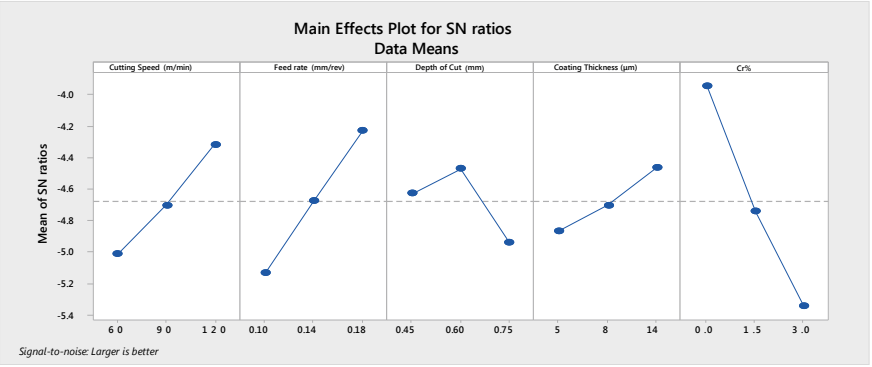

Fig. 5 Main effects plot for grey relation grades

3.3 Non Linear Regression Model for Grey Relation Coefficient

The non-linear regression equation (Eq. 8) indicates that how grey relation grade depends upon the input parameters

$$\begin{aligned} \text{GRD} = {} & 0.4679 + 0.000820\text{*A} + 0.768\text{*B} \\ & - 0.0739\text{*C} + 0.00312\text{*D} - 0.03085\text{*E} \end{aligned} \tag{8}$$

The residual plot of GRG received throughout regression evaluation is presented in Fig. 6.

The normal probability plot is having a straight line with the residuals centered nearer to the straight line. In residual versus fits plot, the residuals appear to be randomly scattered around zero and most of the elements are based on the common outfitted value and the residuals are minimal. The histogram of the residuals suggests the distribution of the residuals for all observations that are skewed towards the left and the bell-shaped curve is formed. Residuals versus order graph plot may also be notably precious in a designed experiment wherein the runsshould not randomize. The residuals in the plot are scattered around the centre line.

4 Confirmation Experiments

The confirmation experiments are performed for optimizing the response parameters by using the optimized parameters in multiple objective optimizations. Base upon optimal values of response parameters, the predicted value of grey relation grade ($\gamma_{\text{Predicted}}$) is estimated as per Eq. 9.

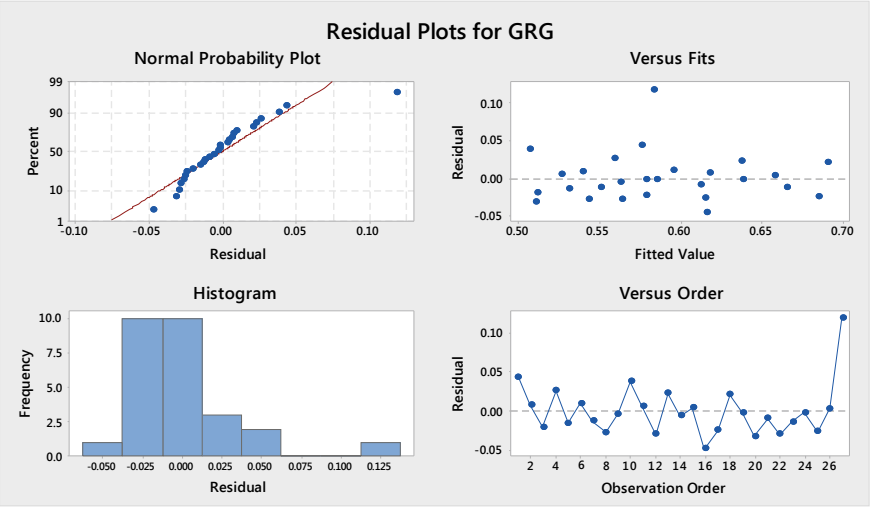

Fig. 6 Residual plots of grey relation grades

$$\gamma_{\mathrm{Pr}edicted} = \gamma_{mean} + \sum_{i=1}^{q}(\gamma_i - \gamma_{mean}) \tag{9}$$

where

γ_{mean} = Mean value of grey relation grades ($\gamma_{mean} = 0.58661$; Table 7).
γ_i = Mean of grey relation grades at the optimal level.
q = Number of significant input parameters. (q = 3; Table 8).

γ_{mean} = Mean value of grey relation grades ($\gamma_{mean} = 0.58661$; Table 7).
γ_i = Mean of grey relation grades at the optimal level.
q = Number of significant input parameters. (q = 3; Table 8).

It is also observed from Table 10 that the experimental value of grey relation grade differ by 2.52% only from the predicted value, means experimental results are validated.

5 Conclusions and Future Perspective

Taguchi analysis followed by a grey relation grade obtained from Taguchi coupled grey relation analysis has been used for the turning of novel Al-10SiC-(0-3)Cr composites with multiple objective optimization of response parameters including material removal rate, surface roughness and tool wear rate. As per results obtained, the following conclusion can be drawn:

Table 10 Results of responses using initial and optimal parameters

	Initial input parameters	Optimum input parameters	
		Predicted	Experimental
Setting level	$V_3F_3A_1T_2C_1$	$V_3F_3A_2T_3C_1$	$V_3F_3A_2T_3C_1$
Surface roughness (μm)	0.34		0.39
Material removal rate (mm^3/min)	8743.62		15,674.32
Tool wear rate (mg/min)	0.914		0.917
Grey relation grade	0.65905	0.69228	0.71021
Improvement in GRG = 0.05116			

1. According to ANOVA test the cutting speed, feed rate and chromium contents are most significant parameters for effecting the surface roughness and tool wear. Speed and feed rate has significant affect on material removal rate, whereas other input parameters are insignificant. Best set of conditions for material removal rate, surface roughness and tool wear rate are $A_3B_3C_3D_2E_1$, $A_3B_3C_3D_3E_1$ and $A_1B_1C_2D_3E_1$ respectively.
2. The Taguchi coupled grey relation analysis suggests a single optimal set of input parameters as $A_3B_3C_2D_3E_1$ i.e. cutting speed 120 m/min, feed rate 0.18, depth of cut of 0.60, coating thickness on carbide insert 14 μm with 0% weightage of chromium contents for all responses.
3. The result of confirmation test indicates that increase in grey relation grade from the set of initial cutting condition to optimal conditions is 0.05116, means the multiple responses of AMCs turning such as material removal rate, surface roughness and tool wear rate is improved together by using grey relation analysis. Also the predicted grey relation grade differs from experimental gray relation grade by 2.52% only and thus the experimental results are validated.

Future Scope

- Another fabrication route like powder metallurgy can be used to develop same composite.
- Composite of reinforcing phase may be change to develop different composites.
- Nano size particles may be used instead of micro size particles.

Acknowledgements The authors would like to thank IKG Punjab Technical University, Kapurthala, Punjab, India for providing an opportunity to do this research work.

Conflict of Interest
The authors declare no conflict of interest.

Funding
This research did not receive any specific grant from funding agencies in the public, commercial, or not-for-profit sectors.

Annexure

Control Log of Experiments

Cutting seed (m/min)	Feed rate (mm/rev)	Depth of cut (mm)	Coating thickness (μm)	Wt% of Cr
1	1	1	1	1
1	1	2	2	2
1	1	3	3	3
1	2	1	2	2
1	2	2	3	3
1	2	3	1	1
1	3	1	3	3
1	3	2	1	1
1	3	3	2	2
2	1	1	2	3
2	1	2	3	1
2	1	3	1	2
2	2	1	3	1
2	2	2	1	2
2	2	3	2	3
2	3	1	1	2
2	3	2	2	3
2	3	3	3	1
3	1	1	3	2
3	1	2	1	3
3	1	3	2	1
3	2	1	1	3
3	2	2	2	1
3	2	3	3	2
3	3	1	2	1
3	3	2	3	2
3	3	3	1	3

References

1. Karabulut Ş (2015) Optimization of surface roughness and cutting force during AA7039/Al2O3 metal matrix composites milling using neural networks and Taguchi method. Measurement 1(66):139–149

2. Lo SP (2002) The application of an ANFIS and grey system method in turning tool-failure detection. Int J Adv Manuf Technol 19(8):564–572
3. Miklaszewski A (2015) Effect of starting material character and its sintering temperature on microstructure and mechanical properties of super hard Ti/TiB metal matrix composites. Int J Refract Metal Hard Mater 1(53):56–60
4. Tjong SC (2014) Processing and deformation characteristics of metals reinforced with ceramic nanoparticles. Nanocryst Mater, 269–304 (Elsevier)
5. Tosun N (2006) Determination of optimum parameters for multi-performance characteristics in drilling by using grey relational analysis. Int J Adv Manuf Technol 28(5–6):450–455
6. Alaneme KK, Aluko AO (2012) Fracture toughness (K1C) and tensile properties of as-cast and age-hardened aluminium (6063)–silicon carbide particulate composites. Sci Iranica 19(4):992–996
7. Devaneyan SP, Senthilvelan T (2014) Electro co-deposition and characterization of SiC in nickel metal matrix composite coatings on aluminium 7075. Procedia Eng 1(97):1496–1505
8. Ho CY, Lin ZC (2003) Analysis and application of grey relation and ANOVA in chemical–mechanical polishing process parameters. Int J Adv Manuf Technol 21(1):10–14
9. Lin JL, Lin CL (2002) The use of the orthogonal array with grey relational analysis to optimize the electrical discharge machining process with multiple performance characteristics. Int J Mach Tools Manuf 42(2):237–244
10. Padmavathi KR, Ramakrishnan R (2014) Tribological behaviour of aluminium hybrid metal matrix composite. Procedia Eng 1(97):660–667
11. Prasad SV, Asthana R (2004) Aluminum metal-matrix composites for automotive applications: tribological considerations. Tribol Lett 17(3):445–453
12. Ranganathan S, Senthilvelan T (2011) Multi-response optimization of machining parameters in hot turning using grey analysis. Int J Adv Manuf Technol 56:455–462
13. Yih-Fong T, Fu-Chen C (2006) Multiobjective process optimisation for turning of tool steels. Int J Mach Mach Mater 1(1):76–93
14. Aramesh M, Shi B, Nassef AO, Attia H, Balazinski M, Kishawy HA (2013) Meta-modeling optimization of the cutting process during turning titanium metal matrix composites (Ti-MMCs). Procedia CIRP 1(8):576–581
15. Arumugam PU, Malshe AP, Batzer SA (2006) Dry machining of aluminum–silicon alloy using polished CVD diamond-coated cutting tools inserts. Surf Coat Technol 200(11):3399–3403
16. Bains PS, Sidhu SS, Payal HS (2016) Fabrication and machining of metal matrix composites: a review. Mater Manuf Processes 31(5):553–573
17. Cao H, Qian Z, Zhang L, Xiao J, Zhou K (2014) Tribological behavior of Cu matrix composites containing graphite and tungsten disulfide. Tribol Trans 57(6):1037–1043
18. Feng GH, Yang YQ, Luo X, Li J, Huang B, Chen Y (2015) Fatigue properties and fracture analysis of a SiC fiber-reinforced titanium matrix composite. Compos B Eng 1(68):336–342
19. James SJ, Venkatesan K, Kuppan P, Ramanujam R (2014) Hybrid aluminium metal matrix composite reinforced with SiC and TiB2. Procedia Eng 1(97):1018–1026
20. Kala H, Mer KK, Kumar S (2014) A review on mechanical and tribological behaviors of stir cast aluminum matrix composites. Procedia Mater Sci 1(6):1951–1960
21. Kalra CS, Kumar V, Manna A (2019) The wear behavior of Al/(Al2O3+SiC+C) hybrid composites fabricated stir casting assisted squeeze. Part Sci Technol 37(3):303–313
22. Kumar J, Singh D, Kalsi NS (2019) Tribological, physical and microstructural characterization of silicon carbide reinforced aluminium matrix composites: a review. Mater Today: Proc 1(18):3218–3232
23. Lin CL, Lin JL, Ko TC (2002) Optimisation of the EDM process based on the orthogonal array with fuzzy logic and grey relational analysis method. Int J Adv Manuf Technol 19(4):271–277
24. Myalski J, Wieczorek J, Dolata-Grosz A (2006) Tribological properties of heterophase composites with an aluminium matrix. J Achievements Mater Manuf Eng 15(1–2):53–57
25. Radhakrishnan R, Nambi M, Ramasamy R (2011) Optimization of cutting parameters for turning Al-SiC(10p) MMC using ANOVA and grey relational analysis. Int J Precis Eng Manuf 12(4):651–656

26. Telang AK, Rehman A, Dixit G, Das S (2010) Alternate materials in automobile brake disc applications with emphasis on Al composites—a technical review. J Eng Res Stud 1(1):35–46
27. Tony Thomas A, Parameshwaran R, Muthukrishanan A, Arvind KM (2014) Development of feeding and stirring mechanism for stir casting of aluminium matrix composites. Procedia Mater Sci 5:1182–1191
28. Uhlmann E, Bergmann A, Gridin W (2015) Investigation on additive manufacturing of tungsten carbide-cobalt by selective laser melting. Procedia CIRP 1(35):8–15

Ultrasound Added Additive Manufacturing for Metals and Composites: Process and Control

Sachin Kumar and Brij Kishor

1 Introduction

The ultrasonic vibrations find their applications in various conventional manufacturing processes to cope with their multiple shortcomings [25]. For example, ultrasonic-assisted machining, forming, welding, friction stir welding are well-established and niche techniques [8, 24, 28, 32, 33, 39]. The ultrasonic vibrations denote the sound waves beyond human hearing range and correspond to the frequency range close to 20 kHz [21, 25]. Based on the frequency ranges, the categorization of sound waves and their corresponding applications has been shown in Fig. 1. The sound waves in the ultrasonic range can be used for various medical and manufacturing processes. Depending on the intrinsic elastic properties and densities, ultrasonic waves can travel with different velocities in different types of mediums [35]. The ultrasonic waves initiate mechanical vibrations into the medium and provoke molecular displacement at the micron level. In the form of the wave, ultrasonic vibrations can travel from one medium to another. However, their movement chiefly depends on ultrasonic vibration frequency, amplitude, and medium of wave propagation, etc. [35]. The ultrasound addition in additive manufacturing processes (AM) process [68] is quite new and has gained serious attention from various researchers across the globe.

The Ultrasonic Additive Manufacturing (UAM) is a solid-state manufacturing process, invented and patented by Dr. White [74], and commercially marketed by Fabrisonic LLC, USA. The UAM is based on the principle of boding the thin metal

S. Kumar (✉)
MOE Key Lab for Liquid-Solid Structure Evolution and Materials Processing, Institute of Materials Joining, Shandong University, Jinan 250061, People's Republic of China

B. Kishor
Department of Materials Science and Engineering, National Institute of Technology, Hamirpur (H.P.), India

S. Mavinkere Rangappa et al. (eds.), *Additive and Subtractive Manufacturing of Composites*, Springer Series in Advanced Manufacturing,
https://doi.org/10.1007/978-981-16-3184-9_3

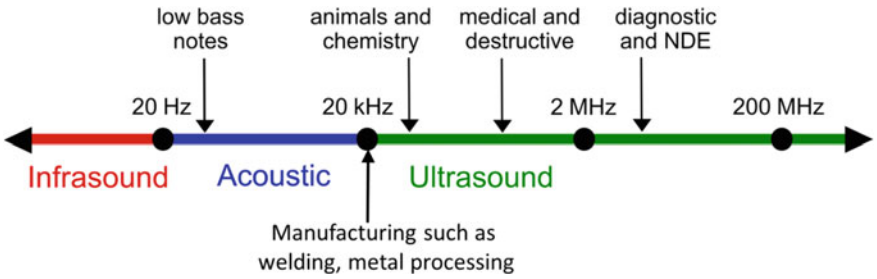

Fig. 1 Wave frequencies with their typical range and applications ('Ultrasound')

foils together sequentially using a similar concept as the ultrasonic metal welding process [14]. The bond formation is done layer by layer on Computer Numerical Control (CNC) machining to cut unwanted material and replicate the desired shape and size (Fig. 2). Therefore UAM can be referred to as the hybrid manufacturing process involving metal addition and subtraction. Typically a UAM process consists of a sequential arrangement of an ultrasonic generator, transducer, booster, and horn/sonotrode. The detailed description of these components has already been given elsewhere hence omitted in the present context [12, 25].

The UAM process involves the generation and transfer of ultrasonic energy from the output end of the transducer to a metallic work-piece via specially designed ultrasonic horn/sonotrode in the form of to and fro oscillations. The simultaneous interaction of normal compressive load with the ultrasonic oscillation permits localized heating of the material intended to work in the close vicinity of contact area, allowing the inter-laminar material flow in that region. It is important to note that the localized rise in material temperature in this process is considerably less to the melting point temperature of respective metal (approximately 50% of the melting temperature). Such a situation permits the metals to have solid-state interaction across their adjoining regions in order to form a bond [37, 69].

This additive buildup by ultrasound-assisted solid-state joining followed by simultaneous selective subtraction can consequent many key manufacturing features such as joining of mechanically and thermally dissimilar materials even of different thicknesses, retaining the original microstructure and grain orientation of parent metals even after joining, safe inclusion/embedding of functional components such as electronic switches or sensors in between the metal foils. The material bonding in the UAM process primarily depends on material processing and ultrasonic parameters such as horn oscillation, the compressive force exerted on the work-piece, and the travel speed of the horn. The selection of optimum values of all these parameters is vital as any deviation may severely degrade the bond quality [22]. In a similar context, Hopkins et al. [18] and Wolcott et al. [76] recognized the horn amplitude and travel speed as the most influential parameters to achieve high strength bonds.

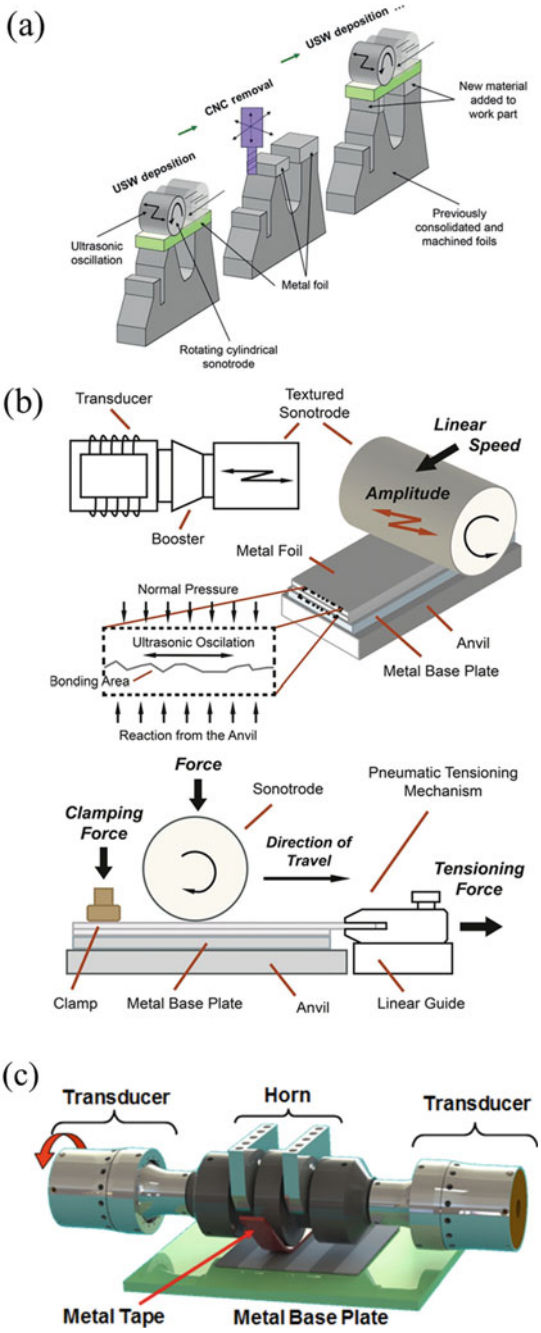

Fig. 2 **a–c** Schematic diagram of UAM process [3, 12, 61] ('Printing Metal 3D Objects Using Sounds')

2 Metallic Bonding of Dissimilar Materials

One of the most promising features of the UAM process is its capability to join dissimilar materials under solid-state conditions even if there is a nominal gap in their melting point temperature. This promising feature makes it stand out among various other additive and traditional manufacturing techniques. In UAM, the inherent mechanical and metallurgical properties of base metals remain intact due to the absence of their melting. Thus makes it applicable for high-strength aerospace aluminum alloys that are not susceptible to be thermally welded without any significant material property loss. The solid-state nature permits the reduction or elimination of brittle intermetallics (IMCs), whose massive formation has been reported in conventional processes. It is essential to mention that brittle IMCs phases attract lateral cracking and therefore severely degrade the structure's joint quality [48, 80]. Several metal combinations that have been processed with ultrasonic welding (USW) may not have been attempted in UAM and therefore can be the hotspot for future research. Figure 3 shows some known metal combinations that are available for USM and UAM processes.

Furthermore, by adding different materials of different thicknesses in a predefined manner, UAM can produce functionally graded laminates with great ease that can be quite cumbersome by other conventional manufacturing methods. The metallic foils can be placed alternatively in layers and welded into a layered structure to form multi-material laminates (Fig. 4). Via placing different materials in different thicknesses, the mechanical properties of the structure can be carefully controlled. For example, Solidica Inc. has used this technique to produce aluminum and titanium in varying ratios to develop armor applications' layered structure.

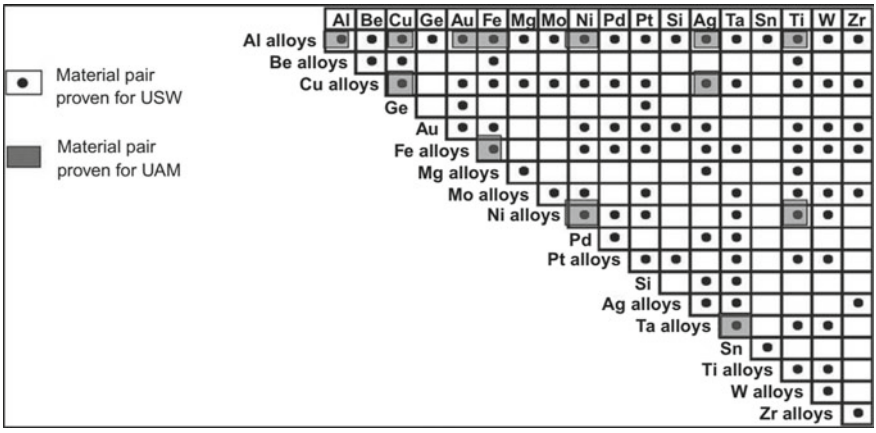

Fig. 3 Material combinations applicable for USM and UAM [12, 19], Image courtesy of the American Welding Society

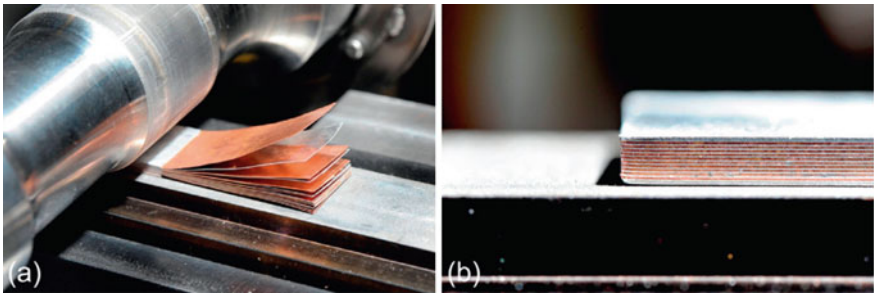

Fig. 4 **a**, **b** UAM dissimilar materials bonding for alternative layers of Al and Cu foils [12], Image courtesy of Loughborough Universities Additive Manufacturing Research Group

The UAM, being an advanced manufacturing technique, can support the manufacturing of complex and challenging to produce shapes with high precision and excellent surface finish. It can be due to the absence of the melting of the respective metals that minimizes the dimensional ambiguities that are usually observed in shrinkages, residual stresses, and distortion of metal parts [58]. The UAM is also effective in producing various manufacturing components of several materials, such as metal matrix composites, parts with embedded wirings, sensors etc., [50]. Frictional heat produced in this process can be regarded as the major source of material bonding. It can be approximately two times that of heat obtained from the plastic deformation of the material [70]. Besides, the ultrasonic addition can add the shear scrubbing that can break up the oxide layer formed on material surfaces. It permits the virgin material surface to interact and bond between the layers [5]. The foils experience intense acoustically induced softening due to ultrasonic vibrations, which affects the material lattice and imparts the plastic deformation [34, 79]. The welds characteristic and their formation mechanism during the ultrasonic-assisted process have been documented by Shimizu et al. [64] by analyzing their microstructural evolution. They observed that acoustic assistance could produce refined and equiaxed grains in the stirred zone (SZ) due to the intense grain refinement and recrystallization occurred by sequential heating and shear deformation. The grain refinement across the joint regions for the first and second layers of the aluminum alloy parts can be seen in Fig. 5 [64]. Dehoff and Babu [6], Mariani and Ghassemieh [45] have analyzed the microstructural evolution during ultrasonic assistance to analyze the possible bonding characteristics during the solidification and recrystallization stage.

To explain the importance and role of ultrasonic vibrations on the bonding mechanism during the UAM process, the microstructural analysis has been investigated by several researchers. For example, Pal and Stucker [52] proposed a finite element model to determine the microstructural evolution in case of the ultrasonic-assisted process by adopting dislocation-density-based crystal plasticity theory. Their work focused on the quasi-static formulation of large plastic deformation, material model based on non-local dislocation density, and process boundary conditions. They concluded that before and after processing, the grain size was reduced to 1.2 μm

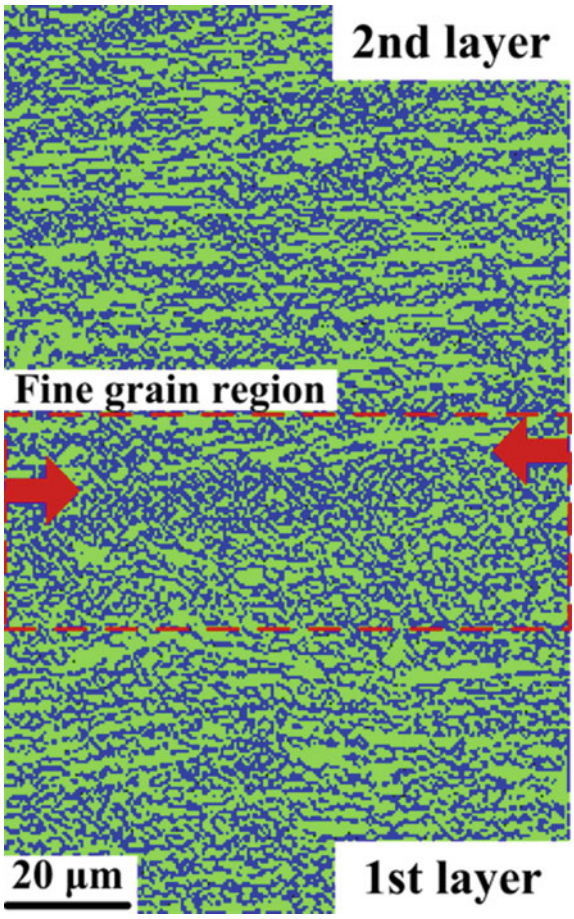

Fig. 5 Fine grains around the interface regions between the first and second layers in the aluminum alloy parts fabricated with ultrasonic addition [49, 64]

from the average value of 13 µm. The simulated results were compared with experimental data and found in good agreement. In the UAM process, the amplitude of ultrasonic vibrations plays an important role in the process parameters' effectiveness. They affect the material flow and plasticity at the region of contact [70]. It has been reported that the parts fabricated with high ultrasonic amplitude can yield better tensile properties that almost approach the value of bulk materials [11]. Apart from that, under the influence of large amplitudes, defects are suppressed greatly, and better bonding is experienced in the fabricated aluminum parts as shown in Fig. 6 [67]. It could be because the large amplitude might induce a significant portion of linear weld density with a more compact foil layer.

It is important to note that higher ultrasonic vibration amplitude induces severe plastic deformation with enhanced material plastic flow that suppresses the defects and improves the bonding [57]. The ultrasonic vibration induced consolidation is also beneficial to produce the metal matrix composites. Their bond strength can also

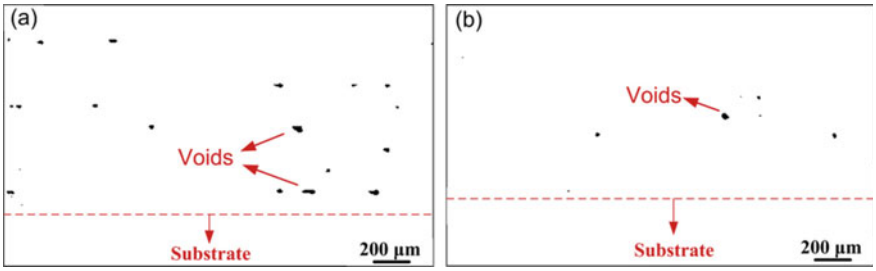

Fig. 6 Optical images of Al alloy parts produced by ultrasonic consolidation process **a** at lower ultrasonic amplitude and **b** at higher ultrasonic amplitude [49, 67]

be analyzed by interface failure which depicts that a higher value of composite length could minimize composite failure probability [16]. To have better knowhow of the interfacial strength, Hehr and Dapino [17] analyzed the interface quality via a single fiber pullout test. They concluded that the bonding was dependent on the fiber surface finish.

Apart from UAM, friction stir welding process (FSW) [2, 20, 55, 66, 77] added with ultrasonic vibration has been found utilizing their virtue to promote the material flow and enhance the bonding of metals across their joining regions [26, 72]. To analyze the virtues of ultrasonic vibrations in the material joining process, recently Kumar et al. [27] have designed and developed an ultrasonic vibration-assisted friction stir welding (UVaFSW) system (Fig. 7) similar to Park [54] and Kumar [24]. This

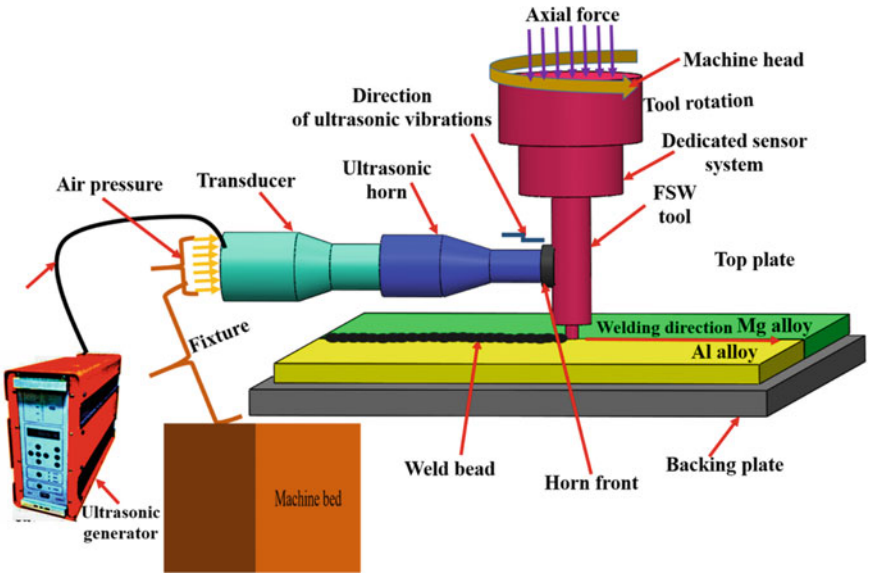

Fig. 7 Schematic of ultrasonic assisted friction stir welding system [29]

ultrasonic vibration is aimed to transfer the acoustic energy in the SZ via welding tool. The aforesaid UVaFSW system comprises a specially designed ultrasonic horn, front attachments, and a welding tool to safeguard the system and safely transfer the ultrasonic energy at the required region. Roller bearings are added to smoothen the process of ultrasonic vibrations from the stationary horn to the rotating FSW tool. In order to gather further details on UVaFSW system, readers can refer the author's previous work Kumar et al. [27, 28, 30], Kumar and Wu [33] have reported major benefits of ultrasonic energy on the joint quality. Additionally, the axial force, torque, and power requirements can also be significantly reduced, which can help to reduce the tool wear and enhance its life. An enhanced material plasticization of the SZ under intense acoustic softening can be reasoned for better joint quality. The ultrasonic addition also favors to reduce the flow stresses and improve the material flow under the vicinity of the ultrasonic vibration zone.

Park et al. [53] enforced the ultrasonic vibrations with the FSW process on the welding tool along the horizontal direction. They found a substantial drop in axial force and marginal rise in weld properties. In a similar ultrasonic addition, Kumar [24] claimed a notable reduction in axial downward force and significant improvement in weldment properties during FSW of Al alloys. However, the frequent failures of horn attachments are evident during experimentation, which restricts their results' reproducibility. Ruilin et al. [60] added a similar mode of ultrasonic energy and reported that the impact of acoustic addition on temperature fields in the FSW process is less effective at lower welding speeds. It can be attributable to additional heat addition due to ultrasonic vibrations. At lower rotation speeds, the peak temperature was identical for both the processes, while a reduction in maximum temperature is higher in the case of FSW than the UVaFSW for higher welding speeds. Ma et al. [44] reported that the weld properties were enhanced during ultrasonic addition in FSW when acoustic intensity was 50%. Amini and Amiri [1] also found a notable reduction in FSW axial force during ultrasonic addition, which could be due to improved weld penetration [1, 24]. Their analysis emphasized that an increase in welding speed in the FSW process could increase the axial force marginally, while the same could be reduced with an increase in rotation speed. The ultrasonic addition could cause better material stirring and enhanced plastic flow. The weld strength and elongation are also improved by ~10% during ultrasonic addition in the FSW process.

Liu et al. [40] designed and developed a novel ultrasonic vibration enhanced FSW (UVeFSW) system via simple linkages, where ultrasonic energy is imparted on the work-piece just ahead the welding tool by the sonotrode inclined at ~ 40°. They obtained better material flow and improved weld properties using such kind of UVeFSW system. Liu et al. [41] discovered that better joint quality in the UVeFSW process is due to intensive material plasticization and reduced HAZ. The weld microstructures analysis reported that the ultrasonic addition could improve the material mixing, deformation in the SZ, and enlarge the thermo-mechanically affected zone (TMAZ). The weld strength was increased marginally due to the improved material flow. Liu et al. [40] analyzed the material flow during the UVeFSW of Al alloy by utilizing a marker insert and sudden stop-action method. During the UVeFSW, they noticed intense material plasticization and improved material flow rate. It could

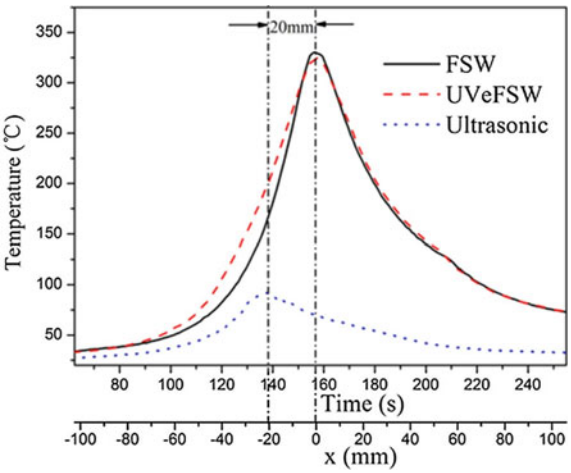

Fig. 8 Temperature variation for FSW and UVeFSW process [81]

be due to supplementary material plasticization under ultrasonic addition. Shi et al. [63] modeled the quasi-steady state of the UVeFSW process. Their model predicted that the better material flow could be due to the ultrasonically influenced stirring and flow stress reduction. The aforesaid ultrasonic-assisted model Shi et al. [63] also discovered that the UVeFSW had minor effects on the overall heat addition and temperature field during the welding. Zhong et al. [81] obtained a notable reduction in tool torque and axial load with ultrasonic addition in FSW process. They also compared the temperature field without ultrasonic addition (FSW) and UVeFSW as shown in Fig. 8. During the weld advancement, the temperature rise in the UVeFSW is reported higher compared to the FSW process. The maximum temperature difference is between the two processes is reported ~40 °C, which occurred 20 s before the peak value. This signifies that ultrasonic vibration heat up the welding material that causes it to experience higher temperature for a considerable time [81].

The weld macrographs at different process parameters for both FSW and UVeFSW processes are shown in Fig. 9. The boundary of pin affected zone of SZ in the case of UVeFSW is surprisingly enlarged than that of FSW. The interface between the SZ and TMAZ across the AS is also smoother for UVeFSW joints.

The FSW joints are found to have defects in the lower section of SZ because of inadequate heat input and poor material mixing. On the contrary, most of the UVeFSW joints are defect-free in SZ. It is attributable to better material mixing and improved material flow [26, 81]. Liu and Wu [42] discovered that the tunnel defects could be eliminated completely with ultrasonic induction in the FSW process. For the FSW and UVeFSW processes, Padhy et al. performed microstructure evolution across the SZ of Al alloy using the advanced microstructure techniques [51]. Their outcomes have shown that acoustic addition has significantly refined the grains and sub-grain formation at the SZ. Finally, ultrasonic addition in the FSW process has been proven robust, beneficial, and superior in context to the process efficacy and joint characteristics than that of the conventional FSW [26]. The acoustic assistance can

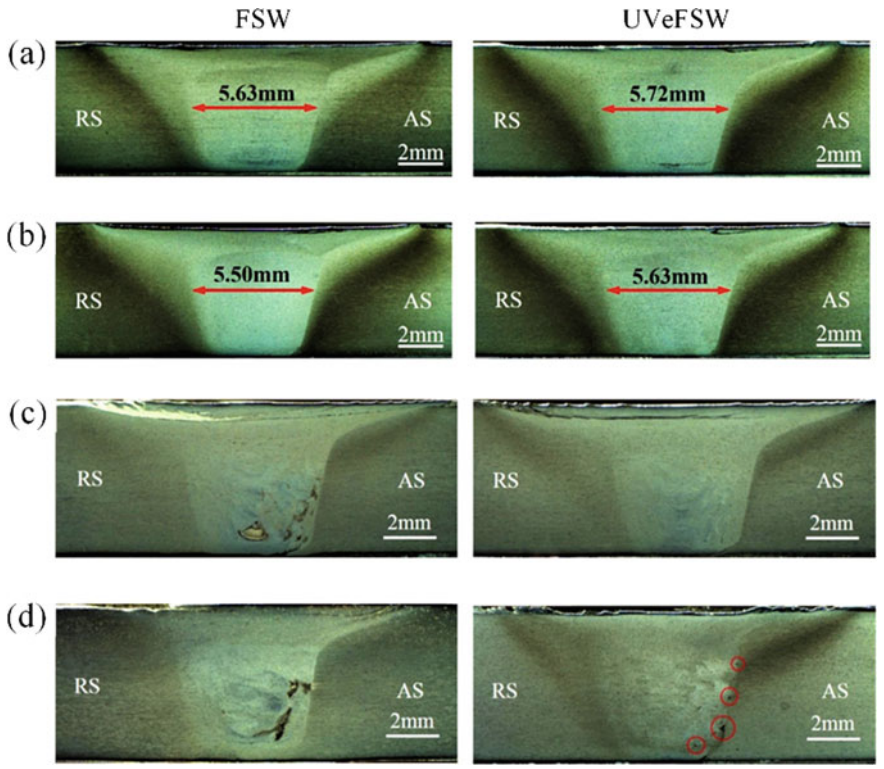

Fig. 9 The optical images of FSW and UVeFSW joints of AA2024-T3 alloy at **a** 200 rpm, 110 mm/min, plunge depth = 0.1 mm, and **b** 400 rpm, 330 mm/min [81]

significantly improve the weld properties and material flow, enlarge process window, suppressed the weld anomalies, and improve the weld quality and microstructure.

Tarasov et al. [71] developed another method to apply for acoustic assistance in front of the welding tool via the backing plate for FSW of Al alloy. They narrated that acoustic energy helped to suppress the recrystallized grain size in SZ at weldment. It is suggested ultrasonication may retard the GP ripening due to the dynamic stabilization of the solid solution. Additionally, the ultrasonic energy might have smoothed the strain-induced dissolution of earlier thought insoluble coarse Al–Cu–Fe–Mn particles. Lv et al. experimented on the FSW of dissimilar Al/Mg alloys by applying ultrasonic vibration system at an angle to the welding tool. They obtained a notable rise in the weld quality and claimed the IMCs phases disappearance across the interface [43]. Besides, they added that with the addition of acoustic assistance, IMCs (Al_3Mg_2 (layer 1) + $Al_{12}Mg_{17}$ (layer 2)) of overall thickness ~3.5 μm gradually became a monolayer (Al_3Mg_2) of overall thickness ~2.5 μm. Kumar et al. [29] performed the scanning electron microscopic (SEM) analysis of the SZ to determine the advantages of ultrasonic energy on the FSW process (Fig. 10). The SZ of both Al and Mg alloys resembles significantly refined and smaller grains as compared to

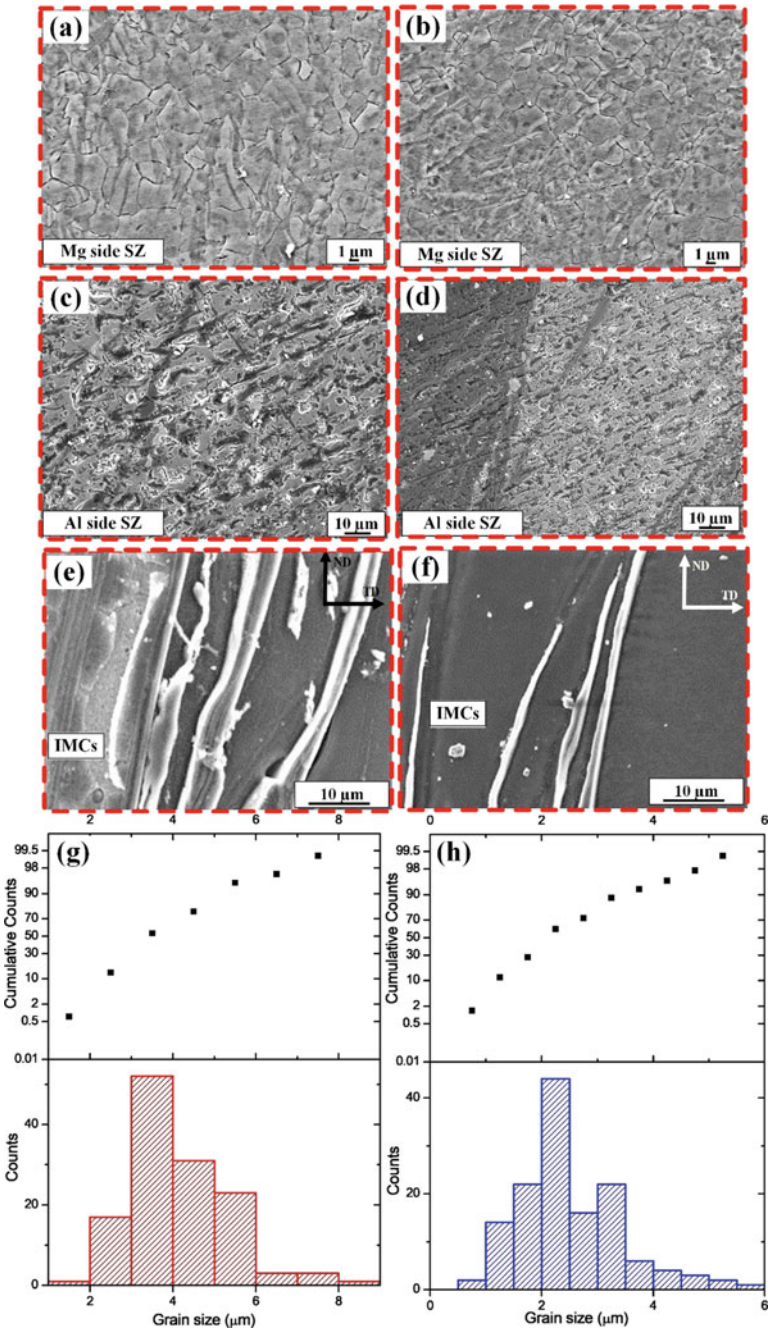

Fig. 10 High magnification images of FSW and UVaFSW joints across the SZ **a**, **b** Mg Side **c**, **d** Al side and **e**, **f** IMCs region **g**, **h** the grain size analysis for Mg side [29]

the base metals (Fig. 10). It is also observed that the grains are recrystallized and finer for the ultrasonic welds at Mg side compared to the conventional FSW joints. The grain analysis of the SZ of the Mg side shows average grain size of ~2.5 and 4.16 μm for ultrasonic and non-ultrasonic welds respectively (Fig. 10a, b, g, h). It implies that acoustic energy is helpful to refine and reduce the grain size. Similarly the grain analysis of SZ region also shows comparatively fine and equiaxed grains for the ultrasonic joints. This region also advocates the intense intermixing of various substrates in a complex manner because of Al alloys' intense material plasticization compared to the Mg alloy [36].

The formation of the dendrite structure in the Al alloys' weld zone in the case of the FSW process is quite common that may be due to constitutional liquation. The phenomenon of constitutional liquation for the FSW process has been reported previously in different studies [4, 7]. During the FSW of Al/ZrB_2 Dinaharan and Murugan [7] have quoted that the constitutional super cooling can originate the dendritic structure during the solidification process. Similarly, in case of dissimilar FSW of Al and Mg alloys, Firouzdor and Kou [9] have also reported dendrites formation of Al_3Mg_2 and $Al_{12}Mg_{17}$. The high magnification images of the IMCs region depicts heavy lumps of intermixed substrates in SZ-TMAZ (Fig. 10e) that may resemble the IMCs of Al and Mg. The origin of heavy lumps of IMCs can be ascribed to the intense intermixing of Al and Mg substrates followed by flow of Al lamellae across the advancing side (AS) and material stirring across shoulder and pin region. The formation of discrete particles is primarily controlled by the SZ region's heat input and formed because of the controlled by inter-diffusion or eutectic transformation [43]. The nature of IMCs formation largely depends on the concentration of Al and Mg substrates [30]. The region where Al concentration dominates attracts Al_3Mg_2 while that of Mg dominated region probably have $Al_{12}Mg_{17}$. The same can be ascribed from the binary phase diagram of Al and Mg alloys [10].

3 Object Embedment

Further application of ultrasonic addition has been experienced by digging out the possibility of embed fibers, electronic circuits, or structures in the metal matrix. Heavy material flow in presence at low temperature permits safe embedment without any harm to embedding material. The embedment process follows the binding of metal foil material with the base metal by the horn/sonotrode. The foil fibers or electronic circuit are added on this, and the second layer of foil is then placed on the top of the embed object followed by sonotrode contact to the sample to bond it with the previous layer. Under the influence of the acoustic plastic behavior of metal foil in contact with the horn pressure and oscillation, the foil is plastically deformed around the embed material. It makes contact with the previous foil layer, thus forming a solid-state bond (Fig. 11).

Following the unique feature of UAM, the embedment of various materials has endeavored in previous literature. Li et al. [38] have attempted the embedment of

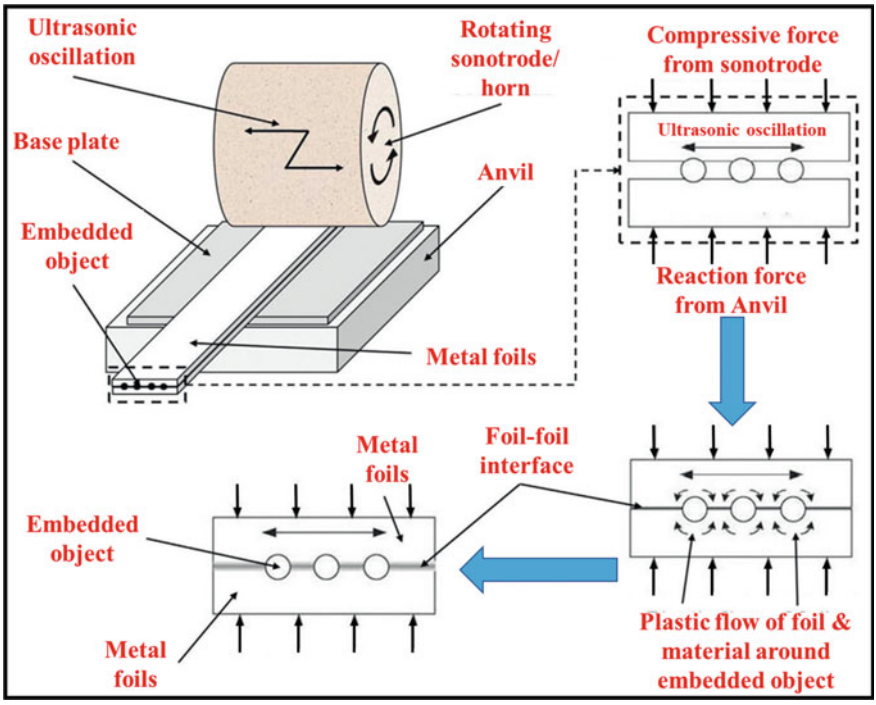

Fig. 11 **a**, **b** The schematic process of object embedment via UAM process [12, 13]

printed electronic pathways in between the Al foils interface. Similarly, Robinson et al. [59] and Siggard et al. [65] have successfully added the pre-packed electronic circuit system in the metal grooves created by the CNC machine. Kong and Soar [23] have carried out the embedment of polymer-based coated and uncoated optical fibers in the Al matrix. In a similar attempt, Monaghan et al. [46] and Mou et al. [47] have also successfully implemented metal-coated optical fibers and Bragg fibers in their research findings. The UAM technique has been advanced by embedding the shape memory alloy fibers in the Al matrix and investigated by Friel and Harris [13] and Hahnlen and Dapino [16]. Their findings have reported appreciable functionality of embedded components and excellent bond strength of adjoining layers. Hence UAM can be considered as one of the most appropriate techniques to develop the embedded structures.

At several places, the UAM is also referred to as a "bond-then-form" technique [15]. It is because, after UAM bonding, subsequent CNC machining is required to add up to cast the anticipated form to the bonded metallic foils. This process is completed in a number of steps followed by layer bonding, it's machining, layer bonding on previously formed part followed by further machining until the required 3D shape is not attained. Similarly, in the "form-then-bond" approach, the required 3D shape is cast in each joined layer (via suitable machining process such as laser

machining) before its binding to the earlier formed part. This method can allow to form the structures to have inner geometry and channels that are quite cumbersome to produce via the "bond-then form technique" [15]. This process has been proven beneficial in developing functional ceramic parts and microfluidic systems via the Computer Aided Manufacturing process ([3], Cawley et al.)

Bournias-Varotsis et al. [3] have analyzed the ultrasonic welding of aluminum foils followed by the geometric machining prior to the commencement of the bonding (Fig. 12). These pre-machined geometries can facilitate to keep the foil in layer by layer in a predefined sequence to host any electronic or fragile components in a required groove, gap, or pocket. For the UAM process, the deformation mechanics of the aluminum foils could be studies and a model was proposed that could facilitate estimation of the final location, shape and size, and tolerances of pre-machined features for a defined combination of process parameters. The proposed model was tested by hosting an electronic component before its encapsulation in a predesigned cavity. In the present example (Fig. 12), the embedment of an electronics item is made however the same can be applied for the fabrication of microfluidic or thermal management devices also. Here, the aluminum foil is machined before being bonded via the UAM process. The cavities and channels are formed layer by layer to form features to host the electronic circuitry. In the process, for the cross-sectioned sample,

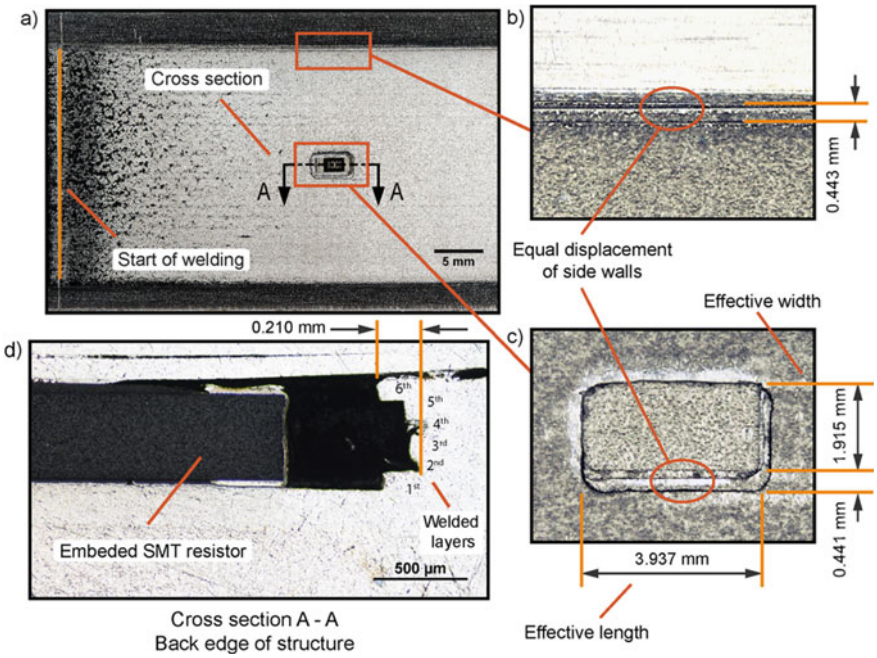

Fig. 12 Representation of multi-layer structure. **a** Top view before encapsulation. **b** Close up of the top edge of the bonded foils. **c** Fabricated structure. **d** Cross-section of the back edge of the structure after encapsulation [3]

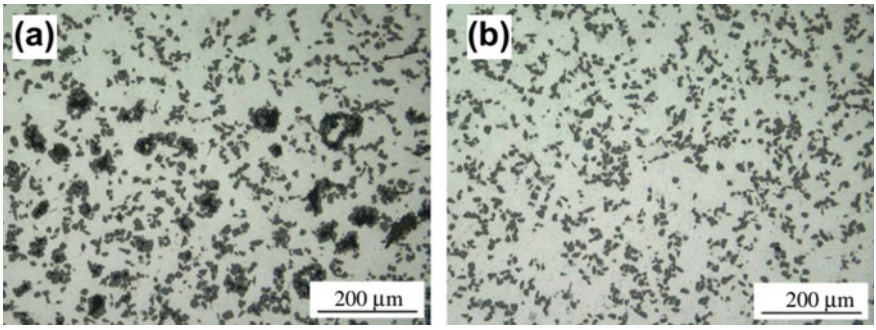

Fig. 13 The microstructure profile of reinforced filler metals **a** via stir casting and **b** via ultrasonic assistance [78]

any visible destruction in the resistor was seen. It is important to note that the effective measured width was found smaller than that of the predicted one in this case. It may be due to human error incurred while foil placement and its alignment before the welding process's commencement.

The UAM has been proven beneficial to fabricate a wide variety of industrially applicable composites. For example, the addition of silicon carbide particulate into the Al matrix may offer several benefits. Wielage et al. [75] performed ultrasonic-assisted soldering of Al_2O_{3p}/6061 metal matrix composites by adding SiC reinforced and Sn-based solders. They reported significantly homogenized reinforced joints of SiC with an appreciable improvement in joint strength than that of a non-reinforced joint. Yan et al. [78] attempted SiC reinforced and Zn-based filler to fabricate the SiC_p/A356 composites with the aid of ultrasonic vibrations. During the joining, the ultrasonic assistance has been proven beneficial to disperse the agglomerates and eliminated the possibility of SiC coagulation. A complete absence of voids and enhanced intermixing of particles in the metal matrix have been observed that may be due to the ultrasonic vibration effects.

The high-resolution microstructure images of SiCp/Zn–Al filler metals have been shown in Fig. 13. Adequate intermixing of stir cast filler with the SiC substrates is observed at subsequent intervals. However, noticeable particle segregation and voids gaps can be seen in the metal matrix (Fig. 13a). With ultrasonic assistance, the localized particle segregation has been considerably reduced while voids' intensity is trimmed, replicating the homogenized mixture of the metal matrix (Fig. 13b).

4 Conclusion and Future Perspective

From the aforesaid discussions, it has been observed that a significant amount of effort has been added to utilize the benefits of ultrasonic vibrations in the form of the ultrasound-assisted manufacturing process. The effect of ultrasonic assistance in

various manufacturing processes has been dealt with in detail and their processing mechanism is discussed to grasp the fundamental concepts. The ultrasound assistance can suppress the defect frequency and improves the material flow that in turn enhance the part quality. With the addition of ultrasound, the surface characteristics and dimensional accuracy can be enhanced than that of the conventional manufacturing processes (without ultrasound). The acoustic assistance can also reduce the frictional contacts between the machine parts, hence the forced required to do the required job can also be reduced. Among these astonishing properties, better arranged high compact density and good surface quality make the ultrasound-assisted as a unique technique in the manufacturing domain. In ultrasonic-assisted compaction, the vibration energy breaks the oxide layer, softens the localized region of contact and results in strong bonding in the case of 3D structures. In case of UAM, the ultrasonic addition can produce non-linear effects for example, acoustic streaming and cavitation. All this can alter the magnitude of heat and mass transfer and thereby the grain refinement and crystal growth. Apart from that, several other special effects such as enhanced stirring, better material mixing and crystal dispersion cum nucleation can be seen in case of melting materials. A better degree of material homogenization by liquid agitation, enhanced particles distribution, and suppressed frequency of porosity and cracks in presence of ultrasonic vibration can be seen from the results reported. As a result the manufactured parts have better quality and precise control in their dimensional accuracy. This short literature review can assist the readers to grasp the basic concepts and application domains of the ultrasonic energy in manufacturing context. It can also be helpful to advance better and effective systems to impart ultrasonic vibrations into the manufactured zone.

References

1. Amini S, Amiri M (2014) Study of ultrasonic vibrations effect on friction stir welding. Int J Adv Manuf 73(1–4):127–135
2. Bansal A, Singla AK, Dwivedi V, Goyal DK, Singla J, Gupta MK, Krolczyk GM (2020) Influence of cryogenic treatment on mechanical performance of friction stir Al–Zn–Cu alloy weldments. J Manuf Process 56:43–53
3. Bournias-Varotsis A, Friel RJ, Harris RA, Engstrøm DS (2018) Ultrasonic Additive manufacturing as a form-then-bond process for embedding electronic circuitry into a metal matrix. J Manuf Process 32:664–675
4. Chen YC, Nakata K (2008) Friction stir lap joining aluminum and magnesium alloys. Scripta Mater 58(6):433–436
5. Chua CK, Leong KF (2014). 3D printing and additive manufacturing: principles and applications (with companion media pack)—Fourth edition of rapid prototyping, 3d printing and additive manufacturing: principles and applications (with companion media pack)—Fourth edition of rapid prototyping
6. Dehoff R, Babu S (2010) Characterization of interfacial microstructures in 3003 aluminum alloy blocks fabricated by ultrasonic additive manufacturing. Acta Mater 58:4305–4315
7. Dinaharan I, Murugan N (2012) Effect of friction stir welding on microstructure, mechanical and wear properties of AA6061/ZrB_2 in situ cast composites. Mater Sci Eng A 543:257–266

8. Dixit US, Pandey PM, Verma GC (2019) Ultrasonic-assisted machining processes: a review. Int J Mechatron Manufact Syst 12(3–4):227–254
9. Firouzdor V, Kou S (2010) Formation of liquid and intermetallics in Al-to-Mg friction stir welding. Metall Mater Trans A 41(12):3238–3251
10. Firouzdor V, Kou S (2010) Al-to-Mg friction stir welding: effect of material position, travel speed, and rotation speed. Metall Mater Trans A 41(11):2914–2935
11. Foster DR, Dapino MJ, Babu SS (2013) Elastic constants of ultrasonic additive manufactured Al 3003–H18. Ultrasonics 53:211–218
12. Friel RJ (2015) Power ultrasonics for additive manufacturing and consolidating of materials. In: Power ultrasonics: applications of high-intensity ultrasound, pp 313–35
13. Friel RJ, Harris RA (2010) A nanometre-scale fibre-to-matrix interface characterization of an ultrasonically consolidated metal matrix composite. Proceed Inst Mech Eng Part L: J Mater: Des Appl 224(1):31–40
14. Friel RJ, Harris RA (2013) Ultrasonic additive manufacturing a hybrid production process for novel functional products. Procedia CIRP 6(1):35–40
15. Gibson I, Rosen DW, Stucker B (2010) Sheet lamination processes. In: Additive manufacturing technologies, pp 223–52
16. Hahnlen R, Dapino MJ (2014) NiTi–Al interface strength in ultrasonic additive manufacturing composites. Compos B Eng 59:101–108
17. Hehr A, Dapino MJ (2015) Interfacial shear strength estimates of NiTi-Al matrix composites fabricated via ultrasonic additive manufacturing. Compos B Eng 77:199–208
18. Hopkins CD, Wolcott PJ, Dapino MJ, Truog AG, Babu SS, Fernandez SA (2012) Optimizing ultrasonic additive manufactured Al 3003 properties with statistical modeling. J Eng Mater Technol Trans ASME 134:011004
19. Johnson K Ultrasonic consolidation—A viable method of smart structure manufacture. In: 4th International conference on rapid manufacturing
20. Kar A, Yadav D, Suwas S, Kailas SV (2020) Role of plastic deformation mechanisms during the microstructural evolution and intermetallics formation in dissimilar friction stir weld. Mater Character 164:110371
21. Kishor B, Chaudhari GP, Nath SK (2014) Cavitation erosion of thermomechanically processed 13/4 martensitic stainless steel. Wear 319:150–159
22. Kong C, Soar RC, Dickens PM (2004) Optimum process parameters for ultrasonic consolidation of 3003 aluminium. J Materi Process 146(2):181–187
23. Kong CY, Soar R (2005) Method for embedding optical fibers in an aluminum matrix by ultrasonic consolidation. Appl Opt 30:6325–6333
24. Kumar S (2016) Ultrasonic assisted friction stir processing of 6063 aluminum alloy. Archiv Civil Mech Eng 16(3):473–484
25. Kumar S, Wu CS, Padhy GK, Ding W (2017) Application of ultrasonic vibrations in welding and metal processing: a status review. J Manuf Process 26:295–322
26. Kumar S, Wu CS (2017b) Ultrasonic vibrations in friction stir welding: state of the art. In: 7th International conference on welding science and engineering (WSE 2017) in conjunction with 3rd international symposium on computer-aided welding engineering (CAWE 2017)
27. Kumar S, Ding W, Sun Z, Wu CS (2018) Analysis of the dynamic performance of a complex ultrasonic horn for application in friction stir welding. Int J Adv Manuf Technol 97(1–4):1269–1284
28. Kumar S, Wu CS, Zhen S, Ding W (2019) Effect of ultrasonic vibration on welding load, macrostructure, and mechanical properties of Al/Mg alloy joints fabricated by friction stir lap welding. Int J Adv Manuf Technol 100(5–8):1787–1799
29. Kumar S, Wu C, Gao S (2020) Process parametric dependency of axial downward force and macro- and microstructural morphologies in ultrasonically assisted friction stir welding of Al/Mg alloys. Metall ater Trans A 51:2863–2881
30. Kumar S, Wu C, Shi L (2020) Intermetallic diminution during friction stir welding of dissimilar Al/Mg alloys in lap configuration via ultrasonic assistance. Metall Mater Trans A 51:5725–5742

31. Kumar S, Wu CS (2017) Review: Mg and its alloy—Scope, future perspectives and recent advancements in welding and processing. J Harbin Inst Technol 24(06):1–37
32. Kumar S, Wu CS (2018) A novel technique to join Al and Mg alloys: ultrasonic vibration assisted linear friction stir welding. Materials Today: Proc 5(9):18142–18151
33. Kumar S, Wu CS (2020) Suppression of intermetallic reaction layer by ultrasonic assistance during friction stir welding of Al and Mg based alloys. J Alloys Compds 827:154343
34. Langenecker B (1966) Effects of ultrasound on deformation characteristics of metals. Trans Sonics Ultrasonics 13(1):1–8
35. Laugier P, Haïat G (2011) Introduction to the physics of ultrasound. In: bone quantitative ultrasound, pp 29–45
36. Lee K-J, Kwon E-P (2014) Microstructure of stir zone in dissimilar friction stir welds of AA6061-T6 and AZ31 alloy sheets. Trans Nonfer Metals Soc China 24(7):2374–2379
37. Levy A, Miriyev A, Sridharan N, Han T, Tuval E, Babu SS, Dapino MJ, Frage N (2018) Ultrasonic additive manufacturing of steel: method, post-processing treatments and properties J Mater Process Technol 256:183–189
38. Li J, Monaghan T, Masurtschak S, Bournias-Varotsis A, Friel RJ, Harris RA (2015) Exploring the mechanical strength of additively manufactured metal structures with embedded electrical materials. Mater Sci Eng, A 639:474–481
39. Li Y, Cheng Z, Chen X, Long Y, Li X, Li F, Li J, Twiefel J (2019) Constitutive modeling and deformation analysis for the ultrasonic-assisted incremental forming process. Int J Adv Manuf Technol 104:2287–2299
40. Liu XC, Wu C, Padhy GK (2015) Characterization of plastic deformation and material flow in ultrasonic vibration enhanced friction stir welding. Scripta Mater 102:95–98
41. Liu XC, Wu CS, Padhy GK (2015) Improved weld macrosection, microstructure and mechanical properties of 2024Al-T4 butt joints in ultrasonic vibration enhanced friction stir welding. Sci Technol Weld Joining 20(4):345–352
42. Liu XC, Wu CS (2016) Elimination of tunnel defect in ultrasonic vibration enhanced friction stir welding. Mater Des 90:350–358
43. Lv XQ, Wu C, Yang C, Padhy GK (2018) Weld microstructure and mechanical properties in ultrasonic enhanced friction stir welding of al alloy to Mg Alloy. J Mater Process Technol 254:145–157
44. Ma H, He DQ, Liu JS (2015) Ultrasonically assisted friction stir welding of aluminium alloy 6061. Sci Technol Welding Joining 20(3):216–221
45. Mariani E, Ghassemieh E (2010) Microstructure evolution of 6061 O Al alloy during ultrasonic consolidation: an insight from electron backscatter diffraction. Acta Mater 58(7):2492–2503
46. Monaghan T, Capel AJ, Christie SD, Harris RA, Friel RJ (2015) Solid-state additive manufacturing for metallized optical fiber integration. Compos A Appl Sci Manuf 76:181–193
47. Mou C, Saffari P, Li D, Zhou K, Zhang L, Soar R, Bennion I (2009) Smart structure sensors based on embedded fibre bragg grating arrays in aluminium alloy matrix by ultrasonic consolidation. Meas Sci Technol 20:34013
48. Moustafa AR, Durga A, Lindwall G, Cordero ZC (2020). Scheil ternary projection (STeP) diagrams for designing additively manufactured functionally graded metals. Additive Manuf 32:101008
49. Ning F, Cong W (2020) Ultrasonic vibration-assisted (UV-A) manufacturing processes: state of the art and future perspectives. J Manuf Process 51:174–190
50. Obielodan J, Stucker B (2014) A fabrication methodology for dual-material engineering structures using ultrasonic additive manufacturing. Int J Adv Manuf Technol 70:277–284
51. Padhy GK, Wu CS, Gao S, Shi L (2016) Local microstructure evolution in Al 6061–T6 friction stir weld nugget enhanced by ultrasonic vibration. Mater Des 92:710–723
52. Pal D, Stucker B (2013) A study of subgrain formation in Al 3003 H-18 foils undergoing ultrasonic additive manufacturing using a dislocation density based crystal plasticity finite element framework. J Appl Phys 113:203517
53. Park K, Kim GY, Ni J (2007) Design and analysis of ultrasonic assisted friction stir welding. In: ASME international mechanical engineering congress and exposition, vol 3

54. Park K (2009) Development and analysis of ultrasonic assisted friction stir welding process. 125
55. Patel V, Li W, Xu Y (2018) Stationary shoulder tool in friction stir processing: a novel low heat input tooling system for magnesium alloy. In: Materials and manufacturing processes, pp 1–6
56. Printing metal 3D objects using sounds. (n.d.). . Retrieved 10 Mar 2021 from https://www.metalworkingworldmagazine.com/printing-metal-3d-objects-using-sounds/
57. Ram G, Yang Y, Stucker BE (2006) Effect of process parameters on bond formation during ultrasonic consolidation of aluminum alloy 3003. J Manuf Syst
58. Ram GDJ, Robinson C, Yang Y, Stucker BE (2007) Use of ultrasonic consolidation for fabrication of multi-material structures. Rapid Prototyping J 13(4):226–235
59. Robinson CJ, Stucker B, Lopes AJ, Wicker R, Palmer JA (2006) Integration of Direct-Write (DW) and Ultrasonic Consolidation (UC) technologies to create advanced structures with embedded electrical circuitry. In: 17th Solid freeform fabrication symposium, SFF 2006
60. Ruilin L, Diqiu H, Luocheng L, Shaoyong Y, Kunyu Y (2014) A study of the temperature field during ultrasonic-assisted friction-stir welding. Int J Adv Manuf Technol 73(1–4):321–327
61. Schomer JJ (2017). Embedding fiber bragg grating sensors through ultrasonic additive manufacturing
62. Schwope LA, Friel RJ, Johnson KE, Harris RA (2009) Field repair and replacement part fabrication of military components using ultrasonic consolidation cold metal deposition. In: RTO-MP-AVT-163-additive technology for repair of military hardware
63. Shi L, Wu CS, Liu XC (2015) Modelling the Effects of Ultrasonic Vibrations in Friction Stir Welding. J Mater Process Technol 222:91–102
64. Shimizu S, Fujii HT, Sato YS, Kokawa H, Sriraman MR, Babu SS (2014) Mechanism of weld formation during very-high-power ultrasonic additive manufacturing of Al Alloy 6061. Acta Mater 74:234–243
65. Siggard EJ, Madhusoodanan AS, Stucker B, Eames B (2006) Structurally embedded electrical systems using ultrasonic consolidation (UC). In: 17th solid freeform fabrication symposium, SFF 2006
66. Singh S, Prakash C, Gupta MK (2020) On friction-stir welding of 3D printed thermoplastics. In: Materials forming, machining and post processing. Springer, pp 75–91
67. Sojiphan K, Sriraman MR, Babu SS (2010) Stability of microstructure in Al3003 builds made by very high power ultrasonic additive manufacturing. In: 21st Annual international solid freeform fabrication symposium—An additive manufacturing conference, SFF 2010
68. Song X, Feih S, Zhai W, Sun CN, Li F, Maiti R, Wei J, Yang Y, Oancea V, Brandt LR, Korsunsky AM (2020). Advances in additive manufacturing process simulation: residual stresses and distortion predictions in complex metallic components. Mater Des 193:108779
69. Sridharan N, Norfolk M, Babu SS (2016) Characterization of steel-Ta dissimilar metal builds made using very high power ultrasonic additive manufacturing (VHP-UAM). Metall Mater Trans A 47(5):2517–2528
70. Sriraman M, Gonser M, Fujii HT, Babu SS, Bloss M (2011) Thermal transients during processing of materials by very high power ultrasonic additive manufacturing. J Mater Process Technol 211:1650–1657
71. Tarasov SY, Rubtsov VE, Fortuna SV, Eliseev AA, Chumaevsky AV, Kalashnikova TA, Kolubaev EA (2017) Ultrasonic-assisted aging in friction stir welding on Al–Cu–Li–Mg aluminum alloy. Welding World 61(4):679–690
72. Thomä M, Gester A, Wagner G, Straß B, Wolter B, Benfer S, Gowda DK, Fürbeth W (2019) Application of the hybrid process ultrasound enhanced friction stir welding on dissimilar aluminum/dual-phase steel and aluminum/magnesium joints. Materialwiss Werkstofftech 50(8):893–912
73. Ultrasound. (n.d.) Retrieved from https://en.wikipedia.org/wiki/Ultrasound
74. White D (2000) Ultrasonic object consolidation. US Patent 6,519,500
75. Wielage B, Hoyer I, Weis S (2007) Soldering aluminum matrix composites. Welding J (Miami, Fla) 86:67–70

76. Wolcott PJ, Hehr A, Dapino MJ (2014) Optimized welding parameters for Al 6061 ultrasonic additive manufactured structures. J Mater Res 29(17):2055–2065
77. Yadav VK, Gaur V, Singh IV (2020) Effect of post-weld heat treatment on mechanical properties and fatigue crack growth rate in welded AA-2024. Mater Sci Eng A 779:139116.
78. Yan J, Xu Z, Shi L, Ma X, Yang S (2011) Ultrasonic assisted fabrication of particle reinforced bonds joining aluminum metal matrix composites. Mater Des 32(1):343–347
79. Yang Y, Ram GJ, Stucker BE (2009) Bond formation and fiber embedment during ultrasonic consolidation. J Mater Process Technol 209(10):4915–4924
80. Zhao Y, Huang L, Zhao Z, Yan K (2016) Effect of travel speed on the microstructure of Al-to-Mg FSW joints. Mater Sci Technol 32(10):1025–1034
81. Zhong YB, Wu CS, Padhy GK (2017) Effect of ultrasonic vibration on welding load, temperature and material flow in friction stir welding. J Mater Process Technol 239:279–283

Processing and Manufacturing Ti6Al4V-Based Structures and Composites Using SLM and EBM: A Review

Sharanjit Singh, Vishal S. Sharma, Anish Sachdeva, Vishal Sharma, Daljit Kaur, Bhargav Reddy Isanaka, and Vinod Kushvaha

1 AM Fabrication Methods

A variety of additive manufacturing (AM) methods are available, most of these are the trademarks of different manufacturers. These methods are broadly categorized as: based on the heat source and feed stock or methods of application of raw material to the build chamber [19]. The raw material used in these AM processes are classified in three forms i.e. powder type, liquid type and solid form type. In all AM processes, an efficient energy source is used for processing of parts in layers according to the CAD geometry. The different process parameters, which are involved in the fabrication of AM parts [10, 58] are broadly classified in four categories as shown in Fig. 1. The parts produced by these processes are desired to have excellent performance, with adequate mechanical properties along with better microstructure and surface finish as well. These requirements can only be achieved by using a better set of optimized processing parameters while processing of parts [54]. The latest progress in the

S. Singh (✉) · V. Sharma
Department of Mechanical Engineering, DAV University, Jalandahar, India
e-mail: sharanjit10027@davuniversity.org; malhi.sharanjit@gmail.com

V. S. Sharma
School of Mechanical, Industrial and Aeronautical Engineering, University of the Witwatersrand, Johannesburg, South Africa

A. Sachdeva
Department of Industrial and Production Engineering, Dr B R Ambedkar National Institute of Technology, Jalandhar, Punjab 144011, India

D. Kaur
Department of Physics, DAV University, Jalandahar, India

B. R. Isanaka · V. Kushvaha
Department of Civil Engineering, Indian Institute of Technology, Jammu 181221, India

S. Mavinkere Rangappa et al. (eds.), *Additive and Subtractive Manufacturing of Composites*, Springer Series in Advanced Manufacturing,
https://doi.org/10.1007/978-981-16-3184-9_4

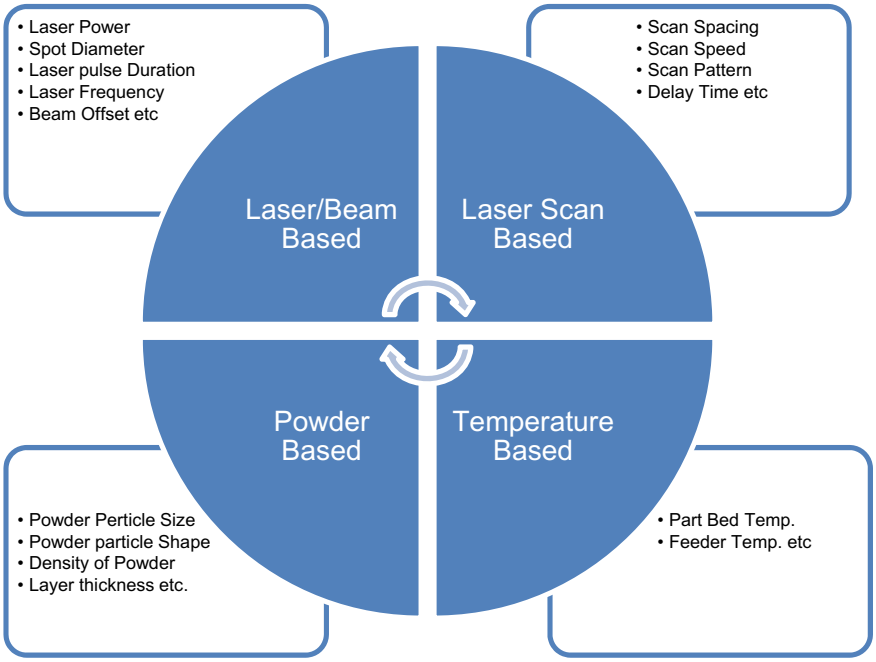

Fig. 1 Classification of different process parameters involved in AM

direction of using AM techniques to fabricate model/solid **parts**, the material and different mechanical properties have progressively **become** more significant [32].

In metallic components, particularly Ti6Al4V based parts are mostly fabricated by using selective laser melting (SLM) and electron beam machining (EBM). The SLM also **known** as laser beam melting, direct metal laser sintering, laser metal fusion and laser CUSING [30]. In spite of different names, all these processes have similar **approaches**: First a CAD drawing is generated, with the use of different CAD software's. **Or with the use of** reverse engineering and **can be with** the data collected from MRI **scans**. The available design file is transformed into **a**.stl file and then further sliced into thin layers in **the** machine setup computer. Physical model is generated in successive layers according to the CAD drawing by melting the raw material in **a part built chamber in an i**nert atmosphere.

The processing of Ti6Al4V a Titanium based alloy using AM techniques for medical implants is only because of the parts having good properties, higher mechanical strength and advanced corrosion resistance [68]. Porous structures having good stiffness and less weight helps to match the properties of implant with the host bone. SLM is **the** only process among **other** AM processes, which is widely used for processing AM parts by fusing metallic powder. In SLM high intensity yttrium fiber laser is used for processing metallic powders having particle size below 40 μm. The powder is spread in layers having layer thickness ranges from 20 μm to 1 mm on **a** machine table in **a** closed temperature controlled (just below the melting temp. of

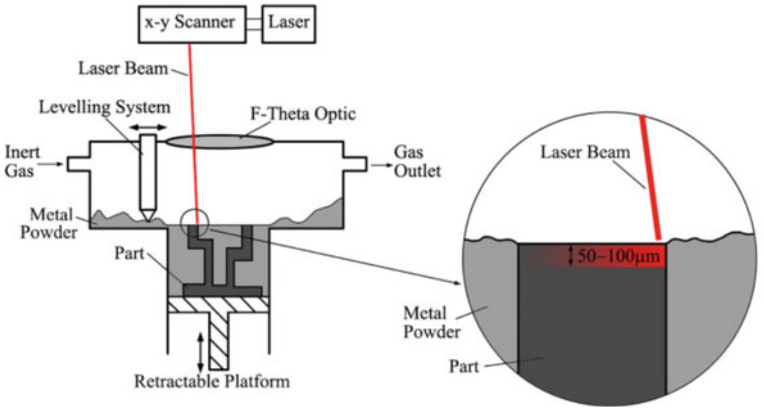

Fig. 2 Schematic diagram of SLM Wang et al. [64, 65]

powder) chamber in presence of inert gas atmosphere (Fig. 2). Laser light scans the powder bed according to CAD drawing and melts the powder particles. During the laser **exposure** it melts the fresh exposed powder layer and also **fuses** it together with the previously sintered layer. After deposition of each layer the build moves downwards and fresh layer is recoated. This procedure repeated again and again until the completion of part. The complete part is taken out from the cake and unfused powder **is** reused for the fabrication of other parts.

The second process i.e. EBM **is** also used for fabrication of metallic powders. The parts fabricated using EBM are of higher density, reduced residual stresses in comparison with SLM [11]. EBM is similar to SLM, first powder is supplied and distributed across the build chamber by a powder deposition mechanism (Fig. 3). Then a defocused beam is used for preheating the powder bed by scanning the bed surface several times. Preheating of powder helps to lessen the thermal stresses in parts by controlling the thermal gradient between different layers of complete part. After this preheating of powder the electron beam scans the top layer and melts the powder particles according to CAD design. Then the build chamber lowers by one layer thickness and new **a** layer is supplied. This cycle repeated again and again until the completion of part.

While scrutiny of literature pertains that EBM and SLM both are widely used by various researchers for fabrication of Ti6Al4V based parts. Both these processes have **advantages** and **disadvantages** over each other as shown below in tabulated form (Table 1). There are some studies in which methods like SLM and EBM are used for the production of Ti6Al4V-based structures.

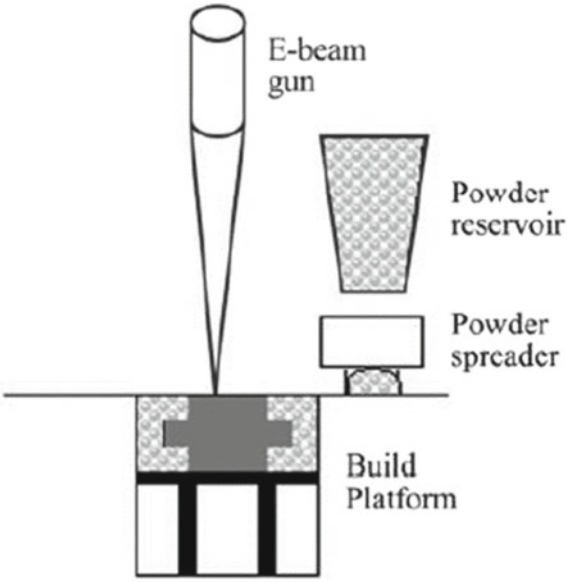

Fig. 3 Schematic of an EBM apparatus [11]

2 Effective Parameters

AM involves a set of parameters that are involved in manufacturing of different parts. These parameters have different **names** and comparative range **depending** on particular process, material used and machine manufacturer. Table 2 contains the major parameters and their tentative range of work used for particular processes [72]. While processing of metallic parts with these technologies, the degree of contamination is higher. So the interlayer bonding and compacting of these metallic powders are higher. But in case of SLM, due to non-uniform thermal gradient, presence of balling effect and because of oxidation occurred between molecules, results in low strength, poor density, weak intermolecular bonding and rough surface finish **among the** produced parts. Therefore AM processes **are** influenced by different processing parameters (Figs. 4 and 5). Table 3 [1] contains a set of processing parameters and characteristics of powder material that influence the processing and quality of products.

Different technologies **use** different power sources for melting and processing of raw materials. While talking about laser power and type of laser, in SLM laser light **transfers** energy to the powder bed via photons. The energy transfer depends upon the capacity of absorption/reflection of powder material. So higher power is used to overcome this effect, but it leads towards spatter generation. Further this can be controlled by pulse shaping and by the control of laser profile. Electrical charge and energy is transferred by electrons in **the** EBM process. If the repulsive forces are higher than particle binding forces the powder particles are ejected from **the**

Table 1 Advantage and disadvantage of SLM and EBM

	Advantage and application	Disadvantage
SLM	• Wide number of materials (metals, polymers and ceramics) can be processed • Feature resolution of produced parts are higher • Surface finish of parts are excellent • The application of parts in: radiation shielding, mass balance in aircrafts and kinetic energy projectiles [80] • Microstructures particularly: tungsten as a multi-pinhole collimator [13] • Dental implants and body prostheses due to their biocompatibility • Localized heating and fast cooling • Lowers the risk of interstitial elements, such as hydrogen, carbon and oxygen etc.	• Energy absorptivity is limited • Scan speed in limited • Cost of parts is higher • Build time is higher • Parts have more residual stress
EBM	• Parts are produced in vaccum, so there is no chance of interstitial elements, such as hydrogen, carbon and oxygen etc. • Scan speed is higher • Cost of parts is lower • Lesser build time • Parts having higher density and lesser porosity • Implant fabrication with customized features for faster rehabilitation [48] • Parts having less residual stresses • Porous titanium alloys manufactured with EBM contained mechanical properties (e.g., stiffness, roughness) that are equivalent to conventional wrought Ti-alloy	• Only metals (conductivity) are processed • Surface finish is poor • Features resolution is moderate

processing area. The ratio of electrical resistivity of powder to bulk density has been taken into account to lower down the powder ejection in EBM.

Scan strategies **are** the traveling path or sequence adopted by processing source during fabrication of parts. Residual stresses of SLM processed parts can be reduced by using island scanning strategies. The scan speed, power and bed temperature must be optimized for a particular scan **strategy** and also influence the porosity and grain morphology [14].

Scan speed is the velocity of **the** beam as it moves to sinter the powder bed. Scan spacing is the gap among two parallel scan lines. As the scan spacing and scan speed increases, poor binding of powder particles and poor densification occurs [9]. With the reverse of this trend the over sintering and re-melting of powder particles occurs as the energy density and penetration is higher. In this situation higher densification occurs due to the instability of the liquid melt pool which occurs as the surface free energy is minimized. The temperature of **the** melt pool also increases which reduces

Table 2 Setup based parameters for SLM and EBM

S. No.	Parameter	Range	
		SLM	EBM
1	Model	SLM 280HL	Arcam A2
2	Build volume	280 mm * 280 mm * 350 mm	250 mm * 250 mm * 400 mm
3	Laser beam size (μm)	70–120	200–1000
4	Build atmosphere	Inert gas (He, N2, Ar)	Low pressure of He
5	Scan speed (mm/s)	Up to 15,000	Up to 8000
6	Feed type (μm)	5–50	25–149
7	Layer thickness (μm)	20–75	20–100
8	Build temp	Mostly naturally heated	640–700 °C
9	Build density (%)	99.7–100	9.4–100
10	Substrate	Without substrate, same material as substrate	Stainless steel

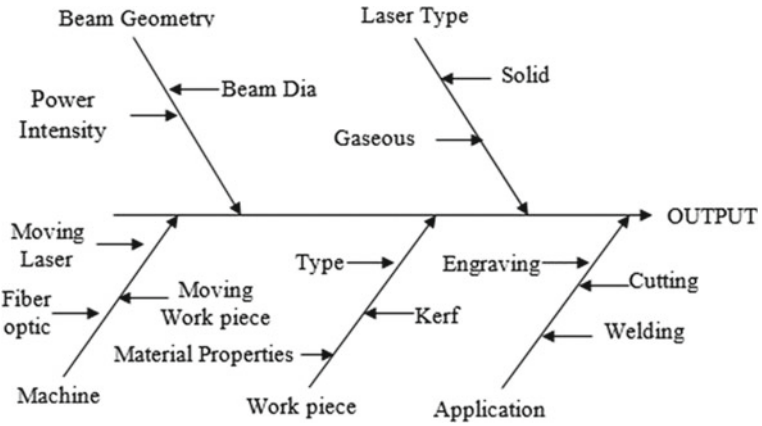

Fig. 4 Cause and effect diagram of SLM

surface tensions as well as melt viscosity. This increase in temperature results in complete melting of powder particles and results in entirely dense parts. Furthermore, the wetting characteristics of powder particles and energy required for rearranging solid particles in the molten form enhances as the liquidity of melt pool enhances, provided the energy density also enhances appropriately.

Depth of penetration depends on energy density (scan spacing, scan speed, laser power and temperature), density of powder, compaction, conductivity, specific heat of powder and powder particle size. A precise amount of energy is provided to powder in a fresh layer for sintering and to adhere with the previous sintered layer. The higher penetration results the unwanted growth in Z direction normally called 'Bonus-Z'

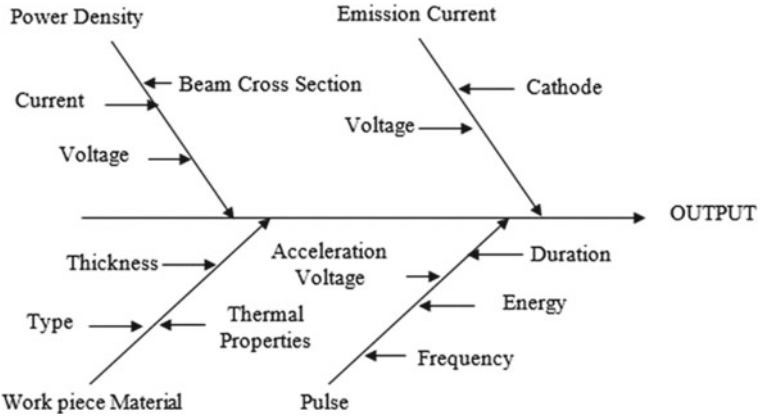

Fig. 5 Cause and effect diagram of EBM

Table 3 Set of different parameters having influence on AM fabricated parts

S. No.	Parameters	Materials properties
1	Scan rate	Surface tension
2	Laser power	Viscosity
3	Scan spacing	Melting temperature
4	Layer thickness	Component ratio
5	Scan length	Emissivity
6	Bed temp	Absorptivity/reflectivity
7	Laser type	Thermal conductivity
8	Machine setup	Chemical composition
9	Scan radius	Specific heat
10	Atmospheric control	Particle size and distribution
11	Gas flow	Particle shape

In AM the atmosphere of **the** build chamber in which the parts are processed, **affects process ability**, flow of heat and properties of parts [56]. In various processing setups according to requirement, the parts are processed in vaccum or with the use of inert gas. When the metal powders are exposed to **the** atmosphere at higher temperature they get oxidized. So it is required to process these metallic powders in **an** inert atmosphere or in **vacuum**. In SLM an inert atmosphere of argon/nitrogen is applied in **the** build chamber. Porosity of parts and heat concentration can be **affected** by flow rate of gases. In EBM the parts are processed in **vacuum**, because electron **beams are** used to melt the powder particles. To avoid charging of build volume a small quantity of helium is inserted in **the** build chamber. Processing in a near-vacuum atmosphere leads towards improved melting, vaporization and exceptional heat transfer consequences.

In both SLM and EBM a build substrate is required to provide the thermal and mechanical support to work parts and **overhanging**. While building **overhanging using** loose powder, the heat is **dissipated** through substrate which is desirable. Heating of **substrates** really **affects** various properties of parts. After fabrication of parts the substrate is removed using wire EDM or abrasive saws. Especially if stainless steel substrate is used for Ti-Al-4V deposition in EBM, it can be easily separated with the application of small force because of poor adherence.

The composition, properties and quality of powder such as shape, size, surface morphology, composition, apparent density and flow ability **affect** the quality of the final product. The powder **particles** with spherical shapes have higher flow ability and apparent density. Interstitial spaces are filled by fine particles between larger particles at the cost of flow ability. In SLM (10–45) μm and in EBM (45–106) μm particle size is nominal. The smaller the size of **the** particle the finer will be the surface finish. In SLM normally a fine distribution of powder is used to enhance surface finish by enabling shorter layer thickness. In **the** EBM process the layer thickness is higher and correspondingly larger size distribution can be accommodated. Further the chemical composition of powder also **affects** the processing of parts and it must be within alloy-specific specifications.

3 Microstructure Characteristics

Both SLM and EBM processes have capabilities to control shapes, grain size, phase composition and phase percentage by setting up process parameters to enhance the appropriate properties in the produced parts. The alteration in the different process parameters (laser power, bed temperature, scan space, scan speed and layer thickness etc.) will affect the nature of microstructure produced [74]. This change in parameters differentiates in energy density and time of interaction, which results **in** different temperature gradient, cooling rate and solidification rate. When the temperature of **the** melt pool is higher it requires more time to cool down and get **solidified**. Meanwhile the temperature of **the** previous sinter layer/substrate **becomes** higher, this reduces cooling rate and temperature gradient at interface [4]. This condition may **result** in the coarse type microstructure. In other **cases** when the temperature of **the** melt pool **is** comparatively lower and temperature gradient at interface is sufficiently high to generate rapid cooling rate. In this situation a finer microstructure may be obtained. The smaller contact area of the melted pool due to lower energy density results in low heat conduction within the **previously** sintered layer and slower cooling rate. The microstructure and cooling rate are affected in case of layered manufactured parts because the previous layers are preheated or partially melted.

In case of Ti alloys both α and β phases are to be made while processing with SLM and EBM. The α phase produced is a ductile phase as compared to β phase, but β phase is stronger. The other biphasic α–β matrix having the properties in between α phase and β phase. The Ti6Al4V parts generated with EBM mainly **have** α phase with **a** small amount of retained β phase. When the Ti6Al4V parts are generated by

using SLM the processing conditions are different and martensitic microstructure is obtained [2]. Similarly the mechanical properties of Ti6Al4V parts also differs while processing with these two different processes i.e. SLM and EBM.

4 Mechanical Properties

The mechanical properties of AM parts **affect** their performance and application. In case of cellular solids: cell topology, relative density, mechanical properties and strut shape (solid distribution in the struts) of the bulk material are four factors that have influence for mechanical properties [78]. The number of researchers worked to test the mechanical properties, especially tensile test to investigate ultimate tensile stress, yield stress and elongation as summarized in Table 4. The mechanical properties may be **affected** by the porosity, but the effect of porosity can be eliminated or minimized by post processing.

4.1 Fatigue Behavior

The fatigue properties of Ti6Al4V parts manufactured with the use of different AM techniques have been investigated under high cycle loading conditions. A comparison between AM manufactured Ti6Al4V parts with the conventionally manufactured Ti6Al4V parts have been shown in Fig. 6. It is observed that fatigue resistance of as build Ti6Al4V is similar to cast and wrought material without HIP treatment. Fatigue testing is a surface critical phenomenon, so rough surface finish of AM manufactured Ti6Al4V parts shows lower fatigue life when compared with fatigue life of machined samples. Rough surface finish of EBM fabricated Ti6Al4V parts shows lower fatigue life when compared with SLM made parts. At end it is concluded that the SLM and EBM fabricated parts cannot be used for fatigue critical application without improving the surface finish.

4.2 Compressive Properties

Compressive properties of Ti6Al4V parts **decrease** with the increase in the mean aspect ratio of the cells (Fig. 7). The cellular parts having spherical pore (supporting effect of the bigger struts) have higher strength as compared to the parts having needle-like pores. The bigger struts provide a supportive network in structure which performs as a retardant in thin walls' buckling deformation. The needle-like-pored cellular structures **show** lower compressive strength in the density range investigations because of thin and long struts that go to plastic buckling with compressive

Table 4 Summary of literature on SLM and EBM for mechanical properties

	Power used/setup	Powder properties	Substrate	Mech properties	Key point/literature outcome
[76]		Strut size-120 μm, porosity-88%, pore size-500 μm	Solid titanium alloy		**Focus**: To study the crystal structure of TiO_2 nanotube for heat treatment effects and nano topographical features of the surface **Findings**: The anodizing of porous Ti alloy structure generates a hierarchical surface containing nano and micro features **Scope**: Findings for the bioactivity of porous Ti structures
[3]	100 W		Titanium base plate	Compressive elastic modulus-11.9 GPa 0.2% offset strength-119 MPa Max. strength-144 MPa	**Focus**: On porous microarchitecture Findings: Compensation strategy improves the discrepancies of lattice structure **Scope**: Compensation scheme for reduction in morphology mismatch

(continued)

Table 4 (continued)

	Power used/setup	Powder properties	Substrate	Mech properties	Key point/literature outcome
[79]	130 W	Fine spherical Powder average particle size 65 μm	Pure Titanium plate	Yield strength-467–862 MPa Youngs modulus—16–85 GPa	**Focus**: Effect of scan spacing on pore characteristics and mechanical properties of porous implants **Findings**: Scan Spacing have max. influence in porous structures increase in scan spacing lowers compression strength 250–450 μm is appropriate range of interconnected pores **Scope**: Fabrication of porous implants having load-bearing bone defect repair and regeneration
Gong et al. [21]	120 W	Mean Particle size of ~30 μm (D10: 17 μm, D90: 44 μm) Powder apparent Density—2.6 g/cm^3		Fatigue limit-350 MPa 0.2% Proof stress (MPa)-1098, 1150, 1066, 932, 813 UTS (MPa)-1237, 1257, 1148, 1112, 978 Elongation (%)-8.8, 8.0, 5.4, 6.6, 3.7 Youngs modulus (GPa)-109, 111, 109, 95, 84	**Focus**: By varying energy density samples are produced and studied for defects and subjected to fatigue, hardness and tensile tests **Findings**: Small pores up to 1 vol.% shows no effect on the mechanical properties At 5 vol%, porosity results drop in tensile properties **Scope**: Outcomes are supportive in standardization and process optimization

(continued)

Table 4 (continued)

	Power used/setup	Powder properties	Substrate	Mech properties	Key point/literature outcome
[22]	130 W	Powder particle size-40 μm			**Focus**: Lattice structure deformation behavior **Findings**: Local strain concentrations, microstructure and process induced pore formation can be controlled by heat treatment Energy absorption capacity of heat treated samples increase due to enhancement in ductility after heat treatment **Scope**: Optimization in the load adapted lattice structure
[77]	42 W	Pore size-450, 500 Strut Size-120, 170, 230	Solid titanium	Yield stress-16–92 MPa Max stress-19–117 MPa	**Focus**: Fatigue behavior of porous structures **Findings**: Change in static mechanical properties of porous structure having micro-architecture Structure having lowest porosity has the higher yield stress

(continued)

Table 4 (continued)

	Power used/setup	Powder properties	Substrate	Mech properties	Key point/literature outcome
Wauthle et al. [66, 67]		Pore size-500 μm Strut size-120 μm Particle size-10 μm to 45 μm	Solid Ti substrate		**Focus**: Static and dynamic compressive properties Ti structures **Findings**: CP Ti is a tremendous material for dynamically loaded porous implants with higher cycle fatigue strength **Scope**: Future implant developments
[69]	150 W	Ti6Al4V amorphous granular Powder-38 μm	Ti6Al4V substrate		**Focus**: Development and evaluation of porous medical implant scaffolds **Findings**: Octahedral lattice having good process ability as compared to circular one Due to transferred heat the powder particles are attached on struts
[31]			Solid titanium build plate		**Focus**: Porous metallic biomaterials for fatigue properties **Findings**: Tool for improved fatigue performance of porous metallic biomaterials Improvement of the fatigue life was achieved

(continued)

Table 4 (continued)

	Power used/setup	Powder properties	Substrate	Mech properties	Key point/literature outcome
[75]	42 W	Strut size—120 μm, Pore size 500 μm	Solid Titanium		**Focus**: To creating nanotube on the surface of porous titanium alloy bone substitutes **Findings**: Cell attachment of porous titanium surfaces improved with heat treatment improved
[42]	117 W, 170 W	The particle size distribution 29, 43 and 68 μm		Effective modulus-7.72 MPa Ultimate compressive strength-163 MPa Yield strength-129 MPa	**Focus**: Heat treatment to determine the microstructural effect on mechanical properties **Findings**: Martensitic α microstructure was observed Thinner struts were obtained, consequently large pores with higher porosity is observed
[38]		Strut dia-348, 540, 612, 720 μm 277, 450, 520, 600 μm Pore size-1080, 1188, 1260, 1452 μm 600, 680, 750, 923 μm	Solid titanium substrate	Youngs modulus (MPa)-511, 1505, 1578, 2178, 3157, 3691, 3694 Yield stress (MPa)-7, 29, 32, 63, 66, 71, 113 Max stress (MPa)-15, 30, 47, 57, 77, 111, 113, 185 Plateau stress (MPa)-8, 11, 29, 38, 40, 64, 82, 142	**Focus**: Failure mechanisms and deformation of porous Ti based biomaterials **Findings**: Diamond unit cells obtained structures were accompanied by the shearing bands of 45°

(continued)

Table 4 (continued)

	Power used/setup	Powder properties	Substrate	Mech properties	Key point/literature outcome
[41]	170 W	Porosity-68% Pore Size-1570 μm Strut size-800 μm			**Focus**: Heat treatment on the mechanical properties of Ti–6Al–4V part **Findings**: The post heat treatment increases the ductility. The decomposition of martensite α′ phase is by the diffusion of excess vanadium from α′ to β phase
[71]	170 W	Powder particle size distribution 3–50 mm Average particle size 20 μm		Micro hardness of 4.0170.34 GPa	**Focus**: Ti based lattices for manufacturability, mechanical properties, and microstructure **Findings**: Biomorphic design and high inter connected porosity with suitable pore size sand stiffness comparable to human bones
[28]		Strut size 433 μm	Solid metal substrate		**Focus**: Tissue regeneration for fatigue and static behavior **Findings**: The addition of polymeric material enhances the fatigue life and mechanical properties of porous structures

(continued)

Table 4 (continued)

	Power used/setup	Powder properties	Substrate	Mech properties	Key point/literature outcome
Wang et al. [64, 65]	280 W	Fine spherical morphology average particle size 38.8 μm Particle size distribution is between 20 and 120 μm	Substrate plate with a solid support		**Focus**: Porous scaffolds for mechanical properties **Findings**: Strength and elastic modulus are decreased with increasing strut size
[15]	100 W	Grain size 15–45 μm Spherical shape			The electro polishing and chemical etching improves the surface finish of implants and remove un-molten grains and open the side surface pores
[45]	4 kW		Ti6Al4V plate	Compressive yield strength-73 ± 8 MPa Ultimate strength-116 ± 10 MPa Young's modulus-2.5 ± 0.5 GPa	**Focus**: To find Mechanical properties with application of compressive tests **Scope**: Orthopedic implants
[44]	EBM S12, Arcam AB	Particle size-(45–100) μm		Young's modulus-1.13 ± 0.04 GPa Ultimate strength-83.8 ± 4.2 MPa	**Focus**: Developed a novel hybrid implant **Scope**: Hybrid implant with long term stability
Gong et al. [21]	Laser power-120 W	Mean powder particle size-73 μm Apparent density of 2.7 g/cm^3		0.2% proof stress-813, 932, 1066, 1098, 1150 MPa UTS-978, 1112, 1148, 1237, 1257 MPa Elongation-3.7, 5.4, 6.6, 8.0, 8.8 Youngs modulus-84, 95, 109, 111 GPa	**Focus**: To evaluate the mechanical properties Findings: Insufficient energy input results macroscopic voids producing serious degradation **Scope**: Process optimization and standardization

(continued)

Table 4 (continued)

	Power used/setup	Powder properties	Substrate	Mech properties	Key point/literature outcome
[27]				Porosity %-65 ± 0.6, 70 ± 0.7, 67 ± 0.6, 70 ± 0.6 Young's modulus-1.6, 1.2, 1.3, 1.4 GPa	**Focus**: Observed the bone bonding strength of diamond-structure porous Ti-alloy **Findings**: No breakage in the porous structure, histological bone ingrowth **Scope**: Potential advantages for weight bearing orthopedic implants such as acetabular cups
[35]	EBM S12; Arcam AB	(Alfa Aesar, Ward Hill, MA)		Porosity%-69 ± 5	**Focus**: Osteointegration capabilities and bone formation **Findings**: Coated implants have tremendous prospects in orthopedic application
[52]	Arcam AB			Porosities varying from 49.75 to 70.32% Stiffness value-0.57(±0.05)-2.29 (±0.17) GPa Compressive strength-7.28 (±0.93)-163.02 (±11.98) MPa grain density—4:423 g/cm^3 UTS-950–990 MPa Yield strength-910–940 MPa Elongation-14–16% Rockwell hardness-30–55 HRC Modulus of elasticity-120 GPa	**Focus**: Mechanical characterization and microstructural analysis

(continued)

Table 4 (continued)

	Power used/setup	Powder properties	Substrate	Mech properties	Key point/literature outcome
[8]	Arcam, Sweden (Arcam A2)	Average powder diameter 30 μm		Density—0.37–1.68 g/cm^3 Porosity%-62.08–91.65 Cell hardness 3.03 ± 0.22–3.51 ± 0.16 GPa Youngs modulus-0.2–6.3 GPa Compressive strength-4–113 MPa	**Focus**: Open cellular structures-reticulated mesh and stochastic foam type **Findings**: Cellular structures having comparable elastic modulus and compressive strength
[49]	ARCAM A2, EBM	Average particle diameter of ~30 μm)		Density—0.47–1.99 g/cm^3 Porosity %-55–89 Stiffness, E-0.48–9.97 GPa	**Focus**: Open cellular foams were fabricated Findings: exhibit tailorable stiffness and strength **Scope**: Aeronautics, biomedical and automotive applications
[50]	ARCAM EBM S12	Powder particle size 45–100 μm		Density—0.13 ± 7 × 10^{-3} to 0.40 ± 7 × 10^{-3} Youngs modulus-0.65 ± 0.05–10.92 ± 0.41	**Focus**: Porous metals for relative density and mechanical properties relationship
[81]	ArcamA1, Arcam	Average particle dia-50 μm		Density—1.57, 1.63, 1.68 Porosity—62.1, 63.2, 64.5 Max strength—196 ± 7.1	**Focus**: Effect of cell shape on compressive fatigue behavior **Findings**: Cellular solids with low modulus and high fatigue strength
[33]	Arcam model A2	Particle size 45–100 μm		Density—0.114–0.291 Flexural strength-26.59–131.60	**Focus**: Open cellular structures proposed for tissue scaffolds and low stiffness implants

(continued)

Table 4 (continued)

	Power used/setup	Powder properties	Substrate	Mech properties	Key point/literature outcome
[29]		Spherical powder Powder particle size-70 μm		Elastic modulus—0.9–18.2 GPa Yield strength—15.2–181 MPa Max strength—21.0–205 MPa Porosity—59.5–81.1	**Focus**: Fabrication of novel cellular structures for orthopaedic applications **Findings**: Reformed bioactive surface of implant with long-term stability
[34]	Arcam AB,	Spherical, average particle size 70 mm			**Focus**: To fabricate regular 3D periodic porous Ti structures
[59]	Arcam AB	Particle size 45–105 μm		Porosity—61.5–82.5	**Focus**: Fabrication of cellular Ti-6Al-4V materials with open-cell pore array structures

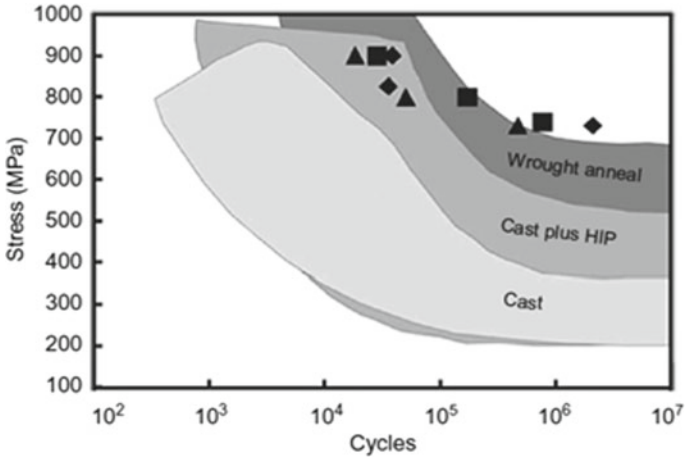

Fig. 6 Comparison of room temperature fatigue properties of AM fabricated Ti6Al4V and conventionally fabricated Ti6Al4V', ■, ⬥ and▲ represent properties in the three orthogonal directions: x, y, and z, respectively (http://www.titanium.org)

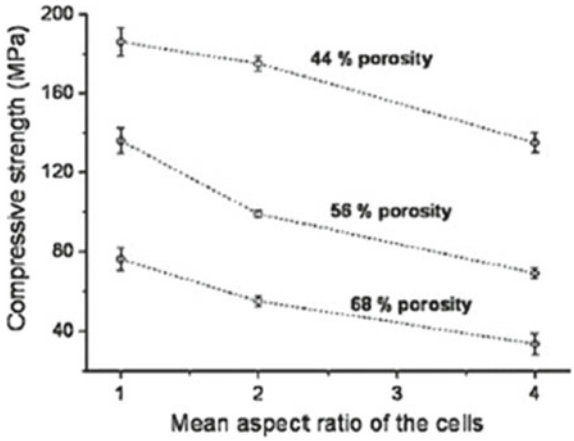

Fig. 7 Comparison of compression strength with aspect ratio of produced titanium foams for different levels of porosity [61]

load. Further the compressive strength is highly **affected** by the other imperfections as the yield stress confirms the strength of the weakest cross section plane of the part.

4.3 Static Mechanical Properties

Table 4 shows different mechanical properties. The material processed by laser based technologies exhibit lower ductility because of martensite α' phase. Ductility can be improved with the application of heat treatment of parts. In case of EBM processed

Ti6Al4V parts have higher ductility as compared to laser processed parts because of reduced residual stress and having α–β microstructure. Porosity present due to entrapped gases can also **affect** the mechanical properties. The factors like process parameters and their range, technique/setup used, geometry of test specimens, orientation, surface roughness and post processing of parts also temper and are main obstacles to compare the mechanical properties of parts. There is a minor effect of direction i.e. X–Y and Z direction on mechanical properties, but in some studies the results of X–Y direction samples are better as compared to Z direction samples because of grain orientation in the samples. For different materials, the effect of aging seems to be **stronger** as compared to orientation of the materials on mechanical properties.

4.4 Corrosion Behavior and Biological Properties

The higher corrosion resistance of Ti6Al4V made parts with SLM and EBM is desired to enhance their application and uses. The parts **that** have higher reactive characteristics, actively participate in crevice corrosion at contacting interfaces. Corrosion resistance shows a substantial effect on biological materials. The materials having low corrosion resistance may react with metallic **ions** which not only leads **to** active reaction, but also damage the organs. Ti6Al4V is highly active, and there is a risk of **developing** a stable surface oxide layer when it is exposed to air or aqueous media. This stable surface oxide layer **prevents** further reaction, **therefore** corrosion resistant capacity of the parts improves.

5 Structural Applications of Titanium and Its Composites

Titanium is one of the strongest **metals** and its **lightweight** property make it an ideal metal for a variety of applications like aerospace, chemical, marine, automobile and **biomedical** industries. Pure titanium exhibits high strength and corrosive resistance, but the titanium alloys retain an equivalent properties and additionally takes on to the greater malleability and flexibility of the metal it is combined with. Due to this, titanium alloy has more applications than that of pure titanium. In general, there are six grades of pure titanium (grade 1, 2, 3, 4, 7 and 11) and different varieties of titanium alloys (https://titaniumprocessingcenter.com/the-element-titanium/). Titanium alloys typically contain traces of aluminum, copper, nickel, cobalt, chromium, iron, manganese, zirconium, tantalum, niobium, vanadium and molybdenum.

Among the all **fields** of applications, **the** aerospace industry has become the main field which was majorly using titanium and its alloys [73]. Particularly titanium was used in airframe systems and **engines** where it comprises 7% and 37% respectively [43]. It has been reported that in the USA, about 70–80% consumption of titanium was for aerospace and the rest is **used** for other industrial applications [16]. In **the** 1980s, the titanium material was started being used in **the** automobile industry which

began with F-1 racing cars primarily, for engine parts. However, due to **the** high cost of titanium and its alloys, their applications in **the** automobile industry are limited except for special and racing purpose cars. In the due period, these titanium alloy applications **were** also extended to other engineering **fields** like marine and chemical. Titanium Matrix composites (TMCs) [7, 47] emerged to enable structural materials in hypervelocity vehicles [60] and advanced aerospace applications such as high performance turbine engines Larsen et al. [40]. TMCs are the initiative of Integrated High Performance Turbine Engine Technology by U.S. Air Force which were used in turbine engine components Larsen et al. [40], Johnson and Mirdamadi [37]. Figure 8 **show** the titanium based structural components in various fields of its applications.

Later the TMCs were widely used for automobile, chemical and industrial applications. The applications of various titanium and its composites are shown in Table 5.

Ti6Al4V is one among all titanium alloys which is widely used for engineering applications like aerospace, marine, chemical, bridge, thermal and bio-medical [25]. In early 1950s, the Ti6Al4V alloy was originally developed and used for structural components of aircraft due to its special properties like low density, high strength,

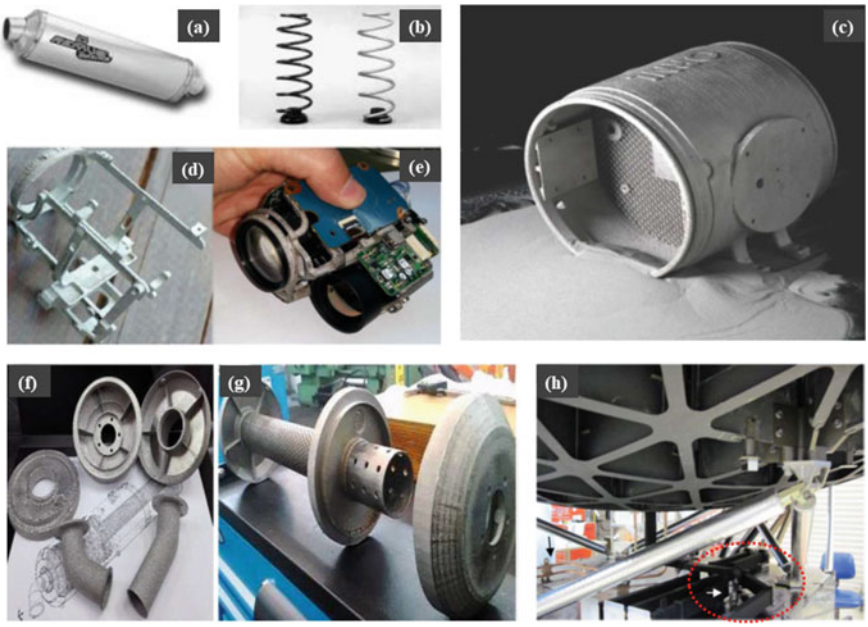

Fig. 8 Structural components manufactured by using titanium material [53, 55] **a** The titanium sports exhaust system (Courtesy: REMUS innovation, Barnbach, Austria), **b** rare axial sprig of the Lupo FSI (left: steel, right: titanium alloy Low Cost Beta (LCB)), **c** hydraulic manifold built using EBM technology (courtesy: ORNL, TN), **d** and **e** titanium EBM manufactured body of Nano-camera, **f** and **g** exhaust gases system for formula technion car by EBM technology, **h** installed titanium wave guide brackets on Juno space craft

Table 5 Applications of various titanium and its composites in different fields of applications Salihu et al. [55], Rawal et al. [53], Kolomiets et al. [39] Veiga et al. [63], Dutta and Froes [17], Gospodinov et al. [24], Bharath et al. [5] and Gofrey et al. [20]

Material (titanium and titanium composites)	Applications (structural systems and parts)
Aerospace applications	
Ti-6Al-4V	Window frames, fan disks and blades, compressor disc, compressor blades, fuselage, nacelles, landing gear, wing, and empennage, and also in the floor support structure, including areas of galleys and lavatories
CP-Ti	Floors, clips and brackets, ducting for the anti-icing
Ti-6Al-2Sn-4Zr-2Mo	Exhaust, tail cone
Ti-10V-2Fe-3Al	Landing gear
Ti-15V-3Cr-3Sn-3Al	Springs and ducts
Ti-6-6-2	Landing gear
Ti-6-2-4-2S	Fan discs and blades, compressor disc, compressor blades and rotors
Ti-35V-1Cr	Compressor stators
TIMETAL 21S	Nozzle assembly
Ti-3Al-2.5V	High pressure hydraulic lines
Ti-5-2.5	Cryogenic applications
Ti-8-1-1	Fan blades of military engines, straps on commercial airframes
Ti-5.5A1-3.5Sn-3Zr-1Nb-0.25Mo-0.3Si	Compressor discs, blades and spacers of the RB-211-535E4 engine, which powers the Boeing 757
Ti-5.SA1-4Sn-3.5Zr-7Nb-0.5Mo-0.35Si-0.06C	Compressor discs
Ti-13 V-11Cr-3A1	Extensively used SR-71 airplane, for wing and body skins, frames, longerons, bulkheads, ribs and rivets
Ti-10-2-3	Landing gear of the 777
Automotive applications	
Ti-6Al-4V	Suspension springs, Armor, outlet valves, intake valves, connecting rods and body
Ti-6.8Mo-4.5Fe-1.5Al	Suspension springs
CP-Ti	Body
ϒTiAl	Outlet valves and Turbocharger rotors
Ti-6Al-2Sn-4Zr-2Mo-0.1Si	Outlet valves
Grade 2	Exhaust system, break guide pins,
Grade 1	Gear shift knob and sealing washer

high fracture toughness and excellent corrosion resistance. This **alloy also exhibits** much better dynamic performance then the others, which will play a vital role in aircraft design. The properties like light weight with high strength of Ti6Al4V alloy helps to save the weight in highly loaded structural components and hence it is an ideal candidate for many air frame components, jet engines and gas turbines Inagaki et al. [6, 36]. Figure 9 shows some of the structural components of Ti6Al4V alloy by additive manufacturing.

Ti6Al4V alloy was initially used as a replacement for aluminum in nacelle and auxiliary power unit (APU) areas and wing anti-icing systems for air frame structures

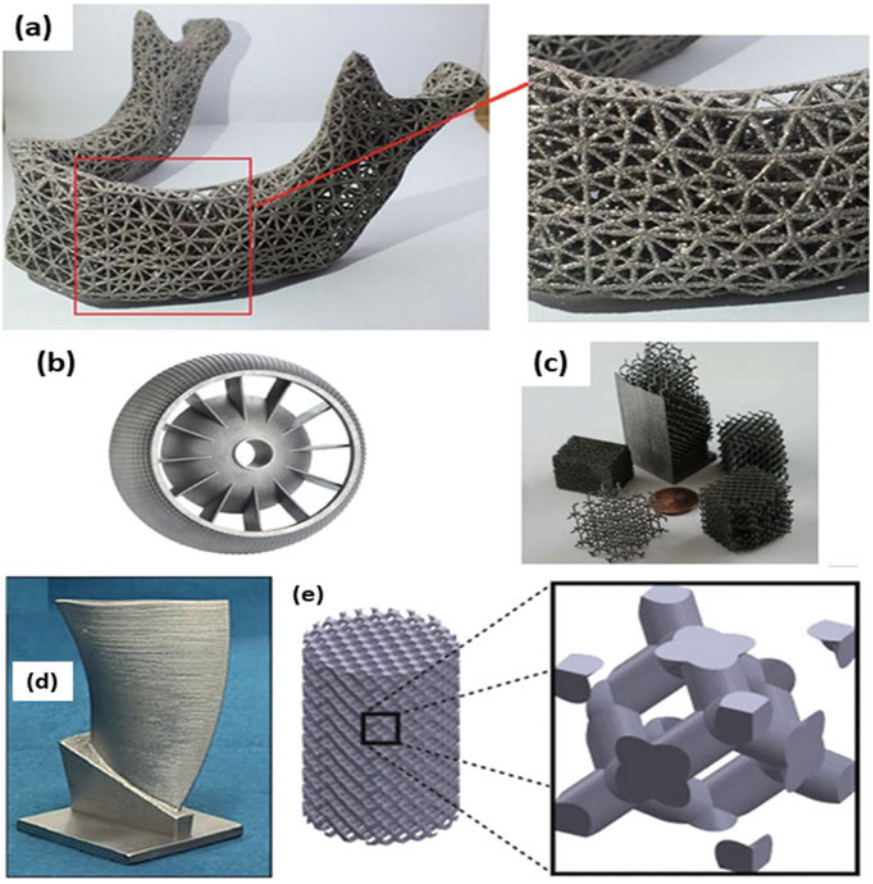

Fig. 9 Structural components of Ti6Al4V by using additive manufacturing (Liu and Shin [46]) **a** 3D mesh Ti6Al4V using EBM [70]. **b** Air duct manufactured by Ti6Al4V manufactured by SLM with high precision (https://www.slm-solutions.com/). **c** Ti6Al4V foams manufactured by using EBM (https://tusharmahale.wixsite.com/home/obtainium). **d** Ti6Al4V blade manufactured by using DED (https://www.rtejournal.de/ausgabe2/233/view?set_language=en). **e** Porous sample of Ti6Al4V alloy and diamond cell built by using SLM (Wauthle et al. [66, 67])

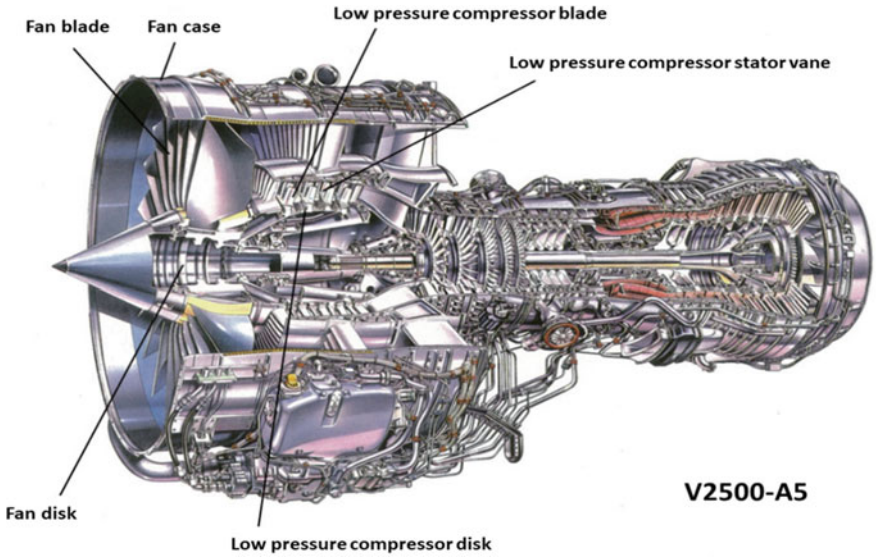

Fig. 10 Different components of titanium alloy used for aero engine (https://www.aerocontact.com/en/virtual-aviation-exhibition/product/441-pratt-and-whitney-v2500-engine)

[6]. Later these applications were extended to other components of aircraft likely for landing gear beams of Boeing 757 and 747. Among the different parts of the aircraft, the Boeing 747 landing gear beam is one of the largest Ti6Al4V forgings which are being produced.

The Ti6Al4V properties like heat resistance, low thermal expansion and resistance to embrittlement at low temperature leads further to extend its usage for aircraft engine components. Figure 10 shows the different components of aero **engines** which are built by using Ti6Al4V.

With the development in aircraft design for its efficiency, about 80–90% of total titanium used in airframe parts (including skin panels, stiffeners, spares, wing boxes etc.) is completely built by using Ti6Al4V alloy. This alloy is also having **an** important role in aero engine parts (around 60% is used by Ti6Al4V). It is not limited to commercial aviation only. It is extended to military fighter jets also. Ti6Al4V plays a major role for the growth of fighter jet development to keep the jet ultra-lightweight and flexible during combat [57]. Blisk of F-35 Lightening-II fighter, fan compressor, cooler parts and other parts which operate below 300 °C are also made by using Ti6Al4V. The forged Ti6Al4V can also withstand the impact (to withstand the bird strike) in cockpit windows [12]. This is also extensively used in rotor heads of helicopters (BK117 and BK105) [62]. The fighter jets like F-15, C-17, F-16, F/A-18E/F, F-2 raptor and F-35 are some of the major **examples** in which Ti6Al4V is used for its airframe.

Apart from the aerospace industry, Ti6Al4V has led to widespread marine, chemical and other industrial applications due to its good corrosion resistance in highly

Table 6 Corrosion behavior of Ti6Al4V alloy in different environment at various temperatures Gurrappa [26]

Environment	Temperature (°C)	Corrosion rate (mils/year)
Chemical	25	227.0
	50	348.9
Marine	25	41.41
	50	96.10
Industrial	25	55.13
	50	116.9

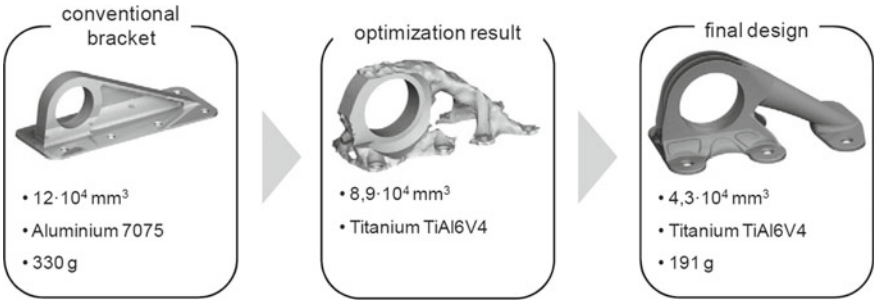

Fig. 11 Optimized design component for additive manufacturing

corrosive environments. During 1990s, this alloy was also used for engineering structures to extract the hydrocarbons in offshore [23]. **A** wide range of literature is available to understand the corrosion behavior of Ti6Al4V alloy which demonstrates that this alloy **plays** a vital role for the ship-building, chemical and industrial applications. Table 6 shows the corrosion behavior of Ti6Al4V in different environments at various temperatures.

Ti6Al4V alloy increases its corrosion rate nearly twice with increase in temperature from 25 to 50 °C in all three environments (chemical, marine and industrial). It **is** also evident that, Ti6Al4V alloy is recommended to build the components that are intended to **be used** in marine environments with minimum surface treatment. Whereas for chemical and industrial applications, it is essential to provide appropriate protective measures, as pitting corrosion occurs in these environments [26, 51].

The applications of Ti6Al4V alloy is not limited for engineering structures (aerospace, marine, chemical, industrial and construction) only but are extended to biomedical applications like hard bone replacements in human body and medical equipment's [18] and Rossman et al. (2016). Due to these wide range of applications in different engineering and medical fields, the demand of Ti6Al4V alloy is extensively increasing and leads to consumption of more material with increase in build cost. To overcome this limitation, new manufacturing methods are needed to be employed. Additive manufacturing of Ti6Al4V alloy based structures by using EBM and SLM is widely **adopted nowadays**. With this manufacturing technique,

Table 7 The main challenge and their solution in fabrication of AM parts

S. No.	Challenge	Solution
1	Residual stresses in SLM made parts	Residual stresses of parts are improved if these are fabricated with new technology i.e. EBM
2	Poor surface finish due to partial melting or sticking of material from surroundings	Use of optimized set of parameters
3	Absence of self-supporting structures can diminish application while producing overhangs	Improve the product design by providing support structures
4	Difference in the microstructure of AM fabricated parts compared to wrought material	Because of rapid heating and cooling of material: control cooling rate
5	AM fabricated parts contained the defects: delamination, unfused layers, porosity and balling	Use optimized set of parameters, and deeply monitors powder based parameters such as flow rate, size distribution, shape of powder particle and alloy chemical composition

an optimized (refer to Fig. 11) intended structures can be developed in its fields of application.

6 Challenges and Solutions

Ti6Al4V based cellular solids made with different AM processes are widely applied for various engineering as well as medical modeling based a**pplications**. The fabricated parts and implants are **performing** up to the expectations, but there is still scope to enhance the applications of these fabricated parts. Table 7 shows the main challenges and the comparative solutions related to each.

There must be the improvement in the reliability of the AM setups that lowers the burden of the operator. The failure of these systems belongs to hardware, skill of operator and poor design. So it is very much required a **collective** action of hardware manufacturer, operators and researchers to **lower operator's** errors on failure and generate reliable setups.

References

1. Agarwala M, Bourell D, Beaman J, Marcus H, Barlow J (1995) Direct selective laser sintering of metals. Rapid Prototyp J 1(1):26–36
2. Ahmed T, Rack HJ (1998) Phase transformations during cooling in α+β titaniumalloys. Mater Sci Eng A 243(1):206–211

3. Bagheri ZS, Melancon D, Liu L, Johnston RB, Pasinin D (2017) Compensation strategy to reduce geometry and mechanics mismatch esin porous biomaterials built with selective laser melting. J Mech Behav Biomed Mater 70:17–27
4. Banerjee D, Williams JC (2013) Perspectives on titanium science and technology. Acta Mater 61(3):844–879
5. Bharath K N, Madhu P, Yashas G T G, Sanjay M R, Kushvaha V, Slengchin S (2020) Alkaline effect on characterization of discarded waste Moringa oleifera Fiber as a pottential eco-friendly reinforcement in biocomposites. J Polym Environ. https://doi.org/10.1007/s10924-020-01818-4
6. Boyer RR (1996) An overview on the use of titanium in the aerospace industry. Mater Sci Eng, A 213(1):103–114. https://doi.org/10.1016/0921-5093(96)10233-1
7. Chan KS, Kim YW (1993) Rate and environmental effects on fracture of a two-phase TiAl-alloy. Metall Trans A 24(1):113–125. https://doi.org/10.1007/BF02669609
8. Cheng XY, Lia SJ, Murr LE, Zhang ZB, Hao YL, Yang R, Medina F, Wicker RB (2012) Compression deformation behavior of Ti–6Al–4V alloy with cellular structures fabricated by electron beam melting. J Mech Behav Biomed, 153–162.
9. Chooa H, Shama KL, Bohlinga J, Ngo A, Xiao X, Ren Y, Depond PJ, Matthews MJ, Garlead E (2019) Effect of laser power on defect, texture, and microstructure of a laser powder bed fusion processed 316L stainless steel. Mater Des 164:107534.
10. Chua CK, Leong KF, Lim CS (2010) Rapid prototyping: principles and applications, 4th edn. World Scientific, Singapore
11. Cormier D, Harrysson O, West H (2004) Characterization of H13 steel produced via electron beam melting. Rapid Prototyp J 10(1):35–41
12. Cui C, Hu B, Zhao L, Liu S (2011) Titanium alloy production technology, market prospects and industry development. Mater Des 32(3):1684–1691. https://doi.org/10.1016/j.matdes.2010.09.011
13. Deprez K, Vandenberghe S, Audenhaege KV, Vaerenbergh JV, Holen RV (2013) Rapid additive manufacturing of MR compatible multi pinhole collimators with selective laser melting of tungsten powder, Medical Physics 14(1) 012501(1–12)
14. Dilip JJS, Zhang S, Teng C, Zeng K, Robinson C, Pal D, Stucker B (2017) Influence of processing parameters on the evolution of melt pool, porosity, and microstructures in Ti-6Al-4V alloy parts fabricated by selective laser melting. Progress Addit Manuf 2:157–167
15. Dobrzański LA, Danikiewicz ADD, Gaweł TG (2017) Computer-aided design and selective laser melting of porous biomimetic materials. Abbreviations, Advan J Mater Process Tech 3(1):70–82
16. Donachie MJ (2000) Titanium: a technical guide, 2nd edn. ASM International
17. Dutta B, Froes FH (2017) The additive manufacturing (AM) of titanium alloys. Met Powder Rep 72(2):96–106. https://doi.org/10.1016/j.mprp.2016.12.062
18. Emmelmann C, Sander P, Kranz J, Wycisk E (2011) Laser additive manufacturing and bionics: redefining lightweight design. Phys Procedia 12:364–368. https://doi.org/10.1016/j.phpro.2011.03.046
19. Gibson I, Rosen DW, Stucker B (2010) Additive manufacturing technologies. In: Rapid prototyping to direct digital manufacturing. Springer, New York
20. Gofrey TMT, Goodwin PS, Ward Close CM (2000) Titanium particulate metal matrix composites—reinforcement, production methods, and mechanical properties. Adv Eng Mater 2(3):85–91. https://doi.org/10.1002/(SICI)1527-2648(200003)2:3%3c85::AID-ADEM85%3e3.0.CO;2-U
21. Gong H, Rafi K, Gu H, Ram GDJ, Starr T, Stucker B (2015a) Influence of defects on mechanical properties of Ti–6Al–4 V components produced by selective laser melting and electron beam melting. Mater Des 86:545–554
22. Gorny B, Niendorf T, Lackmann J, Thoene M, Troester T, Maier HJ (2011) In situ characterization of the deformation and failure behavior of non-stochastic porous structures processed by selective laser melting. Mater Sci Eng A 528:7962–7967

23. Gorynin IV (1999) Titanium alloys for marine application. Mater Sci Eng, A 263(2):112–116. https://doi.org/10.1016/S0921-5093(98)01180-0
24. Gospodinov D, Ferdinandov N, Dimitrov S (2016) Classification, properties and application of titanium and its alloys
25. Gupta MK, Song Q, Liu Z, Sarikaya M, Jamil M, Mia M, Kushvaha V, Singla AK, Li Z (2020) Ecological, economical and technological perspectives based sustainability assessment in hybrid-cooling assisted machining of Ti-6Al-4V alloy. Sustain Mater Technol 26 (December):e00218. https://doi.org/10.1016/j.susmat.2020.e00218
26. Gurrappa I (2003) Characterization of titanium alloy Ti-6Al-4V for chemical, marine and industrial applications. Mater Charact 51(2):131–139. https://doi.org/10.1016/j.matchar.2003.10.006
27. Hara D, Nakashima Y, Sato T, Hirata M, Kanazawa M, Kohno Y, Yoshimoto K, Yoshihara Y, Nakamura A, Nakao Y, Iwamoto Y (2016) Bone bonding strength of diamond-structured porous titanium-alloy implants manufactured using the electron beam-melting technique. Mater Sci Eng C 59:1047–1052
28. Hedayati R, Janbaz S, Sadighi M, Aghdam MM, Zadpoor AA (2017) How does tissue regeneration influence the mechanical behavior of additively manufactured porous biomaterials. J Mech Behav Biomed Mater 65:831–841
29. Heinl P, Muller L, Korner C, Singer RF, Muller FA (2008) Cellular Ti–6Al–4V structures with interconnected macro porosity for bone implants fabricated by selective electron beam melting. Acta Biomater 4:1536–1544
30. Herzog D, Seyda V, Wycisk E, Emmelmann C (2016) Additive manufacturing of metals. Acta Mater 117:371–392
31. Hooreweder BV, Apers Y, Lietaert K, Kruth JP (2017) Improving the fatigue performance of porous metallic biomaterials produced by selective laser melting. Acta Biomater 47:193–202
32. Hopkinson N, Hague R, Dickens P (2006) Rapid manufacturing: an industrial revolution for a digital age. Wiley, Chichester
33. Horn TJ, Harrysson OLA, Little DJM, West HA, Lascelles BDX, Aman R (2014) Flexural properties of Ti6Al4V rhombic dodecahedron open cellular structures fabricated with electron beam melting. Addit Manuf 1–4:2–11
34. Hrabe NW, Heinl P, Bordia RK, Korner C, Fernandes RJ (2013) Maintenance of a bone collagen phenotype by osteoblast-like cells in 3D periodic porous titanium (Ti-6Al-4V) structures fabricated by selective electron beam melting. Connect Tissue Res 54(6):351–360
35. Huang H, Lan PH, Zhang YQ, Li XK, Zhang X, Yuan CF, Zheng XB, Guo Z (2015) Surface characterization and in vivo performance of plasma-sprayed hydroxyapatite-coated porous Ti6Al4V implants generated by electron beam melting. Surf Coat Tech 283:80–88
36. Inagaki I, Takechi T, Ariyasu YSN (2014) Application and Features of Titanium for the Aerospace Industry
37. Johnson WS, Mirdamadi M (1993) Analysis of Thermal Mechanical Fatigue in Titanium Matrix Composites 14 (n.d.)
38. Kadkhodapour J, Montazerian H, Darabic AC, Anarakia AP, Ahmadid SM, Zadpoord AA, Schmauder S (2015) Failure mechanisms of additively manufactured porous biomaterials: effects of porosity and type of unit cell. J Mech Behav Biomed Mater 50:180–191
39. Kolomiets A Jr, Popov VV, Strokin E, Muller G (2018) Benefits of titanium additive manufacturing for industrial, 9
40. Larsen JM, Russ SM, Jones JW (1995) An evaluation of fiber-reinforced titanium matrix composites for advanced high-temperature aerospace applications. Metall and Mater Trans A 26:3211–3223. https://doi.org/10.1007/BF02669450
41. Levaa ES, Carama R, Jardinib AL, Fogagnoloa JB (2016) Ductility improvement due to martensite α' decomposition inporous Ti–6Al–4V parts produced by selective laser melting for orthopedic implants. J Mech Behav Biomed Mater 54:149–158
42. Levaa ES, Jardinib AL, Fogagnoloa JB (2013) Microstructure and mechanical behavior of porous Ti–6Al–4V parts obtained by selective laser melting. J Mech Behav Biomed Mater 26:98–108

43. Leyens C, Peters M (2003) Titanium and titanium alloys: fundamentals and applications. Wiley (n.d.). Wiley.com.
44. Li X, Luo Y, Wang C (2012) Preparation and characterization of porous Ti6Al4V/alginate hybrid implant by combination of electron beam melting and freeze-drying. Mater Lett 81:23–26
45. Li X, Wang C, Zhang W, Li Y (2009) Fabrication and characterization of porous Ti6Al4V parts for biomedical applications using electron beam melting process. Mater Lett 63:403–405
46. Liu S, Shin YC (2019) Additive manufacturing of Ti6Al4V alloy: a review. Mater Des 164:107552. https://doi.org/10.1016/j.matdes.2018.107552
47. Malakondaiah G, Nicholas T (1996) High-temperature low-cycle fatigue of a gamma titanium aluminide alloy Ti-46Al-2Nb-2Cr. Metall and Mater Trans A 27(8):2239. https://doi.org/10.1007/BF02651878
48. Murr LE, Esquivel EV, Quinones SA, Gaytan SM, Lopez MI, Martinez EY, Medina F, Hernandez DH, Martinez E, Martinez JL, Stafford SW, Brown DK, Hoppe T, Meyers W, Lindhe U, Wicker RB (2009) Microstructures and mechanical properties of electron beam-rapid manufactured Ti–6Al–4V biomedical prototypes compared to wrought Ti–6Al–4V. Mater Charact 60(2):96–105
49. Murr LE, Gaytan SM, Medina F, Martinez E, Martinez JL, Hernandez DH, Machado BI, Ramirez DA, Wicker RB (2010) Characterization of Ti–6Al–4V open cellular foams fabricated by additive manufacturing using electron beam melting. Mater Sci Eng A 527:1861–1868
50. Nava EH, Smith CJ, Derguti F, Williams ST, Léonard F, Withers PJ, Todd I, Goodall R (2015) The effect of density and feature size on mechanical properties of isostructural metallic foams produced by additive manufacturing. Acta Mater 85:387–395
51. Oryshchenko AS, Gorynin IV, Leonov VP, Kudryavtsev AS, Mikhailov VI, Chudakov EV (2015) Marine titanium alloys: present and future. Inorg Mater Appl Res 6(6):571–579. https://doi.org/10.1134/S2075113315060106
52. Parthasarathy J, Starly B, Raman S, Christensen A (2010) Mechanical evaluation of porous titanium (Ti6Al4V) structures with electron beam melting (EBM). J Mech Behav Biomed 3:249–259
53. Rawal S, Brantley J, Karabudak N (2013). Additive manufacturing of Ti-6Al-4V alloy components for spacecraft applications. In 2013 6th International conference on recent advances in space technologies (RAST), pp 5–11. Presented at the 2013 6th international conference on recent advances in space technologies (RAST). https://doi.org/10.1109/RAST.2013.6581260
54. Sachdeva A, Singh S, Sharma VS (2013) Investigating surface roughness of parts produced by SLS process. Int J Adv Manuf Tech 64:1505–1516
55. Salihu SA, Suleiman YI, Eyinavi AI (2019) Classification, properties and applications of titanium and its alloys used in automotive industry—a review. Am J Eng Res, 7
56. Sames WJ, List FA, Pannala S, Dehoff RR, Babu SS (2016) The metallurgy and processing science of metal additive manufacturing. Int Mater Rev 1–46
57. Singh P, Pungotra H, Kalsi NS (2017) On the characteristics of titanium alloys for the aircraft applications. Materials Today: Proceedings 4(8):8971–8982. https://doi.org/10.1016/j.matpr.2017.07.249
58. Singh S, Sharma VS, Sachdeva A (2016) Progress in selective laser sintering using metallic powders: a review. Mater Sci Technol 32:760–772
59. Smith G, Brown I, Kirchner A, Ryan M, McGavin P, Sharp M (2016) Engineering properties of cellular ti-6al-4v structures fabricated by electron beam melting. Key Eng Mater 704:318–324
60. Thornton EA (1996) Thermal structures for aerospace applications. AIAA
61. Tuncer N, Arslan G, Maire E, Salvo L (2011) Influence of cell aspect ratio on architecture and compressive strength of titanium foams. Mater Sci Eng A 528:7368–7374
62. Uhlmann E, Kersting R, Klein TB, Cruz MF, Borille AV (2015) Additive Manufacturing of titanium alloy for aircraft components. Procedia CIRP 35:55–60. https://doi.org/10.1016/j.procir.2015.08.061
63. Veiga C, Davim J, Loureiro A (2012) Properties and applications of titanium alloys: a brief review. Rev Adv Mater Sci 32:133–148

64. Wang M, Lin X, Huang W (2016a) Laser additive manufacture of titanium alloys. Mater Technol 31(2):90–97.
65. Wang Y, Chen J, Yuan Y (2016b) Influence of the unit cell geometrical parameter to the mechanical properties of Ti6Al4V open-porous scaffolds manufactured by selective laser melting. Appl Mech Mater 851:201–210
66. Wauthle R, Ahmadi SM, Yavari SA, Mulier M, Zadpoor AA, Weinans H, Humbeeck JV, Kruth JP, Schrooten J (2015a) Revival of pure titanium for dynamically loaded porous implants using additive manufacturing. Mater Sci Eng C 54:94–100
67. Wauthle R, Vrancken B, Beynaerts B, Jorissen K, Schrooten J, Kruth J-P, Van Humbeeck J (2015b) Effects of build orientation and heat treatment on the microstructure and mechanical properties of selective laser melted Ti6Al4V lattice structures. Addit Manuf 5:77–84. https://doi.org/10.1016/j.addma.2014.12.008
68. Wieding J, Souffrant R, Mittelmeier W, Bader R (2013) Finite element analysis on the biomechanical stability of open porous titanium scaffolds for large segmental bone defects under physiological load conditions. Med Eng Phys 35(4):422–432
69. Xu-bin SU, Yong-qiang Y, Peng YU, Jian-feng S (2012) Development of porous medical implant scaffolds via laser additive manufacturing. Trans Nonferrous Met Soc China 22:181–187
70. Yan R, Luo D, Huang H, Li R, Yu N, Liu C, Rong Q (2018) Electron beam melting in the fabrication of three-dimensional mesh titanium mandibular prosthesis scaffold. Sci Rep 8(1):750. https://doi.org/10.1038/s41598-017-15564-6
71. Yan C, Hao L, Hussein A, Young P (2015) Ti–6Al–4V triply periodic minimal surface structures for bone implants fabricate dvias elective laser melting J Mech Behav Biomed Mater 51:61–73.
72. Yan M, Yu P, (2015) An overview of densification, microstructure and mechanical property of additively manufactured Ti-6Al-4V Comparison among selective laser melting, electron beam melting, laser metal deposition and selective laser sintering, and with conventional powder metallurgy. In: Lakshmanan A (ed) Sintering techniques of materials, Intech. https://doi.org/10.5772/59275.
73. Yang X, Liu CR (1999) Machining titanium and its alloys. Mach Sci Technol 3(1):107–139. https://doi.org/10.1080/10940349908945686
74. Yang J, Yu H, Yin J, Gao M, Wang Z, Zeng X (2016) Formation and control of martensite in Ti-6Al-4V alloy produced by selective laser melting. Mater Des 108:308–318
75. Yavari SA, Chai YC, Böttger AJ, Wauthle R, Schrooteng J, Weinans H, Zadpoor AA (2015) Effects of anodizing parameters and heat treatment on nano topographical features, bioactivity, and cell culture response of additively manufactured porous titanium. Mater Sci Eng C 51:132–138
76. Yavari SA, Wauthle R, Böttger AJ, Schrooten J, Weinans H, Zadpoor AA (2014) Crystal structure and nano topographical features on the surface of heat-treated and anodized porous titanium biomaterials produced using selective laser melting. Appl Surf 290:287–294
77. Yavari SA, Wauthle R, Stok JVD, Riemslag AC, Janssen M, Mulier M, Kruth JP, Schrooten J, Weinans H, Zadpoor AA (2013) Fatigue behavior of porous biomaterials manufactured using selective laser melting. Mater Sci Eng C 33:4849–4858
78. Zargarian A, Esfahanian M, Kadkhodapour J, Rad SZ (2016) Numerical simulation of the fatigue behavior of additive manufactured titanium porous lattice structures. Mater Sci Eng C 60:339–347
79. Zhang S, Wei Q, Cheng L, Li S, Shi Y (2014) Effects of scan line spacing on pore characteristics and mechanical properties of porous Ti6Al4V implants fabricated by selective laser melting. Mater Des 63:185–193
80. Zhang D, Cai Q, Liu J, Li R (2011) Research on process and microstructure formation of w-ni-fe alloy fabricated by selective laser melting. J Mater Eng Perf 20(6):1049–1054
81. Zhao S, Lia SJ, Hou WT, Hao YL, Yang R, Misra RDK (2016) The influence of cell morphology on the compressive fatigue behavior of Ti-6Al4V meshes fabricated by electron beam melting. J Mech Behav Biomed 59:251–264

Laser Drilling of Superalloys and Composites

Shoaib Sarfraz, Essam Shehab, Konstantinos Salonitis, and Wojciech Suder

Nomenclature

A	Material absorptivity
A_s	Cross-sectional area of the laser spot (mm^2)
D_{Max}	Maximum hole diameter (mm)
D_{Min}	Minimum hole diameter (mm)
D_{ent}	Entrance hole diameter (mm)
D_{ex}	Exit hole diameter (mm)
D_p	Pulse duration (s)
E_{abs}	Energy absorbed by the material (J)
F_l	Focal length (mm)
H_c	Hole circularity
P	Applied laser power (W)
P_d	Laser power density (W/mm^2)
P_e	Pulse energy (J)
S_d	Spot diameter (mm)

S. Sarfraz (✉) · K. Salonitis · W. Suder
Manufacturing Department, School of Aerospace, Transport and Manufacturing, Cranfield University, Cranfield MK43 0AL, Bedfordshire, UK
e-mail: engr.shoaibsial@gmail.com

K. Salonitis
e-mail: k.salonitis@cranfield.ac.uk

W. Suder
e-mail: w.j.suder@cranfield.ac.uk

E. Shehab
Mechanical and Aerospace Engineering Department, School of Engineering and Digital Sciences, Nazarbayev University, Nur-Sultan 010000, Kazakhstan
e-mail: essam.shehab@nu.edu.kz

S. Mavinkere Rangappa et al. (eds.), *Additive and Subtractive Manufacturing of Composites*, Springer Series in Advanced Manufacturing,
https://doi.org/10.1007/978-981-16-3184-9_5

t	Material thickness (mm)
θ	Taper angle
Ø	Beam divergence (angle)

1 Introduction

Aircraft engine components usually operate under elevated temperature (above 1000 °C) and high-pressure conditions (more than 1 MPa) [42]. Materials with outstanding thermo-mechanical properties are required for effective performance in such hot sections of an aeroengine. Superalloys are the ideal candidate for use in aforesaid extreme operating conditions because of excellent corrosion and wear resistance, and high creep strength properties [71]. Superalloys are majorly classified into four categories, (Ni) nickel-based, (Ti) titanium-based, (Co) cobalt-based and (Fe) iron-based alloys. A significant portion (70%) of superalloys is used by aerospace industries and approximately 50% of the aerospace components are manufactured using Ni-based superalloys [24]. The characteristics of high strength, excellent thermal and fatigue resistivity enabled these alloys to be used in various applications, such as aeroengine components, space shuttles, nuclear reactors and tooling.

Composite materials have become popular in a wide range of industries due to their enhanced properties, including high strength to wear ratio, lower weight, and better corrosion and high-temperature resistance. Metal matrix composites (MMCs) are a comparatively new class of material structured by embedding high-strength ceramic fibres into a tough metal matrix [38]. These composites have superior properties comparable to superalloys and are used in both commercial and industrial applications especially in the aerospace sector [2, 35].

Conventional machining of these materials is challenging because of higher tool wear and the low material removal rate [3, 60]. The significance of using non-conventional machining processes (electrical discharge machining (EDM), laser machining and water-jet machining) for superalloys and MMCs has been discussed by Bains et al. [5] and Majumdar and Manna [47]. It is noted that non-conventional machining processes produce high quality products with better surface characteristics. Of all the available non-conventional machining processes, laser processing is a fast and flexible machining process specifically when drilling of aerospace components is considered [48].

There are different ways to drill a particular hole geometry. They can be divided based upon drilling processes such as single-pulse, percussion and trepanning. For a particular process, there is a range of parameters involved which control the material removal, hole quality and manufacturing cost. Furthermore, there are different factors which influence the laser drilling manufacturing cost. All of these aspects are discussed in this chapter.

2 Drilling in the Aerospace Industry

Advancements in aeroengine efficiency are associated with an enhancement of exhaust gases and combustion temperatures in aircraft gas turbines [52]. Although superalloys can sustain these elevated temperatures, supplementary cooling of components is necessary for effective engine performance. This can be achieved through drilling multiple cooling holes in hot-section components. Hole dimensions as well as the number of holes vary in different components as shown in Table 1.

Different methods are available to drill these holes. These include electrochemical machining (ECM), electrodischarge machining (EDM) and laser drilling. The latter method has an advantage over ECM and EDM because of the following reasons [20, 21, 46, 54, 92]:

i. There is no direct contact with the material surface and therefore no tool wear or breakage is involved.
ii. Proper design of the motion-control system and beam delivery facility enables the achievement of high precision and repeatability.
iii. The laser beam can be focused precisely on the defined area, which allows drilling of holes of various shapes and sizes.
iv. It is easy to program and automate the laser drilling process.
v. A wide range of materials can be operated on including composites, plastics, silicon, rubber or metals.
vi. The process duration is shorter as compared to EDM and ECM techniques.
vii. Some of the laser machines are versatile and it is possible to perform multiple functions using the same laser, such as welding or cutting.

However, there are some limitations of laser drilling which must be considered; these are provided below [20, 21, 46, 54, 92].

i. High capital cost is needed to buy a laser drilling setup.
ii. Laser drilling is associated with some inherent defects, such as hole taper, circularity, recast layer thickness (RLT), heat affected zone (HAZ), surface roughness, spatter and microcracks.
iii. Appropriate laser safety precautions need to be implemented.

Table 1 Hole dimensions of gas turbine components [53]

Components	Wall thickness (mm)	Diameter (mm)	Angle to the surface (°)	Number of holes
Nozzle guide vane	1.0–4.0	0.3–1.0	15	25–200
Turbine blade	1.0–3.0	0.3–0.5	15	25–200
Baseplate	1.0	0.5–0.7	30–90	10,000
Afterburner	2.0–2.5	0.4	90	40,000
Cooling ring	4.0	0.78–0.84	79	4200
Seal ring	1.5	0.95–1.05	50	180

iv. Optical setup needs regular maintenance.

Therefore, this chapter is focused on the laser drilling process taking into consideration both cost and quality aspects.

3 Laser Drilling

Laser drilling is a non-traditional machining process, which is extensively used in the aerospace industry for the machining of high strength and high-temperature resistant metals and alloys. Recently, the application of laser drilling for producing holes in aluminium matrix/silicon carbide reinforcement (Al/SiC) MMCs has been reported by researchers [49, 51, 93]. This technique is preferable compared to other manufacturing processes, especially in the drilling of aerospace components [52, 73]. It has been extensively adopted for producing cooling holes for aerospace gas turbine components, in particular combustors, nozzle guide vanes and high-pressure turbine blades [6].

In the laser drilling process, a high power laser beam is directed on the surface of the workpiece, where the optical energy of the laser beam is thermalized and rapidly heats the base material and converts it into its molten state as a result of thermal diffusion. Some of the energy is lost due to scattering and reflection of the laser beam. Depending on laser intensity material is removed in both the liquid and/or vapour states. The process of hole formation during laser drilling is shown in Fig. 1. If the laser intensity is high enough, the vaporisation will generate plasma and recoil pressure which helps in the ejection of molten metal and results in the formation of a hole cavity (Fig. 2a) [83]. To make the liquid metal removal more efficient high pressure assist gas can be used, as presented in Fig. 2b. Kinetic energy of the assist gas is used to expel liquid metal where the process doesn't need to rely on the vapour pressure. Assist gas pressure together with plasma and recoil pressures control material expulsion in the laser drilling process [66, 82].

Different types of methods are available for the laser drilling operation, which include single-pulse, percussion and trepan laser drilling. The following section outlines the description of these methods.

4 Methods of Laser Drilling

Laser drilling can be performed using different methods and laser types. Depending on the required applications, a particular method and laser are selected as indicated in Fig. 3.

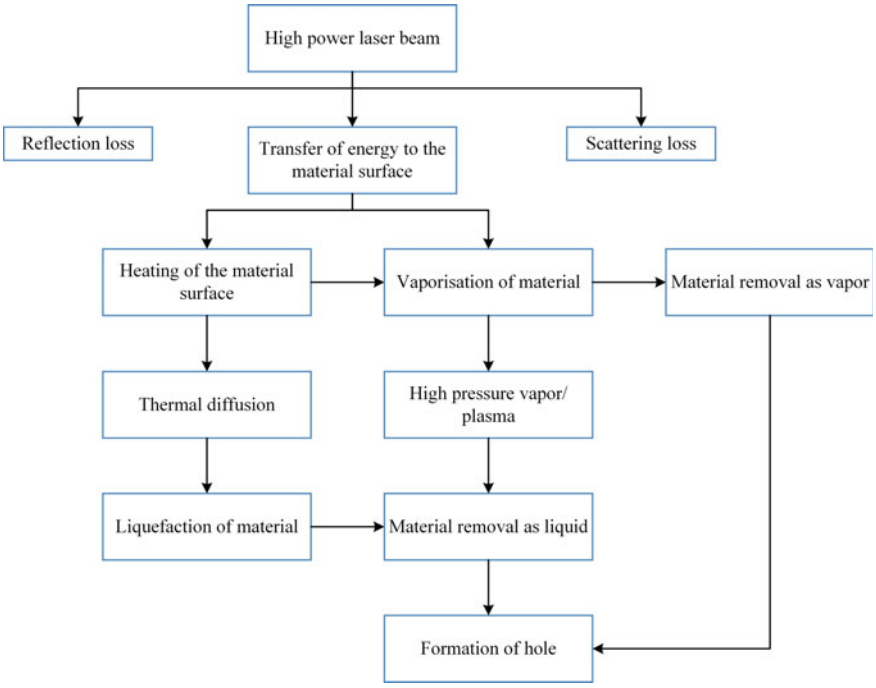

Fig. 1 Hole formation physical mechanism in the laser drilling process [56]

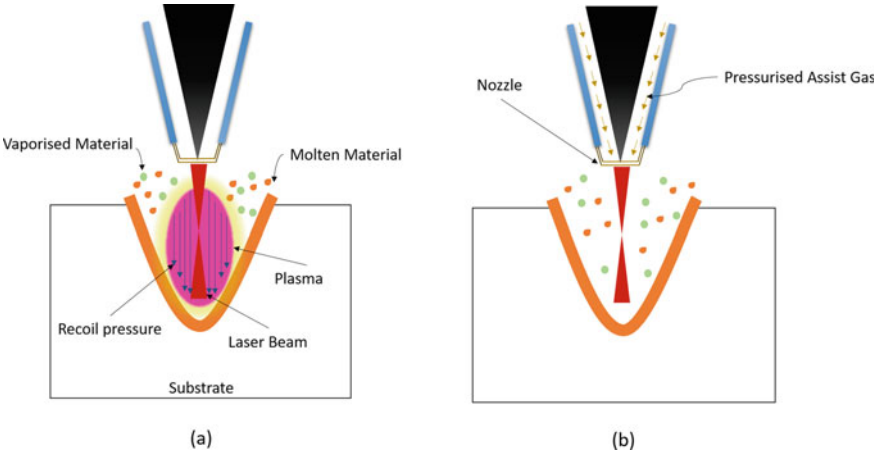

Fig. 2 Schematic of the laser drilling process: **a** vapour driven melt expulsion, **b** assist gas melt expulsion

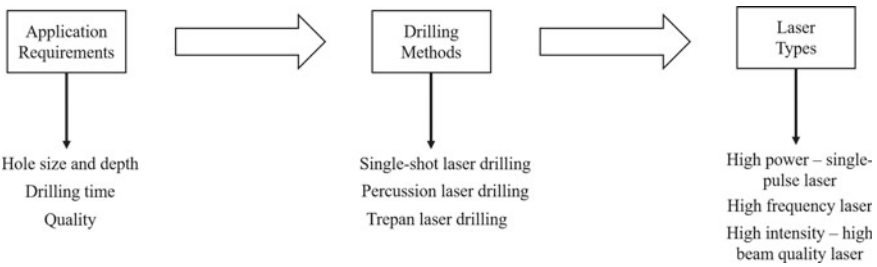

Fig. 3 Laser drilling methods and their application requirements

4.1 Single-Pulse Laser Drilling

Single-pulse laser drilling, also known as single-shot laser drilling is a simple method of drilling holes. It involves the use of a single pulse with high energy to create a hole throughout the material thickness. The maximum thickness of material that can be drilled is limited by the pulse energy of the laser. The hole size and quality depend on material thickness and spatial as well as temporal profiles of the laser beam [70].

Using this method, a large number of holes can be produced in a relatively short amount of time. This depends on laser frequency and the speed of the motion system. Single-pulse drilling is a better choice when productivity is the priority compared to quality [79]. It is to be noted that above certain thickness very high pulse energy lasers are required which are expensive, therefore this method is suitable for producing holes in thin sheet materials.

4.2 Percussion Laser Drilling

Percussion laser drilling involves a series of laser pulses fired at a particular spot of a material where each pulse generates a proportion of the hole. The productivity of this process is a function of pulse energy (edge depth per pulse) and pulse frequency.

Better hole quality can be attained with percussion drilling which depends on laser beam quality and its intensity profile; however, this process is slower in comparison to single-pulse drilling and requires more energy to drill a hole [79].

4.3 Trepan Laser Drilling

Trepan laser drilling or trepanning is employed to drill large diameter holes. This process begins by piercing a central hole into the material similar to percussion drilling; the laser beam is then moved in a spiral configuration using a motion control system to cut the required size hole. A significant benefit of this method is the delivery

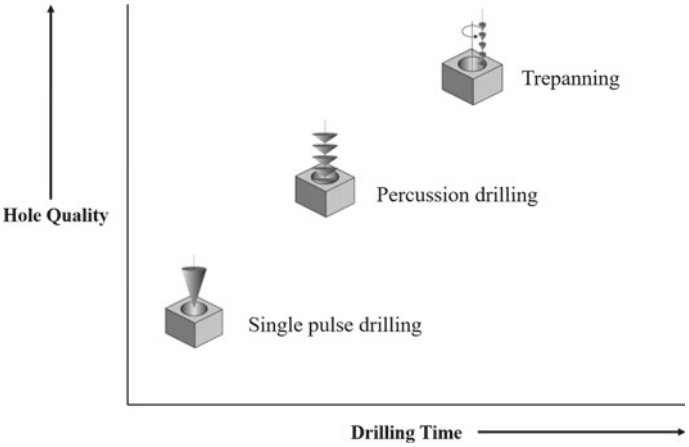

Fig. 4 Correlation between hole quality and drilling time for different laser drilling methods. *Source* Gautam and Pandey [25]

of good quality holes but it takes a more time compared to other methods [48]. Figure 4 shows hole quality and drilling time associated with various laser drilling methods. It is evident that trepanning is the best choice when hole quality is the priority. In trepanning, hole quality depends on the accuracy of the motion system [55].

5 Performance Measures

Performance of the laser drilling process depends upon efficient removal of (molten) material, hole quality and manufacturing cost. These performance measures are described in the following sections.

5.1 Material Removal Volume

Material removal is a key feature of the machining process. Laser drilling process involves the removal of molten material to produce a hole cavity. Material removal volume (MRV) indicates the volume of material removed per unit time when it is correlated with the process time, specified as mm^3/s [79]. It helps the users to calculate the speed of the drilling of any arbitrary hole by knowing the volume of material needed to be removed per hole. It also defines the energy efficiency of the process that is associated with the amount of material removed per unit joule of energy, usually measured in mm^3/J [23]. Energy consumption is also an important

cost driver of the laser drilling process, therefore it is reasonable to achieve higher MRV with lower energy consumption.

5.2 Hole Quality

Hole quality is of supreme concern in the aerospace industry. Several characteristics are used to judge the quality of laser drilled holes i.e. geometrical features (hole circularity, hole taper and surface roughness) and metallurgical features (microcracks, recast layer, spatter and heat affected zone) [25]. Detailed quality attributes are provided in the following sections.

5.2.1 Hole Circularity

Hole circularity defines the roundness of a hole. It varies with the deviation of the hole diameter across the circumference of a drilled hole as shown in Fig. 5. It is always important to increase hole circularity, which can be calculated by the following relation (1). In single-pulse and percussion drilling, hole circularity depends on the roundness of the laser spot and laser beam intensity profile. Whereas in trepanning it is influenced by the accuracy of the motion system.

$$H_c = \frac{D_{Min}}{D_{Max}} \tag{1}$$

where:

H_c = Hole circularity.
D_{Min} = Minimum hole diameter (mm).
D_{Max} = Maximum hole diameter (mm).

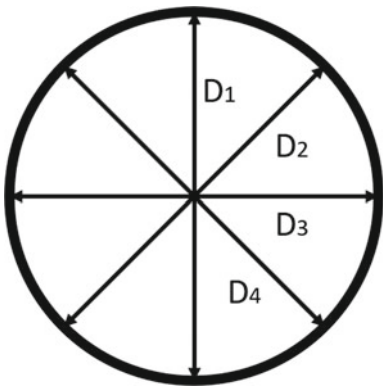

Fig. 5 Measurement of hole circularity

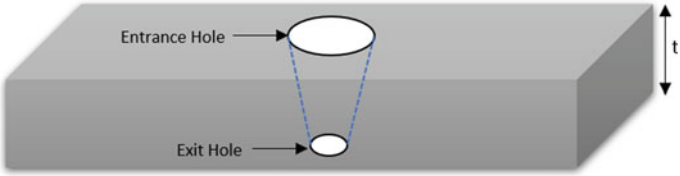

Fig. 6 Schematic representation of a (positive) hole taper

5.2.2 Hole Taper

Taper formation is an inherent characteristic of laser material processing. It is an important attribute which significantly influences drilled hole quality [4]. Near-zero hole taper is always desirable specifically in aeroengine components where close tolerances and high quality are strict requirements [7].

Hole taper angle is based on the entry and exit hole diameters of the drilled hole and can be calculated using the following relation (2).

$$\tan \theta = \frac{D_{ent} - D_{ex}}{2 \times t} \tag{2}$$

where:

θ = Taper angle.
D_{ent} = Entrance hole diameter (mm).
D_{ex} = Exit hole diameter (mm).
t = Material thickness (mm).

Taper angle can be positive or negative depending upon entrance and exit hole diameters. Figure 6 shows the position of hole taper where the exit hole side is smaller than the entry side (positive hole taper). The major cause of this drawback is the diffraction of the laser beam inside the hole cavity.

5.2.3 Surface Roughness

Surface roughness is one of the important factors considered for quality evaluation of laser drilled parts [86]. It refers to surface irregularities formed on the inner side of the hole which is a product of recast layer. It also reflects the dynamics of the liquid film prior to solidification and local reflectivity of the laser beam. It is usually measured as the arithmetic mean of absolute values of the vertical deviations of the actual surface from the ideal or nominal surface profile over the defined evaluation length, as presented in Fig. 7. A small deviation presents a smooth surface and if the deviation is large the surface obtained is rough. A smooth and uniform surface is required to ensure smooth airflow and avoid turbulence specifically for turbine blades [33]. Surface roughness is majorly influenced by laser intensity, laser power and trepan speed [86, 88].

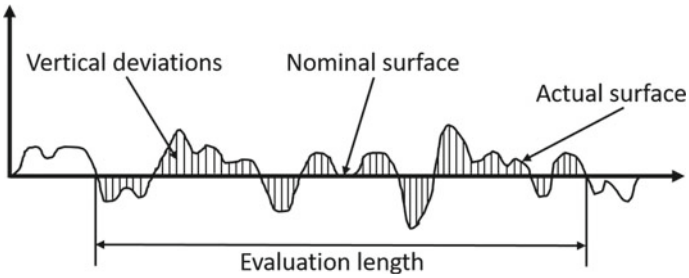

Fig. 7 Average surface roughness (Ra) representation [91]

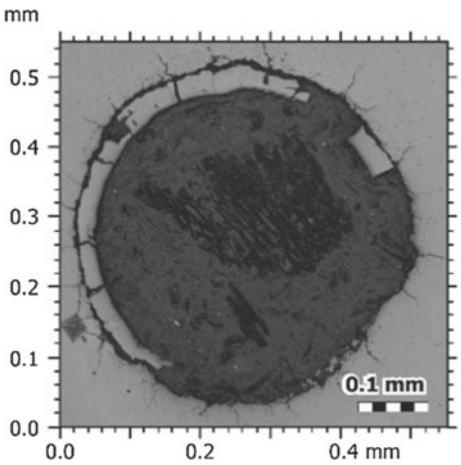

Fig. 8 Microcracks formation around a drilled hole (0.5 mm thick yttria-stabilized zirconia) [22]

5.2.4 Microcracks

Rapid drilling induces a high cooling rate in the material and in some cases may lead to the formation of microcracks [25]. Microcracks normally arise when drilling is performed in brittle or hard materials. The propagation of these cracks in operation affects the fatigue life of components leading to failure [59]. Figure 8 indicates microcracks formed on the laser drilled surface. Microcracks can be avoided by minimising thermal input into the material.

5.2.5 Recast Layer

During the laser drilling operation, some of the melted material is not removed appropriately and is re-solidified along the walls of the hole. This is known as a recast layer [25]. This layer has contrasting properties compared to the parent material. Sometimes, microcracks are also formed in the recast layer which adversely affect the component's integrity and its lifespan [59]. Therefore, recast layer formation

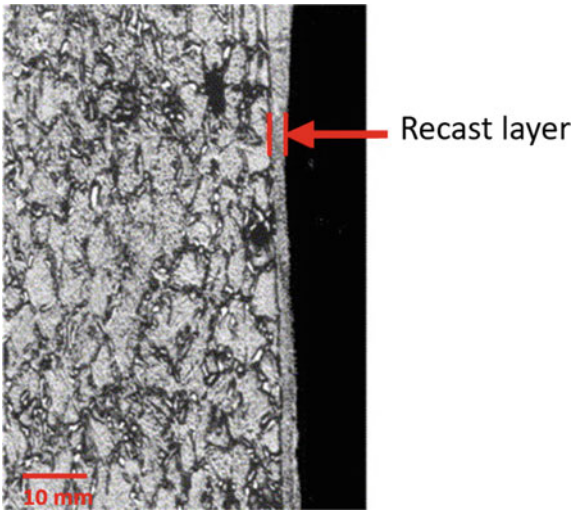

Fig. 9 Recast layer in a percussion drilled hole (4 mm thick IN 718) [7]

must be avoided. Figure 9 shows the recast layer in a percussion drilled hole. For a given material, recast layer depends on laser beam intensity. Higher the laser beam intensity more efficient is the material removal which ultimately reduces the chances of recast layer formation.

5.2.6 Spatter

Incomplete expulsion of melted material occasionally causes the scattering of molten droplets around the edges of the hole, which later resolidify. These droplets get stuck to the hole surface and are known as spatter [32]. It is an innate defect of the laser drilling process and is not desirable especially for effusion cooling applications, whereby the material surface is important for the efficiency and flow of the cooling air [45]. Figure 10 depicts the spatter area formed near the edges of laser drilled holes of a Nimonic sheet.

5.2.7 Heat Affected Zone

Laser drilling is a thermal process which involves the interaction of a laser beam with the surface of the workpiece. Higher temperature is involved in the process due to which the (mechanical, physical and chemical) properties of the workpiece surrounding the interaction area are changed. This results in the creation of a distinct zone known as a heat affected zone. The HAZ area is not melted, though lateral heat conduction produces a significant change in the microstructure. The microstructure interface clearly differentiates HAZ from the base material and the recast layer as shown in Fig. 11. HAZ is directly linked to pulse duration and laser beam intensity.

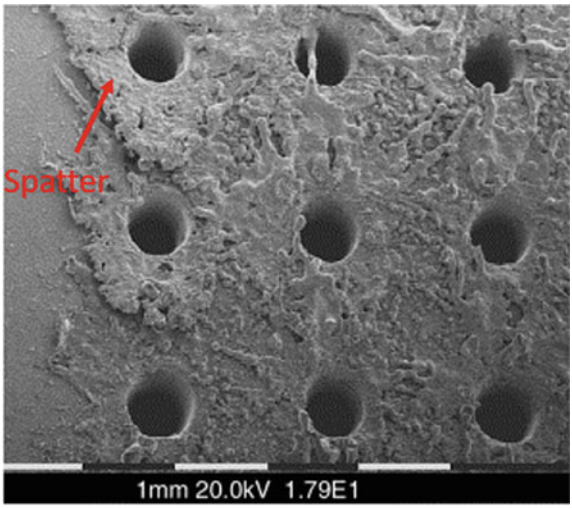

Fig. 10 SEM image of spatter deposited over the periphery of the holes (2.05 mm thick Nimonic PK 33) [45]

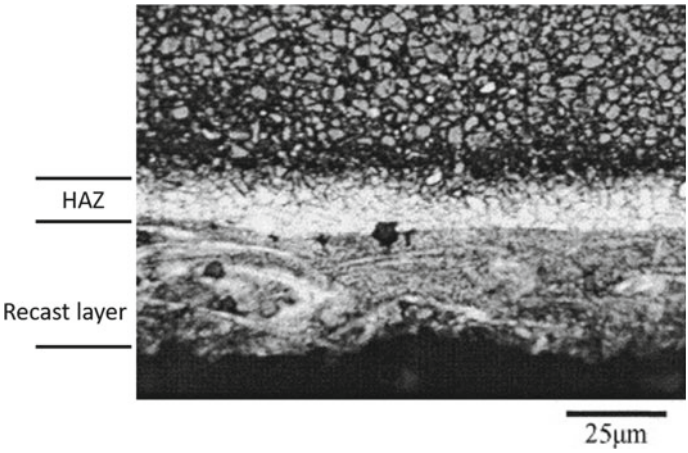

Fig. 11 HAZ and recast layer in laser drilled hole (8.0 mm thick IN 718) [6]

Low pulse duration allows less time for the energy to dissipate into the material. On the contrary, high laser beam intensity leads to efficient removal of molten material and results in less contact time between the hot liquid and bare material.

5.3 Manufacturing Cost

Manufacturing cost of a product plays an important role in its successful design and production. It is used for making several types of decisions for product designing and manufacturing. These decisions include:

- Material type to be utilised for the product
- Manufacturing process type to be used for the product
- Number of products to be manufactured
- Whether to buy or make the part/product
- Product design.

Product manufacturing cost is a major cost element of its selling price i.e. 40% (shown in Fig. 12), which further consists of various elements: labour cost (direct & indirect), material cost, equipment depreciation, energy and plant cost as illustrated in Fig. 13 [81]. It is important to estimate manufacturing cost as it assists the manufacturing companies to evaluate their performance and effectiveness [16].

There are different ways of drilling and each of them has a different quality and associated manufacturing cost which is essential to understand for the user. With single-pulse drilling, manufacturing cost can be reduced but at the expense of hole quality; on the other hand, trepanning gives good hole quality but the manufacturing cost is higher. This shows that there is a trade-off between quality and manufacturing cost. All these factors depend on the process parameters which are discussed in the following sections.

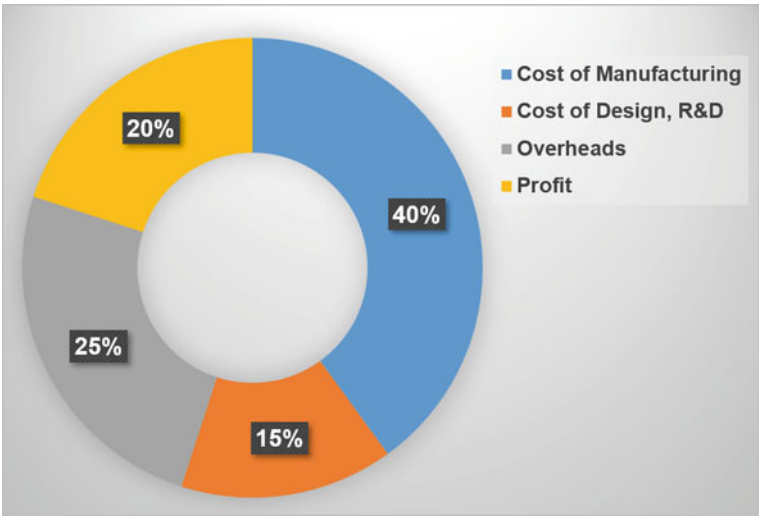

Fig. 12 Product selling price cost elements [81]

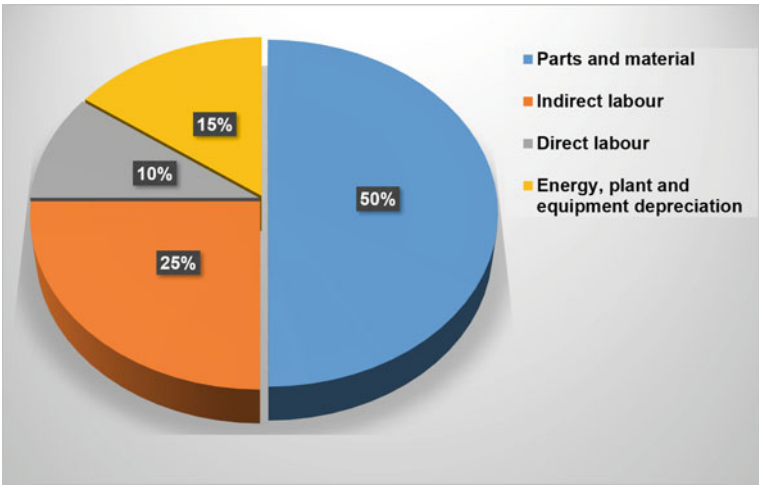

Fig. 13 Manufacturing costs elements [81]

6 Laser Drilling Process Parameters

Different parameters are involved in the practical implementation of the laser drilling process. Yeo et al. [92] grouped these parameters into five main categories, as shown in Fig. 14. Laser pulse parameters include pulse energy, pulse duration, pulse frequency and the number of pulses. Environment conditions are the surrounding temperature and humidity level. Material based parameters include material reflectivity, thickness and type of material. Optical setup involves beam shape, intensity profile, focal length and focal position of the laser beam. Assist gas based parameters are gas pressure, nozzle design and the type of assist gas employed. The performance and efficiency of the process depend on an appropriate selection of these parameters.

6.1 Pulse Energy and Pulse Duration

Pulse energy and pulse duration are the critical process parameters of laser drilling. Pulse energy provides the energy to melt or vaporise a proportion of the material. Pulse duration or pulse width determines the duration at which this energy is applied as shown in Fig. 15. Depending on laser specifications, the ranges of pulse duration and pulse energy can be varied and have a significant impact on the hole characteristics [25].

Both of these parameters are interdependent (see Eq. 3) and define the laser peak power that controls the rate at which pulse energy is applied into the material [48]. To attain the same pulse energy with a short pulse width, higher peak power is required. There is a significant impact of peak power on the material removal process. Higher

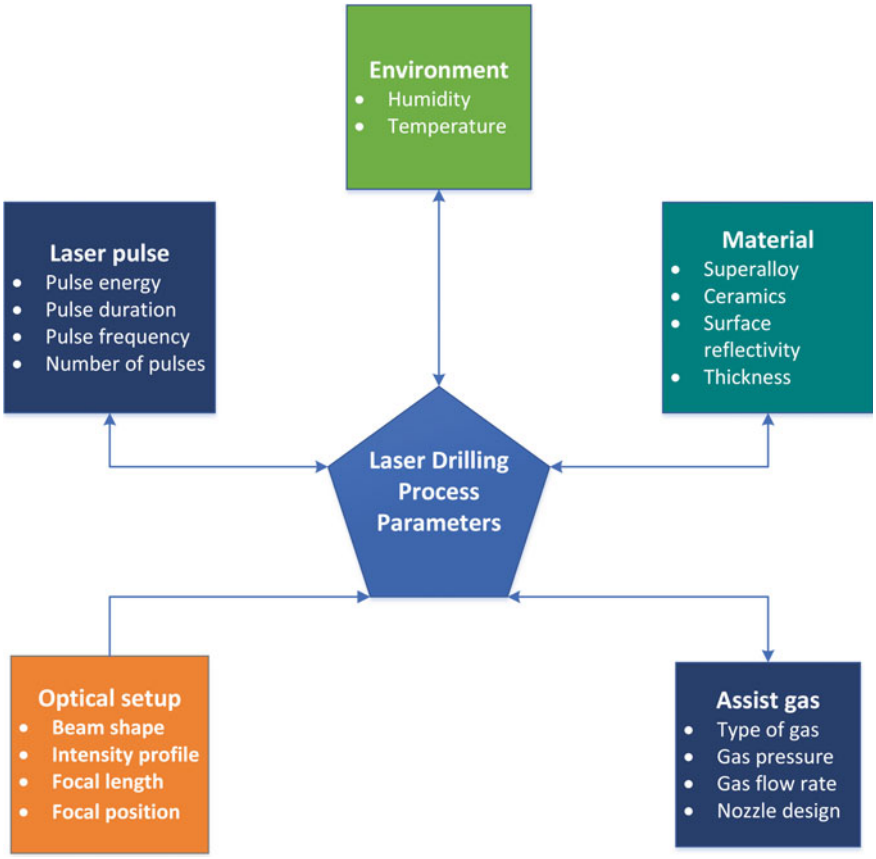

Fig. 14 Classification of process parameters

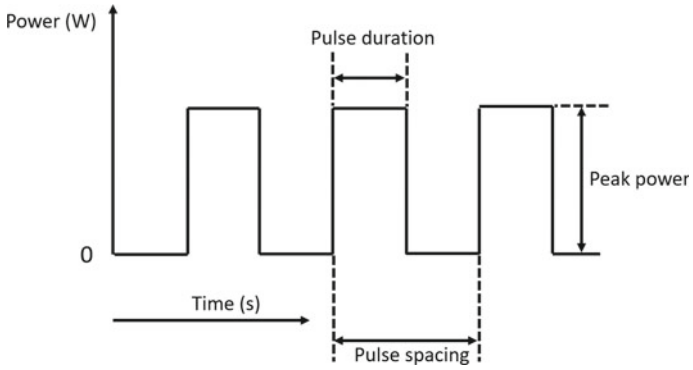

Fig. 15 Laser pulse waveform

peak power with short pulse duration typically leads to rapid melting and high vapour pressure which subsequently accelerates liquid (molten metal) removal [79]. It has been noted that drilling with high peak power significantly reduces hole taper [31, 57], recast layer thickness [6, 14, 61] and microcracks [59].

$$Peak\ power = \frac{Pulse\ energy}{Pulse\ duration} = \frac{joule(J)}{second(s)} = watt(W) \tag{3}$$

It is clear from Eq. (3) that peak power is directly proportional to pulse energy and inversely proportional to pulse duration. High pulse energy helps to remove the molten material outside the hole cavity and therefore reduces the RLT [14] and microcracking [15]. On the other hand, hole taper increases with an increase in pulse energy [12, 78]. Generally, long pulse duration produces large diameter and deeper hole because of sufficient laser beam-workpiece interaction time [8], however, too long pulse duration is not ideal for laser drilling as it produces a large HAZ [57]. Short pulse duration is found to produce a very small difference between entry hole and exit hole diameters because of the high-power intense laser beam [12, 30] and also reduces microcracking [15]. The above mentioned studies have revealed a significant influence of pulse energy and pulse duration on drilled hole quality, therefore it is important to select a suitable value for these parameters.

6.1.1 Single-Pulse Drilling

Single-pulse drilling employs one high-energy laser pulse to perform the drilling operation. The laser pulse can be of a short pulse duration with high peak power (Fig. 16a) or long pulse duration with low peak power (Fig. 16b), each has a significant impact on hole characteristics. The combination of short pulse width with high peak power is recommended as it improves repeatability of hole diameter [65] and hole circularity [28, 65].

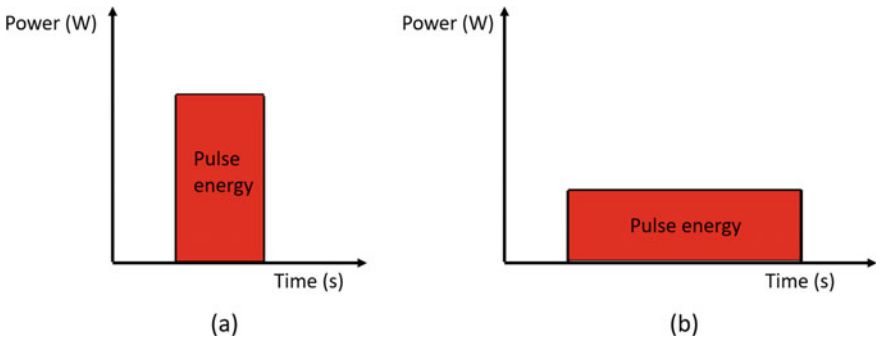

Fig. 16 Schematic representation of single-pulse drilling regimes: **a** higher peak power, **b** lower peak power

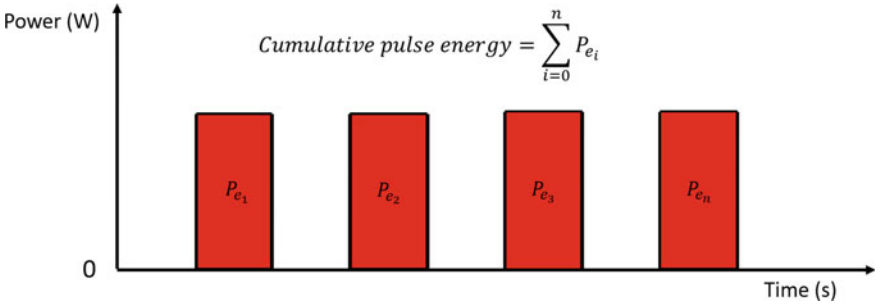

Fig. 17 Schematic representation of cumulative pulse energy—percussion drilling

6.1.2 Percussion

In case of percussion drilling, more than one number of pulses are involved therefore the energy transferred to the material is calculated as cumulative pulse energy i.e. a total sum of energy associated with each pulse, as shown in Fig. 17. Typically, the cumulative pulse energy required to drill a hole is higher in comparison to single-pulse drilling due to pulse off stage in percussion drilling which allows the molten metal to solidify. Laser pulse off time depends on the duty cycle and pulse frequency. This indicates that the number of pulses and pulse frequency are also important parameters. These are explained in the following sections.

6.2 Number of Pulses

In laser drilling an increase in the number of pulses helps to remove material from the bottom side of a hole, after the formation of through-hole, and consequently produces lower hole taper [26, 29, 41, 64, 79]. Circularity of holes also improves with higher number of pulses [34]. However, spatter volume can be minimised using a smaller number of pulses [90].

6.3 Pulse Frequency

Pulse frequency controls the number of laser pulses fired per second. It also defines the average power of the laser that can be calculated by using the following Eq. (4).

$$\begin{aligned} Average\ power &= Pulse\ energy \times Pulse\ frequency \\ &= (joule(J)) \times 1/(second(s)) = watt(W) \end{aligned} \tag{4}$$

Hole quality is significantly influenced by the change in pulse frequency [63]. At high pulse frequency, the time gap between consecutive pulses is short which reduces the chances of heat loss due to convection and allows sufficient energy to enter into the workpiece material [79]. Lower hole taper with less RLT can be obtained with high pulse frequency [6, 12, 29, 57, 68]. On the contrary, HAZ increases with pulse frequency [57]. High average power (frequency) lasers and high energy lasers are expensive; therefore the type of process and laser used should be carefully selected.

6.4 Material Properties and Environment

Material properties have a considerable effect on laser drilling performance. The (reflective) characteristics of a material surface directly influence the amount of energy absorbed during the laser drilling operation. Reflectivity or absorptivity is required to calculate the amount of energy absorbed by the material as indicated in Eq. (5) [74]. Single-pulse drilling is more sensitive to material reflectivity, whereas in percussion drilling there is a preheating effect and absorptivity increases with subsequent pulses.

$$E_{abs} = A \times P \times D_p \tag{5}$$

where:

E_{abs} = Energy absorbed by the material (J).
A = Material absorptivity (1 − Reflectivity).
P = Applied laser power (W).
D_p = Pulse duration (s).

In addition to this, the thermal conductivity of material also affects process efficiency. It is obvious that materials with high thermal conductivity transfer heat quickly throughout the workpiece instead of rapidly heating the targeted zone, therefore more time is needed to reach the melting state [84]. Material thickness is a significant influencing factor related to the geometry and metallurgical features of hole quality. Hole taper decreases with an increase in material thickness. On the contrary, spatter and recast layer increase when thicker material is used [6].

Environmental factors including humidity, mist, dust, ambient temperature and machine vibration also influence laser performance. Moreover, the surface of optical elements should be cleaned and contain no oil vapour or dust particles as these damage the optical system [75].

6.5 Beam Shape and Intensity Profile

The temporal profile of a laser beam defines the intensity distribution and material removal capability of a laser pulse [92]. Gaussian beam profile is generally used in

the laser drilling process as it provides a small focused spot and high laser beam intensity which results in efficient removal of molten material [87]. Diameter and roundness of a laser beam directly affect the dimensions of a hole. The size of a hole is directly dependent on beam size. The smallest beam size of a particular laser system is determined by its optics and the optical settings.

6.6 Focal Length and Focal Position

Focal length is the distance from the centre of the lens to the focal point (see Fig. 18). Hole characteristics are greatly influenced by a change in focal length since this directly effects the beam spot size that is related with the laser power density, as shown in Eqs. (6) and (7) [1]. High power density is associated with shorter focal length and therefore results in higher melt removal. On the other hand, the spatter area increases with shorter focal length [43].

$$S_d = F_l \times \emptyset \tag{6}$$

$$P_d = \frac{P}{A_s} = \frac{4P}{\pi S_d^2} \tag{7}$$

where:

S_d = (min) spot diameter (mm).
F_l = Focal length (mm).
$\emptyset$ = Beam divergence (angle).
P_d = (max) Laser power density (W/mm^2).
P = Applied laser power (W).
A_s = Cross-sectional area of the laser spot (mm^2).

Focal position of a laser beam is divided into three categories based on its position relative to the workpiece surface (see Fig. 19) [34]:

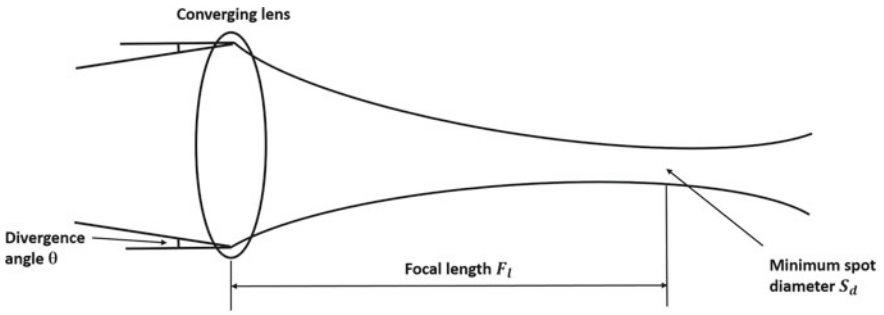

Fig. 18 Focus pattern of a laser beam

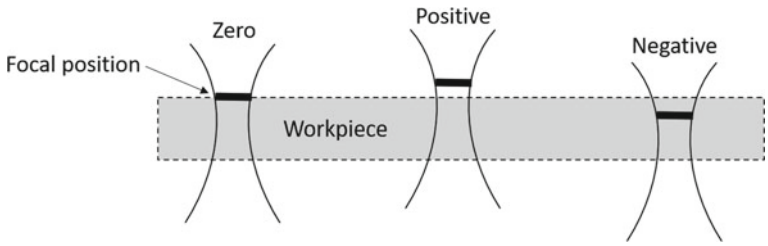

Fig. 19 Schematic diagram showing the variation of focal position [27]

Zero: when the focal position of the laser beam is located exactly at the workpiece surface
Positive: when the focal position of the laser beam is located above the workpiece surface
Negative: when the focal position of the laser beam is located below the workpiece surface.

Focal position significantly affects the quality and geometry of a hole. Minimum RLT was noticed by Marimuthu et al. [48] and Leigh et al. [41] when the focal position of the laser beam was maintained exactly at the workpiece surface. The circularity of holes has also been shown to increase with zero focal plane position [34]. Shin and Mazumder [85] found a significant improvement in the values of hole taper with zero focal plane position.

6.7 Assist Gas

In the laser drilling process, an assist gas is employed to facilitate the removal of molten material and to blow out the recast layer and spatter which is deposited inside and on the top of the hole cavity, respectively. Different types of assist gases are utilised for the laser drilling operation. They are broadly classified as reactive gases or inert gases. Reactive gases provide additional exothermic energy as a result of chemical reaction between the molten metal and the gas and subsequently improve drilling efficiency. Oxygen and compressed air are categorised as reactive gases [72]. On the other hand, inert gases only provide kinetic energy to evacuate the molten material from the hole cavity without undergoing any chemical reaction. Nitrogen and argon fall under this category. The quality of the drilled hole is significantly affected by the type of assist gas employed [4]. Low et al. [44] observed lower spatter thickness with weak bonding strength when using oxygen as the assist gas. On the contrary, the drilling edge is oxidised which requires further cleaning [89]. Compressed air is the cheapest option but the disadvantages associated with this gas are the formation of dross and an oxidised surface. Using inert gases (nitrogen and argon), these oxidation scales can be avoided. Marimuthu et al. [49] compared

the quality of laser drilled holes using different assist gases. A regular hole profile with minimum RLT was obtained with argon and nitrogen compared to oxygen and compressed air.

The gas pressure must be enough to overcome the surface tension holding the liquid (molten) metal so that the liquid can be ejected. The value of gas pressure influences hole quality. Higher gas pressure facilitates the removal of molten material along the sidewalls and therefore results in less RLT [14, 48] and lower hole taper [12]. On the other hand, excessive gas pressure is also not desirable as it results in the formation of microcracks due to the phenomena of rapid solidification [14].

The nozzle design also affects hole quality. Biffi and Previtali [10] designed an innovative nozzle and achieved a significant decrease in spatter compared to a standard nozzle. Low values of recast layer were reported by Khan et al. [39] when a small nozzle diameter was used.

Proper control of these process parameters is necessary as they significantly influence performance of the process. Influence of laser drilling process parameters on the selected performance measures is provided below.

7 Effect of Process Parameters on MRV

The laser drilling process is associated with the removal of molten material to produce a particular hole geometry. Process efficiency depends on the volume of material removed versus the amount of energy applied. Higher MRV is always desirable with less energy input as it improves process efficiency. Additionally, MRV and process duration define the productivity of the process where higher MRV with less process duration is required for improved productivity.

There are various process parameters which influence MRV in laser drilling. This section covers previous research work conducted by researchers to study MRV in connection with the laser drilling process.

Low et al. [43] examined the laser drilling parameters influencing melt removal during percussion drilling. They concluded that pulse width and peak power directly influence MRV.

Fysikopoulos et al. [23] examined the impact of laser power and pulse frequency on the energy efficiency of the laser drilling process. For energy efficiency, MRV was calculated against the energy applied. It was revealed that increase in laser power and pulse frequency enhances process efficiency.

Panda et al. [68] selected oxygen as an assist gas and studied the variation in MRR. It was found that higher gas flow rate increases MRR. Goyal and Dubey [30] reported that higher gas pressure provides sufficient drag force that facilitates in removing the melt material. Wang et al. [89] analysed the effects of assist gas including oxygen and argon on drilling efficiency. Improved efficiency was reported using oxygen as an assist gas due to its combustible-supportability that generates excessive heat and results in higher MRV.

Sarfraz et al. [79] investigated the effects of laser drilling parameters on IN718 superalloy using three different laser drilling processes. Material removal rate (MRR) was calculated using MRV and drilling time. The results showed that pulse width, number of pulses and trepan speed are the most important parameters that influence MRR.

Biscaia et al. [11] conducted experiments on nickel superalloy using trepan laser drilling to explore the influence of process parameters on MRR. Results indicated trepan speed as the significant parameter influencing MRR. Higher trepan speed produced higher MRV with reduced drilling time.

An investigation was performed by Parthipan and Ilangkumaran [69] to examine the material removal rate and surface roughness of laser drilled holes in Cu-Ni-Tib_2 MMC. Response surface methodology (RSM) approach was used to describe the relationship between material removal rate and drilling parameters. Then the optimal process parameters (pulse energy, laser power, gas pressure) were determined for higher MRR and better surface roughness.

8 Effect of Process Parameters on Hole Quality

Different experimental studies have been performed by researchers to study the impact of laser drilling process parameters on hole quality. These aim to enhance the quality attributes of the laser drilled holes.

Taper control is the most important issue during the laser drilling process. High value manufacturing industries dealing with aircraft engine components demand holes without any taper. Different factors influence hole taper, the following studies address the significant process parameters.

Bandyopadhyay et al. [7] investigated the hole taper of laser drilled holes produced in titanium alloy and nickel superalloy sheets. Pulse duration, pulse energy and focal position were found to be significant parameters affecting hole taper. Low levels of pulse duration and pulse energy with zero focal position resulted in improvement of hole taper. In another study, Bandyopadhyay et al. [6] found that increase in material thickness caused improvement in hole taper.

Kacar et al. [37] observed the influence of pulse duration and peak power on hole taper using alumina ceramic. An increase in pulse duration and peak power produced an improvement in hole taper.

A study was conducted by Mishra and Yadava [58] on laser drilling of IN 718 sheet. Results showed improvement in hole taper with an increase in pulse frequency. Bathe and Padmanabham [9] reported the influence of laser drilling parameters using TBC (thermal barrier coated) IN 718 as a substrate. Pulse duration produced a significant impact on hole taper. Decreasing pulse duration produced a reduction in hole taper.

Goyal and Dubey [30] investigated the impact of laser drilling parameters on hole taper of laser drilled IN 718 sheet. Hole taper was found to decrease with an increase in trepan speed and pulse frequency. Similar findings were reported by Dhaker and Pandey [18].

Bahar et al. [4] showed the importance of laser power and laser frequency in the laser drilling process. They reported that higher laser power and increased pulse frequency help to improve hole taper. The study also revealed that comparing the effect of compressed air, oxygen and nitrogen on hole taper, improved hole quality was obtained with compressed air and nitrogen. Shin and Mazumder [85] stated that hole taper can be improved when higher laser power is applied with lower trepan speed and zero focal position.

Chatterjee et al. [12] explored studies on laser drilling of titanium alloy. Pulse duration, pulse energy, pulse frequency and gas pressure were varied to observe their effects on hole taper. They stated that increasing pulse frequency and gas pressure resulted in improvement of hole taper. It was also discovered that hole taper was increased by increasing pulse energy and pulse width. Chatterjee et al. [13] conducted another study on stainless steel (AISI 316). Similar results were found for this material except for gas pressure and pulse energy effects due to a difference in material properties.

Sarfraz et al. [79] conducted experiments to investigate the impacts of pulse energy, pulse frequency, number of pulses, pulse duration and trepan speed on hole taper. Pulse duration and pulse energy produced the most significant effect on hole taper.

Padhee et al. [67] examined the impact of number of pulses and pulse width on the taper angle of drilled holes produced on (Al/SiC) MMC. Improvement in taper angle was observed when lower number of pulses and lower pulse width was applied. Moreover, the impact of concentration (wt%) of SiC particulates on hole taper was studied. It was noted that higher concentration of SiC increases hole taper.

Marimuthu et al. [49] studied the characteristics of holes during laser drilling of (Al/SiC) MMC. It was observed that less energy is required to drill holes with acceptable quality in (Al/SiC) MMC in contrast to isotropic metals or alloys. In another study, Marimuthu et al. [50] investigated the water jet guide (WJG) laser drilling of the same material. WJG laser drilling produced better hole quality with less taper, no recast layer and improved hole circularity compared to conventional laser drilling.

9 Effect of Process Parameters on Manufacturing Cost

The laser drilling process depends on several process parameters that affect process efficiency and product quality as described above. Sarfraz et al. [76, 78] specified that these process parameters also influence manufacturing cost. These researchers provided a cost breakdown structure of the laser drilling process and identified cost drivers involved in the process. Detailed work has been reported by Sarfraz et al. [80] depicting the laser drilling process parameters impact on manufacturing cost. Pulse duration was reported as the most significant parameter affecting the drilling cost followed by gas flow rate and pulse energy. However, the work was only limited to the single-pulse drilling process.

Besides the laser processing parameters, there are other factors involved which contribute to the laser drilling manufacturing cost. These factors are discussed in the following section.

10 Cost of Laser Drilling

Manufacturing cost estimation is essential for companies targeting to become successful in the current competitive scenario. One of the important tasks of cost estimation is to establish a work breakdown structure (WBS). The main purpose of a WBS is to provide a uniform structure incorporating all the elements of the process that will be specified by the cost estimate, where each element represents the cost required to execute that process. When a WBS includes all the cost information, it may serve directly as a cost breakdown structure [62]. The operating costs breakdown structure of a laser drilling process is presented in Fig. 20.

Cost estimation requires an identification of cost drivers i.e. those factors which significantly influence the cost. The total cost is changed with a small modification to a single cost driver. It is possible to generate a comprehensive cost estimate for a particular process only if all of its cost drivers are identified [62].

The main cost drivers relevant to the laser drilling process are provided in Table 2. Equipment running cost, maintenance, material and labour costs are the key drivers in laser drilling cost estimation. It was identified that equipment running cost further consists of equipment depreciation, electrical (power) consumption, components replacement, gas consumption, component handling and overhead costs. When all cost drivers are finalised, a cost is allocated to each driver and the total process cost can be calculated.

The selection of an appropriate laser source is also important as it affects the cost efficiency of the process [19]. Nd:YAG and fibre lasers are the most commonly used laser sources for drilling in the industry. A comparison between these two lasers is

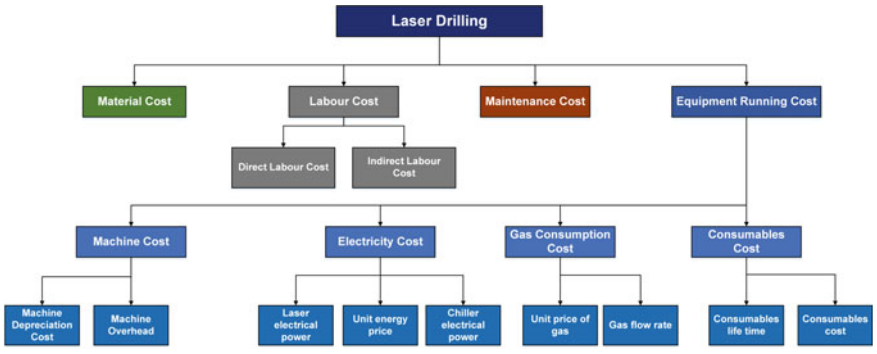

Fig. 20 Cost breakdown structure

Table 2 Cost drivers of the laser drilling process

Cost drivers	Yeo et al. [92]	Baisev and Powell [8]	Ion [36]	Dahotre and Harimkar [17]	Sarfraz et al. [77]
Equipment running cost	Equipment depreciation	Equipment depreciation	Equipment depreciation	Equipment depreciation	Equipment depreciation
	Electrical consumption	Electrical consumption	Electrical consumption	Electrical (power) consumption	Electrical consumption
	Replaceable components (lenses, flash lamp, filters)	Replaceable components (lenses, laser pumps)	Replaceable components (lenses, flash lamps)		Replaceable components (lenses, flash lamp, filters, nozzle)
	Gas consumption		Gas consumption		Gas consumption
		Component handling		Component handling	Component handling
		Overhead	Overhead	Overhead	Overhead
Maintenance		Equipment maintenance	Equipment maintenance		Equipment maintenance
Material				Material cost	Material cost
Labour		Labour (operator) cost	Labour (laser operators and engineers) cost	Labour cost	Labour cost

provided in Table 3. It is noted that the purchase cost of a fibre laser is higher than Nd:YAG but its running cost is much lower because of higher electrical efficiency and longer operating life. Nd:YAG laser does require periodic maintenance and service for the alignment, cleaning and replacement of optics, on the other hand, a fibre laser is maintenance free. It is important to mention that these laser sources have different beam quality, which ultimately affects hole quality and productivity [19, 40]. Therefore, it is important to evaluate the laser source being used for the drilling.

Table 3 Fibre laser and Nd:YAG laser comparison

	Fibre laser	Nd:YAG laser
Laser capital cost	Higher	Lower
Laser operating cost	Lower	Higher
Electrical efficiency	Higher	Lower
Operating life	Longer	Shorter
Maintenance	Low	High

11 Concluding Remarks and Future Perspectives

11.1 Conclusions

Laser drilling is a well-established technology exclusively in the aerospace sector, where this process involves large volume production of holes. In this chapter, single-shot, percussion and trepan laser drilling methods are discussed. Performance measures of the laser drilling process including material removal volume, hole quality attributes and manufacturing cost are explained.

Different laser drilling process parameters are extensively discussed, and the existing literature depicting the attention of several authors towards this advanced machining process is presented. The performance of the laser drilling process can be enhanced when proper selection and control of process parameters are applied. Furthermore, the cost factors of the laser drilling process are explained within this chapter. It is observed that the laser source affects the cost efficiency of the drilling process along with productivity and hole quality.

11.2 Future Research Trends

Because of their superior properties, metal matrix composites are potential candidate materials for use in aeroengine components. However, limited documented knowledge is available discussing the performance of laser drilling of MMCs. Exploring the behaviour of MMCs against the applied laser drilling parameters is, therefore, necessary to find out the best combination of process parameters for optimum hole quality.

It is noted that the laser drilling process parameters have a substantial impact on the manufacturing cost of the process. Therefore, there is a need to examine the impact of process parameters on the manufacturing cost along with the economic implications of the laser drilling process.

It is also specified that the product quality and the manufacturing cost are interdependent and both depend on the applied process parameters. Consequently, connecting the quality attributes with the manufacturing cost is a knowledge gap that can be covered in a future study.

Different types of laser drilling methods are available to perform the drilling operation. From the available literature, it has been found that there is a lack of research characterising laser drilling methods in terms of economic and quality perspectives. Therefore, a model can be developed to provide a comprehensive understanding for the designers and practitioners to select a suitable laser drilling technique for the required cost and quality attributes.

References

1. Adelmann B, Hellmann R (2015) Rapid micro hole laser drilling in ceramic substrates using single mode fiber laser. J Mater Process Technol 221:80–86. https://doi.org/10.1016/j.jmatprotec.2015.02.014
2. Akhil R (2018) A study on recent trends in the applications of metal matrix composites. Int J Res Appl Sci Eng Technol 6:172–180. https://doi.org/10.22214/ijraset.2018.5027
3. Anderson M, Patwa R, Shin YC (2006) Laser-assisted machining of Inconel 718 with an economic analysis. Int J Mach Tools Manuf 46:1879–1891. https://doi.org/10.1016/j.ijmachtools.2005.11.005
4. Bahar ND, Marimuthu S, Yahya WJ (2016) Pulsed Nd: YAG laser drilling of aerospace materials (Ti-6Al-4V). IOP Conf Ser Mater Sci Eng 152:012056. https://doi.org/10.1088/1757-899X/152/1/012056
5. Bains PS, Sidhu SS, Payal HS (2016) Fabrication and machining of metal matrix composites: a review. Mater Manuf Process 31:553–573. https://doi.org/10.1080/10426914.2015.1025976
6. Bandyopadhyay S, Sundar JKS, Sundararajan G, Joshi SV (2002) Geometrical features and metallurgical characteristics of Nd:YAG laser drilled holes in thick IN718 and Ti-6Al-4V sheets. J Mater Process Technol 127:83–95. https://doi.org/10.1016/S0924-0136(02)00270-4
7. Bandyopadhyay S, Gokhale H, Sundar JKS et al (2005) A statistical approach to determine process parameter impact in Nd:YAG laser drilling of IN718 and Ti-6Al-4V sheets. Opt Lasers Eng 43:163–182. https://doi.org/10.1016/j.optlaseng.2004.06.013
8. Basiev TT, Powell RC (2004) Handbook of laser technology and applications. Institute of Physics Publishing, Bristol, Philadelphia
9. Bathe R, Padmanabham G (2014) Evaluation of laser drilling of holes in thermal barrier coated superalloys. Mater Sci Technol 30:1778–1782. https://doi.org/10.1179/1743284713Y.0000000477
10. Biffi CA, Previtali B (2013) Spatter reduction in nanosecond fibre laser drilling using an innovative nozzle. Int J Adv Manuf Technol 66:1231–1245. https://doi.org/10.1007/s00170-012-4402-y
11. Biscaia RVB, Ribas MT, Júnior AB (2020) Effects of processing parameters on the micro-drilling through fast hole electroerosion and laser trepanning in Inconel 718. Int J Adv Manuf Technol 106:31–45. https://doi.org/10.1007/s00170-019-04394-7
12. Chatterjee S, Mahapatra SS, Bharadwaj V et al (2018) Drilling of micro-holes on titanium alloy using pulsed Nd:YAG laser: parametric appraisal and prediction of performance characteristics. Proc Inst Mech Eng Part B J Eng Manuf 233:1872–1889. https://doi.org/10.1177/0954405418805604
13. Chatterjee S, Mahapatra SS, Bharadwaj V et al (2018) Quality evaluation of micro drilled hole using pulsed Nd:YAG laser: a case study on AISI 316. Lasers Manuf Mater Process 5:248–269. https://doi.org/10.1007/s40516-018-0067-1
14. Chien WT, Hou SC (2007) Investigating the recast layer formed during the laser trepan drilling of Inconel 718 using the Taguchi method. Int J Adv Manuf Technol 33:308–316. https://doi.org/10.1007/s00170-006-0454-1
15. Corcoran A, Sexton L, Seaman B et al (2002) The laser drilling of multi-layer aerospace material systems. J Mater Process Technol 123:100–106. https://doi.org/10.1016/S0924-0136(01)01123-2
16. D'Urso G, Quarto M, Ravasio C (2017) A model to predict manufacturing cost for micro-EDM drilling. Int J Adv Manuf Technol 91:2843–2853. https://doi.org/10.1007/s00170-016-9950-0
17. Dahotre NB, Harimkar S (2008) Laser fabrication and machining of materials. Springer Science & Business Media, New York, USA
18. Dhaker KL, Pandey AK (2019) Particle swarm optimisation of hole quality characteristics in laser trepan drilling of Inconel 718. Def Sci J 69:37–45. https://doi.org/10.14429/dsj.69.12879
19. Dietrich J, Blaesius C, Brief S, Kelbassa I (2011) Drilling with fiber lasers. In: International congress on applications of lasers & electro-optics. Laser Institute of America, pp 473–477

20. Dubey AK, Yadava V (2008) Laser beam machining-a review. Int J Mach Tools Manuf 48:609–628. https://doi.org/10.1016/j.ijmachtools.2007.10.017
21. Dubey AK, Yadava V (2008) Experimental study of Nd:YAG laser beam machining—an overview. J Mater Process Technol 195:15–26. https://doi.org/10.1016/j.jmatprotec.2007.05.041
22. Feng D, Shen H (2019) Hole quality control in underwater drilling of yttria-stabilized zirconia using a picosecond laser. Opt Laser Technol 113:141–149. https://doi.org/10.1016/j.optlastec.2018.12.019
23. Fysikopoulos A, Stavropoulos P, Salonitis K, Chryssolouris G (2012) Energy efficiency assessment of laser drilling process. Phys Procedia 39:776–783. https://doi.org/10.1016/j.phpro.2012.10.100
24. Ganji DK, Rajyalakshmi G (2020) Influence of alloying compositions on the properties of nickel-based superalloys: a review. In: Recent advances in mechanical engineering. Springer, pp 537–555
25. Gautam GD, Pandey AK (2018) Pulsed Nd:YAG laser beam drilling: a review. Opt Laser Technol 100:183–215. https://doi.org/10.1016/j.optlastec.2017.09.054
26. Ghoreishi M, Low DKY, Li L (2002) Statistical modelling of laser percussion drilling for hole taper and circularity control. Proc Inst Mech Eng Part B J Eng Manuf 216:307–319. https://doi.org/10.1243/0954405021519988
27. Ghoreishi M, Low DKY, Li L (2002) Comparative statistical analysis of hole taper and circularity in laser percussion drilling. Int J Mach Tools Manuf 42:985–995. https://doi.org/10.1016/S0890-6955(02)00038-X
28. Ghoreishi M (2006) Statistical analysis of repeatability in laser percussion drilling. Int J Adv Manuf Technol 29:70–78. https://doi.org/10.1007/s00170-004-2489-5
29. Ghoreishi M, Nakhjavani OB (2008) Optimisation of effective factors in geometrical specifications of laser percussion drilled holes. J Mater Process Technol 196:303–310. https://doi.org/10.1016/j.jmatprotec.2007.05.057
30. Goyal R, Dubey AK (2014) Quality improvement by parameter optimization in laser trepan drilling of superalloy sheet. Mater Manuf Process 29:1410–1416. https://doi.org/10.1080/10426914.2014.912313
31. Goyal R, Dubey AK (2016) Modeling and optimization of geometrical characteristics in laser trepan drilling of titanium alloy. J Mech Sci Technol 30:1281–1293. https://doi.org/10.1007/s12206-016-0233-3
32. Guo D, Cai K, Yang J, Huang Y (2003) Spatter-free laser drilling of alumina ceramics based on gelcasting technology. J Eur Ceram Soc 23:1263–1267. https://doi.org/10.1016/S0955-2219(02)00299-6
33. Gurav MM, Gupta U, Dabade UA (2019) Quality evaluation of precision micro holes drilled using pulsed Nd:YAG laser on aerospace nickel-based superalloy. Mater Today Proc 19:575–582. https://doi.org/10.1016/j.matpr.2019.07.736
34. Han W, Pryputniewicz RJ (2004) Modeling and characterization of laser drilling of small holes on metal sheets. In: Proceedings of the ASME 2004 international mechanical engineering congress and exposition. ASME, Anaheim, California, USA, pp 189–197
35. Hooker JA, Doorbar PJ (2000) Metal matrix composites for aeroengines. Mater Sci Technol 16:725–731. https://doi.org/10.1179/026708300101508414
36. Ion J (2005) Laser processing of engineering materials: principles, procedure and industrial application. Butterworth-Heinemann, Oxford
37. Kacar E, Mutlu M, Akman E et al (2009) Characterization of the drilling alumina ceramic using Nd:YAG pulsed laser. J Mater Process Technol 209:2008–2014. https://doi.org/10.1016/j.jmatprotec.2008.04.049
38. Kainer KU (2006) Basics of metal matrix composites. In: Metal matrix composites: custom-made materials for automotive and aerospace engineering. Wiley, pp 1–54
39. Khan A, Celotto S, Tunna L et al (2007) Influence of microsupersonic gas jets on nanosecond laser percussion drilling. Opt Lasers Eng 45:709–718

40. Kudesia SS, Rodden WSO, Hand DP, Jones JDC (2001) Effect of beam quality on single pulse laser drilling. In: International congress on applications of lasers & electro-optics. Laser Institute of America, pp 1439–1448
41. Leigh S, Sezer K, Li L et al (2010) Recast and oxide formation in laser-drilled acute holes in CMSX-4 nickel single-crystal superalloy. Proc Inst Mech Eng Part B J Eng Manuf 224:1005–1016. https://doi.org/10.1243/09544054JEM1541
42. Li ZY, Wei XT, Guo YB, Sealy MP (2015) State-of-art, challenges, and outlook on manufacturing of cooling holes for turbine blades. Mach Sci Technol 19:361–399. https://doi.org/10.1080/10910344.2015.1051543
43. Low DKY, Li L, Byrd PJ (2000) The effects of process parameters on spatter deposition in laser percussion drilling. Opt Laser Technol 32:347–354. https://doi.org/10.1016/S0030-3992(00)00079-7
44. Low DKY, Li L, Corfe AG (2000) Effects of assist gas on the physical characteristics of spatter during laser percussion drilling of NIMONIC 263 alloy. Appl Surf Sci 154–155:689–695. https://doi.org/10.1016/S0169-4332(99)00427-4
45. Low DKY, Li L, Byrd PJ (2003) Spatter prevention during the laser drilling of selected aerospace materials. J Mater Process Technol 139:71–76. https://doi.org/10.1016/S0924-0136(03)00184-5
46. Majumdar JD, Manna I (2003) Laser processing of materials. Sadhana 28:495–562. https://doi.org/10.1007/BF02706446
47. Majumdar JD, Manna I (2011) Laser material processing. Int Mater Rev 56:341–388. https://doi.org/10.1179/1743280411Y.0000000003
48. Marimuthu S, Antar M, Dunleavey J, Hayward P (2019) Millisecond fibre laser trepanning drilling of angular holes. Int J Adv Manuf Technol 102:2833–2843. https://doi.org/10.1007/s00170-019-03389-8
49. Marimuthu S, Dunleavey J, Liu Y et al (2019) Characteristics of hole formation during laser drilling of SiC reinforced aluminium metal matrix composites. J Mater Process Technol 271:554–567. https://doi.org/10.1016/j.jmatprotec.2019.04.030
50. Marimuthu S, Dunleavey J, Liu Y et al (2019) Water-jet guided laser drilling of SiC reinforced aluminium metal matrix composites. J Compos Mater 53:3787–3796. https://doi.org/10.1177/0021998319848062
51. Marimuthu S, Dunleavey J, Smith B (2019) Laser based machining of aluminum metal matrix composites. Procedia CIRP 85:243–248. https://doi.org/10.1016/j.procir.2019.09.007
52. Mazumder J (2010) Lasers in aerospace industry manufacturing. Encycl Aerosp Eng 1–20. https://doi.org/10.1002/9780470686652.eae208
53. McNally CA, Folkes J, Pashby IR (2004) Laser drilling of cooling holes in aeroengines: state of the art and future challenges. Mater Sci Technol 20:805–813. https://doi.org/10.1179/026708304225017391
54. Meijer J (2004) Laser beam machining (LBM), state of the art and new opportunities. J Mater Process Technol 149:2–17. https://doi.org/10.1016/j.jmatprotec.2004.02.003
55. Misawa H, Juodkazis S (2006) 3D laser microfabrication: Principles and applications. Wiley-VCH, Weinheim
56. Mishra S, Yadava V (2013) Modeling and optimization of laser beam percussion drilling of nickel-based superalloy sheet using Nd: YAG laser. Opt Lasers Eng 51:681–695. https://doi.org/10.1016/j.optlaseng.2013.01.006
57. Mishra S, Yadava V (2013) Modelling of hole taper and heat affected zone due to laser beam percussion drilling. Mach Sci Technol 17:270–291. https://doi.org/10.1080/10910344.2013.780554
58. Mishra S, Yadava V (2013) Prediction of hole characteristics and hole productivity during pulsed Nd:YAG laser beam percussion drilling. Proc Inst Mech Eng Part B J Eng Manuf 227:494–507. https://doi.org/10.1177/0954405413475616
59. Morar NI, Roy R, Mehnen J et al (2018) Investigation of recast and crack formation in laser trepanning drilling of CMSX-4 angled holes. Int J Adv Manuf Technol 95:4059–4070. https://doi.org/10.1007/s00170-017-1481-9

60. Müller F, Monaghan J (2001) Non-conventional machining of particle reinforced metal matrix composites. J Mater Process Technol 118:278–285. https://doi.org/10.1016/S0924-0136(01)00941-4
61. Naeem M (2006) Laser percussion drilling of aerospace material using high peak power fiber delivered lamp-pumped pulsed Nd: YAG laser. In: International congress on applications of lasers & electro-optics. Laser Institute of America, p 308
62. NASA (2015) NASA cost estimating handbook (CEH). Version 4.0, National Aeronautics and Space Administration
63. Nath AK (2014) Laser drilling of metallic and nonmetallic substrates. In: Comprehensive materials processing. Elsevier, pp 115–175
64. Nawaz S, Awan MB, Saeed B, Abbas N (2019) Experimental investigation of taper angle during millisecond laser drilling of 18CrNi8 steel under multiple parameters and defocused plane. Mater Res Express 6:086531. https://doi.org/10.1088/2053-1591/ab17a9
65. Ng GKL, Li L (2001) The effect of laser peak power and pulse width on the hole geometry repeatability in laser percussion drilling. Opt Laser Technol 33:393–402. https://doi.org/10.1016/S0030-3992(01)00048-2
66. Ng GKL, Crouse PL, Li L (2006) An analytical model for laser drilling incorporating effects of exothermic reaction, pulse width and hole geometry. Int J Heat Mass Transf 49:1358–1374. https://doi.org/10.1016/j.ijheatmasstransfer.2005.10.002
67. Padhee S, Pani S, Mahapatra SS (2012) A parametric study on laser drilling of Al/SiC p metal-matrix composite. Proc Inst Mech Eng Part B J Eng Manuf 226:76–91. https://doi.org/10.1177/0954405411415939
68. Panda S, Mishra D, Biswal BB (2011) Determination of optimum parameters with multi-performance characteristics in laser drilling—a grey relational analysis approach. Int J Adv Manuf Technol 54:957–967. https://doi.org/10.1007/s00170-010-2985-8
69. Parthipan N, Ilangkumaran M (2020) Material synthesis, characterization and performance measurement of laser drilling for stir casted Cu-Ni-Tib2 metal matrix. Mater Today Proc 21:392–400. https://doi.org/10.1016/j.matpr.2019.06.137
70. Ready JF, Farson DF, Feeley T (2001) LIA handbook of laser materials processing. Laser Institute of America, Orlando
71. Reed RC (2008) The superalloys: fundamentals and applications. Cambridge University Press, Cambridge
72. Riveiro A, Quintero F, Lusquiños F et al (2011) The role of the assist gas nature in laser cutting of Aluminum alloys. Phys Procedia 12:548–554. https://doi.org/10.1016/j.phpro.2011.03.069
73. Rockstroh TJ, Scheidt D, Ash C (2002) Advances in laser drilling of turbine airfoils. Ind Laser Solut Manuf 17:15–21
74. Salonitis K, Stournaras A, Tsoukantas G et al (2007) A theoretical and experimental investigation on limitations of pulsed laser drilling. J Mater Process Technol 183:96–103. https://doi.org/10.1016/j.jmatprotec.2006.09.031
75. Sarfraz S, Shehab E, Salonitis K (2017) A review of technical challenges of laser drilling manufacturing process. In: Proceedings of the 15th International conference on manufacturing research. IOS Press, University of Greenwich, UK, pp 51–56
76. Sarfraz S, Shehab E, Salonitis K et al (2018) Evaluation of productivity and operating cost of laser drilling process—a case study. In: Proceedings of the 16th International conference on manufacturing research. IOS Press, University of Skövde, Sweden, pp 9–14
77. Sarfraz S, Shehab E, Salonitis K et al (2018) Towards cost modelling for laser drilling process. In: Proceedings of the 25th ISPE Inc. International conference on transdisciplinary engineering. IOS Press, University of Modena and Reggio Emilia, Italy, pp 611–618
78. Sarfraz S, Shehab E, Salonitis K et al (2019) An experimental investigation of productivity, cost and quality for single-pulse laser drilling process. In: Proceedings of the 15th International conference on manufacturing research. IOS Press, Queen's University, Belfast, pp 334–339
79. Sarfraz S, Shehab E, Salonitis K, Suder W (2019) Experimental investigation of productivity, specific energy consumption, and hole quality in single-pulse, percussion, and trepanning drilling of in 718 superalloy. Energies 12:4610. https://doi.org/10.3390/en12244610

80. Sarfraz S, Shehab E, Salonitis K et al (2020) An integrated analysis of productivity, hole quality and cost estimation of single-pulse laser drilling process. Proc Inst Mech Eng Part B J Eng Manuf. https://doi.org/10.1177/0954405420968161
81. Scallan P (2003) Process planning: the design/manufacture interface. Butterworth-Heinemann, Oxford
82. Schaaf P (2010) Laser processing of materials: fundamentals, applications and developments. Springer-Verlag, Berlin, Heidelberg
83. Schneider M, Girardot J, Berthe L (2011) Recoil pressure and surface temperature in laser drilling. In: International congress on applications of lasers & electro-optics. Laser Institute of America, pp 478–481
84. Shen ZH, Zhang SY, Lu J, Ni XW (2001) Mathematical modeling of laser induced heating and melting in solids. Opt Laser Technol 33:533–537. https://doi.org/10.1016/S0030-3992(01)00005-6
85. Shin J, Mazumder J (2016) Shallow angle drilling of Inconel 718 using a helical laser drilling technique. J Manuf Sci Eng 139:031004. https://doi.org/10.1115/1.4034718
86. Solati A, Hamedi M, Safarabadi M (2019) Comprehensive investigation of surface quality and mechanical properties in CO_2 laser drilling of GFRP composites. Int J Adv Manuf Technol 102:791–808. https://doi.org/10.1007/s00170-018-3164-6
87. Steen WM, Mazumder J (2010) Laser material processing, 4th edn. Springer, London
88. Tewari R, Singh MK, Zafar S, Powar S (2020) Parametric optimization of laser drilling of microwave-processed kenaf/HDPE composite. Polym Polym Compos 096739112090570. https://doi.org/10.1177/0967391120905705
89. Wang H, Ren N, Zhang W et al (2017) Influence of assist gases on pulsed laser drilling of nickel-based superalloy. In: 2017 Conference on lasers and electro-optics Pacific rim (CLEO-PR). IEEE, pp 1–4
90. Wang R, Wang K, Dong X et al (2018) An experimental investigation into the defects of laser-drilled holes in thermal barrier coated Inconel 718 superalloys. Int J Adv Manuf Technol 96:1467–1481. https://doi.org/10.1007/s00170-018-1592-y
91. Whitehouse DJ (2002) Surfaces and their measurements. Hermes Penton Science, London
92. Yeo CY, Tam SC, Jana S, Lau MWS (1994) A technical review of the laser drilling of aerospace materials. J Mater Process Tech 42:15–49. https://doi.org/10.1016/0924-0136(94)90073-6
93. Yunus M, Alsoufi MS (2019) Mathematical modeling of multiple quality characteristics of a laser microdrilling process used in Al7075/SiCp metal matrix composite using genetic programming. Model Simul Eng 2019:1–15. https://doi.org/10.1155/2019/1024365

Subtractive Manufacturing of Different Composites

Italo Tomaz, Munish Kumar Gupta, and Danil Yu. Pimenov

1 Introduction

When two or more distinct materials are combined to provide properties that cannot obtained by any traditional material a composite materials a composite material is obtained and they can be classified in in three major types: Polymer Matrix Composites, MMCs Metal Matrix Composites (MMCs) and Ceramic Matrix Composites (CMCs) (Fig. 1).

These materials present an extensive variety of chemical and mechanical properties that allow them to be used in many different applications. However, they usually exhibit anisotropy, inhomogeneity and non-ductile behavior which increase the complexity and the cost of their shaping process which limit their use in some applications [20]. Most of composite components are submitted to machining processes in the finishing step to achieve the desired geometry, tolerances and surface finishing. When compared to machining of conventional materials, machining processes of composites differs considerably in various aspects and many of them can be classified as difficult to machine. The inhomogeneity, anisotropy and sometimes the high hardness make the machining process complex generating elevated tool wear

I. Tomaz (✉)
SEAM Research Centre, Waterford Institute of Technology, Waterford X91TX03, Ireland

Instituto Federal Fluminense—Laboratory of Materials Testing (LEMat), Cabo Frio/Búzios Road, Cabo Frio, RJ, Brazil

M. K. Gupta
Key Laboratory of High Efficiency and Clean Mechanical Manufacture, Ministry of Education, School of Mechanical Engineering, Shandong University, Jingshi Road, Jinan 250061, China

D. Yu. Pimenov
Department of Automated Mechanical Engineering, South Ural State University, Lenin Prosp. 76, Chelyabinsk 454080, Russia
e-mail: danil_u@rambler.rus

S. Mavinkere Rangappa et al. (eds.), *Additive and Subtractive Manufacturing of Composites*, Springer Series in Advanced Manufacturing,
https://doi.org/10.1007/978-981-16-3184-9_6

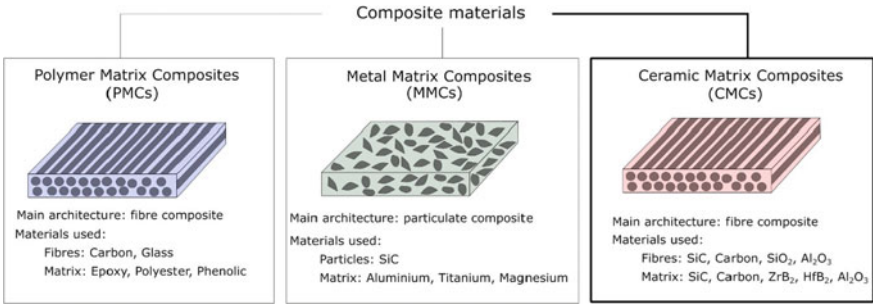

Fig. 1 Classification of composite materials [36]

and poor surface finishing and dimensional accuracy which increases the machining costs and compromises the surface integrity of components.

When machining composite materials the chip formation mechanism is originated in distinct failure modes that occurs simultaneously that are ruled by a number of variables including cutting parameters and also composite characteristics such as fibre orientation [11]. Lopresto et al. [70] reported the existence of two major types of surface damage that are induced by machining process which are the matrix cracking on fibres direction and the out-of-plane displacement.

Because of these motives many researches have been conducted to create new machining techniques and also improve the traditional process and tools in order to obtain elevated surface finishing quality with reasonable costs. The following sections will discuss the challenges and the advances in the machining process of PMCs, MMCs and CCs.

2 Machining of Polymer Matrix Composites (PMC)

This type of polymer is used in many applications in different industries such as aerospace, automotive, naval, sport and even medical industry. They are known by its high strength to weight ratio when compared to metals [70]. The increasing number of applications results in higher demand and consequently the availability of manufacturing technologies that are able to achieve large scale manufacturing requirements regarding cost and product quality. Despite the recent progress in non-tradional machining process such as Laser Beam Machining (LBM) and Electrical Discharge Machining (EDM), conventional machining processes still being the most used due to the considerably lower cost. Many investigations have been done to understand the cutting mechanism of PMCs and identify the best manufacturing strategy to obtain high quality components with reasonable cost [4, 45, 71]. These works showed that the cutting mechanism is mainly influenced by reinforcing fibre orientation but other parameters like cutting depth, tool geometry and composition also have essential role in subtractive manufacturing process of composites.

Different from ductile metals in which the material is removed as continuous chip, in PMCs the chip is generated by a series of fractures that occur transversely and in the direction of the fibres. The cutting mechanism of PMCs is more complex, depending not only on the mechanical properties of the fibres and the matrix but also on orientation angle between the fibres and the cutting directions (Fig. 2). The types of chips and their correlation with fibres orientation angle was described by Palanikumar et al. [84] Sheikh-Ahmad [101] and Voss et al. [124].

Palanikumar et al. [84] defined four groups of fibre orientation interval which results in different chip formation mechanisms. These groups are presented in Fig. 2. The first chip mechanism occurs when $\theta = 0°$ and the fibres are cut in axial direction. When cutting direction is perpendicular to fibres orientation ($\theta = 90°$) the third mechanism takes place. Type II and IV of chip formation mechanisms occurs when $15° < \theta < 75°$ and $105° < \theta < 165°$ respectively. An angular gap of 15° exists between

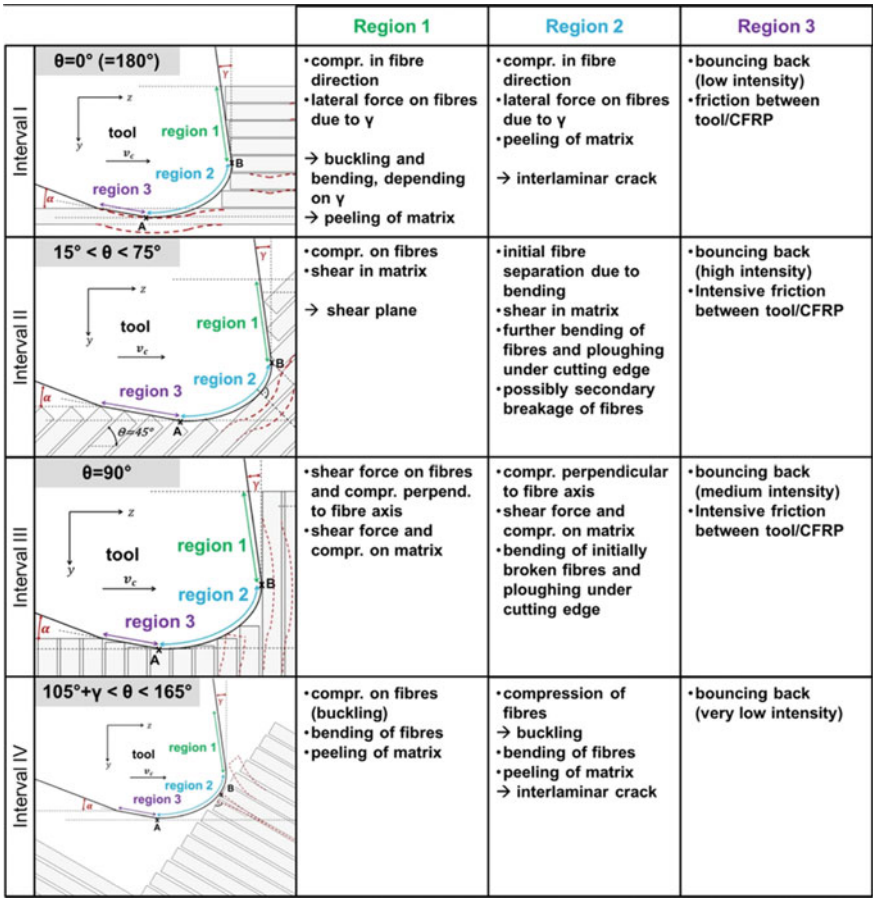

Fig. 2 Cutting mechanism according to fibre direction [124]

each type. They have studied the influence of fibre orientation angle on surface roughness of glass fibre reinforced polymer and observed surface roughness rapidly increased for fibre orientation angles beyond 30º. According to many authors this is the main parameter to be taken in consideration during machining process of PMCs.

3 Drilling of PMC

In aerospace industry, most of PMCs components are fixed using riveted or bolted joints which require a high number of holes. The main challenges of PMCs drilling process are due to their inhomogeneity, anisotropy and hard nature of fibres that cause drilling-induced damages and rapid tool wear [1].

The main drilling-induced damage is the delamination corresponding to 60% of all components nonconformity at the assembly stage [41]. This damage occurs in the drilled hole periphery usually at the hole entry or exit of. It is called peel-up delamination when it occurs in the hole entry and push-out delamination when it occurs in the hole exit [38]. As drill moves through the workpiece, the thickness of the uncut layers decreases and lose strength against deformation generated by the feed force and the push-out delamination occurs as illustrated by Fig. 3b. Peel-up delamination occurs when drill touches the surface and a peeling force is produced through the slope of the drill flute. This effect separates the top layers causing the peel-up delamination (Fig. 3a) [1].

Other common types of drilling-induced damage are chipping, fuzzing, matrix/fibre de-bonding, spalling, fibre pull-out, fibre breaking, uncut fibres and resin loss which were described by Feito et al. [29], Fernández-Pérez et al. [31], Giasin et al. [41], Haeger et al. [44] and are illustrated in Fig. 4. Drilling-induced

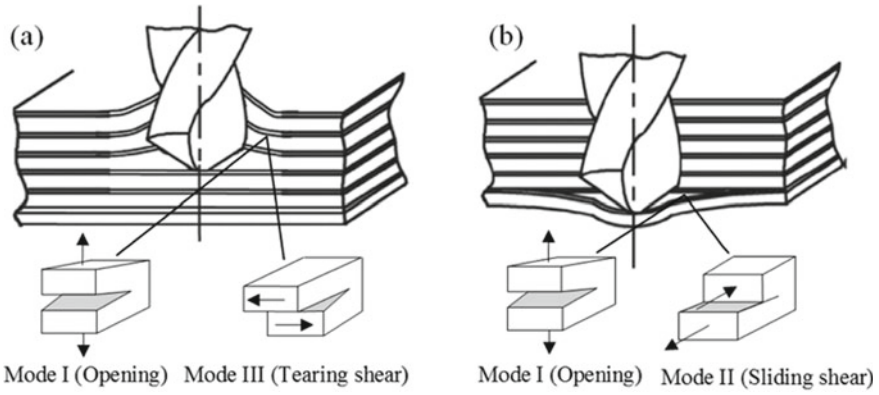

Fig. 3 Delamination mechanism in composite drilling. **a** Peel-up delamination. **b** Push-out delamination [38]

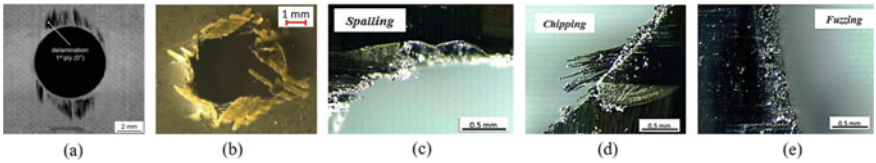

Fig. 4 Different drilling-induced damage. **a** Delamination in CFRP [44]. **b** Fibre fraying in CFRP [31]. **c** Spalling in CFRP [29]. **d** Chipping in CFRP [29]. **e** Fuzzing in CFRP [29]

damages not only reduces the dimension accuracy but also reduces fatigue life and the strength of the PCMs degrading their performance in the long-term [16, 33, 131].

Therefore, the investigation of the influence of drilling parameters in surface quality and dimension accuracy have been the interest of many authors and a damage free process is still a challenge to overcome. M'Saoubi et al. [72] have presented recent advances in machining process oriented to aerospace industry and highlighted the importance of the cutting conditions in the drilling of PCM. In their review of Machinability of natural fibre reinforced composites, [80] discussed challenges on PCM machining and pointed that the heat produced during the process can be a problem. Although the increase of temperature reduces machining force it can also melt the polymeric matrix and burn the fibres. The use of traditional coolant can result in other problems such as its absorption by the fibres and a possible solution would be the use of air or mist as coolant. Gaitonde et al. [33] evaluated the effects of drilling conditions on the delamination and revealed that higher cutting speed decreases delamination tendency. They showed that high-speed machining has an important role in reducing drilling-induced damage and the combination of point angle and low feed is also vital to minimize delamination damage during the drilling process. Campos Rubio et al. [12] also used high speed drilling in glass fibre reinforced polymers demonstrating that delamination damage decreased when higher cutting speed were used. Voss et al. [123] compared the conventional drilling with the process of orbital drilling (OD) in which the tool travels along a helical path. However orbital drilling produced a higher quality hole under lower machining forces it required a more elaborated machine tool. The axial feed force during the drilling process was reduced by three when OD was used resulting in less hole exit damages. The major disadvantage is the great increase in the process time. Other studies such as [78] and [119] analyzed the use of different drills materials and coatings and types of drills. Xia et al. [132] evaluated the cryogenic cooling-induced drilling performance and surface integrity of carbon fibre reinforced polymers and concluded that cryogenic cooling improves the performance of drill bit with regard to wear, generates better borehole surface, and minimizes diameter error. Although is does not reduce delamination for the tested drilling parameter.

It is possible to notice the there is still challenges to overcome the drilling process of PMCs and the selection of the proper tool and machining parameters is vital to ensure the proper quality of the holes avoiding drilling-induced damage.

4 Milling of PMC

Considering most PMCs parts are produced to near net-shape [39], milling processes are generally performed as a finishing machining operation to remove the excess material in order to control tolerances and surface roughness [34]. Milling PMCs is a complex process due to its heterogeneity and the machining-induced damage such as delamination (Fig. 5) [46]. The selection of the proper parameters and tools depends on several factors, including matrix volume fraction, reinforcement architecture and fibre type.

Because of their high thermal conductivity and hardness, carbide coated and PCD tools are the most used materials for PMCs milling [49, 70, 83]. El-Hofy et al. [28] investigated the use of diamond like carbon (DLC) coated carbide and PCD cutting tool materials in the milling process of carbon fibre reinforced plastic and observed the PCD present greater life time. Sheikh-Ahmad et al. [102] created new tool life criterion derived from the existence of delamination, and the optimum machining conditions to reduce delamination were obtained by a tool life equation.

Many studies have been done to understand the cutting mechanism of PMCs and identify the best conditions (tool geometry and material, cutting parameters, cutting fluid or mist application etc.) to ensure the obtaining of the required surface quality and the economic viability of the machined parts. Çolak and Sunar [19] studied the influence of different machining parameters and fibre orientation on the PMCs milling process and found that increment of feed rate or decrease of cutting speed have increased the cutting force and the surface roughness. Chen et al. [15] evaluated the machining performance of diamond-coated rhombic milling tool on the machining process of carbon fibre reinforced polymer and observed that when coating fell off, the machining forces increased largely till the cutter failed to work. Azmi et al. [5]

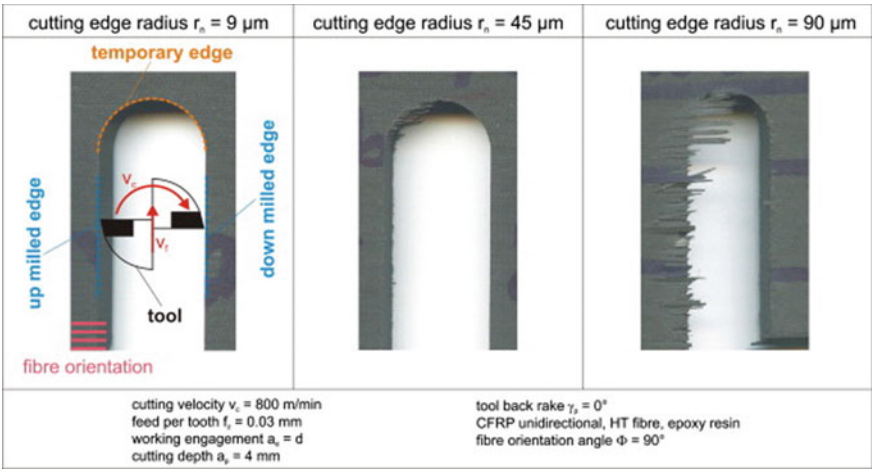

Fig. 5 Delamination as function of tool wear [48]

evaluated the end milling process of glass fibre reinforced polymer using ANOVA (Analysis of Variance) combined with Taguchi analysis. They reported that feed rate is the most important variable affecting all the output parameters (surface roughness, machining forces and tool life). When higher cutting speeds were used a change in the chips formation occurs leading to a decrease in machining forces was observe by Uhlmann et al. [121]. It can be employed to use higher feeds at the same tool life or elongate tool life when the same feed rate is used. Gara and Tsoumarev [34] evaluated the slotting of carbon fibre reinforced polymer and also observed that feed rate is the most relevant variable affecting surface finishing.

The process complexity and the many differences from the cutting mechanism of metals also motivate the development of mechanistic and numerical models to better understand and optimize the process and address the current challenges [125]. Hintze and Hartmann [47] developed a model applicable for any carbon fibre reinforced polymer laminate with unidirectional top layers that can be applied to deduce the limits for permissible tool wear or cutting force. A two-dimensional finite element model was used by Ghafarizadeh et al. [39] to simulate the mechanism of chip formation, cutting forces and machining-induced damage in the milling process of unidirectional carbon fibre reinforced polymer. The author validated the simulates results with SEM images of the workpiece machined surface and experimentally measured cutting forces. Thakur et al. [116] used ANOVA and response surface method to find out the effect of different machining parameters like spindle speed, feed rate and weight of graphene on delamination factor and surface finishing of graphene doped glass fibre reinforced polymer.

In order to optimize the milling process of PMCs reducing the costs, increasing dimensional accuracy and surface roughness new technologies and have been developed and tested. The use of Minimum Quantity Lubrication (MQL) technique in the slotting process of carbon fibre reinforced polymer was investigated by Iskandar et al. [53]. Low frequency (<30 Hz) oscillated milling was proposed by Szallies et al. [114] to improve surface quality. Lower delamination was obtained when compared to the conventional milling. A direct laser-assisted machining technique (DLAM) was applied in cutting process of carbon fibre reinforced polymer by Park et al. [85]. In this method, the laser beam passes through a light transmissive sapphire cutting tool and irradiates directly in the workpiece/tool interface. DLAM succeeded in reduce machining forces and reduced the surface roughness. In [76] slot milling performance of carbon fibre reinforced polymers was evaluated using different machining parameters and cryogenic environment based on immersing of the workpiece into the liquid nitrogen. The cryogen bath resulted in the increment of cutting forces and the decrease of surface damage due to the increase the chip breakability.

5 Turning of PMC

Tuning is applied in the finishing processes of PMCs rotation-symmetric components, such as tubes, shafts, spindles, gears etc. Along with drilling and milling, turning

stands out as one of the most used machining processes in PMCs [115]. Just as in the milling process, in the turning process the selection of cutting tool and machining parameter is vital to obtain the required surface quality and control toll wear rate.

Petropoulos et al. [86] evaluated the turning of Polyethere-therketone (PEEK) reinforced with carbon and glass fibres applying different cutting parameters and tool materials. Feed rate was the parameter that most influenced surface roughness for all the tested composites. PCD tool provided lower surface roughness when compared to carbide tool. The influence of turning parameters of surface roughness was also studied by Rajasekaran et al. [92] who machined carbon fibre reinforce polymer leading to the same conclusion that feed rate was the parameter that most influenced surface roughness. Fetecau and Stan [32] carried out an investigation into the turning of two types of polytetrafluoroethylene (PTFE) composites reinforced with 32% carbon and 3% graphite and 15% regenerated graphite. When PTFE composite was reinforced with carbon it presented low machinability and feed rate was the most important parameter to both surface finishing and machining force. Rajasekaran et al. [91] used Taguchy method and RSM to identify the optimum catting parameter in the turning process. RSM succeed to predict surface roughness results and the lower feed rate associated with the higher cutting speed offered the best roughness result.

Efforts have also been made to develop method to simulated and predicted outputs of PMCs turning processes. Bagci and Işık [6] studied the turning process of unidirectional glass fibre reinforced polymer using cermet tools. They investigated the influence of depth of cut, cutting speed and feed rate on surface quality. An artificial neural network and RSM were used to predict surface roughness. Işık and Kentli [52] proposed a multicriteria optimization to select the machining parameters capable of to minimize machining forces and maximize MRR (Material Removal Rate) in turning of uni-directional GFRP rods. Pradhan and Das [87] used gray relation analysis with fuzzy logic to optimize the CNC turning process of glass fibre reinforced plastic and concluded that method significantly improved the turning process. Chang [14] developed oblique three-dimensional cutting model and obtained good correlations between simulated and experimental data of FEM and Inverse heat transfer solution in tool temperature in CFRP turning. In [126, 128] a three-dimensional finite element model of an orthogonal cutting was developed and validated by the experimental results. The model was capable to predict cutting forces and cutting induced damage in the turning process of uni-directional CFRP.

6 Grinding of PMC

Considering the small tolerance required in the assembly of some mechanical parts, grinding for finishing is often performed on PMCs materials [18]. Investigations have been done to identify the best techniques and grinding parameters that are able to provide great surface integrity without increment in the processes costs. Hu and Zhang [50] investigated the surface grinding performance of the multidirectional CFRP, with a focus on the material removal mechanism, chip formation, grinding

force characteristics and ground surface features. The machining forces of grinding operation of multidirectional PMC increased almost linearly with the increment in grinding depth and the surface roughness changed strongly with the local fibre orientations. Chockalingam and Kuang [17] evaluated the grinding of chopped glass fibre reinforced polymer laminates using two abrasive types, alumina, and cubic boron nitride. They also tested surface roughness and grinding force ratio under various machining variable, such as feed, depth of cut and speed. Maximum grinding force ratio was found at high feed, low speed, and low cutting depth for both abrasive types. Although CBN grinding wheel produced higher grinding forces it performed better than alumina grinding wheel, resulting in lower surface roughness.

The grinding performance of CFRP when using internal coolant supply was evaluated by Sasahara et al. [98]. They investigated the effect of this technology on the surface roughness and delamination and also measured the grinding temperature and forces during the process. The experiments showed that matrix resin loading on grinding wheel decreased when the internal coolant supply was used. The considerable increment on surface quality confirmed the high performance of internal coolant supply for this application. Liu et al. [66, 68] presented a mathematical model for cutting force in rotary ultrasonic face grinding of CFRP. In this method the tool oscillates at high frequency during the process which lead to some benefits such as reducing the cutting force, reducing the cutting temperature, reducing tool wear and improve surface integrity [67, 129]. The predicted effect by mathematical model was then validated with the experimental data.

7 Non-conventional Machining of PMC

To overcome the challenges of the traditional machining of PMCs material, the use of different non-conventional machining process has been investigated. In this context, three methods stand out because of their characteristics: LBM, Water Jet (WJ)/Abrasive Water Jet (AWJ) and EDM. These methods exhibit high productivity and are widely used in the operation of cutting, trimming and drilling of PMCs.

LBM is a promising emerging technology for the machining of PMCs because it is a non-contact process, which avoid the contact induced damage and completely eliminates the tool wear. Although, the inherent heat input in this process may cause thermal damage to both fibres and matrix of the PMC which is the main challenge to be overcome in the LBM of PMC. The interaction between the laser beam and the workpiece generates a heat affected zone (HAZ) which can lead to delamination, matrix recession and fibres distortion [11]. The influence of LBM process parameters (pulse energy, pulse duration and spot overlap) on HAZ extension was investigated by Leone and Genna [63]. The authors performed cutting testes of CFRP plates, 1 mm in thickness, using a 150 W pulsed Nd:YAG laser with different process parameters. The maximum heat affected zone extension occurred at the center of the laminate in correspondence of unidirectional lamina and varied in the range 170–1600 μm. Shyha [104] carried out an investigation of trimming CFRP and GFRP composites

using CO_2 laser beam to understand the impact of process parameters on surface integrity and productivity in order to determine the best set of process factors. They reported cutting speed as the main factor affecting the surface quality and volumetric material removal rate. Stock et al. [110] proposed the introduction of absorbent soot particles into the composite matrix to improve the laser cut quality and reported a decrease in workpiece defects.

The use of water jet and abrasive water jet for machining of PMCs have been object of study of many researchers. The use of these machining processes is a great alternative to avoid the problems related to the contact between the tool and the PMCs workpiece such as delamination and high tool wear rates. When compared to LBM their main advantage is the lack of heat input which does not produce the HAZ that I the biggest problem associated with LBM. They also have advantage when compared to EDM because it can be used to any kind of composite material and is limited to conductive materials [27]. Ruiz-Garcia et al. [97] evaluated the influence of AWJ variables on the quality of straight cuts and holes in CFRP. The authors reported the absence of thermal damage and delamination in the cutting and holing of CFRP with the used process parameter. In [74] the trimming of hybrid carbon/glass fibre reinforcement polymer composites using AWJ was evaluated. The experimental results and statistical analysis showed that the stand-off distance followed was the main factor regarding the reducing of kerf ratio. In [51] A numerical optimization was performed to select the optimized set of cutting parameters for superior surface quality, improve productivity generating less reduction in strength and lower cost of hole making in glass fibre reinforced composite.

EDM is also an alternative to avoid the machining-induced damaged caused by the traditional machining processes. Considering this process does not uses mechanical loads and removes material from electrically conducting, it does not face problems associated with the high hardness, strength, toughness, or abrasiveness which commonly observed in the reinforcement fibres of PMCs The great disadvantage is its limited application to conductive materials but when the composite matrix is non-conductive and the fibre is conductive, the material removal by EDM can be applied [11]. Sheikh-Ahmad [100] evaluated the mechanism of material removal and the machining-induced damage in the EDM drilling of carbon fibre reinforce polymer and reported that material removal occurs by decomposition of the epoxy matrix, vaporization of the fibres and also thermally induced fracture of the fibres. Kumar et al. [60] performed holes of diameter 120 μm in CFRP using micro electrical discharge drilling with three types of tool geometries (double notch, single notch and solid). The authors concluded that EDM is suitable for drilling micro holes of high aspect ratio.

8 Machining of Metal Matrix Composites (MMC)

Metal matrix composites are a category of composite materials in which a ductile metal matrix is reinforced by addition of hard particles, whiskers or fibres. Most

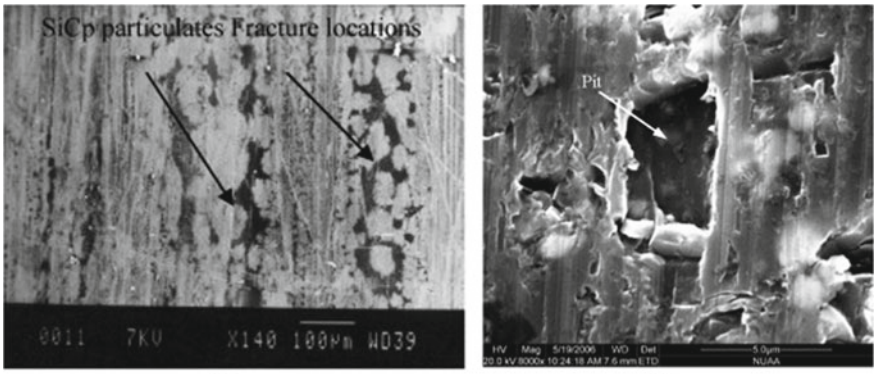

Fig. 6 Example of machining induced damage. **a** Particle fracture [9]. **b** Particle pull-out [37]

common matrix metallic alloys are aluminum, titanium, copper alloys and magnesium while reinforcement material are generally a brittle ceramic material such as silicon carbide, boron carbide, graphite and TiC [81, 90]. Their mechanical properties make them suitable for use in defense, aerospace, sports, electronics and automotive industries. Particulate and fibre reinforced MMCs have a very important difference between them regarding directionality of properties. While fibre reinforced MMCs are generally anisotropic, particulate reinforced MMCs present isotropic properties as conventional metallic material making them a great alternative to some applications [75].

Although MMCs are generally manufactured in near-net shape, further machining operations are required to achieve final geometry and surface quality. The machining process of these materials is still a challenge because of highly abrasive nature of most reinforcement materials [58] and also the anisotropic properties when it comes to the fibre reinforced MMCs. Understand the effects of machining process on MMCs surface integrity and metallurgical state is essential to ensure that the mechanical components will present the desired mechanical and geometry properties [65]. The investigation of machining process of MMCs have been concern of many researchers who reported the reinforcement type and orientation, tool type and geometry and cutting conditions are the main parameters affecting MMCs machinability. The most common machining-induced damage are debonding at the fibre or particle and matrix interface, fibre/particle pullout, delamination and particle fracture [103] (Fig. 6).

9 Milling of MMC

Milling of MMCs differs from the milling of conventional metal alloys in many aspects and because of his it has been object of study of many researchers. The

machinability of aluminum alloy matrix reinforced with SiC reinforcement particles were studied by Suresh Kumar Reddy et al. [112]. The study shows the importance of the proper selection of milling parameters to improve the machining process of Al/SiC MMC making viable its use in wide variety of industries. In [57] Taguchi method, RSM and ANN were used to determine the best set of cutting parameters for the milling process of aluminum 7039-based MMCs reinforced with B4C and SiC particles. The authors reported optimal set of machining parameters at highest value of cutting speed, lowest feed rate and the largest cutting depth for both tested MMC. Sridhar et al. [108] studied the effect of cutting parameters in the end milling process of Al/SiC metal matrix composite. Different nose radius, helix angle, rake angle, feed rate, cutting speed and depth of cut were used, and the authors reported a good correlation between predicted and experimental results.

Different techniques have been used to predict the influence of milling parameters in the surface quality, tool wear and cutting forces. The proper prediction of this results allows the implementation of optimizing methods that will lead to reduce the process costs and improve machined surface integrity. In [136] a micromechanical model was used to understand the relationship between the macroscopic behaviors and microstructure fracture and deformation properties. They investigated residual stresses, surface and subsurface damage and edge breakout. Finite element method was carried out using the Johnson–Cook damage model for the aluminum matrix and the elastic-brittle failure model for the SiC reinforcements. The authors reported good agreement between the simulated and experimental results. The surface roughness increased with the increment of depth of cut which also contributed to the presence of edge breakout. On the other hand, cutting speed had small effect edge breakout and should be used as high as possible. The analysis of residual stresses did not show any significative dependence on cutting speed or cutting depth. The effect of reinforcement particles size and machining parameters on responses variables were analyzed by Ajith Arul Daniel et al. [3]. An ANN model was proposed, and its performance was compared with a linear regression analysis. The authors also used and genetic algorithm to identify the set of input parameters that was able to give the better multi-objective results. The use of higher percentage of reinforcement particles weight resulted in higher cutting forces, temperature, surface roughness and lower material removal rate. On the other hand, increment in particles sizes generated lower surface roughness, temperature, cutting forces and higher material removal rate. The proposed ANN model showed better performance than linear regression in the prediction of all response parameters and genetic algorithm found lower reinforcement percentage, depth of cut, feed, speed and higher particle size as the best set of input parameters. Rajeswari and Amirthagadeswaran [93] proposed a mathematical model using response surface method to investigate the effect of machining parameters in the milling of end milling AA7075 MMC. Multi-response optimization by response surface method showed that minimum tool wear, cutting force, surface finishing and MRR were obtained at feed rate of 0.033 mm/rev, depth of cut of 1.6 mm, spindle speed of 1210 rpm and 5% of SiC. Song et al. [106] evaluated the machinability of MMC when laser assisted machining (LAM) was used. A multi-objective optimization of Ra and cutting force was used to analyze

the effect of machining parameters. Surface roughness and cutting forces increased with a decrease in the rotational speed, and an increase in the feed rate. The use of ultrasonic assisted machining in the milling process of SiCp/Al composites was studied by Niu et al. [82]. They reported a detrimental effect of high amplitudes and when it was increased to 3 μm, the cutting force and surface roughness suddenly increased.

10 Turning of MMC

As one of the most used traditional machining processes turning is widely used the finishing steps of MMCs components. Considering its relevance and the complexity and many experimental and theoretical work have been made to optimize the turning process, using statics analysis and simulation or even employing new manufacturing technologies.

The machinability of Al-SiC MMCs in turning process was investigated by Tomac et al. [117] who compared the performance of PCD and coated tungsten carbide tools. They reported that higher feed rates were able to reduce tool wear and machining forces due to the increment temperature which result in thermal softening of the MMC. They also reported a much higher performance of PCD tools presenting much higher tool life under similar cutting conditions. A design of optimization of machining variables for turning MMC using orthogonal arrays was performed by Davim [22] that reported the cutting in speed as the main factor contribution to tool wear and feed rate as the main parameter affecting surface finishing.

In order to optimize the turning process of MMCs many researchers have been using analytical methods, simulation methods and artificial intelligence algorithms that are able to find satisfactory results in the prediction of parameters such as tool life time, surface roughness and cutting forces. Pramanik et al. [88] developed a mechanics model for predicting the forces in the turning process of aluminum MMCs reinforced with ceramic particles. The model, based on Merchant's shear plane analysis, Griffith theory and slip line field theory, showed an excellent agreement when comparing predicted and experimental results. Chan et al. [13] used parametric analysis, cutting mechanics analysis, finite element method and power spectrum analysis to investigate the factors affecting the ultra-precision turning of Al6061/SiC. They found that the surface integrity can be considerably improved by using high feed rate and spindle speed. Among other findings they stated that two different cutting mechanisms were observed. The first of them occurs when the SiC particles are cut through and results in a better surface finishing, without pits and cracks. In the second cutting mechanism the SiC particles were pulled out during the turning process cracks and pits are generated in the machining surface, resulting in poor surface finish (Fig. 7).

The detrimental effect of particles pull out from machining surface was also reported by Ge et al. [37] who evaluated the surface integrity on ultra-precision machining of SiCp/ZL101A and SiCp/2024Al MMCs. The authors used PCD and single point diamond tool (SPDT) tools and observed a smoother surface finishing

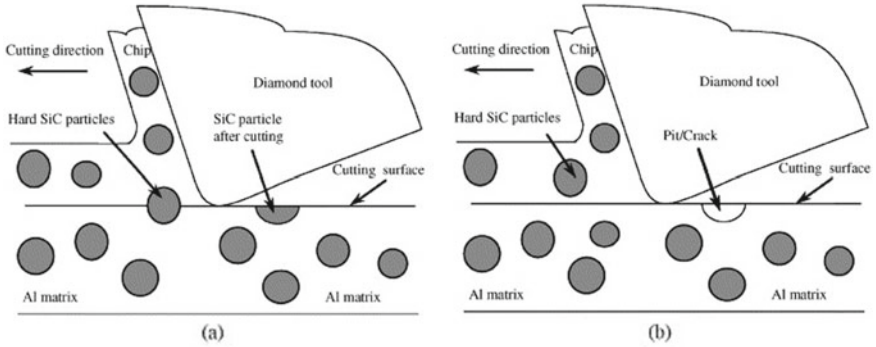

Fig. 7 MMC particle reinforced cutting mechanisms. **a** Cut through. **b** Pull-out [13]

when SPDT were used which could be explained by the fact that more SiC particle was cut through instead of being pulled out when this type of tool was used. Used a Taguchi based grey relational analysis to the multi-objective optimization in turning of Rock dust reinforced Aluminum MMC. As reported by other authors, feed rate was the most important machining variable affecting the surface finishing and its increment resulted in higher roughness. The multi-objective considered not only machining parameters but also composite manufacturing variables such as particles size and reinforcements weight. Furthermore, to obtain better surface finishing without compromising material removal rate the best parameters set was found to be 20 μm particle size, 10% of reinforcement by weight, 1273 rpm speed, 0.6 mm depth of cut and 0.1 mm/rev feed rate [107]. The use of new promising technologies can also improve the quality and reduces the costs of MMCs turning. The use of MQL in the machining of Mg/μ.Al_2O_3/n.Al_2O_3 hybrid MMC was studied by Suneesh and Sivapragash [111] who also used grey relation analysis and TOPSIS to perform the multi-objective optimization process. TOPSIS presented a better performance and was used to the confirmation test showing great agreement with experimental results. They observed that, in general, the MQL method provided better results when compared to dry turning. The use of MQL in the turning of MMCs was also investigated by Vishwas et al. [122] who used Taguchi analysis to determine the best machining parameters in the turning of Al-6082/SiC MMC. Another practical solution to enhance tool life in the turning process of MMCs is the use of laser-assisted machining (LAM). Bejjani et al. [10] reported an increment in tool lifetime related to the change in the tool-particle interaction when LAM was used. Because of the thermal softening generated by LAM the hard particles area able to displace the matrix instead of breaking and causing abrasion wear. On the other hand, the LAM turning presented worst surface finishing when compared to traditional process. The use LAM in the turning process of MMCs was also studied by Kong et al. [59]. The authors used Taguchi method to optimize the cutting parameters of LAM of Al/SiCp/45% MMC and observed that LAM was able to provide a larger MRR under the same surface finishing when compared to conventional

machining. The ultrasonic machining is also another promising technology when it come to the turning of difficult-to-cut material such as MMCs. A study comparing conventional turning and ultrasonic assisted turning of SiC-particle-reinforced Al MMC using different cutting tools and machining parameters was conducted by Bai et al. [7]. They concluded that ultrasonic assisted process was able to both reduce machining forces and improve surface finishing. In [135] conventional turning and ultrasonic assisted turning of an aluminum matrix MMC reinforced with SiC particles were compared and lower surface roughness was obtained when ultrasonic assisted machining was used.

11 Drilling of MMC

Drilling is also a critical process to MMCs and many investigations have been done to identify the conditions that are able to avoid premature tool wear. Balamurugan et al. [8] used different input variables such as feed rate, spindle speed and type of drilling tool to identify tis influence on the tool wear and chip morphology during the drilling process of Mg/SiC composite. Different wear mechanisms were observed depending on the drill diameter and improved surface profile was obtained with larger drill diameter. In [105], the authors attempted to evaluated the effect of cutting edges of the drill point geometry in the machinability of Al-6063/10% SiC MMC using Taguchi methodology. The modified drill geometry was able to perform a drill without burr formation in the entrance and exit of the drilled hole. The author also reported feed rate and cutting speed as the most important parameters influencing surface roughness. Tosun [118] conducted a study to determine the optimal conditions for the drilling process of Al/SiCp MMC. Drill type and feed were reported as the most important parameters influencing surface roughness. An optimum set of drilling parameters for the best surface finishing was achieved using the analysis of S/N ratio and the confirmation tests showed that it is feasible to improve surface finishing considerably by using the proposed technique.

Grey relational analysis was used by Udaya Prakash et al. [120] to identify the optimal conditions in the drilling process of aluminum-based MMC. A multi-objective optimization was used and the confirmation experiments showed a small error (3.9%) associated with the thrust force confirming the efficiency of the applied method. Doomra et al. [25] proposed a three-dimensional finite element model to simulate the drilling process of MMCs. The comparison of the predict and the experimental the data was done and it was proved that the developed finite element model was efficient in the simulation of the resulting thrust force on the drilling process of Al1100/10% SiC MMCs. Gowda et al. [43] studied the estimation of drilling aluminum silicon nitride composite output parameters (surface roughness, circularity and cylindricity) using an artificial neural network. The authors stated that, for 6% Si_3N_4, the proposed model was able to represent properly the measured parameters with 70% training set that the relationship between the was well represented by w reinforcement material.

The investigation of new machining technique is also vital to improve the drilling of MMCs. [21] used a laser assisted machining (LAM) method in the drilling of long-fibre reinforced Al-2%Cu/Al_2O_3 composite and also performed a 2-D multi-phase finite element analysis to model the process and predict the drilling-induced damage. Surface roughness, cutting energy, fibre pull-out and tool wear were significantly reduced when LAM was used and the proposed model succeeded in the prediction of machining induced damage as a function of cutting temperature showing that higher material removal temperatures resulted in lower damage. An empirical study of ultrasonic-assisted drilling process of Al/SiC metal matrix composite was performed by Kadivar et al. [56]. The authors investigated the drilling force and burr size when ultrasonic assisted of the tool and workpiece was used. The results showed that ultrasonic vibration technique improved the drilling of Al/SiC MMC.

12 Grinding of MMC

Grinding is an essential operation to reach final geometry and surface finishing in the manufacturing process of MMCs. Nandakumar et al. [79] evaluated the performance of minimum quantity lubrication grinding process of Nano SiC reinforced aluminum MMC using cashew nutshell oil and Nano TiO_2 filled cashew nutshell oil. The authors reported depth of cut and wheel speed as the most important parameters that influence the responses. The best results were obtained when cashew nutshell Oil + NanoTiO_2 based MQL was used. The grinding process of aluminum-based MMCs reinforced with SiC particles were studied by Kwak and Kim [61] whose work used Taguchi design of experiments. Using RSM, the authors were able to define the optimal set of machining parameters to improve the surface roughness and reduce grinding forces.

A review of the application of soft computing methods in machining process of particle reinforced MMC was performed by Laghari et al. [62]. The authors presented the most advanced modelling techniques being used to simulate and optimize machining processes of MMCs. Many methods such as RSM, Taguchi techniques, genetic algorithms, ANN and fuzzy logic have proved its efficiency in the prediction of responses of machining processes of MMCs. In [133] the authors studied the material removal mechanism of SiCp/Al MMC by theoretical modeling, simulation and experimental procedure. They have reported consistent results when comparing the results of theory, simulation and experiment. Liu et al. (2017) used a back-propagation ANN optimized by particle swarm optimization algorithm to predict the grinding temperature if titanium MMC which presented better results when compared to other ANN models. The prediction accuracy of particle swarm optimized back propagation artificial neural network is up to 94.13%, which indicates that it can predict the grinding temperature accurately.

13 Non-conventional Machining of MMC

Non-conventional machining methods have shown very promising results in the manufacturing of MMCs. These techniques are able to increase productivity, reduce costs and generate better surface integrity when compared to conventional processes. Müller and Monaghan [77] used an experimental investigation involving LBM, AWJ and EDM machining of SiC reinforced Al MMC. Considering each of these processes have a material removal mechanism they also present different results in machined surface quality and productivity. EDM presented low productivity and crater-like surface. Laser beam machining showed high productivity but poor surface quality and also significant thermal induced microstructural changes in heat affected zone. AWJ also presented poor surface quality but no thermal induced damage was observed.

Suresh Kumar et al. [113] investigated the EDM process of AleSiC and AleSi-CeB4C parts using different machining parameters. They reported an increment in surface roughness when higher current was used, and crater diameter was also raised when higher material removal rate was applied.

The use of laser beam machining was studied by Ghosal and Manna [40] that developed a statistical model to correlate the interactive and higher order effects of the different cutting parameters, such as the modulation frequency, laser power, wait time, gas pressure and pulse width on the tapering phenomena and metal removal rate. They reported that laser process parameter can be controlled for effective drilling of Al/Al_2O_3-MMC and the developed model could satisfactory evaluate the MRR and taper angle under various machining parameters. Marimuthu et al. [73] also investigated the use of LBM in the machining process of aluminum based MMCs. They reported that the process is challenging because of the great difference in the melting temperature of Al and Al_2O_3 presenting a minimum heat affected zone of 300 μm.

Srivastava et al. [109] investigated the abrasive water jet of tuning of MMC of A359/Al_2 O_3 /B4 C. They stated that abrasive waterjet turning can be used in rough turning process for material removal, avoiding the problems generated by conventional turning of MMCs and the traverse speed is one of the most important process parameters of AWJ turning influencing on surface roughness and material removal. The SEM images revealed pits formation, internal cracks, and brittle fracture of reinforcement particles on the machined surface which increased when higher traverse speed was used. The machinability of aluminum 7075 MMCs by an AWJM method was investigated by Sasikumar et al. [99] that, based on the results, proved the feasibility of this method in the machining of aluminum 7075 composites. Using ANOVA, they suggested that AWJM parameters such as jet speed water, jet pressure and standoff distance impact directly on kerf characteristics such as surface finish and top kerf width. They also observed that higher level of water jet pressure provided better surface finish.

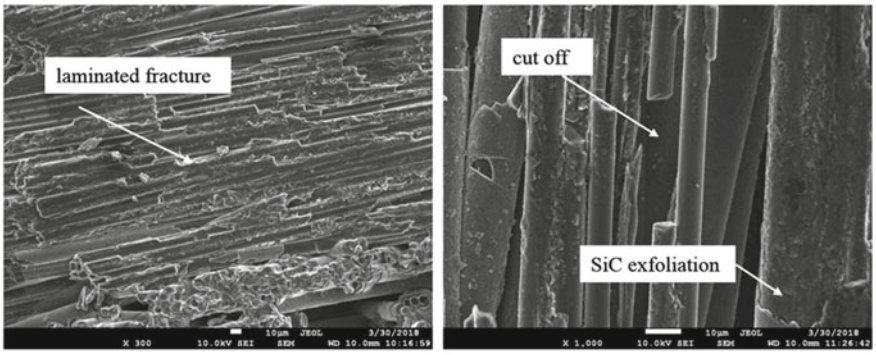

Fig. 8 Example of machine-induced damage. **a** Extruding vault and fibre fracture. **b** Fibre pull-out [26]

14 Machining of Ceramic Matrix Composites (CMC)

Ceramic Matrix Composites have been used in applications in which resistance to elevated temperature is required such as gas turbine engines components and in rocket nozzles. This type of composite also stands out as a good alternative for frictional applications such as cars or aircrafts braking systems [35]. The growing demand for ceramic matrix composites justifies the efforts in understanding its machining process. As the other types of composites, CMCs are manufactured net-shape, but further machining process is still required to reach proper geometry and surface quality requirements. Unlike PMCs and MMCs, CMCs possess a brittle matrix which makes its machinability and cutting mechanism completely different. Ceramic matrix composites are hard materials, which easily produces defects, such as burrs, chipping, fibres pull-out/fracture, delamination and surface/subsurface micro-cracks during the machining (Fig. 8). Due to its characteristics they are very unlikely to be machined by conventional methods.

The most commonly used conventional machining processes of CMCs are grinding and drilling. Due to the difficulty in using conventional machining processes in CMCs, new non-conventional machining techniques have been investigate [94] presenting promising results.

15 Milling of CMC

Considering the high strength, high hardness and the abrasive nature of CMCs traditional milling process is not feasible or not economically viable. In this scenario techniques such as ultrasonic assisted machining and laser assisted machining (LAM) have been investigated. Rozzi and Barton [96] integrated a laser and a conventional

machine tool and demonstrated the feasibility of the use of LAM machining of CMC components. The authors reported a reduction in 40% of cutting forces using LAM as compared to conventional. In [24] tool wear progression and tool life in micro milling of CMC materials were investigated. The authors also proposed a three-dimensional FEM model to simulate temperature distributions and assist in the selection of optimal cutting parameters for laser assisted micro milling. The obtained results showed that the total cost of the process could be significantly reduced to 32.3% of the cost of conventional micromachining when laser assisted method is used.

Another promising method is the rotary ultrasonic machining which was applied by Yuan et al. [134] in the side milling of C/SiC composites. The authors developed a mechanistic model to predict cutting forces and understand its relationship with machining parameters. The cutting force increased with the increment of feed rate and depth of cut while the increase in spindle speed lead to decrease in cutting force. They also reported that the developed model was compared with experimental data and the obtained error was less than 10% for most set of values. In [64] the material removal mechanism of brittle fracture of C/SiC by rotary ultrasonic machining was investigated using a cutting force simulation. Machining parameters were optimized by the algorithm to reduce the machining force and the results were compared with experimental data. Rotary ultrasonic machining achieved the high machining efficiency. Surface roughness was improved while cutting tool cost was reduced by a half when compared to conventional method. Wang et al. (2017) also obtained great results when using rotary ultrasonic method in the milling of MMC. They observed a dramatical reduce in cutting forces when the technique was used in in the machining of C/SiC composites.

16 Drilling of CMC

Drilling is still a required manufacturing step even for net-shape manufactured CMCs components. Although, it is very challenging because of the appearance of severe drilling-induced defects [23]. When traditional methods and tools are used, tools tend to undergo severe wear in short cutting time and generate poor quality finishing [115]. To overcome this problem new techniques have been studied to make the drilling of CMCs feasible. In this manner ultrasonic drilling stands out with great results.

In [127] the authors studied the rotary ultrasonic drilling and effect of longitudinal-torsional coupled vibration drilling in the cutting forces of carbon fibre-reinforced silicon carbide (C/SiC) CMCs comparing the results with those obtained in longitudinal vibration. They showed that longitudinal- torsional coupled vibration method was able to induce a 50% reduction in cutting force. Feng et al. [30] performed a factorial experimental investigation of rotary ultrasonic machining (RUM) of C/SiC to investigate the drilling-induced tearing defects. The authors reported that RUM was able to reduce both tearing defect (Fig. 9) and thrust force and increments in

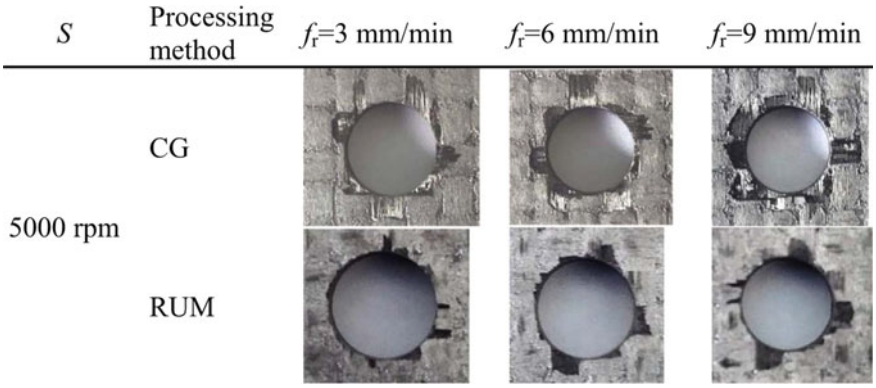

Fig. 9 Images of drilled holes exits varying the drilling methods in C/SiC CMC [30]

the spindle speed and ultrasonic amplitude or decreasing the feed rate were able to reduce the tearing factor at hole exit.

Torque prediction and axial drilling force model was proposed by Islam et al. [54] and the results were validated using experimental data of rotary ultrasonic drilling on C/SiC CMCs. Feed rate, spindle speed and ultrasonic power were the input variables for the model development. Axial drilling force and torque were predicted with and error of 14% and 10% respectively.

17 Grinding of CMC

The grinding process of C/SiC CMCs were studied by Du et al. [26] that among other findings concluded that fibre orientation plays an important role in the obtained cutting forces and increments in feed rate results in more poor surface quality. Adibi et al. [2] evaluated the influence on MQL grinding process of C/SiC composites comparing the results with flood and dry techniques using different grinding parameters (depth of cut, feed rate and cutting speed). They reported that the use MQL resulted in the reduction of cutting forces when compared to the other two techniques. MQL also reduces significantly the tool wear and produced a slightly better surface finishing. Dry machining presented the worst results for all the output variables (specific grinding energy, grinding forces, grinding ratio, wheel wear and surface roughness). In [42], the authors systemically analyzed the effect of grinding parameter in the machining efficiency and surface quality of SiC and 2.5 D needled Cf/SiC composite materials. They observed that fibre orientation has a substantial effect on the SiC matrix and higher grinding forces were observed SiC when compared to 2.5 D needled Cf/SiC composite. Qu et al. [89] evaluated the effect of fibre orientation and grinding depth on the grinding quality of unidirectional Cf/SiC CMC. The grinding quality was evaluated based on surface quality, grinding chips and grinding

forces. The grinding depth and the fibre orientation were reported as the most important parameters influencing on grinding quality. When grinding depth was reduced surface quality was improve and grinding forces and maximum undeformed chip thickness increased.

18 Non-conventional Machining of CMC

Considering all the problems associated with the conventional machining of CMCs many efforts have been made to optimize the application of non-conventional machining such as laser machining, abrasive water jet machining, abrasive jet machining and electric discharged machining in the machining process of these materials. In their review, [36] discussed the use of these techniques and pointed that although the number of publications regarding the machining processes of CMCs have grown in the last few years there is still a lack of study specially for abrasive water jet machining, abrasive jet machining and electric discharged machining.

Ridealgh et al. [95] studied the laser cutting of a glass ceramic matrix composite reinforced with continuous fibres of SiC. They observed that laser cutting produced better surface quality when compared to the results obtained by high speed diamond saw. Author concluded that the use of this process in industrial scale may be viable but a more extend work is required. Liu et al. [69] discussed the use of different machining parameters, such as rate of laser spot, overlap, helical line, feeding speeds and energy density in the drilling process of micro-holes on SiC/SiC CMCs. The authors used femtosecond laser irradiation technique to perform the ablation of CMS and then perform the micro-holes. They reported that spot overlap ratio influenced on the depth of micro-holes and when higher overlap rate was used more effective removal of material was generated, increasing the depth of the holes. Feed rate was one of the most significative factors affecting the quality of micro-holes. In [55] the abrasive water jet machining of zirconia (ZrO_2) composite was evaluated using Taguchi L27 orthogonal array. The authors reported that the technique is capable and adequate to machine zirconia (ZrO_2) composites and also stated that the adopted method successfully predicted the optimal cutting conditions as shown by the experimental confirmation tests.

Wei et al. [130] used EDM process in advanced CMC with ceramic fibre reinforcements. They evaluated the machinability of the material and identified the set parameters to improve the process using ANOVA. They investigated the influence of electrode vibration in the process. Tool vibration and dielectric deep flushing increased the MRR and surface integrity. The authors also reported that the material removal mechanism of the ceramic matrix occurs by crack expansion, cracking and stripping-off.

19 Conclusion

The subtractive manufacturing process of composites materials is still a challenge to be overcome due to the wide range and the complex mechanical and chemical properties found in this type of material. The increment in demand for components manufactured with composite materials stimulates the interesting of researchers in carrying out investigations to optimize the machining processes of these material, improving the surface quality of the components and reducing costs to achieve industrial requirements. In this context, this review demonstrated that many efforts have been done not only to improve conventional machining processes but also to develop new techniques that can be applied in the subtractive manufacturing process of Polymer Matrix Composites (MMCs), Metal Matrix Composites (MMCs) and Ceramic Matrix Composites (CMCs). Although the results achieved in the recent years it is possible to conclude that more investigating is required to define the best techniques and parameters to obtain high quality components with feasible costs, especially when it comes to the machining processes of CMCs.

References

1. Aamir M, Tolouei-Rad M, Giasin K, Nosrati A (2019) Recent advances in drilling of carbon fiber–reinforced polymers for aerospace applications: a review. Int J Adv Manuf Technol 105:2289–2308. https://doi.org/10.1007/s00170-019-04348-z
2. Adibi H, Esmaeili H, Rezaei SM (2018) Study on minimum quantity lubrication (MQL) in grinding of carbon fiber-reinforced SiC matrix composites (CMCs). Int J Adv Manuf Technol 95:3753–3767. https://doi.org/10.1007/s00170-017-1464-x
3. Ajith Arul Daniel S, Pugazhenthi R, Kumar R, Vijayananth S (2019) Multi objective prediction and optimization of control parameters in the milling of aluminium hybrid metal matrix composites using ANN and Taguchi-Grey relational analysis. Def Technol 15:545–556. https://doi.org/10.1016/j.dt.2019.01.001
4. Altin Karataş M, Gökkaya H (2018) A review on machinability of carbon fiber reinforced polymer (CFRP) and glass fiber reinforced polymer (GFRP) composite materials. Def Technol 14:318–326. https://doi.org/10.1016/j.dt.2018.02.001
5. Azmi AI, Lin RJT, Bhattacharyya D (2013) Machinability study of glass fibre-reinforced polymer composites during end milling. Int J Adv Manuf Technol 64:247–261. https://doi.org/10.1007/s00170-012-4006-6
6. Bagci E, Işık B (2006) Investigation of surface roughness in turning unidirectional GFRP composites by using RS methodology and ANN. Int J Adv Manuf Technol 31:10–17. https://doi.org/10.1007/s00170-005-0175-x
7. Bai W, Roy A, Sun R, Silberschmidt VV (2019) Enhanced machinability of SiC-reinforced metal-matrix composite with hybrid turning. J Mater Process Technol 268:149–161. https://doi.org/10.1016/j.jmatprotec.2019.01.017
8. Balamurugan K, Uthayakumar M, Thirumalai Kumaran S et al (2019) Drilling study on lightweight structural Mg/SiC composite for defence applications. Def Technol 15:557–564. https://doi.org/10.1016/j.dt.2019.01.002
9. Basheer AC, Dabade UA, Joshi SS et al (2008) Modeling of surface roughness in precision machining of metal matrix composites using ANN. J Mater Process Technol 197:439–444. https://doi.org/10.1016/j.jmatprotec.2007.04.121

10. Bejjani R, Shi B, Attia H, Balazinski M (2011) Laser assisted turning of Titanium metal matrix composite. CIRP Ann 60:61–64. https://doi.org/10.1016/j.cirp.2011.03.086
11. Caggiano A (2018) Machining of fibre reinforced plastic composite materials. Materials (Basel) 11:442
12. Campos Rubio J, Abrao AM, Faria PE et al (2008) Effects of high speed in the drilling of glass fibre reinforced plastic: evaluation of the delamination factor. Int J Mach Tools Manuf 48:715–720. https://doi.org/10.1016/j.ijmachtools.2007.10.015
13. Chan K, Cheung C, Ramesh M et al (2001) A theoretical and experimental investigation of surface generation in diamond turning of an Al6061/SiCp metal matrix composite. Int J Mech Sci 43:2047–2068. https://doi.org/10.1016/S0020-7403(01)00028-5
14. Chang CS (2015) A study of cutting temperatures in turning carbon-fiber-reinforced-plastic (CRFP) composites with nose radius tools. Key Eng Mater 649:38–45. https://doi.org/10.4028/www.scientific.net/KEM.649.38
15. Chen T, Xiang J, Gao F et al (2019) Study on cutting performance of diamond-coated rhombic milling cutter in machining carbon fiber composites. Int J Adv Manuf Technol 103:4731–4737. https://doi.org/10.1007/s00170-019-03902-z
16. Chen W-C (1997) Some experimental investigations in the drilling of carbon fiber-reinforced plastic (CFRP) composite laminates. Int J Mach Tools Manuf 37:1097–1108. https://doi.org/10.1016/S0890-6955(96)00095-8
17. Chockalingam P, Kuang KC (2015) Effects of abrasive types on grinding of chopped strand mat glass fiber-reinforced polymer composite laminates. Mach Sci Technol 19:313–324. https://doi.org/10.1080/10910344.2015.1018534
18. Chockalingam P, Kuang KC, Vijayaram TR (2013) Effects of grinding process parameters and coolants on the grindability of GFRP laminates. Mater Manuf Process 28:1071–1076. https://doi.org/10.1080/10426914.2013.792411
19. Çolak O, Sunar T (2016) Cutting forces and 3D surface analysis of CFRP milling with PCD cutting tools. Procedia CIRP 45:75–78. https://doi.org/10.1016/j.procir.2016.03.091
20. Dandekar CR, Shin YC (2012) Modeling of machining of composite materials: a review. Int J Mach Tools Manuf 57:102–121. https://doi.org/10.1016/j.ijmachtools.2012.01.006
21. Dandekar CR, Shin YC (2009) Laser-assisted machining of a fiber reinforced metal matrix composite. In: ASME 2009 international manufacturing science and engineering conference, vol 2. ASMEDC, pp 579–588
22. Davim JP (2003) Design of optimisation of cutting parameters for turning metal matrix composites based on the orthogonal arrays. J Mater Process Technol 132:340–344. https://doi.org/10.1016/S0924-0136(02)00946-9
23. Ding K, Fu Y, Su H et al (2014) Experimental studies on drilling tool load and machining quality of C/SiC composites in rotary ultrasonic machining. J Mater Process Technol 214:2900–2907. https://doi.org/10.1016/j.jmatprotec.2014.06.015
24. Dong X, Shin YC (2017) Improved machinability of SiC/SiC ceramic matrix composite via laser-assisted micromachining. Int J Adv Manuf Technol 90:731–739. https://doi.org/10.1007/s00170-016-9415-5
25. Doomra VK, Debnath K, Singh I (2015) Drilling of metal matrix composites: experimental and finite element analysis. Proc Inst Mech Eng Part B J Eng Manuf 229:886–890. https://doi.org/10.1177/0954405414534227
26. Du J, Ming W, Ma J et al (2018) New observations of the fiber orientations effect on machinability in grinding of C/SiC ceramic matrix composite. Ceram Int 44:13916–13928. https://doi.org/10.1016/j.ceramint.2018.04.240
27. El-Hofy M, Helmy MO, Escobar-Palafox G et al (2018) Abrasive water jet machining of multidirectional CFRP laminates. Procedia CIRP 68:535–540. https://doi.org/10.1016/j.procir.2017.12.109
28. El-Hofy MH, Soo SL, Aspinwall DK et al (2011) Factors affecting workpiece surface integrity in slotting of CFRP. Procedia Eng 19:94–99. https://doi.org/10.1016/j.proeng.2011.11.085
29. Feito N, Díaz-Álvarez J, Díaz-Álvarez A et al (2014) Experimental analysis of the influence of drill point angle and wear on the drilling of woven CFRPs. Materials (Basel) 7:4258–4271. https://doi.org/10.3390/ma7064258

30. Feng P, Wang J, Zhang J, Zheng J (2017) Drilling induced tearing defects in rotary ultrasonic machining of C/SiC composites. Ceram Int 43:791–799. https://doi.org/10.1016/j.ceramint.2016.10.010
31. Fernández-Pérez J, Díaz-Álvarez J, Miguélez MH, Cantero JL (2021) Combined analysis of wear mechanisms and delamination in CFRP drilling. Compos Struct 255:112774. https://doi.org/10.1016/j.compstruct.2020.112774
32. Fetecau C, Stan F (2012) Study of cutting force and surface roughness in the turning of polytetrafluoroethylene composites with a polycrystalline diamond tool. Measurement 45:1367–1379. https://doi.org/10.1016/j.measurement.2012.03.030
33. Gaitonde VN, Karnik SR, Rubio JC et al (2008) Analysis of parametric influence on delamination in high-speed drilling of carbon fiber reinforced plastic composites. J Mater Process Technol 203:431–438. https://doi.org/10.1016/j.jmatprotec.2007.10.050
34. Gara S, Tsoumarev O (2016) Effect of tool geometry on surface roughness in slotting of CFRP. Int J Adv Manuf Technol 86:451–461. https://doi.org/10.1007/s00170-015-8185-9
35. Gavalda Diaz O, Axinte DA (2017) Towards understanding the cutting and fracture mechanism in ceramic matrix composites. Int J Mach Tools Manuf 118–119:12–25. https://doi.org/10.1016/j.ijmachtools.2017.03.008
36. Gavalda Diaz O, Garcia Luna G, Liao Z, Axinte D (2019) The new challenges of machining Ceramic Matrix Composites (CMCs): review of surface integrity. Int J Mach Tools Manuf 139:24–36. https://doi.org/10.1016/j.ijmachtools.2019.01.003
37. Ge YF, Xu JH, Yang H et al (2008) Workpiece surface quality when ultra-precision turning of SiCp/Al composites. J Mater Process Technol 203:166–175. https://doi.org/10.1016/j.jmatprotec.2007.09.070
38. Geng D, Liu Y, Shao Z et al (2019) Delamination formation, evaluation and suppression during drilling of composite laminates: a review. Compos Struct 216:168–186. https://doi.org/10.1016/j.compstruct.2019.02.099
39. Ghafarizadeh S, Chatelain J-F, Lebrun G (2016) Finite element analysis of surface milling of carbon fiber-reinforced composites. Int J Adv Manuf Technol 87:399–409. https://doi.org/10.1007/s00170-016-8482-y
40. Ghosal A, Manna A (2013) Response surface method based optimization of ytterbium fiber laser parameter during machining of Al/Al_2O_3-MMC. Opt Laser Technol 46:67–76. https://doi.org/10.1016/j.optlastec.2012.04.030
41. Giasin K, Ayvar-Soberanis S, Hodzic A (2015) An experimental study on drilling of unidirectional GLARE fibre metal laminates. Compos Struct 133:794–808. https://doi.org/10.1016/j.compstruct.2015.08.007
42. Gong Y, Qu S, Yang Y et al (2019) Some observations in grinding SiC and silicon carbide ceramic matrix composite material. Int J Adv Manuf Technol 103:3175–3186. https://doi.org/10.1007/s00170-019-03735-w
43. Gowda BMU, Ravindra HV, Ullas M et al (2014) Estimation of Circularity, Cylindricity And Surface Roughness In Drilling Al-Si 3 N 4 metal matrix composites using artificial neural network. Procedia Mater Sci 6:1780–1787. https://doi.org/10.1016/j.mspro.2014.07.208
44. Haeger A, Schoen G, Lissek F et al (2016) Non-destructive detection of drilling-induced delamination in CFRP and its effect on mechanical properties. Procedia Eng 149:130–142. https://doi.org/10.1016/j.proeng.2016.06.647
45. Hassanpour H, Sadeghi MH, Rasti A, Shajari S (2016) Investigation of surface roughness, microhardness and white layer thickness in hard milling of AISI 4340 using minimum quantity lubrication. J Clean Prod 120:124–134. https://doi.org/10.1016/j.jclepro.2015.12.091
46. Hintze W, Brügmann F (2018) Influence of spatial tool inclination on delamination when milling CFRP. J Mater Process Technol 252:830–837. https://doi.org/10.1016/j.jmatprotec.2017.10.041
47. Hintze W, Hartmann D (2013) Modeling of delamination during milling of unidirectional CFRP. Procedia CIRP 8:444–449. https://doi.org/10.1016/j.procir.2013.06.131
48. Hintze W, Hartmann D, Schütte C (2011) Occurrence and propagation of delamination during the machining of carbon fibre reinforced plastics (CFRPs)—an experimental study. Compos Sci Technol 71:1719–1726. https://doi.org/10.1016/j.compscitech.2011.08.002

49. Hosokawa A, Hirose N, Ueda T, Furumoto T (2014) High-quality machining of CFRP with high helix end mill. CIRP Ann 63:89–92. https://doi.org/10.1016/j.cirp.2014.03.084
50. Hu NS, Zhang LC (2003) A study on the grindability of multidirectional carbon fibre-reinforced plastics. J Mater Process Technol 140:152–156. https://doi.org/10.1016/S0924-0136(03)00704-0
51. Ibraheem HMA, Iqbal A, Hashemipour M (2015) Numerical optimization of hole making in GFRP composite using abrasive water jet machining process. J Chin Inst Eng 38:66–76. https://doi.org/10.1080/02533839.2014.953240
52. Işık B, Kentli A (2009) Multicriteria optimization of cutting parameters in turning of UD-GFRP materials considering sensitivity. Int J Adv Manuf Technol 44:1144–1153. https://doi.org/10.1007/s00170-009-1927-9
53. Iskandar Y, Tendolkar A, Attia MH et al (2014) Flow visualization and characterization for optimized MQL machining of composites. CIRP Ann 63:77–80. https://doi.org/10.1016/j.cirp.2014.03.078
54. Islam S, Yuan S, Li Z (2020) Mathematical modeling and experimental studies on axial drilling load for rotary ultrasonic drilling of C/SiC composites. Int J Adv Manuf Technol 107:1309–1326. https://doi.org/10.1007/s00170-020-05052-z
55. Jagadish, Gupta K (2020) Abrasive water jet machining of ceramic composites, pp 51–71
56. Kadivar MA, Akbari J, Yousefi R et al (2014) Investigating the effects of vibration method on ultrasonic-assisted drilling of Al/SiCp metal matrix composites. Robot Comput Integr Manuf 30:344–350. https://doi.org/10.1016/j.rcim.2013.10.001
57. Karabulut Ş, Gökmen U, Çinici H (2018) Optimization of machining conditions for surface quality in milling AA7039-based metal matrix composites. Arab J Sci Eng 43:1071–1082. https://doi.org/10.1007/s13369-017-2691-z
58. Kim J, Bai W, Roy A et al (2019) Hybrid machining of metal-matrix composite. Procedia CIRP 82:184–189. https://doi.org/10.1016/j.procir.2019.04.162
59. Kong X, Yang L, Zhang H et al (2017) Optimization of surface roughness in laser-assisted machining of metal matrix composites using Taguchi method. Int J Adv Manuf Technol 89:529–542. https://doi.org/10.1007/s00170-016-9115-1
60. Kumar R, Kumar A, Singh I (2018) Electric discharge drilling of micro holes in CFRP laminates. J Mater Process Technol 259:150–158. https://doi.org/10.1016/j.jmatprotec.2018.04.031
61. Kwak JS, Kim YS (2008) Mechanical properties and grinding performance on aluminum-based metal matrix composites. J Mater Process Technol 201:596–600. https://doi.org/10.1016/j.jmatprotec.2007.11.139
62. Laghari RA, Li J, Laghari AA, Wang S (2019) A review on application of soft computing techniques in machining of particle reinforcement metal matrix composites. Arch Comput Methods Eng. https://doi.org/10.1007/s11831-019-09340-0
63. Leone C, Genna S (2018) Heat affected zone extension in pulsed Nd:YAG laser cutting of CFRP. Compos Part B Eng 140:174–182. https://doi.org/10.1016/j.compositesb.2017.12.028
64. Li Z, Yuan S, Zhang C (2016) Research on the rotary ultrasonic facing milling of ceramic matrix composites. Procedia CIRP 56:428–433. https://doi.org/10.1016/j.procir.2016.10.077
65. Liao Z, Abdelhafeez A, Li H et al (2019) State-of-the-art of surface integrity in machining of metal matrix composites. Int J Mach Tools Manuf 143:63–91. https://doi.org/10.1016/j.ijmachtools.2019.05.006
66. Liu C, Ding W, Li Z, Yang C (2017a) Prediction of high-speed grinding temperature of titanium matrix composites using BP neural network based on PSO algorithm. Int J Adv Manuf Technol 89:2277–2285. https://doi.org/10.1007/s00170-016-9267-z
67. Liu JW, Baek DK, Ko TJ (2014) Chipping minimization in drilling ceramic materials with rotary ultrasonic machining. Int J Adv Manuf Technol 72:1527–1535. https://doi.org/10.1007/s00170-014-5766-y
68. Liu S, Chen T, Wu C (2017b) Rotary ultrasonic face grinding of carbon fiber reinforced plastic (CFRP): a study on cutting force model. Int J Adv Manuf Technol 89:847–856. https://doi.org/10.1007/s00170-016-9151-x

69. Liu Y, Zhang R, Li W et al (2018) Effect of machining parameter on femtosecond laser drilling processing on SiC/SiC composites. Int J Adv Manuf Technol 96:1795–1811. https://doi.org/10.1007/s00170-017-1163-7
70. Lopresto V, Caggiano A, Teti R (2016) High performance cutting of fibre reinforced plastic composite materials. Procedia CIRP 46:71–82. https://doi.org/10.1016/j.procir.2016.05.079
71. M'Saoubi R, Outeiro JC, Chandrasekaran H et al (2008) A review of surface integrity in machining and its impact on functional performance and life of machined products. Int J Sustain Manuf 1:203. https://doi.org/10.1504/IJSM.2008.019234
72. M'Saoubi R, Axinte D, Soo SL et al (2015) High performance cutting of advanced aerospace alloys and composite materials. CIRP Ann 64:557–580. https://doi.org/10.1016/j.cirp.2015.05.002
73. Marimuthu S, Dunleavey J, Liu Y et al (2019) Laser cutting of aluminium-alumina metal matrix composite. Opt Laser Technol 117:251–259. https://doi.org/10.1016/j.optlastec.2019.04.029
74. Iw MM, Azmi A, Lee C, Mansor A (2018) Kerf taper and delamination damage minimization of FRP hybrid composites under abrasive water-jet machining. Int J Adv Manuf Technol 94:1727–1744. https://doi.org/10.1007/s00170-016-9669-y
75. Mohamed SB, Rashid RA, Muhamad M, Ismail J (2019) Composite materials and types of machining, pp 1–14
76. Morkavuk S, Köklü U, Bağcı M, Gemi L (2018) Cryogenic machining of carbon fiber reinforced plastic (CFRP) composites and the effects of cryogenic treatment on tensile properties: a comparative study. Compos Part B Eng 147:1–11. https://doi.org/10.1016/j.compositesb.2018.04.024
77. Müller F, Monaghan J (2000) Non-conventional machining of particle reinforced metal matrix composite. Int J Mach Tools Manuf 40:1351–1366. https://doi.org/10.1016/S0890-6955(99)00121-2
78. Murphy C, Byrne G, Gilchrist MD (2002) The performance of coated tungsten carbide drills when machining carbon fibre-reinforced epoxy composite materials. Proc Inst Mech Eng Part B J Eng Manuf 216:143–152. https://doi.org/10.1243/0954405021519735
79. Nandakumar A, Rajmohan T, Vijayabhaskar S (2019) Experimental evaluation of the lubrication performance in MQL grinding of nano SiC reinforced Al matrix composites. SILICON 11:2987–2999. https://doi.org/10.1007/s12633-019-0088-1
80. Nassar MMA, Arunachalam R, Alzebdeh KI (2017) Machinability of natural fiber reinforced composites: a review. Int J Adv Manuf Technol 88:2985–3004. https://doi.org/10.1007/s00170-016-9010-9
81. Nicholls CJ, Boswell B, Davies IJ, Islam MN (2017) Review of machining metal matrix composites. Int J Adv Manuf Technol 90:2429–2441. https://doi.org/10.1007/s00170-016-9558-4
82. Niu Q, Jing L, Wang C et al (2020) Study on effect of vibration amplitude on cutting performance of SiCp/Al composites during ultrasonic vibration–assisted milling. Int J Adv Manuf Technol 106:2219–2225. https://doi.org/10.1007/s00170-019-04796-7
83. Ozkan D, Sabri Gok M, Oge M, Cahit Karaoglanli A (2019) Milling behavior analysis of carbon fiber-reinforced polymer (CFRP) composites. Mater Today Proc 11:526–533. https://doi.org/10.1016/j.matpr.2019.01.024
84. Palanikumar K, Karunamoorthy L, Karthikeyan R (2006) Assessment of factors influencing surface roughness on the machining of glass fiber-reinforced polymer composites. Mater Des 27:862–871. https://doi.org/10.1016/j.matdes.2005.03.011
85. Park CI, Wei Y, Hassani M et al (2019) Low power direct laser-assisted machining of carbon fibre-reinforced polymer. Manuf Lett 22:19–24. https://doi.org/10.1016/j.mfglet.2019.10.001
86. Petropoulos G, Mata F, Davim JP (2008) Statistical study of surface roughness in turning of peek composites. Mater Des 29:218–223. https://doi.org/10.1016/j.matdes.2006.11.005
87. Pradhan V, Das PP (2018) Parametric optimization of CNC turning on glass-fibre-reinforced plastic (GFRP) pipes: a grey-fuzzy logic approach. IOP Conf Ser Mater Sci Eng 377:012180. https://doi.org/10.1088/1757-899X/377/1/012180

88. Pramanik A, Zhang LC, Arsecularatne JA (2006) Prediction of cutting forces in machining of metal matrix composites. Int J Mach Tools Manuf 46:1795–1803. https://doi.org/10.1016/j.ijmachtools.2005.11.012
89. Qu S, Gong Y, Yang Y et al (2019) Grinding characteristics and removal mechanisms of unidirectional carbon fibre reinforced silicon carbide ceramic matrix composites. Ceram Int 45:3059–3071. https://doi.org/10.1016/j.ceramint.2018.10.178
90. Rai RN, Datta GL, Chakraborty M, Chattopadhyay AB (2006) A study on the machinability behaviour of Al–TiC composite prepared by in situ technique. Mater Sci Eng A 428:34–40. https://doi.org/10.1016/j.msea.2005.11.040
91. Rajasekaran T, Palanikumar K, Arunachalam S (2013) Investigation on the turning parameters for surface roughness using Taguchi analysis. Procedia Eng 51:781–790. https://doi.org/10.1016/j.proeng.2013.01.112
92. Rajasekaran T, Palanikumar K, Vinayagam BK (2012) Turning CFRP composites with ceramic tool for surface roughness analysis. Procedia Eng 38:2922–2929. https://doi.org/10.1016/j.proeng.2012.06.341
93. Rajeswari B, Amirthagadeswaran KS (2018) Study of machinability and parametric optimization of end milling on aluminium hybrid composites using multi-objective genetic algorithm. J Brazilian Soc Mech Sci Eng 40:377. https://doi.org/10.1007/s40430-018-1293-3
94. Rayat MS, Gill SS, Singh R, Sharma L (2017) Fabrication and machining of ceramic composites—a review on current scenario. Mater Manuf Process 32:1451–1474. https://doi.org/10.1080/10426914.2017.1279301
95. Ridealgh JA, Rawlings RD, West DRF (1990) Laser cutting of glass ceramic matrix composite. Mater Sci Technol 6:395–398. https://doi.org/10.1179/mst.1990.6.4.395
96. Rozzi JC, Barton MD (2009) The laser-assisted edge milling of ceramic matrix composites. In: ASME 2009 international manufacturing science and engineering conference, vol 1. ASMEDC, pp 845–852
97. Ruiz-Garcia R, Mayuet Ares P, Vazquez-Martinez J, Salguero Gómez J (2018) Influence of abrasive waterjet parameters on the cutting and drilling of CFRP/UNS A97075 and UNS A97075/CFRP stacks. Mater (Basel) 12:107. https://doi.org/10.3390/ma12010107
98. Sasahara H, Kikuma T, Koyasu R, Yao Y (2014) Surface grinding of carbon fiber reinforced plastic (CFRP) with an internal coolant supplied through grinding wheel. Precis Eng 38:775–782. https://doi.org/10.1016/j.precisioneng.2014.04.005
99. Sasikumar K, Arulshri K, Ponappa K, Uthayakumar M (2018) A study on kerf characteristics of hybrid aluminium 7075 metal matrix composites machined using abrasive water jet machining technology. Proc Inst Mech Eng Part B J Eng Manuf 232:690–704. https://doi.org/10.1177/0954405416654085
100. Sheikh-Ahmad JY (2016) Hole quality and damage in drilling carbon/epoxy composites by electrical discharge machining. Mater Manuf Process 31:941–950. https://doi.org/10.1080/10426914.2015.1048368
101. Sheikh-Ahmad JY, Davim JP (2012) Cutting and machining of polymer composites. In: Wiley encyclopedia of composites. Wiley, Hoboken
102. Sheikh-Ahmad JY, Dhuttargaon M, Cheraghi H (2017) New tool life criterion for delamination free milling of CFRP. Int J Adv Manuf Technol 92:2131–2143. https://doi.org/10.1007/s00170-017-0240-2
103. Shin YC, Dandekar C (2012) Mechanics and modeling of chip formation in machining of MMC. Machining of metal matrix composites. Springer, London, London, pp 1–49
104. Shyha I (2013) An investigation into CO_2 laser trimming of CFRP and GFRP composites. Procedia Eng 63:931–937. https://doi.org/10.1016/j.proeng.2013.08.200s
105. Singh S (2016) Effect of modified drill point geometry on drilling quality characteristics of metal matrix composite (MMCs). J Mech Sci Technol 30:2691–2698. https://doi.org/10.1007/s12206-016-0530-x
106. Song H, Dan J, Du J et al (2019) Multiresponse optimization for laser-assisted machining of fused silica using response surface methodology. SILICON 11:3049–3063. https://doi.org/10.1007/s12633-019-00101-z

107. Soorya Prakash K, Gopal PM, Karthik S (2020) Multi-objective optimization using Taguchi based grey relational analysis in turning of rock dust reinforced Aluminum MMC. Measurement 157:107664. https://doi.org/10.1016/j.measurement.2020.107664
108. Sridhar R, Perumal Subramaniyan S, Ramesh S (2019) Optimization of machining and geometrical parameters to reduce vibration while milling metal matrix composite. Trans Indian Inst Met 72:3179–3189. https://doi.org/10.1007/s12666-019-01783-0
109. Srivastava AK, Nag A, Dixit AR et al (2017) Surface integrity in tangential turning of hybrid MMC A359/B 4 C/Al_2O_3 by abrasive waterjet. J Manuf Process 28:11–20. https://doi.org/10.1016/j.jmapro.2017.05.017
110. Stock J, Zaeh MF, Conrad M (2012) Remote laser cutting of CFRP: improvements in the cut surface. Phys Procedia 39:161–170. https://doi.org/10.1016/j.phpro.2012.10.026
111. Suneesh E, Sivapragash M (2019) Parameter optimisation to combine low energy consumption with high surface integrity in turning Mg/Al_2O_3 hybrid composites under dry and MQL conditions. J Brazilian Soc Mech Sci Eng 41:89. https://doi.org/10.1007/s40430-019-1587-0
112. Suresh Kumar Reddy N, Kwang-Sup S, Yang M (2008) Experimental study of surface integrity during end milling of Al/SiC particulate metal–matrix composites. J Mater Process Technol 201:574–579. https://doi.org/10.1016/j.jmatprotec.2007.11.280
113. Suresh Kumar S, Uthayakumar M, Thirumalai Kumaran S et al (2019) Investigating the surface integrity of aluminium based composites machined by EDM. Def Technol 15:338–343. https://doi.org/10.1016/j.dt.2018.08.011
114. Szallies K, Siebert N, Bergmann JP (2017) Low frequency oscillated milling of carbon fiber-reinforced plastics. Procedia CIRP 66:153–158. https://doi.org/10.1016/j.procir.2017.03.298
115. Teti R (2002) Machining of composite materials. CIRP Ann 51:611–634. https://doi.org/10.1016/S0007-8506(07)61703-X
116. Thakur RK, Sharma D, Singh KK (2019) Optimization of surface roughness and delamination factor in end milling of graphene modified GFRP using response surface methodology. Mater Today Proc 19:133–139. https://doi.org/10.1016/j.matpr.2019.06.153
117. Tomac N, Tannessen K, Rasch FO (1992) Machinability of particulate aluminium matrix composites. CIRP Ann 41:55–58. https://doi.org/10.1016/S0007-8506(07)61151-2
118. Tosun G (2011) Statistical analysis of process parameters in drilling of AL/SICP metal matrix composite. Int J Adv Manuf Technol 55:477–485. https://doi.org/10.1007/s00170-010-3103-7
119. Tsao CC, Hocheng H (2005) Effects of exit back-up on delamination in drilling composite materials using a saw drill and a core drill. Int J Mach Tools Manuf 45:1261–1270. https://doi.org/10.1016/j.ijmachtools.2005.01.015
120. Udaya Prakash J, Sarala Rubi C, Rajkumar C, Jebarose Juliyana S (2020) Multi-objective drilling parameter optimization of hybrid metal matrix composites using grey relational analysis. Mater Today Proc. https://doi.org/10.1016/j.matpr.2020.04.570
121. Uhlmann E, Richarz S, Sammler F, Hufschmied R (2016) High speed cutting of carbon fibre reinforced plastics. Procedia Manuf 6:113–123. https://doi.org/10.1016/j.promfg.2016.11.015
122. Vishwas CJ, Gajanan MN, Sachin B et al (2019) Study on surface roughness in minimum quantity lubrication turning of Al-6082/SiC metal matrix composites. Appl Mech Mater 895:127–133. https://doi.org/10.4028/www.scientific.net/AMM.895.127
123. Voss R, Henerichs M, Kuster F (2016) Comparison of conventional drilling and orbital drilling in machining carbon fibre reinforced plastics (CFRP). CIRP Ann 65:137–140. https://doi.org/10.1016/j.cirp.2016.04.001
124. Voss R, Seeholzer L, Kuster F, Wegener K (2019) Analytical force model for orthogonal machining of unidirectional carbon fibre reinforced polymers (CFRP) as a function of the fibre orientation. J Mater Process Technol 263:440–469. https://doi.org/10.1016/j.jmatprotec.2018.08.001
125. Wan M, Li S-E, Yuan H, Zhang W-H (2019) Cutting force modelling in machining of fiber-reinforced polymer matrix composites (PMCs): a review. Compos Part A Appl Sci Manuf 117:34–55. https://doi.org/10.1016/j.compositesa.2018.11.003

126. Wang D, He X, Xu Z et al (2017) Study on damage evaluation and machinability of UD-CFRP for the orthogonal cutting operation using scanning acoustic microscopy and the finite element method. Materials (Basel) 10:204. https://doi.org/10.3390/ma10020204
127. Wang J, Feng P, Zhang J, Guo P (2018) Reducing cutting force in rotary ultrasonic drilling of ceramic matrix composites with longitudinal-torsional coupled vibration. Manuf Lett 18:1–5. https://doi.org/10.1016/j.mfglet.2018.08.002
128. Wang J, Zhang Q, Feng P (2017b) Preliminary investigation on rotary ultrasonic face milling of ceramic matrix composite C/Sic: design of experiments. In: Proceedings of the 2017 international conference on mechanical, electronic, control and automation engineering (MECAE 2017). Atlantis Press, Paris, France
129. Wang X, Zhou M, Gan JG-K, Ngoi B (2002) Theoretical and experimental studies of ultra-precision machining of brittle materials with ultrasonic vibration. Int J Adv Manuf Technol 20:99–102. https://doi.org/10.1007/s001700200130
130. Wei C, Zhao L, Hu D, Ni J (2013) Electrical discharge machining of ceramic matrix composites with ceramic fiber reinforcements. Int J Adv Manuf Technol 64:187–194. https://doi.org/10.1007/s00170-012-3995-5
131. Won MS, Dharan CKH (2002) Drilling of aramid and carbon fiber polymer composites. J Manuf Sci Eng 124:778–783. https://doi.org/10.1115/1.1505854
132. Xia T, Kaynak Y, Arvin C, Jawahir IS (2016) Cryogenic cooling-induced process performance and surface integrity in drilling CFRP composite material. Int J Adv Manuf Technol 82:605–616. https://doi.org/10.1007/s00170-015-7284-y
133. Yin G, Gong Y, Li Y et al (2019) Modeling and evaluation in grinding of SiCp/Al composites with single diamond grain. Int J Mech Sci 163:105137. https://doi.org/10.1016/j.ijmecsci.2019.105137
134. Yuan S, Fan H, Amin M et al (2016) A cutting force prediction dynamic model for side milling of ceramic matrix composites C/SiC based on rotary ultrasonic machining. Int J Adv Manuf Technol 86:37–48. https://doi.org/10.1007/s00170-015-8099-6
135. Zhong ZW, Lin G (2006) Ultrasonic assisted turning of an aluminium-based metal matrix composite reinforced with SiC particles. Int J Adv Manuf Technol 27:1077–1081. https://doi.org/10.1007/s00170-004-2320-3
136. Zhou L, Cui C, Zhang PF, Ma ZY (2017) Finite element and experimental analysis of machinability during machining of high-volume fraction SiCp/Al composites. Int J Adv Manuf Technol 91:1935–1944. https://doi.org/10.1007/s00170-016-9933-1

Mechanical, Electrical and Thermal Behaviour of Additively Manufactured Thermoplastic Composites for High Performance Applications

Praveenkumara Jagadeesh, Madhu Puttegowda, Yashas Gowda Thyavihalli Girijappa, Sanjay Mavinkere Rangappa, Munish Kumar Gupta, and Suchart Siengchin

1 Introduction

In the past decades during the development of composites, there is always an extending interest towards the development of high performance and lightweight structures in engineering sector [15]. These required sustainable properties leads to the coining of fiber reinforced polymer composites. The same or different thin polymer layers which are adhesive bounded by matrix are comprised of FRP materials [87]. FRPs has many attractive exceptional properties such as high stiffness, durability, corrosion resistance, higher mechanical properties, higher strength to weight ratio and wear resistance property. These attractive features are led the applications of FRPs in automotive, biomedical, design and construction, marine and aerospace sectors [78]. To meet the current days demand for high volume production of materials suitable for potential automobile applications, the thermoplastic composites are

P. Jagadeesh
Department of Mechanical Engineering, University Visvesvaraya College of Engineering, Bangalore University, Bangalore, India

M. Puttegowda (✉)
Department of Mechanical Engineering, Malnad College of Engineering, Hassan, Visvesvaraya Technological University, Belagavi, Karnataka, India
e-mail: pm@mcehassan.ac.in

M. Puttegowda · Y. G. T. Girijappa · S. M. Rangappa · S. Siengchin
Natural Composites Research Group Lab, Department of Materials and Production Engineering, The Sirindhorn International Thai-German Graduate School of Engineering (TGGS), King Mongkut's University of Technology North Bangkok (KMUTNB), Bangkok, Thailand

M. K. Gupta
Key Laboratory of High Efficiency and Clean Mechanical Manufacture, Ministry of Education, School of Mechanical Engineering, Shandong University, Jingshi Road, Jinan, China

S. Mavinkere Rangappa et al. (eds.), *Additive and Subtractive Manufacturing of Composites*, Springer Series in Advanced Manufacturing,
https://doi.org/10.1007/978-981-16-3184-9_7

preferred. The thermoplastic resins are having numerous advantages over thermosetting resins (epoxy, vinyl ester, phenols) especially impact and energy absorption properties [90]. The thermoplastic resins are having a superior ability of soften after heating above the specific temperature and it retains his property after cooled. Hence, this property adds the advantage for welding the two similar or dissimilar thermoplastic composite [7]. The short fiber reinforced thermoplastic composite offers lesser production cost, higher volume production rate, light in weight, able to withstand cyclic loads and these are suitable for production of complex geometries [69]. The processing of thermoplastic composite was done by using fusion bonding by the supplement of pressure and heat at the bonding interface and hence the process is happened quickly without the requirement of autoclave curing. Their further interest towards the development is elevated due to increase in damage tolerance, resistant to chemicals and solvents, long shelf life, less storage cost and good weldability, recyclability. However, the viscous and stiff nature of the thermoplastic results in the requirement of higher temperature and pressure values for processing. It is difficult to obtain a mechanical property at an autoclave level due to rapid heating rate and cooling of composites and also autoclave pressure is lower than the pressure applied at a short duration of time [77, 103, 104], The thermoplastic resins' usage has an economic benefits because of tooling without application of heat, lesser manufacturing cycle time and collection of raw material from used part. The used composites part contains internally stored energy, hence the recovering of these parts constituents gives the economic benefits [23]. Nowadays producing thermoplastic materials has simple structure as compared to others because of lesser deformation of reinforced fibers, insertion of thermoplastic matrix phase for the development of thermoplastics [96]. The carbon fiber reinforced thermoplastics plays a dominant role in automobile industry. The reduction of automobile vehicle weight improves the fuel efficiency of the vehicles. The current automobile companies focusing towards the development of hybrid cars using green sources. The weight reduction is the current challenge for engine and body components of the vehicles, hence carbon reinforced thermoplastics in automobiles contributes the material cost reduction and vehicle economy. The conductive thermoplastic composites extends its applications in electromagnetic interface shielding and thermal related applications [13, 101].

Additive manufacturing (AM) is also called as 3-D printing, which is a process of combining multiple layers of materials to fabricate a three-dimensional object from.stl (Surface Tessellation Language) file which is designed from a CAD software. The object structures were built by laying one layer on X–Y plane at a time, further adding additional layer on Z-direction. The first 3-D printable apparatus was first introduced in the year 1986 by Charles Hull [61, 94]. This AM technology was utilized to produce a high volume structures of thermoplastic materials. The different AM techniques and their working process is tabulated in Table 1. AM has an ability to fabricate a complex structural geometry of different constituents of material, which is not easily produced from conventional manufacturing technologies due to difficulty in obtaining (extracting) a particular structure from a bulk raw material [66]. AM technique involves reduction in product design manufacturing cycle, and also possibility of reduced in production cost with effective manufacturing processes.

Table 1 Additive manufacturing (AM) technique and their process

AM technique	Abbreviation	Process	Reference
SLA	Stereolithography apparatus	Liquid layer is solidified by using laser light source (photopolymerization)	[54]
SLS	Selective laser sintering	The powder material was sintered using laser source	[34]
LOM	Laminated object manufacturing	Adhesive coated materials are bonded together and cut into 3-D shape	[50]
FDM	Fused deposition modelling	Deposition of melted thermoplastics as per particular pattern	[48]
SLM	Selective laser melting	High power laser density is utilized for the melting and fusing of metallic powders	[9]
LDM	Liquid deposition modeling	3-D printing technique uses liquid suspension where data obtained from digital file	[81]
-	Material jetting	Build a 3-D structure utilizing polymer droplets and cured using UV source	[102]
-	Binder jetting	Binder material is particularly deposited on the powder bed, together bonding of these areas forms 3-D structure	[57]

As compared to subtractive manufacturing technique, the AM reduces the 90% of material waste [71]. AM is a preferable technique for prototype and tooling jigs manufacturing, also small volume and customized production. Hence, AM reduces the tooling cost, storage cost, scrap materials and reduction in short lead time [45]. AM process involves multiple steps, where it begins from virtually representation of model and it shows the complete outline of geometry using surface representation model or a solid body model. To simplify the structure, the software pre-processer breaks the 3-D structure into different cross-sections depends on each process layer resolution. The layer thickness affects the total quality of the 3-D structure. Each of the divided cross-section is identified with particular pattern and this will be the main base for defining the deposition technique for each layer. Once the deposition technique is fixed, the construction starts by feeding the pattern into automated additive system [15]. AM technique has several challenges for the fabrication of 3-D complex parts. The fabricated parts with layered manufacturing has some variable mechanical properties at different levels which depends on the AM technique. And also there is a less choice for selection of materials for AM technique [5].

2 Mechanical Properties of Thermoplastic Composites

Usually the material performance is determined by mechanical properties. The tensile, flexural and impact properties were reported in the literature. These properties calculate the material capacity and to identify the ability of working under various mechanical conditions suitable for potential engineering applications [73]. Dutra et al. [28] fabricated a carbon-Nylon fiber reinforced thermoplastic composite using fused filament fabrication (FFF) technique. The mechanical results obtained from asymptotic homogenization technique reveals that 3-D printed nylon matrix embedded carbon fiber reinforced composite possesses higher ratio of elastic moduli to fiber volume fraction as compared to thermoset composites. The SEM images of nylon matrix embedded at the top and bottom of the carbon fiber reveals the changes in composition at the core, top and bottom layers. The finite element analysis of continuous carbon fiber reinforced thermoplastic (CFRTP) composites for tensile specimens shows the internal stresses stored in the material and also it reveals the effect of test specimen structure on mechanical properties. The fiber deposition is one of the parameter for stress concentration in 3-D printed structures and it may lead to the early failure of specimens at irregular locations. Along with that placing of fibers at the end structures and fixing of specimens also affect the material sustainability which are observed in FEM simulation software [68]. Wang et al. [99] evaluated the mechanical properties of Polyether ether ketone (PEEK) filament reinforced thermoplastic composite using FFF process. The author suggested the influencing parameters like nozzle diameter, nozzle temperature and printing speed on the mechanical properties of composites. The parameter combination of nozzle diameter 0.4 mm, nozzle temperature of 430 °C and 5 mm/s printing speed gives the optimum bending strength. The 0.2 mm is favorable nozzle diameter to get the best bending modulus and internal defects were reduced by high nozzle temperature and slow printing speed. The better compression properties were obtained by increasing the nozzle diameter above 0.6 mm. The conductive composite is prepared using Poly lactic acid (PLA) as a matrix with multi-walled carbon nano tubes (MWCNTs) constituents by fused deposition modeling (FDM) method. The combination of PLA with 5% MWCNTs achieves maximum tensile strength of 78.4 ± 12.4 MPa with elongation at break is 94.4 ± 14.3%. Further, increasing the filler content above 5% forms an agglomeration, which causes decrease in load transferring capacity, increase in brittleness and decreases material toughness [63]. Iragi et al. [47] studied the mechanical properties of 3-D printed cellulose filled thermoplastic materials. The 10 wt% filler loaded recycled thermoplastic shows weaker tensile properties (Tensile strength, modulus, elongation at break) but the slightly improvement is found in virgin PLA composite. The tensile strength and elastic modulus of PLA-C composite was enhanced by 28 and 3% respectively. The reduction of mechanical properties in recycled thermoplastic composite is due to the material aging during usage, additives, impurities and thermomechanical action while processing. The author proposed an in-house fabrication work of ABS filament based thermoplastics using FDM method. The in-house fabricated one FDM filament cartridge saves around 93% of cost on

FDM filament. The optimum tensile strength is obtained for FDM parameters such as 40 rpm screw speed and 145 °C barrel temperature. The mathematical models were developed to measure the accuracy of tensile strength, modulus, deviation outputs which is around 99.51%, 98.54% and 97.96% respectively [85]. Calignano et al. [10] fabricated a carbon/nylon thermoplastic composite using in-house FFF process and mechanical properties were evaluated. The results are evident based on the filling percentage and building direction of thermoplastic material. The samples produced at XZ plane with 80 and 100% filling shows higher hardness value as compared to other planes and also production time, material cost are also elevated. The XZ plane produced component possess higher stiffness value in comparison with XY plane and also young's modulus, stress at break is higher for XZ component. The 100% filling density provides good properties but it also causes some negative impact on the production process. The filling factor also affects the material behavior, which impacts the development of non-linear relation between filling factor and the mechanical properties. Chacón et al. [16] carried out a studies on effect of filament build orientation, feed rate and layer thickness on mechanical response of PLA structures manufactured using FDM process. The on edge orientation and flat samples exhibits better tensile, flexural and ductile behavior and the failure occurs at trans-layer whereas the upright orientation possess brittle behavior with lower stiffness and strength value and failure occurs at inter-layer. The upright orientation samples also possess higher tensile and flexural strength in case of higher layer thickness value, for the on-edge, flat orientations the mechanical properties were significant in the layer thickness range of 0.12–0.24 mm. The mechanical properties vary inversely with the feed rate for upright samples. From these observations, author recommend that higher layer thickness and lower feed rate values for upright, on-edge orientations whereas lower thickness value and higher feed rate is recommended for on-edge, flat orientations. Guan et al. [39] evaluated the mechanical properties of carbonyl iron powder filled PLA composite fabricated using FDM process. The 3-D printed pure PLA composite achieves a tensile strength and elongation at break of 55 ± 5.68 MPa and $20.5 \pm 0.024\%$, which is higher than compared to traditionally manufactured pure PLA composites (40–60 MPa and 4–10%). Because 3-D printed parts achieves higher plasticity of PLA and maintains the composite strength, and also there exist a strong adhesion between the layers of 3-D printed parts. The added filler particles improves the adhesion, carries some of the applied load and absorbs the deformation energy. These particles embedded with the matrix enhances the mechanical properties of PLA structures. Goh et al. [35] studied the mechanical properties of carbon fiber/nylon thermoplastic which is fabricated using 3-D printing technology. By the observation of stress–strain curve, the pure nylon thermoplastic possess higher energy absorbing capacity with a nature of plastic behavior. The carbon fiber reinforced nylon composite has elastic behavior where the modulus value enhanced by 337 MPa to 53,000 MPa and tensile strength increased from 48 to 923 MPa because there exist a strong adhesion between carbon and nylon fibers. From the observation of S–N curve, the fatigue life is more for carbon/nylon composite as compared to pure nylon matrix composite. The carbon fiber plays a crucial role and adds the

fatigue life to the composite and these fibers are comparatively insensitive to the fatigue loading.

3 Thermoplastic Matrix Reinforced Polymer Composites

The polymers whose physical properties are not altered after melting, molding and remolding are called Thermoplastic polymers. As compared to thermosets, thermoplastic matrix has good damage tolerance, impact resistant, tough and less brittle nature. Hence, thermoplastic matrix composite repair is easy and it can be easily remolded, recyclable. These materials are suggested for critical weight applications due to less density as compared to thermosets and excellent properties which are tabulated in Table 2. Their manufacturing process involves higher cost due to requirement of high temperature and pressure for the melting of plastics and for binding the fibers. There are many types of thermoplastic matrices such as nylon, polyamide, polycarbonate, polypropylene, polyurethane, polyether ether ketone etc. Some of the thermoplastic matrix composites were discussed in the following sections.

3.1 Polylactic Acid (PLA) Thermoplastic Composites

PLA is one of the economically preferred popular matrix material which is produced from the renewable sources. As per 2010 survey, PLA occupies second position in top consumed bio-plastics in the world. The monomer of PLA is produced from natural plants starch obtained from sugarcane, root of tropical tree and corn [70]. Hu et al. [46] fabricated a long carbon fiber reinforced PLA thermoplastic composites for the analysis mechanical, thermal and surface characterization of 3-D printed composite. The 5 wt% carbon fiber filled CF/PLA composite obtained enhancement of tensile strength by 89.14%, whereas 70.71% of enhanced tensile modulus if found in 7.5 wt% CF composite. The 15 wt% CF filled composite claims the highest elevated flexural strength and modulus value by the amount of 43% and 185.29% respectively. The highest thermal conductivity achieved is 0.1350 W/m. K and it is for 5 wt% CF composites. As per experimental results the best performance is obtained for 5 wt% CF filled PLA composites and as per Gaussian process modeling, the optimum performance is predicted for 7.5 wt% CF filled PLA composites. Karakoç et al. [53] conducted an experiment on thermomechanical evaluation of cellulosic PLA filled glass/carbon fiber reinforced thermoplastics using FDM method. TGA analysis results shows that PLA and its composites stability is less and it is higher for glass fiber reinforced polyamide based composites. The crystallinity of the polymer matrix is enhanced by the addition of nano diamond filler particles and cellulosic, carbon, glass fibers has no effect on crystallinity of the composites. The highest tensile strength is achieved for PLA, polyamide based composites whose values are higher

Table 2 Properties of different thermoplastic composites

Studies	Matrix	Reinforcement	Manufacturing method	Processing temperature	Observations
De León et al. [25]	ABS	Thermoplastic polyurethane (TPU)	FFF	230 °C	Addition of TPU improves the interfacial adhesion of printed parts, TPU blends uniformly distributed in ABS matrix
Wang et al. [100]	PEEK	Glass fiber, carbon fiber	FDM	360–400 °C	Incorporation of CF/GF increases the tensile, flexural strength at cost of ductility and strength is more due to fiber alignment along printing direction
[2]	PEEK	Carbon nanostructures (CNN), Graphene nanoplatelets (GNPs)	FFF	390–410 °C	Addition of CNC increases the degree of crystallinity. GNP addition decreases modulus value by 5% and increases strength value by nearly 5%
[67]	Polyethylene Terephthalate Glycol	Carbon fiber	FFF	230 °C	Addition of CF increases modulus, hardness value by 30%, 27% and decreases compressive strain by 66%. Average damping capacity was reduced by the addition of CF into PETG

(continued)

Table 2 (continued)

Studies	Matrix	Reinforcement	Manufacturing method	Processing temperature	Observations
[89]	Polypropylene	Glass fiber	Extrusion based AM	175–185 °C	The addition of glass spheres enhances the toughness and tensile properties of PP filled thermoplastics
[105]	ABS	Carbon Black	FDM	230 °C	Resistivity is more in horizontally printed parts as compared to vertically printed parts. Resistivity is anisotropic in printed parts due to the internal structures
Dickson et al. [26]	Nylon	Carbon fiber	3D printing	245 °C	The woven specimen has bearing strength of maximum 214 MPa and double shear bearing strength of maximum 276 MPa, which is 29% and 63% higher as compared to hole drilled equivalent composite

(continued)

Table 2 (continued)

Studies	Matrix	Reinforcement	Manufacturing method	Processing temperature	Observations
[75]	Nylon	Carbon, glass, kevlar	FDM	200–260 °C	Fatigue response is more in 0° printed carbon reinforced nylon thermoplastics. The specimens with higher humidity shows yield failure at low load cycles
Camineo et al. 2018	Nylon	Glass, kevlar, carbon	FDM	232–273 °C	With the increasing layer thickness, impact strength increases in flat samples and decreases for on-edge specimens. Glass fiber reinforced nylon composite has higher impact strength
[4]	Polyamide 11	MWCNTs	Laser assisted manufacturing	189 °C	Incorporation of CNT with PA 11 improves the impact strength by 9.48 kJ/m^2 and crystallinity percentage of 64.2%

than manufacturer quoted values. The injection molding parameters like temperature, speed, and infill percentage affects the strength of the composites. The PLA filament reinforced with short carbon fibers composite manufactured using fused filament fabrication process results in enhancement of tensile strength and stiffness of 47.1%, 179.9% respectively as compared to plane PLA composite. The strong bonding performance was observed in flat and on-edge orientations and hence inter laminar shear strength is high, whereas lower ILSS was observed in up-right orientation. The SEM micrographs of fractured tensile surfaces shows a brittle behavior in up-right orientations and higher plastic deformation is observed in on-edge, flat

orientations [79]. Fan et al. [29] fabricated a composite made of 0.1, 0.5, 1 and 2 mm short carbon fiber reinforced PLA structures and studies reveals that 38 MPa of tensile strength is obtained for 0.5 wt% fiber content in single layer, which is 15% higher than plane resin matrix. Further, increasing short fibers leads to development of voids results in decrease of mechanical properties. When the carbon fiber length is added about 0.5 and 1 mm (more than critical fiber length), the composite exhibits higher mechanical performance due to better bonding quality with the matrix. The 2 mm fiber reinforced composite shows lower mechanical properties due to overlapping of fibers which creates poor adhesion with the matrix material. Further 3-D printed parts were subjected to post treatment for the enhancement of the properties (significantly within 5%), normally the post treatment temperature is maintained above the glass transition temperature (T_g) and hence strong interface is formed between 3-D printed layers due to fusion. The prepared composites were further heated using laser source, which increases the temperature at inter layers. The 10 W laser power utilization elevates the tensile strength to 59.20 MPa which is 56.78% higher than composites without the post treatment. Csenge and Kovács [24] manufactured a composite reinforced with glass, carbon, basalt fibers with PLA matrix using FFF process. In longitudinal directionally (0°) printed 5 wt% all samples possess increased tensile properties, but in 90° printed samples only basalt fibers reinforced samples exhibit elevation in the strength. Addition of more percentage of fiber content results in decrement of tensile property by the amount of 5% reduction in development. Major flexural strength values depends on the printed orientation of fibers and it is higher for glass fiber reinforced composites. The parallel infill orientation of 5 wt% glass and carbon fibers have higher impact strength. The ductility index value decreases with increasing fibers content because PLA matrix is more rigid than the reinforced fibers. The porosity is observed in the SEM micrographs of thermoplastic samples which is due irregular flow of material while printing and this porosity may be reduced by elevating the feed rate or reduction of draw speed. Another study reveals the comparison of mechanical properties of pure PLA composite and short carbon fiber reinforced PLA structures. The 15 wt% CF reinforced PLA has tensile modulus value 2.2 times greater than neat PLA composite in the plane printing direction and it is 1.2 times higher in transversely printed direction. From the examination of tensile strengths both in plane printing direction and transverse to printing direction noticed that there is no much alteration of quantities by the short carbon fibers practically and majority of loading stresses were carried by PLA matrix at failure loading stage both in PLA and PLA + CF composites. The chopped carbon fibers of small length 60 μm doesn't play dominant role in improving the strength and also adhesive nature is decreased with the matrix material [30]. Li et al. [60] manufactured a continuous carbon fiber reinforced PLA composites using 3-D printing and compared the properties of 3-D printed composites with and without preprocessing of carbon fiber bundle. The pane PLA composite possess 28 MPa of tensile strength, for carbon fiber reinforced PLA has 80 MPa and modified carbon reinforced PLA withstand 91 MPa of tensile strength. The carbon fiber modified PLA composite has 13.8% and 164% elevated tensile and flexural strength as compared to untreated one. These mechanical performances were observed in Fig. 1. Due to the modification of

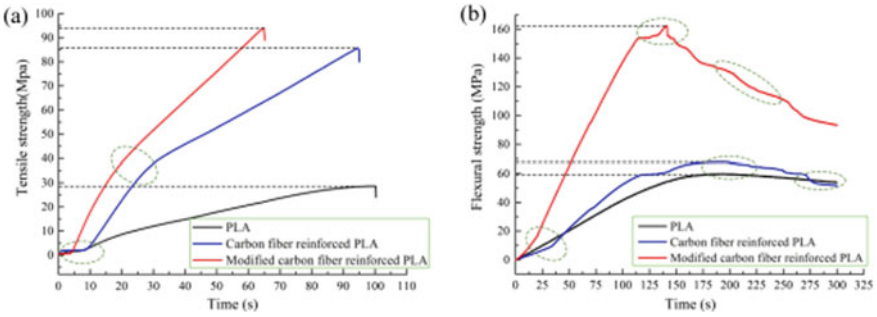

Fig. 1 Mechanical properties of three different materials printed by the same process condition. **a** Tensile strength of PLA, carbon fiber reinforced PLA and modified carbon fiber reinforced PLA. **b** Flexural strength of PLA, carbon fiber reinforced PLA and modified carbon fiber reinforced PLA. (Reused with the permission from Elsevier, License No: 4991340859318)

fiber, the adhesive property is increases and hence the interfacial strength between the fiber and PLA is more. The DMA analysis of three types samples were shown in Fig. 2. The storage modulus value is higher for all the three kinds at initially and decreases for further raise in temperature. The peak value of the loss tangent curve is identified as a glass transition temperature (T_g) and this attributes the PLA matrix molecular mobility. As compared to storage modulus curves, the modified sample possess higher value at the beginning stiffness elevated due to modification of carbon

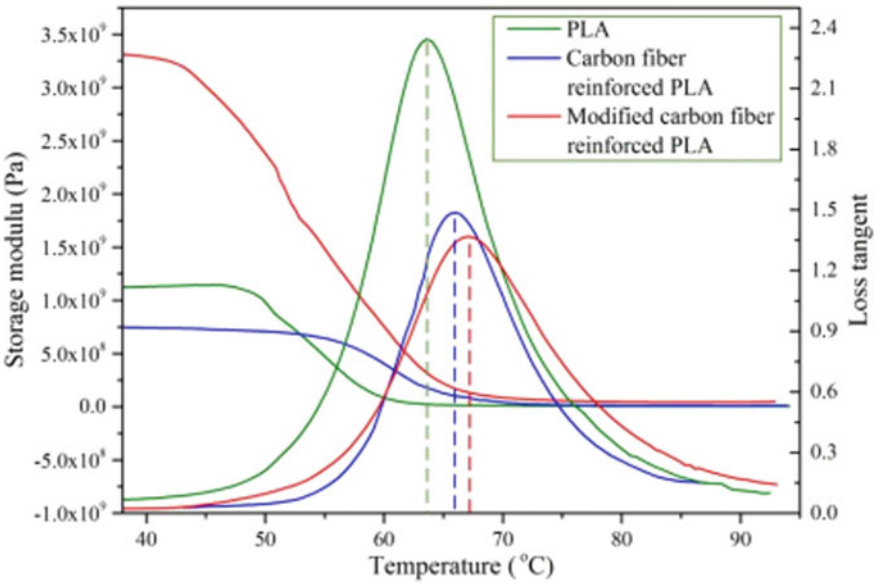

Fig. 2 Storage modulus and loss tangent of three kinds of printed materials (Reused with the permission from Elsevier, License No: 4991341504425)

fiber and majority of stress is withstood by the carbon fiber at the carbon-PLA interface. The 66.8 °C T_g value shows the higher thermal stability of modified carbon PLA composite and achieves lower loss target as compared to other two kinds.

3.2 Polyetheretherketone (PEEK) Thermoplastic Composites

The high performance PEEK belongs to the family of polyaryletherketone and it was synthesized in the year 1962 by Bonner. This consists of molecular aromatic ring with ethers and ketones as a functional group. These carbonyl functional groups with benzene ring, ethers forms the bond with intermolecular attraction and results in PEEK structure. The PEEK addition enhances the tribological conditions, stiffness, strength and toughness of the composites [58]. [95] fabricated and evaluated the mechanical, thermal analysis of PEEK thermoplastic which is produced by robotic 3-D printer. By the TGA analysis, PEEK thermal decomposition occurs in two stages with nitrogen atmosphere at 10 °C heating rate. In the first phase of decomposition there exist a random chain separation in bonds of ether and ketones and also phenol (main content) degradation occurs with lesser amount of benzene and dibenzofuran compounds. In the next phase, splitting of carbonyl bonds were takes place, this forms intermediate more stabled radicals because of resonance effect. PEEK produces a residue weight of 58.6%, 55.68%, 52.62%, 52% at 600 °C, 650 °C, 700 °C and 800 °C respectively. The maximum ultimate tensile strength, modulus of elasticity achieved is 300.07 N/mm^2, 5114 N/mm^2 for 390 °C extrusion temperature and 40 mm/s printing speed. Arif et al. [3] evaluated the performance of PEEK matrix used Graphene nanoplatelets (GNP) and carbon nanotubes composites which were fabricated using FFF AM technique. The addition of CNT enhances the degree of crystallinity and crystallization temperature of PEEK composites and printing direction influence the formation and extend of voids with the variation of density value. The addition of 5% GNP, 3% CNT into PEEK matrix reduces the coefficient of thermal expansion value by 26% and 18% respectively and these nanocomposites withstands optimum dimensional stability. The young's modulus and storage modulus are found to be increased by 66%, 77% for 5% GNP composite and 20%, 23% for 3 wt% CNT loaded composite. Both the GNP, CNT filled composites are having superior wear rate but it has lower coefficient of friction value because of less hardness value, existence of more porous percentage. Another study reveals the fabrication of PEEK composite with 1% and 5% CNTs and it is fabricated using FDM technique. The PEEK was extruded easily with the temperature range of 350–380 °C and for 390 °C PEEK was degraded at the nozzle outlet. The smooth and denser surface was observed in PEEK structure fabricated at 350 °C and cavities formed were observed at 365 °C and 380 °C PEEK composites. Initially the filament is dried to remove the moisture content, but in some cases the environment moisture enter into the filament and evaporates after the deposition process, which forms the cavity at that position. The highest porosity was observed in 5% CNT filled PEEK with 4.67% of voids. The 1% CNT PEEK has the highest tensile strength and 5% CNT loading has lowest due to

the formation of agglomeration while region is formed at the specimen. The short beam shear strength is similar for plane PEEK and 1% CNT loaded PEEK about 33 ± 10 MPa and it is decreased to 21 ± 5 MPa for 5% CNT loaded PEEK because of change in surface characteristics like adhesion with molten material, surface tension and wettability, which are different from 1% CNT PEEK, plane PEEK composites [6]. Chang et al. [19] prepared a continuous carbon fiber reinforced PEEK composite using Laser assisted Laminated Object AM technique. This composite withstands the highest flexural strength and modulus of 670.5 MPa and 89.7 GPa respectively which is higher than FFF printed same composite. The Hot press postprocessing (HPP) is one of the main reason for increased flexural properties and it also reduces the interface delamination. Without HPP the specimens exhibit 1212.9 MPa of tensile strength, 113.8 GPa of elastic modulus whereas with HPP exhibits 1513.8 MPa of tensile strength and 133.1 GPa of elastic modulus value [0° orientation]. The mechanical properties were reduced for 45 and 90° orientation which is due to fiber pull-out and delamination of printed surface. Han et al. [40] conducted a studies on mechanical evaluation of CF/PEEK composite and analyzed the effect of surface roughness of material on biocompatible nature and cell adhesive nature using sandblasting and polishing methods. The slightly higher tensile properties were observed in CF/PEEK as compared to plane PEEK composites and compression strength is nearly equal for the composites. The SEM images reveals that the peaks and valleys were disappeared completely on the sandblasted, polished surfaces and rough surface is found on the untreated composite. The smooth morphology is observed on polished surfaces and very fewer defects were found on CF/PEEK composite. The cells attachment is more in untreated surface with good adhesive nature and hence cell density is higher than compared to treated surfaces. Rahman et al. [76] manufactured a PEEK composite using FFF process with extruder temperature of 340 °C and quoted the advantage of FFF process over selective laser sintering (SLS) technique. The 0° raster orientation combination shows average ultimate tensile strength of 73 MPa, compression strength of 80.9 MPa and 90° oriented raster combination has average of 54 MPa tensile strength, whereas alternating 0°/90° raster orientation possess intermediate strength of 66.5 MPa and compression strength of 72.8 MPa. The maximum bending strength achieved is about 111.7 MPa, 79.7 MPa, 95.3 MPa for 0°, 90° and 0°/90° raster oriented combination respectively. Author also quoted the advantages of FFF process such as less equipment cost, easy usage, less material contamination, degradation and user safety while using the equipment. Luo et al. [64] studied the inter layer bonding behavior of extruded continuous carbon reinforced PEEK composites. Extrusion performance of the composite material was influenced by the melt viscosity, but PEEK has higher viscosity, melting point and hence it is challenging for 3-D printing. The ILSS test is conducted for two types of PEEK (450 G, 150 G), the melt viscosity value and ILSS were decreased as the increase of melt flow rate, which results in poor bonding between the layers. The zig-zag variations were observed in the stress–strain curve, which implies the inter layers delamination and exist a poor infusion between CF and PEEK. The 10 W laser source is used for preheating of material surface during the extrusion process and it is also one of the reason for elevated ILSS value. The delamination of inter layers is due to the two

main reasons: (i) The surface temperature of the 3-D printed layer is lower than the glass transition temperature (T_g), which reduces the bonding of PEEK molecular chains end with the neighbor layers and it causes poor bonding between the layers, (ii) Fluidity value is lesser for PEEK material which is difficult to penetrate into the CF fiber sufficiently, hence weaker inter layer bonding and macro pores were developed.

3.3 Nylon Thermoplastic Composites

Nylon was the first thermoplastic polymer synthesized commercially in the year 1935 and it is composed of repeating units of amide link (polyamide). Nylon doesn't get affected by alkalis, oxidizing agents, reducing agents, microorganisms and it has higher insulating properties. Nylon is used in fabrication of flame resistant product, machine parts, high strength wires and nets, clothes, ropes, vehicle tires and in some military applications [93]. Dong et al. [27] evaluated the mechanical properties of kevlar fiber reinforced nylon thermoplastic composites manufactured using FDM process. The thermoplastics reach a maximum elastic modulus value of 27 GPa and ultimate strength of 333 MPa and this improvement was found due to the continuous fiber reinforcement. When the fiber is aligned in a direction perpendicular to the tensile loading, the elastic modulus value falls to 0.84 GPa and it is also observed the weak bonding exist between the nylon layer and kevlar layer. The debonding of layers occurs mainly because of existence in different Poisson's ratios of kevlar, nylon layers. The elastic modulus value is not affected by the position of fibers and author suggested the 5 layers of nylon for part surface. Another study reveals the effect of moisture content on the mechanical properties of carbon fiber reinforced nylon thermoplastic, which is fabricated using 3-D printing. To study the water absorption behavior, Fickian model and Langmuir model were used. The analysis of pure nylon behavior is done by Fickian model above the glass transition temperature and the diffusivity (D) depends on moisture content and temperature. The moisture content reduces the T_g value and for the thick material, the diffusion coefficient changes with heterogeneous water contents (Langmuir behavior). The nylon samples has 9.7% of moisture content in wet condition and 3% in ambient condition. The equilibrium of moisture content depends on the volume percentage of matrix material (hygroscopic), hence increase of fiber volume percentage decreases the moisture intake percentage. The pure nylon possess a tensile modulus of 206.1 MPa and 1074.9 MPa in wet and dry condition respectively. For the wet condition, CF/PA possesses the modulus and ultimate stress values of 35.1 MPa and 522 MPa respectively, and for dry condition it is 41.2 GPa and 598 MPa. The ductile behavior was observed in the wet samples, whereas in dry samples light brittle nature and plastic deformation is observed [56]. Chacón et al. [17] found the effect of process parameters on FDM printed continuous fiber reinforced (glass, carbon, kevlar) nylon thermoplastics. There is no much effect of layer thickness on the mechanical properties of nylon matrix specimens and in most of the cases flat oriented samples withstands higher

tensile and flexural strength as compared to on-edge oriented samples. The carbon fiber reinforced composite has higher stiffness, tensile strength, flexural strength value as compared to other two composites and kevlar fiber reinforced thermoplastics possess lower mechanical properties. The kevlar fiber exhibits anisotropic property and hence compressive strength is lower than the carbon and glass fibers, which results in composite failure. The fiber pull-outs and fiber breakages were observed due to the inappropriate coating of matrix material (Nylon) on the continuous fiber surface while fabrication of composites. The experimental results evident that the strength and stiffness values elevated as the increase of fiber volume percentage and also depends on the build orientation. Blok et al. [8] studied the quality and mechanical performance of continuous carbon fiber/nylon printed using Mark Forged Mark One printer and discontinuous carbon fiber/nylon produced using desktop 3-D printer. The MarkOne printed composite has 986 MPa of average strength, 31.16 MPa of shear stress and 62.5 GPa of stiffness value and it is heard that high frequency sound of fiber fracture is found at 200 MPa lower stress, after that no sound was heard before the failure of composite. The flexural strength and flexural modulus were noted as 485 MPa and 41.6 GPa respectively and these values were lower than the tensile values which might due to poor quality of parts. The 3-D printed discontinuous CF/Nylon has tensile strength of 33.5 MPa, stiffness value of 1.85 GPa, flexural strength of 55.3 MPa, shear strength of 19.02 MPa and flexural stiffness value of 3.0 GPa. There exists a disadvantage of continuous fiber printing, there is not much control over the printing of continuous fiber and it creates voids during printing of complex shapes. Hence, to overcome these problems, a short fiber with a length of above critical length is preferred for printing process. Caminero et al. [11, 12] conducted a studies on inter-laminar bonding performance of continuous fiber reinforced thermoplastics and also studied the effect of fiber volume and layer thickness. The ILSS strength value is directly related to the layer thickness and slightly decrease of ILSS is observed with increase of layer thickness (Fig. 3a). The decrease of layer thickness results in overlapping of thin fiber layers, which reduces the formation of voids and hence ILSS strength was elevated. For the analysis of fiber/nylon thermoplastics ILSS performance, two kinds' fiber percentages were considered (A-27.2% reinforcement, B-73.2% reinforcement). Type B reinforced composite possess higher ILSS value as compared to type A and the value is higher for carbon fiber reinforced thermoplastics. There is no much effect of fiber volume percentage in kevlar fiber reinforced thermoplastics and less ILSS strength was observed due to poor wettability (Fig. 3b). These composites were compared with ILSS values of other 3-D printed thermoplastic composites and also with thermoset matrix based composites which are produced using traditional manufacturing methods (Fig. 3c). The carbon fiber reinforced thermoplastics withstands higher indentation force before the indentation reaches to 3.8 mm when carbon fiber sheets breaks which is having isotropic properties at plane. The 1078 N of indentation force is recorded to the maximum extent and the indentation energy is noted about 6530 J for 10.62 mm of displacement and the sudden indentation force drop is due to catastrophic failure of specimens. Foe the glass fiber thermoplastics the maximum indentation achieved before the 7.68 mm of indentation and this value is higher than compared to carbon fiber due

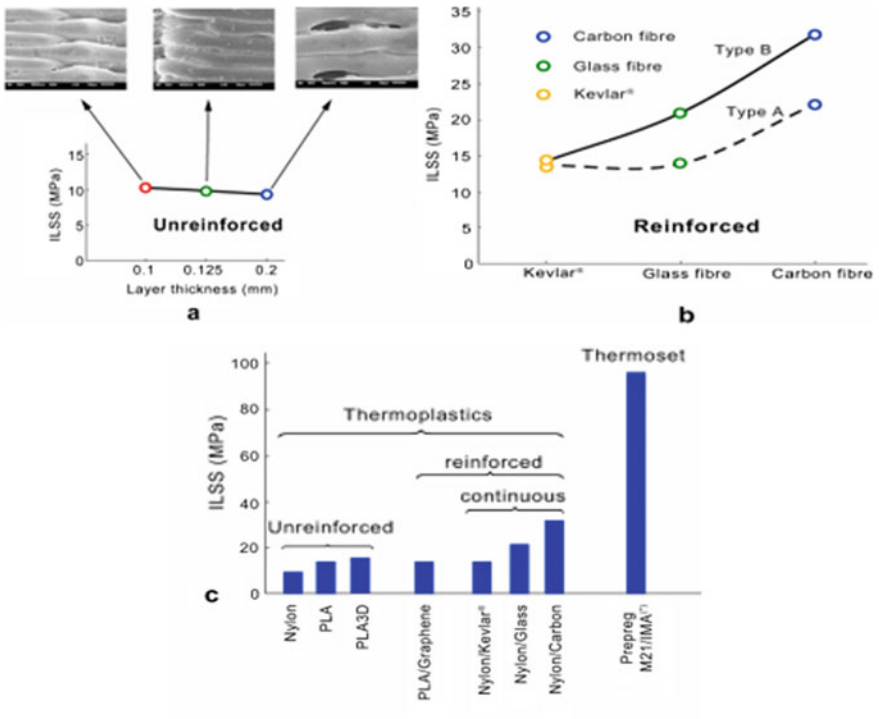

Fig. 3 Graphical comparison of average maximum ILSS of specimens. **a** He effect of layer thickness in unreinforced ILSS samples. **b** The effect of fibre volume content. **c** Comparison of different 3D printed thermoplastic materials (unreinforced and reinforced) and prepreg M21/IMA thermoset-matrix composite. (Reused with the permission from Elsevier, License No: 4991350480889)

to the lower young's modulus and flexural modulus value of glass fiber. The glass fiber thermoplastics achieves 1406 N of indentation force and 7046 J of indentation energy which is calculated upto the displacement of 12.12 mm [36].

3.4 Polyurethane Thermoplastic Composites

Polyurethane (PU) is a versatile plastic material, which contains the soft copolymer segments of macrodiol and hard segment components obtained from the di-isocyanate. PU has certain excellent properties such as high elasticity, flexibility, shock absorbing capacity and abrasive resistance nature. It also has some drawbacks such as lower thermal stability, mechanical properties and these properties can be boosted by coating of clay or layered polymer silicates [51]. Chen et al. [20] studied the biocompatible nature of PU/PLA/Graphene oxide (GO) filled nanocomposites printed using FDM process. The addition of GO elevates the compression modulus

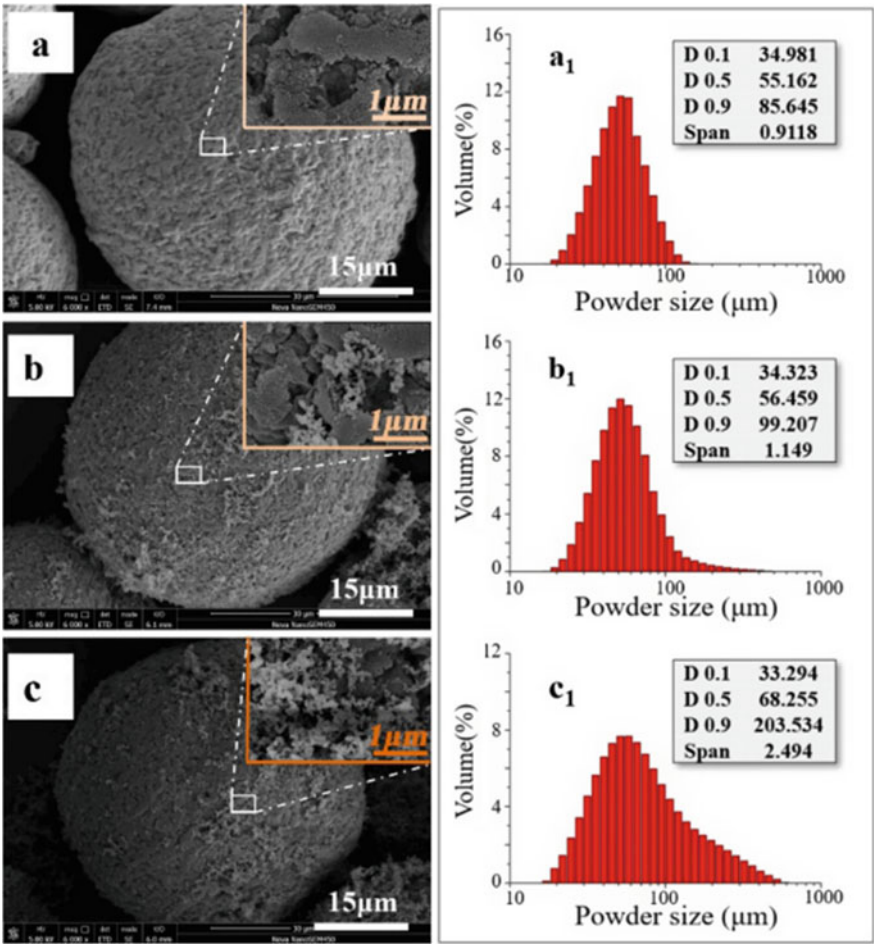

Fig. 4. A **a–c** SEM images of PA12, 2CB/PA12 and 4CB/PA12 raw powders; (**a1-c1**) corresponding powder size and size distribution. (Reused with the permission from Elsevier, License No: 4991350759209)

value of standing specimen (height direction printing) by 56% and for lying specimen (width direction printing) it is 167%. The tensile properties were optimum for 0.5 wt% loading of GO and further addition reduces the properties which might be due to reaching the above percolation threshold value. At 90 °C degradation temperature, the composite possess improved thermal stability with the formation of good newly build crystalline structures. The controlled addition of GO fillers doesn't provide toxicity for the growth of cells and this addition is advantage for cell proliferation. Leng et al. [59] fabricated a PU components reinforced with in Situ PLA microfibers and studied the influence of deposition-induced effect. The author

developed a customized CSBED system which works on the principle of screw rotation and it is adopted to FDM to use fiber pellets directly as a feedstock because it is difficult for printing in commercial FDM printer. The DSC analysis reveals that the composite produced from FDM process has higher crystallinity as compared to compression molding technique and the variation rate is from 17.72% to 24.92% above. Hence, these reasons increase the tensile strength and Young's modulus values of FTP specimens as compared to CTP specimens. The effect of printing speed is less on mechanical properties and fiber morphology of specimens. Shen et al. [83] studied the energy absorption behavior of PUs based 3-D lattice structures fabricated via selective laser sintering (SLS) using modeling and prediction. The prepared 3-D model is subjected to cyclic loading applied in y-direction for compression test with a load rate of 1.5×10^{-3} s^{-1} and 17 mm displacement is set for nominal strain of 25%. The load–displacement curves shows a small deviation of fourth cycle forces about 10% as compared to experimental data. These deviations arise during the above 50% of loading process and before 50% of unloading process. The numerical calculations were done to study the effect of strain on energy absorption and the two models withstands a maximum energy absorption of 0.00494 and 0.01866 per unit volume. The energy absorption value is elevated after reaching the strain value above 0.1. The predicated model indicates the non-linear relationship among energy absorption value and compression value. It is also observed the relationship between porosity and compression force, which means that the prepared spherical 3-D lattice model strength value is sensitive to porosity and the energy absorption value is higher for lower porosity. Gorbunova et al. [37] synthesized a urea-based PU thermoplastic for bio-medical applications by controlling the physical parameters. The mechanical properties, thermal properties, shape memory of adaptive materials were controlled by physical structural parameters like degree of crystallinity and crystallization rate of soft blocks. These physical parameters were controlled by varying the polyether-dioles types and ratio and also the nature of isocyanate group present in the rigid blocks. The author also reported the influence of two crystllaizable blocks such as poly-ε-caprolactone diol (PCL) and polybutylene glycol adipate diol (PBA) on structure and thermal properties of urea based PU thermoplastic elastomers. Kim et al. [55] investigated the mechanical and piezoresistive behavior of MWCNTs filled (2%, 3%, 4%, 5%) PU thermoplastic nanocomposites. The plan PU thermoplastic possess lower strength value, addition of MWCNT increases the young's modulus and true stress value and the strength is higher for 5 wt% MWCNT filled PU thermoplastic nanocomposite. The stable electrically conductive network is formed at 5 wt% filler composite and this is the percolation threshold value to get the higher electrical conductivity. Piezo resistivity is measured for 5% CNT by using variation of resistance under loading and it is measured upto the 1.4 stretch. The rate of increase in resistance is faster in longitudinal direction as compared to transverse direction. The piezo resistivity is measured with cyclic deformation to know the reliable nature of the 3-D printed composite. The resistance peak decreases with increasing number of cycles and the small peaks were observed at lower strain limit. The increase in CNT length and diameter reduces the piezo resistivity and smaller significant difference were observed in the prepared model.

3.5 Polyamide Thermoplastic Composites

Polyamides (PAs) are the synthetic polymers formed by the repeating units of amides linkages, where these polymers applications ranges from textile to automotive applications. There exist a two types PAs such as aromatic polyamides (aromatic rings) and aliphatic polyamides (aliphatic chains), synthesizing of aliphatic PAs is easy by condensation polymerization and synthesizing of aromatic PAs is difficult by diacids and diamines due to less reactive nature of aromatic amines [92]. Chabaud et al. [18] investigated the mechanical behavior of glass, carbon fiber reinforced polyamide thermoplastics which are produced using commercial 3-D printer. The optical observations were done on as received filaments and it reveals that there exist a variation in diameters of carbon and glass fibers due to improper coating of filaments during processing and also inhomogeneity was found in impregnated fibers with agglomeration formation. Tensile modulus and ultimate stress value is higher for higher fiber volume percentage (30%), further increasing fiber percentage above 30% of GF/PA composite results in lower ultimate stress value due to change in failure mode by debonding instead of fiber breakages. Both the fiber reinforcement exhibits higher mechanical properties as compared pure PA composite, where ultimate stress value is 23 times higher for carbon fiber and 19 times higher for glass fiber, similarly tensile modulus value is elevated to 137 times, 63 times for carbon and glass fibers respectively. Silva et al.[86] studied the hybrid processing approach for the fabrication of carbon fiber reinforced PA thermoplastic using Fiber Yarn Fused Fabrication (FYFF) system. The tensile and three point bending tests were conducted for two types of yarns 1 K and 3 K with varying sample thickness. The 3 K yarn 4 layers specimen possess maximum 153.62 MPa of rupture stress with 5.16% of standard deviation. The 2.12 mm of mean displacement is observed at break with 0.61% of standard deviation. The addition of less dense carbon fiber lowers the tensile strength and standard deviation value is within the expectation because of the produced components has higher anisotropic mechanical properties as per manufacturing directions. The flexural results show that increasing the fiber yarn layers from 2 to 4 elevates the break strength to 366% and 325% for 3 K and 1 K yarn types respectively. Hong et al. [44] evaluated the mechanical, electrical properties of carbon black (CB)/polyamide 12 (PA12) composite using two-step approach based on SLS system. In the first step, these material powders were prepared with predesigned coating structure and then sintering was done in the subsequent SLS steps. Morphology images shows the good absorbing of CB particles in the PA12 power surface and the powder size impact is negligible. The quantitative analysis of power size and distribution is shown in Fig. 4. The raw powders median diameter value (D 0.5) and span of distribution increases with addition of CB particles. The higher content of CB creates the agglomeration of particles and it is observed in Fig. 4c. The 2% CB/PA12 composite has uniform distribution of CB particles and it is shown in Fig. 4b. The two-step approach increases the higher electrical conductivity of CB/PA composite due to formation of 3-D segregated conductive network. The young's modulus value increased with higher CB contents and CB demonstrate

the irregular effect on the tensile strength and elongation at break at different SLS conditions. [49] characterized the ply and interlaminar behavior of continuous carbon fiber reinforced PA composite fabricated using FFF process. The mechanical performance obtained through FFF process in longitudinal direction is equivalent to same produced using hot compression molding process. The mechanical response during transverse and shear loading is strongly affected by manufacturing defects and this drawback is less in HCM process. The defects such as voids, non-uniform distribution of fibers, poor intralaminar bonding were identified in between the layers and the beads. These defects lower the thermo-mechanical strength of the materials during fabrication which arises due to rapid cooling of 3-D printed composite below the T_g value. The carbon fibers have good dispersibility with the PA12 matrix material and these fibers aligned in the printing direction. The DSC curves recorded the highest crystallization peak temperatures with the addition of higher carbon fiber content, because these carbon fibers behaves as a nucleating agents for the crystallization of PA12 matrix phase. This nucleating behavior of fibers changes the mode from homogeneous nucleation to heterogeneous nucleation, which reduces the nucleation free energy and it leads to the orderly arrangement of molecular chains on the surfaces of carbon fiber. The plane PA12 and CF/PA12 DSC heating curve shows the very less difference of melt peak temperatures and addition of CF doesn't affect the melt process. The carbon fiber shows a two opposite faces for the failure of material, one is it may increase the defect density in the composite, which results in crack beginning. Another it is efficient to avoid the crack propagation because the carbon fiber orientation is perpendicular to the direction of crack propagation. Along the printing direction, the thermal conductivity value enhanced by 227.8% as compared to neat PA12 and it is 0.835 W/mK [62]. Wang et al. [98] analyzed the effect of infill pattern, infill density and strain rate on mechanical performance of polyamide based thermoplastic composites. The composites with hexagonal structure unit's has higher tensile modulus and strength value but having lower elongation at break as compared to triangular unit structures. The failure and deformation mode is affected by infill pattern and it is caused due to printing path defects. The triangular unit composite structure failure is started from internal node and propagates towards the neighbor nodes. The beginning of failure at the internal node is due to imperfections in manufacturing (overlapping of printing path). The hexagonal structured composite failure begins from circumferential walls which is due to strain at the wall edges and imperfection at the cellular joint. The young's modulus and tensile strength value increases with increasing infill density, this infill density improves the resistance to deformation.

3.6 *Acrylonitrile Butadiene Styrene (ABS) Thermoplastic Composites*

ABS is an amorphous engineering thermoplastic material, which is composed of monomers like styrene, acrylonitrile and butadiene. Acrylonitrile monomer increases the chemical resistance, butadiene contributes for the toughness, styrene increases the processability and these properties attracts the variety of applications. ABS is non conducting material having an excellent properties like ductility at lower temperature, rubber toughness, good dimensional stability and good chemical resistance [72]. The 20% CF reinforced thermoplastic has most dominant elastic properties and they are having high shear thinning at different dynamic frequencies. The dynamic mechanical properties were depending on the printing direction, the T_g value is highest in xy direction than the z direction printed sample by 4 °C. The storage modulus, loss modulus value is 58 MPa and 19.5 MPa respectively in the xy direction [1]. Conway et al. [22] studied the crazing behavior of additive manufactured ABS thermoplastic and compared the results with compression molded ABS. The AM ABS has yield strength of 33 MPa and compression molded (CM) ABS has 31 MPa of yield strength. The crazing was observed in AM ABS material at 0.78σ and it is observed in CM ABS after the material is subjected to yielding. The uniform and thin crazes were found in AM ABS specimens with 10 μm width and it is not originated from any particular one point, but uniformly distributed over the entire crossectional area, particularly observed at thinnest sections. Further loading elaborates the crazes size, upon increasing the load results in initiating crazes developing outside the gage sections, which is due to more crazes begins to nucleate from the stress concentration region over the gage section. The crazes were found to be denser at middle of dog bone shaped specimen at the smallest crossectional area and the density is decreased towards the gripping section. The internal voids were not found in the CM ABS material and found in AM ABS specimen due to printing errors. During loading, the internal voids were grown till the material cracked at the region of craze initiation. [33] fabricated a sandwich composite composed of carbon fiber reinforced ABS thermoplastic for complex structure build by FDM process. The reinforcing of one layer carbon fiber on bottom and top of the ABS enhances the ultimate strength from 0.63 ± 0.1 GPa to 4.03 ± 0.7 GPa and the elastic modulus value by 0.63 ± 0.1 GPa to 4.03 ± 0.7 GPa, similarly for two carbon layers it is increased by 43 ± 2.3 MPa of ultimate tensile strength and the elastic modulus value achieved is 7.3 ± 0.7 GPa and for three carbon layers the tensile strength and modulus is 83.3 ± 1.5 MPa and 11.2 ± 1.7 GPa respectively. The failure in CF/ABS/CF composite begins from carbon layers, further followed by core material failure and the failure occurs by the mode of fiber pull-outs and carbon layer delamination. During tensile loading, the sandwich composite exhibits brittle behavior while pure ABS samples has ductile behavior. The artificial neural network model is prepared to check the accuracy of elastic modulus and specific strength value and the results reveal the excellent accuracy of tensile values proposed by ANN model as compared to experimental data. [84] investigated the effect of MWCNTs (1, 3, 5, 7 and 10 wt%) on ABS

material fabricated using 3 D printing. The ultimate tensile strength (UTS) is higher for 7 wt% MWCNT filled composite and UTS is reduced for 10 wt% due to the improper particles' agglomeration. The total UTS value is 288% higher for 7 wt% as compared to neat ABS composite. The pure ABS samples nonconducting electric behavior and adding 3 wt% of MWCNT makes insulating to conductive material for the raster angle [0, 90]. The mechanical properties and electrical conductivity is higher for [0, 90] raster angle as compared to [−45, + 45] rater angle. The maximum electrical conductivity achieved is 232 e^{-2} S/cm and lowest melt flow index (MFI) value achieved is 0.03 g/10 mm for 10 wt% MWCNT filled ABS thermoplastic composite. The MFI reduction is due to clogging of filler particles at the extruder nozzle while printing the filaments with higher concentration filler rate. The addition of CNT filler with the ABS matrix enhances the tensile strength upto 5wt5 of CNT and the percentage was elevated, which is equal to five times the weight percentage of CNT filler material. CNT also improves the young's modulus value estimated for 100% increase for 3wt% filler composite and the 10 wt% CNT/ABS composite shows brittle behavior with reduction of strength value. The adhesive nature between the layers is not affected by CNT upto 3 wt%, further increasing above 2 wt% reduces the fracture toughness value and slight increase was observed at 1 wt% CNT composites. The anisotropic conductivity values were observed in less than 5 wt% CNT filled composite and the conductivity is high in in-layer direction as compared to through layer conductivity. The piezo resistance changes were observed in CNT/ABS nanocomposites at the strained tension condition and the resistance value sudden change is observed when the material deformation reaches to plastic zone [91].

3.7 Polypropylene (PP) Thermoplastic Composites

Polypropylene is a low density popular thermoplastic material, discovered in the year 1954 and it is prepared by the catalytic action from the propylene. The major advantage of the polymer is resistance to high temperature and chemical activity, which makes the advantage in clinical environment applications. This polymer is free color material having a superior mechanical property as compared to polyethylene [65]. Grigorescu et al. [38] developed a thermoplastic composite composed of recycled polypropylene (rPP), styrene butadiene block copolymer (SBS) and waste printed circuit board (WPCB) powder as a filler material and Irganox as a compatible element. The 30% WPCB filled increases the impact strength of the composites by the addition of two block copolymers and without the filler the impact strength reduced by 62–85%. The malenized block copolymer (elastomer) addition enhances the impact strength value three times higher than compared to rPP with same percentage of filler material, it is due to the better compatibility between the rPP and copolymer. The copolymer addition with rPP increases the elongation at break value of composites and it becomes ductile one (initially brittle). [52] prepared a polypropylene/ micro crystalline cellulose (MCC) composite using additive manufacturing and MCC surface is treated with different silanes. The results indicate

the improvement in mechanical properties due to good dispersion of MCC in the PP matrix material. The good quality of the filament and good mechanical properties of AM printed parts suggests that the compounded homogeneous composite could be reprocessed into the filaments for ME-AM and it can also be reshaped into the 3D structures. [74] evaluated the mechanical properties of unidirectional GF/PP composites and bidirectional GF/PP which are built by laser assisted AM technique. The SEM crossectional images shows the orientation of fibers aligned in 0°/90° direction in bidirectional composites whereas the fiber orientation is one direction in unidirectional composite. The PP matrix exhibits semi-crystalline structure and it was bonded with diffusion with the application of heat and pressure. The strong bonding mechanism and diffusion is observed in both the mechanisms without any visibility of gaps or voids (Fig. 5). The adhesive nature of prepreg layer T-peel test using laser source and the T-peel strength is higher for bidirectional composite. The stronger adhesion can be obtained setting the parameters like 26 W laser bonding power and 2 mm/s of fixed roller speed. As compared to hot compaction method, this laser assisted AM has 50% of higher peel strength and 96% of lap shear strength. The 300%, 150%, 100% of higher tensile strength, tensile modulus and flexural modulus values were obtained as compared to FDM printed short fiber reinforced thermoplastic composites. [88] studied the anisotropic properties of short carbon

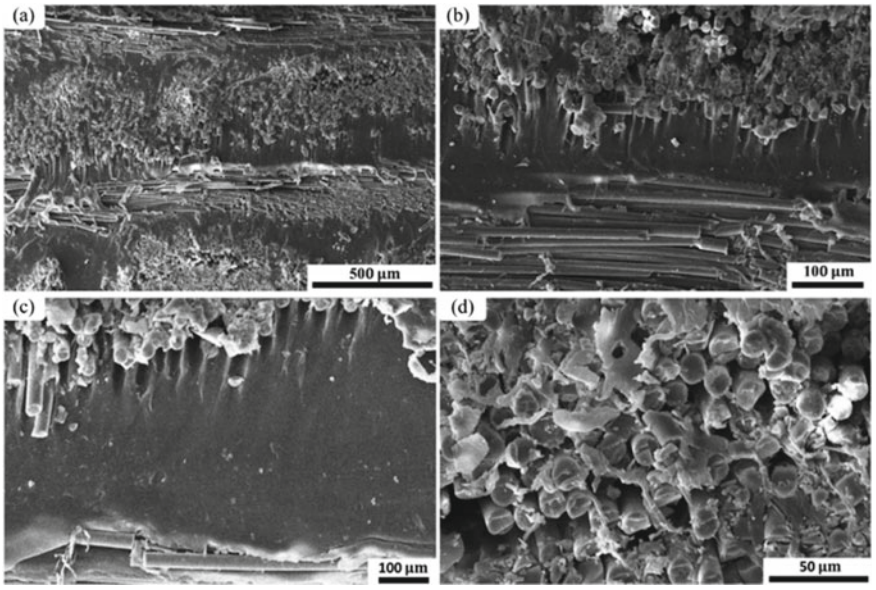

Fig. 5 Cross-sectional SEM images of unidirectional samples demonstrating interfacial bonding after laser assisted additive manufacturing. **a** Cross-ply fiber orientation (0/90) evident from cross-sectional micrograph, **b**, **c** interfacial area between two layers with 90° angle of fiber orientation, and **d** fibers in unidirectional tape. (Reused with the permission from Elsevier, License No: 4991351004332)

fiber reinforced polypropylene composite built by extrusion-based AM technique. The SEM images reveals the good compatibility between the fiber-matrix interfaces and also there exist a good interaction between the compatibiliser reactive group and the carbon fiber surface. The more fiber pull-outs and the holes in the cryo-fracture were observed in more than 10% carbon reinforced composite due to reduction of compatible nature with the addition of more reinforcement. The composite PP/10CF exhibits proper alignment of fibers in the printing direction and uniform distribution together. The addition of 10% CF with PP increases 100% of filament yield stress, filament young's modulus of more than 400% and decrease of 50% in yield strain as compared to neat PP composite. The thermal conductivity value is higher in printing direction fiber alignment and lower in fiber alignment opposite to printing direction composite. By the application of impact load, the composite with different fiber orientation shows almost similar trend in flexural test. The composite PP/CF10 shows more brittle nature than neat PP and exhibits plastic deformation at smaller zones, results in decrease of impact energy by 2–4 times as compared to neat PP.

4 Applications

The thermoplastic composites are attracted for manufacturing industries due to light weight, high mechanical performance, ease of manufacturing, low processing cost and these materials are suitable for high volume production with complex structures. Further enhancement of properties were done by selecting suitable additive manufacturing technique instead of traditional methods. Some of the applications were tabulated in Table 3. The carbon fiber reinforced PEEK thermoplastic built by laser sintering technique possess isotropic properties and the part property exhibited by dry blends causes' difference in spatial directions. These developed composites have light in weight, higher stiffness and these are suggested for aerospace applications like air ducts, exhausts and the interior customized parts of aircrafts [31]. Flowers et al. [32] developed a thermoplastic composite suitable for electronic components and conductive thermoplastic used electronic circuits. The material composed of hatch box PLA and bronze fill PLA has a dielectric materials and graphene based PLA, carbon black PLA has a conductive material fabricated using FFF process. The author prepared a small electric applicability components such as horn antenna having thin walls pyramid structure, LED embedded thermoplastic component and 3-D printed high pass filter L-C circuit. Additive manufacturing is one of the efficient techniques for the fabrication of 3-D printed PEEK dentistry models during the requirement of exact fitting model. It makes the surgeons jobs easier and the dentist can be able to transfer their requirements into the real 3D model innovative and these PEEK material has an ability to replace the tooth which is economical for the dentists. Due to their biocompatible nature and safeties, the PEEK based implants were used in medical applications instead of metallic implants. The lightweightness of PEEK promotes the application in robust denture which helps for the patients [41].

Table 3 Applications of thermoplastic composites

References	Matrix	Reinforcement/additives	AM technique	Observations	Application
[80]	Polyurethane blends	Encapsulated paraffin blends	FDM	Prepared material withstands the cyclic stress both in tensile and compressive phenomenon	Thermal energy storage and release application
[82]	Polyimide	Polyetherimide, Polyethylene glycol diacrylate	FFF	Inkjet printing modifies the material surface and increases the RF performance	Printed electronics and RF devices
Wang et al. [97]	Poly ether ether ketone (PEEK)	–	FDM	High biocompatible nature PEEK and mechanical properties promotes for medical devices	Dental implantology
[21]	Polyurethane	Multiwalled carbon nanotube	FDM	Addition of MWCNT enhances strength, electrical conductivity and initial elastic modulus value. Good adhesion and no degradations were observed	Elastic strain sensors

(continued)

Table 3 (continued)

References	Matrix	Reinforcement/additives	AM technique	Observations	Application
[14]	Cyclo-olefin polymer	$MgCaTiO_2$, TiO_2, $Ba_{0.55}Sr_{0.45}TiO_3$	FDM	The optimum relative permittivity and loss tangent values were obtained by the addition of ceramic fillers	Microwave components
[33]	Acrylonitrile butadiene styrene (ABS)	Carbon fiber	FDM	Addition of CFRP layers improves the stiffness and specific strength suitable for UAV applications	Aerial vehicle applications
[43]	PEEK	-	FFF	Inexpensive 3D printing technique advantages for surgical planning and reduction of time for implant production	Surgical applications
[42]	Polyurethane	MWCNTs	FFF	The composite with 3 and 4 wt% MWCNT shows optimum repeatable and conductivity behavior (frequency independent) suitable for actuating applications	Pneumatic actuators

5 Conclusion

The advanced manufacturing sector is attracted by Additive Manufacturing (AM) due to its rapid prototyping action, flexibility and application oriented parts can be developed easily. This present review work demonstrates the properties of different thermoplastic composites fabricated using various AM techniques with their potential applications in various field. The addition of high stiffness reinforcements (carbon, glass, kevlar) with the thermoplastic matrix fabricated using AM technique increases the potentiality of the composite, especially the continuous fiber reinforcements has higher mechanical, thermal and electrical properties as compared to short fiber reinforcements. The properties of printed parts were affected by process parameters like nozzle temperature, printing speed and also the printing direction. The AM fabricated composite possess higher material properties as compared to other traditionally manufactured composites due to strong adhesion exist between the printed layers. The AM fabricated thermoplastics has less manufacturing defects, involves less processing time and complex structured prototypes can be produced quickly. The biocompatible nature of PEEK thermoplastics plays dominant role in medical applications and the AM produced PEEK utilized especially by surgeons for prototyping of newly developed tools and implant applications. The major advantages of AM printed thermoplastics are high impact resistance, ductile nature, recyclable nature, corrosion resistance and they have higher thermal stability as compared to thermosets. These attractive properties and AM advantages add up the applications in manufacturing field. Further research work must be needed for the fabrication of different thermoplastics using various additive manufacturing techniques.

6 Future Scope

This work constitutes some portion of thermoplastic composite, further work is needed on polyaryletherketones, polycarbonate, polyetherimide based thermoplastic composites. Some of the thermoplastics are having poor resistance to high polar solvents, organic solvents and hydrocarbons, these factors influence the filament chemical treatment before the printing. Postprocessing is required for 3D printed parts and also difficult to produce large volume complex structures. The fiber pull-outs, delaminations, voids formation is more in additively manufactured composites due to improper adhesiveness and care must be taken while selecting the suitable process parameters for the particular material, over melting of filaments leads to the development of improper structure, uneven material deposition, which can be reduced by selecting the proper filament melting temperature before printing. Hence further research work is needed more on potential thermoplastics and to overcome the drawbacks exist in the current additive manufacturing techniques.

Acknowledgements The work was financed by Thailand Science Research and Innovation Fund and King Mongkut's University of Technology North Bangkok (KMUTNB), Thailand with Contract no. KMUTNB-BasicR-64-16 and KMUTNB-62-Post-08.

References

1. Ajinjeru C, Kishore V, Chen X, Hershey C, Lindahl J, Kunc V, Duty C (2019) Rheological survey of carbon fiber-reinforced high-temperature thermoplastics for big area additive manufacturing tooling applications. J Thermoplast Compos Mater 0892705719873941
2. Alam F, Varadarajan KM, Koo JH, Wardle BL, Kumar S (2020) Additively manufactured polyetheretherketone (PEEK) with carbon nanostructure reinforcement for biomedical structural applications. Adv Eng Mater 22(10):2000483
3. Arif MF, Alhashmi H, Varadarajan KM, Koo JH, Hart AJ, Kumar S (2020) Multifunctional performance of carbon nanotubes and graphene nanoplatelets reinforced PEEK composites enabled via FFF additive manufacturing. Compos Part B Eng 184:107625
4. Bai J, Yuan S, Shen F, Zhang B, Chua CK, Zhou K, Wei J (2017) Toughening of polyamide 11 with carbon nanotubes for additive manufacturing. Virtual Phys Prototyping 12(3):235–240
5. Banoriya D, Purohit R, Dwivedi RK, Baghel U (2019) development and testing of polyurethane based composites using rapid prototyping techniques for biomedical applications-a review. Mater Today Proc 18:5410–5415
6. Berretta S, Davies R, Shyng YT, Wang Y, Ghita O (2017) Fused deposition modelling of high temperature polymers: exploring CNT PEEK composites. Polym Testing 63:251–262
7. Bhudolia SK, Gohel G, Leong KF, Islam A (2020) Advances in ultrasonic welding of thermoplastic composites: a review. Materials 13(6):1284
8. Blok LG, Longana ML, Yu H, Woods BK (2018) An investigation into 3D printing of fibre reinforced thermoplastic composites. Addit Manuf 22:176–186
9. Calandri M, Manfredi D, Calignano F, Ambrosio EP, Biamino S, Lupoi R, Ugues D (2018) Solution treatment study of inconel 718 produced by SLM additive technique in view of the oxidation resistance. Adv Eng Mater 20(11):1800351
10. Calignano F, Lorusso M, Roppolo I, Minetola P (2020) Investigation of the mechanical properties of a carbon fibre-reinforced nylon filament for 3D printing. Machines 8(3):52
11. Caminero MA, Chacón JM, García-Moreno I, Reverte JM (2018) Interlaminar bonding performance of 3D printed continuous fibre reinforced thermoplastic composites using fused deposition modelling. Polym Test 68:415–423
12. Caminero MA, Chacón JM, García-Moreno I, Rodríguez GP (2018) Impact damage resistance of 3D printed continuous fibre reinforced thermoplastic composites using fused deposition modelling. Compos B Eng 148:93–103
13. Cardenas JA, Tsang H, Tong H, Abuzaid H, Price K, Cruz MA, Lazarus N (2020) Flash ablation metallization of conductive thermoplastics. Addit Manuf 36:101409
14. Castro J, Rojas-Nastrucci EA, Ross A, Weller TM, Wang J (2017) Fabrication, modeling, and application of ceramic-thermoplastic composites for fused deposition modeling of microwave components. IEEE Trans Microw Theory Tech 65(6):2073–2084
15. Cerneels J, Voet A, Ivens J, Kruth JP (2013) Additive manufacturing of thermoplastic composites. Compos Week@ Leuven 1–7
16. Chacón JM, Caminero MA, García-Plaza E, Núnez PJ (2017) Additive manufacturing of PLA structures using fused deposition modelling: Effect of process parameters on mechanical properties and their optimal selection. Mater Des 124:143–157
17. Chacón JM, Caminero MA, Núñez PJ, García-Plaza E, García-Moreno I, Reverte JM (2019) Additive manufacturing of continuous fibre reinforced thermoplastic composites using fused deposition modelling: Effect of process parameters on mechanical properties. Compos Sci Technol 181:107688

18. Chabaud G, Castro M, Denoual C, Le Duigou A (2019) Hygromechanical properties of 3D printed continuous carbon and glass fibre reinforced polyamide composite for outdoor structural applications. Addit Manuf 26:94–105
19. Chang B, Li X, Parandoush P, Ruan S, Shen C, Lin D (2020) Additive manufacturing of continuous carbon fiber reinforced poly-ether-ether-ketone with ultrahigh mechanical properties. Polym Test 106563
20. Chen Q, Mangadlao JD, Wallat J, De Leon A, Pokorski JK, Advincula RC (2017) 3D printing biocompatible polyurethane/poly (lactic acid)/graphene oxide nanocomposites: anisotropic properties. ACS Appl Mater Interfaces 9(4):4015–4023
21. Christ JF, Aliheidari N, Ameli A, Pötschke P (2017) 3D printed highly elastic strain sensors of multiwalled carbon nanotube/thermoplastic polyurethane nanocomposites. Mater Des 131:394–401
22. Conway KM, Pataky GJ (2019) Crazing in additively manufactured acrylonitrile butadiene styrene. Eng Fract Mech 211:114–124
23. Cousins DS, Suzuki Y, Murray RE, Samaniuk JR, Stebner AP (2019) Recycling glass fiber thermoplastic composites from wind turbine blades. J Clean Prod 209:1252–1263
24. Csenge T, Kovács KN (2020) Characterization of short fiber-reinforced polylactic acid composites produced with Fused Filament Fabrication (FFF). In: IOP conference series: materials science and engineering IOP publishing, vol 903, issue no 1, p 012031
25. De León AS, Domínguez-Calvo A, Molina SI (2019) Materials with enhanced adhesive properties based on acrylonitrile-butadiene-styrene (ABS)/thermoplastic polyurethane (TPU) blends for fused filament fabrication (FFF). Mater Des 182:108044
26. Dickson AN, Dowling DP (2019) Enhancing the bearing strength of woven carbon fibre thermoplastic composites through additive manufacturing. Compos Struct 212:381–388
27. Dong G, Tang Y, Li D, Zhao YF (2018) Mechanical properties of continuous kevlar fiber reinforced composites fabricated by fused deposition modeling process. Procedia Manuf 26:774–781
28. Dutra TA, Ferreira RTL, Resende HB, Guimarães A (2019) Mechanical characterization and asymptotic homogenization of 3D-printed continuous carbon fiber-reinforced thermoplastic. J Braz Soc Mech Sci Eng 41(3):133
29. Fan C, Shan Z, Zou G, Zhan L, Yan D (2020) Performance of short fiber interlayered reinforcement thermoplastic resin in additive manufacturing. Materials 13(12):2868
30. Ferreira RTL, Amatte IC, Dutra TA, Bürger D (2017) Experimental characterization and micrography of 3D printed PLA and PLA reinforced with short carbon fibers. Compos B Eng 124:88–100
31. Fischer S, Pfister A, Galitz V, Lyons B, Robinson C, Rupel K, Kubiak S (2015) A high performance material for aerospace applications: development of carbon fiber filled PEKK for laser sintering. In: Proceedings of the 26th annual international solid freeform fabric symposium, Austin, TX, USA, pp 10–12
32. Flowers PF, Reyes C, Ye S, Kim MJ, Wiley BJ (2017) 3D printing electronic components and circuits with conductive thermoplastic filament. Addit Manuf 18:156–163
33. Galatas A, Hassanin H, Zweiri Y, Seneviratne L (2018) Additive manufactured sandwich composite/ABS parts for unmanned aerial vehicle applications. Polymers 10(11):1262
34. Geng LC, Ruan XL, Wu WW, Xia R, Fang DN (2019) Mechanical properties of selective laser sintering (SLS) additive manufactured chiral Auxetic cylindrical stent. Exp Mech 59(6):913–925
35. Giannakis E, Koidis C, Kyratsis P, Tzetzis D (2019) Static and fatigue properties of 3D printed continuous carbon fiber nylon composites. Int J Mod Manuf Technol 11:69–76
36. Goh GD, Dikshit V, Nagalingam AP, Goh GL, Agarwala S, Sing SL, Yeong WY (2018) Characterization of mechanical properties and fracture mode of additively manufactured carbon fiber and glass fiber reinforced thermoplastics. Mater Des 137:79–89
37. Gorbunova MA, Shukhardin DM, Lesnichaya VA, Badamshina ER, Anokhin DV (2019) New polyurethane urea thermoplastic elastomers with controlled mechanical and thermal properties for medical applications. In Key engineering materials. Trans Tech Publications Ltd. vol 816, pp 187-191

38. Grigorescu RM, Ghioca P, Iancu L, David ME, Andrei ER, Filipescu MI, Bucurica IA (2020) Development of thermoplastic composites based on recycled polypropylene and waste printed circuit boards. Waste Manage 118:391–401
39. Guan XN, Xu XN, Kuniyoshi R, Zhou HH, Zhu YF (2018) Electromagnetic and mechanical properties of carbonyl iron powders-PLA composites fabricated by fused deposition modeling. Mater Res Express 5(11):115303
40. Han X, Yang D, Yang C, Spintzyk S, Scheideler L, Li P, Rupp F (2019) Carbon fiber reinforced PEEK composites based on 3D-printing technology for orthopedic and dental applications. J Clin Med 8(2):240
41. Haleem A, Javaid M (2019) Polyether ether ketone (PEEK) and its manufacturing of customised 3D printed dentistry parts using additive manufacturing. Clin Epidemiol Glob Health 7(4):654–660
42. Hohimer CJ, Petrossian G, Ameli A, Mo C, Pötschke P (2020) 3D printed conductive thermoplastic polyurethane/carbon nanotube composites for capacitive and piezoresistive sensing in soft pneumatic actuators. Addit Manuf 101281
43. Honigmann P, Sharma N, Okolo B, Popp U, Msallem B, Thieringer FM (2018) Patient-specific surgical implants made of 3D printed PEEK: material, technology, and scope of surgical application. BioMed Res Int 2018:1–8
44. Hong R, Zhao Z, Leng J, Wu J, Zhang J (2019) Two-step approach based on selective laser sintering for high performance carbon black/polyamide 12 composite with 3D segregated conductive network. Compos Part B Eng 176:107214
45. Holmes M (2019) Additive manufacturing continues composites market growth. Reinf Plast 63(6):296–301
46. Hu C, Hau WNJ, Chen W, Qin QH (2020) The fabrication of long carbon fiber reinforced polylactic acid composites via fused deposition modelling: experimental analysis and machine learning. J Compos Mater 0021998320972172
47. Hyvärinen M, Kärki T (2020) Tensile Properties of cellulose-filled recycled thermoplastic composite filaments for 3D printing. In: Key engineering materials. Trans Tech Publications Ltd. vol 841, pp 87–93
48. Ilyés K, Kovács NK, Balogh A, Borbás E, Farkas B, Casian T, Nagy ZK (2019) The applicability of pharmaceutical polymeric blends for the fused deposition modelling (FDM) 3D technique: material considerations–printability–process modulation, with consecutive effects on in vitro release, stability and degradation. Eur J Pharm Sci 129:110–123
49. Iragi M, Pascual-Gonzalez C, Esnaola A, Lopes CS, Aretxabaleta L (2019) Ply and interlaminar behaviours of 3D printed continuous carbon fibre-reinforced thermoplastic laminates; effects of processing conditions and microstructure. Addit Manuf 30:100884
50. Jeong S, Sim J, Kim H, Shin D, Hong D (2017) Application of LOM for freeform architecture. J Korean Soc Precision Eng 34(12):903–909
51. John B (2014 Structural and physical properties of polyurethane nanocomposites and foams. In: Handbook of polymer nanocomposites processing performance and application. Springer, Berlin, Heidelberg, pp 341–359
52. Kaynak B, Spoerk M, Shirole A, Ziegler W, Sapkota J (2018) Polypropylene/cellulose composites for material extrusion additive manufacturing. Macromol Mater Eng 303(5):1800037
53. Karakoç A, Rastogi VK, Isoaho T, Tardy B, Paltakari J, Rojas OJ (2020) Comparative screening of the structural and thermomechanical properties of FDM filaments comprising thermoplastics loaded with cellulose, carbon and glass fibers. Materials 13(2):422
54. Khadilkar A, Wang J, Rai R (2019) Deep learning–based stress prediction for bottom-up SLA 3D printing process. Int J Adv Manuf Technol 102(5–8):2555–2569
55. Kim M, Jung J, Jung S, Moon YH, Kim DH, Kim JH (2019) Piezoresistive behaviour of additively manufactured multi-walled carbon nanotube/thermoplastic polyurethane nanocomposites. Materials 12(16):2613
56. Kikuchi BC, Bussamra FLDS, Donadon MV, Ferreira RTL, Sales RDCM (2020) Moisture effect on the mechanical properties of additively manufactured continuous carbon fiber-reinforced Nylon-based thermoplastic. Polym Compos 41(12):5227–5245

57. Kumar AY, Bai Y, Eklund A, Williams CB (2018) The effects of Hot Isostatic Pressing on parts fabricated by binder jetting additive manufacturing. Addit Manuf 24:115–124
58. Kumar D, Rajmohan T, Venkatachalapathi S (2018) Wear behavior of PEEK matrix composites: a review. Mater Today Proc 5(6):14583–14589
59. Leng J, Wu J, Zhang J (2019) Preparation of thermoplastic polyurethane parts reinforced with in situ polylactic acid microfibers during fused deposition modeling: the influences of deposition-induced effects. Ind Eng Chem Res 58(47):21476–21484
60. Li N, Li Y, Liu S (2016) Rapid prototyping of continuous carbon fiber reinforced polylactic acid composites by 3D printing. J Mater Process Technol 238:218–225
61. Lim CWJ, Le KQ, Lu Q, Wong CH (2016) An overview of 3-D printing in manufacturing, aerospace, and automotive industries. IEEE Potentials 35(4):18–22
62. Liao G, Li Z, Cheng Y, Xu D, Zhu D, Jiang S, Zhu Y (2018) Properties of oriented carbon fiber/polyamide 12 composite parts fabricated by fused deposition modeling. Mater Des 139:283–292
63. Luo J, Wang H, Zuo D, Ji A, Liu Y (2018) Research on the application of MWCNTs/PLA composite material in the manufacturing of conductive composite products in 3D printing. Micromachines 9(12):635
64. Luo M, Tian X, Shang J, Zhu W, Li D, Qin Y (2019) Impregnation and interlayer bonding behaviours of 3D-printed continuous carbon-fiber-reinforced poly-ether-ether-ketone composites. Compos A Appl Sci Manuf 121:130–138
65. Maddah HA (2016) Polypropylene as a promising plastic: a review. Am J Polym Sci 6(1):1–11
66. Manapat JZ, Chen Q, Ye P, Advincula RC (2017) 3D printing of polymer nanocomposites via stereolithography. Macromol Mater Eng 302(9):1600553
67. Mansour M, Tsongas K, Tzetzis D, Antoniadis A (2018) Mechanical and dynamic behavior of fused filament fabrication 3D printed polyethylene terephthalate glycol reinforced with carbon fibers. Polym-Plast Technol Eng 57(16):1715–1725
68. Majko J, Ságа M, Vaško M, Handrik M, Ságová Z (2020) FE modeling of continuous fiber reinforced thermoplastic composite structures produced by additive manufacturing. In: IOP conference series: materials science and engineering IOP publishing, vol 776, issue no 1, p 012080
69. Mortazavian S, Fatemi A (2017) Fatigue of short fiber thermoplastic composites: a review of recent experimental results and analysis. Int J Fatigue 102:171–183
70. Nagarajan V, Mohanty AK, Misra M (2016) Perspective on polylactic acid (PLA) based sustainable materials for durable applications: Focus on toughness and heat resistance. ACS Sustain Chem Eng 4(6):2899–2916
71. Ning F, Cong W, Qiu J, Wei J, Wang S (2015) Additive manufacturing of carbon fiber reinforced thermoplastic composites using fused deposition modeling. Compos B Eng 80:369–378
72. Olivera S, Muralidhara HB, Venkatesh K, Gopalakrishna K, Vivek CS (2016) Plating on acrylonitrile–butadiene–styrene (ABS) plastic: a review. J Mater Sci 51(8):3657–3674
73. Omar NWY, Shuaib NA, Ab Hadi MHJ, Azmi AI (2019) Mechanical properties of carbon and glass fibre reinforced composites produced by additive manufacturing: a short review. In: IOP conference series: materials science and engineering IOP publishing, vol 670, issue no 1, p 012020
74. Parandoush P, Tucker L, Zhou C, Lin D (2017) Laser assisted additive manufacturing of continuous fiber reinforced thermoplastic composites. Mater Des 131:186–195
75. Pertuz A D, Diaz-Cardona S, González-Estrada OA (2020) Static and fatigue behaviour of continuous fibre reinforced thermoplastic composites manufactured by fused deposition modelling technique. Int J Fatigue 130: 105275
76. Rahman KM, Letcher T, Reese R (2015) Mechanical properties of additively manufactured PEEK components using fused filament fabrication. In: ASME international mechanical engineering congress and exposition. Ame Soc Mech Eng 57359:V02AT02A009
77. Ray D, Comer AJ, Lyons J, Obande W, Jones D, Higgins RM, McCarthy MA (2015) Fracture toughness of carbon fiber/polyether ether ketone composites manufactured by autoclave and laser-assisted automated tape placement. J Appl Polym Sci 132(11)

78. Rajak DK, Pagar DD, Menezes PL, Linul E (2019) Fiber-reinforced polymer composites: Manufacturing, properties, and applications. Polymers 11(10):1667
79. Reverte JM, Caminero MÁ, Chacón JM, García-Plaza E, Núñez PJ, Becar JP (2020) Mechanical and geometric performance of PLA-based polymer composites processed by the fused filament fabrication additive manufacturing technique. Materials 13(8):1924
80. Rigotti D, Dorigato A, Pegoretti A (2021) Low-cycle fatigue behavior of flexible 3D printed thermoplastic polyurethane blends for thermal energy storage/release applications. J Appl Polym Sci 138(3):49704
81. Rosenthal M, Henneberger C, Gutkes A, Bues CT (2018) Liquid deposition modeling: a promising approach for 3D printing of wood. Eur J Wood Wood Prod 76(2):797–799
82. Roach DJ, Roberts C, Wong J, Kuang X, Kovitz J, Zhang Q, Qi HJ (2020) Surface modification of fused filament fabrication (FFF) 3D printed substrates by inkjet printing polyimide for printed electronics. Add Manuf 36: 101544
83. Shen F, Yuan S, Guo Y, Zhao B, Bai J, Qwamizadeh M, Zhou K (2016) Energy absorption of thermoplastic polyurethane lattice structures via 3D printing: modeling and prediction. Int J Appl Mech 8(07):1640006
84. Sezer HK, Eren O (2019) FDM 3D printing of MWCNT re-inforced ABS nano-composite parts with enhanced mechanical and electrical properties. J Manuf Process 37:339–347
85. Singh R, Singh S, Mankotia K (2016) Development of ABS based wire as feedstock filament of FDM for industrial applications. Rapid Prototyping J
86. Silva M, Pereira AM, Alves N, Mateus A, Malça C (2017) A hybrid processing approach to the manufacturing of polyamide reinforced parts with carbon fibers. Procedia Manuf 12:195–202
87. Siddika A, Al Mamun MA, Alyousef R, Amran YM (2019) Strengthening of reinforced concrete beams by using fiber-reinforced polymer composites: a review. J Build Eng 25:100798
88. Spoerk M, Savandaiah C, Arbeiter F, Traxler G, Cardon L, Holzer C, Sapkota J (2018) Anisotropic properties of oriented short carbon fibre filled polypropylene parts fabricated by extrusion-based additive manufacturing. Compos A Appl Sci Manuf 113:95–104
89. Spoerk M, Savandaiah C, Arbeiter F, Sapkota J, Holzer C (2019) Optimization of mechanical properties of glass-spheres-filled polypropylene composites for extrusion-based additive manufacturing. Polym Compos 40(2):638–651
90. Tan W, Falzon BG (2016) Modelling the crush behaviour of thermoplastic composites. Compos Sci Technol 134:57–71
91. Thaler D, Aliheidari N, Ameli A (2019) Mechanical, electrical, and piezoresistivity behaviors of additively manufactured acrylonitrile butadiene styrene/carbon nanotube nanocomposites. Smart Mater Struct 28(8):084004
92. Vasanthan N (2009) Polyamide fiber formation: structure, properties and characterization. Woodhead Publishing, In Handbook of textile fibre structure, pp 232–256
93. Vagholkar P (2016) Nylon (Chemistry, Properties and Uses). Chemistry 5(9)
94. Valino AD, Dizon JRC, Espera Jr AH, Chen Q, Messman J, Advincula RC (2019) Advances in 3D printing of thermoplastic polymer composites and nanocomposites. Prog Poly Sci 98:101162
95. Velu R, Vaheed N, Ramachandran MK, Raspall F (2020) Experimental investigation of robotic 3D printing of high-performance thermoplastics (PEEK): a critical perspective to support automated fibre placement process. Int J Adv Manuf Technol 108(4):1007–1025
96. Velmurugan P, Manohar J, Kannan CR, Manivannan S, Vairamuthu J, Stalin B (2020) a study on development of induction welding of thermoplastic composites. In: IOP Conference Series: Materials Science and Engineering, IOP Publishing, vol 988 (1), p 012109
97. Wang Y, Müller WD, Rumjahn A, Schwitalla A (2020) Parameters influencing the outcome of additive manufacturing of tiny medical devices based on PEEK. Materials 13(2):466
98. Wang K, Xie X, Wang J, Zhao A, Peng Y, Rao Y (2020) Effects of infill characteristics and strain rate on the deformation and failure properties of additively manufactured polyamide-based composite structures. Results Phys 18:103346

99. Wang Y, Müller WD, Rumjahn A, Schmidt F, Schwitalla AD (2020) Mechanical properties of fused filament fabricated PEEK for biomedical applications depending on additive manufacturing parameters. J Mech Behav Biomed Mater 104250
100. Wang P, Zou B, Ding S, Huang C, Shi Z, Ma Y, Yao P (2020) Preparation of short CF/GF reinforced PEEK composite filaments and their comprehensive properties evaluation for FDM-3D printing. Compos Part B Eng 108175
101. Wei H, Nagatsuka W, Lee H, Ohsawa I, Sumimoto K, Wan Y, Takahashi J (2018) Mechanical properties of carbon fiber paper reinforced thermoplastics using mixed discontinuous recycled carbon fibers. Adv Compos Mater 27(1):19–34
102. Yap YL, Wang C, Sing SL, Dikshit V, Yeong WY, Wei J (2017) Material jetting additive manufacturing: an experimental study using designed metrological benchmarks. Precis Eng 50:275–285
103. Yassin K, Hojjati M (2018) Processing of thermoplastic matrix composites through automated fiber placement and tape laying methods: a review. J Thermoplast Compos Mater 31(12):1676–1725
104. Yousefpour A, Hojjati M, Immarigeon JP (2004) Fusion bonding/welding of thermoplastic composites. J Thermoplast Compos Mater 17(4):303–341
105. Zhang J, Yang B, Fu F, You F, Dong X, Dai M (2017) Resistivity and its anisotropy characterization of 3D-printed acrylonitrile butadiene styrene copolymer (ABS)/carbon black (CB) composites. Appl Sci 7(1):20

Applications of Additive Manufacturing

Siddharth Srivastava, Aanchna Sharma, and Vinod Kushvaha

1 Introduction

Additive Manufacturing (AM), better known as 3D printing, is the process of manufacturing a 3D object layer by layer. This requires the use of computer aided designing (CAD) to create a 3D model for the object to be printed. As parts are built by addition of material one layer at a time, it eliminates the need of fixture and cutting tools. Due to this, the conventional methods of subtractive manufacturing like boring, drilling, milling, etc. look primitive as compared to modern techniques.

The 3D printing process can be explained through a flowchart as shown in Fig. 1. First a 3D model of the object needs to be created using CAD. Then the file format is changed into STL which is recognized by a 3D printer. The STL file and the input parameters are then fed into the AM system which creates slices of the digital model. Then the layer by layer printing process starts. Upon completion, the user can remove the part and after proper post-processing, the final product is ready for application.

3D printing was first introduced in 1980s. Since then, it has evolved over the years and involves various methods, materials and equipments. Wohler's Associates have calculated that the AM industry has grown by 26.2% in over 27 years [56]. From $4.2 billion in 2014, it now holds a market share of $9.32 billion in 2018. They have also predicted that about 50% of 3D printing will revolve around the fabrication of commercial products in 2020 [4]. Figure 2a shows the growth of 3D printing in recent years. But to understand how this technology succeeded, we must learn about

S. Srivastava · A. Sharma · V. Kushvaha (✉)
Department of Civil Engineering, IIT Jammu, Jammu, India
e-mail: vinod.kushvaha@iitjammu.ac.in

S. Srivastava
e-mail: 2018uce0031@iitjammu.ac.in

A. Sharma
e-mail: 2018rce0035@iitjammu.ac.in

S. Mavinkere Rangappa et al. (eds.), *Additive and Subtractive Manufacturing of Composites*, Springer Series in Advanced Manufacturing,
https://doi.org/10.1007/978-981-16-3184-9_8

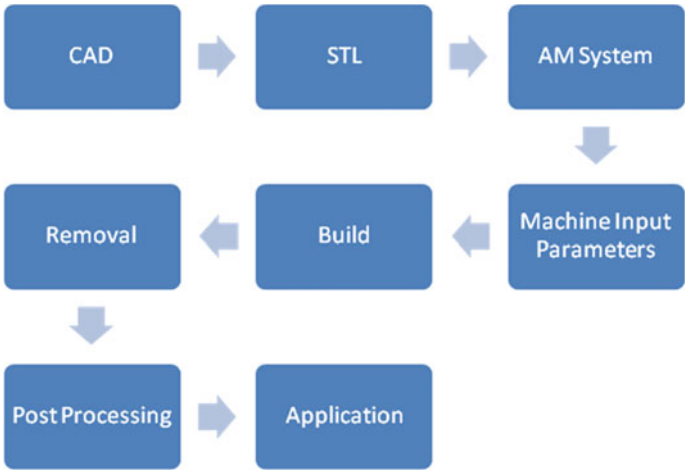

Fig. 1 Steps involved in 3D printing

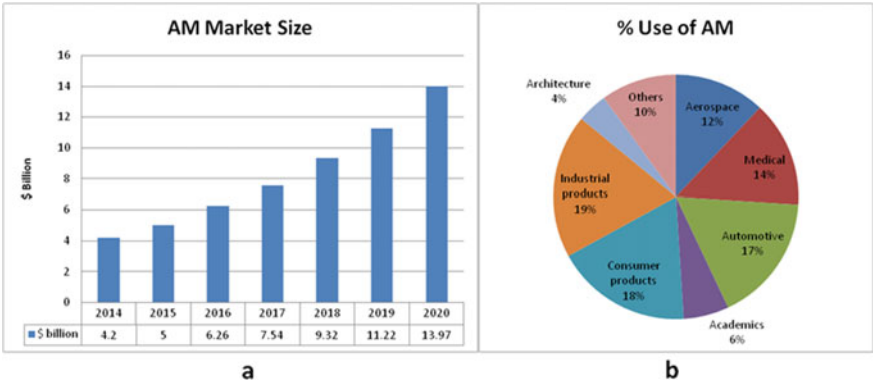

Fig. 2 **a** The values from 2014–2018 are based on actual data and values 2018 onwards are predicted by SmarTech Publishing. **b** Percentage use of AM in each sector in 2013

rapid prototyping and rapid manufacturing. Rapid prototyping is the technique to quickly fabricate a prototype model using CAD. In fact, additive manufacturing is a direct consequence of rapid prototyping. On the other hand, rapid manufacturing is the technique where software automation is used to accelerate the manufacturing process. This worked in parallel with AM to enable mass customization and mass production. These two techniques are together responsible for the enormous growth of 3D printing in the twenty-first century.

Until a few years ago, 3D printing was only limited to prototyping. However, with rapid growth in additive manufacturing, this technique is being intensively used in biomedical sector, aerospace and automotive industries and many other areas like fashion, jewelry and food. It has also found use in construction and marine industry

although with limited applicability. Recent developments have even made it possible for 3D printing to extend its applications to school, universities and laboratories for education and research work. A pie chart showing percentage use of AM in each sector is shown in Fig. 2b.

AM technologies can be broadly divided into 4 categories:

Vat-polymerization based printing: In this method, a light wave of certain frequency is subjected on a vat containing photocurable resin. This cures the resin layer by layer as the printing continues. Techniques involved are Stereolithography (SLA), Digital Light Processing (DLP), etc.

Powder-based printing: In this method, localized heating is used to fuse powdered material. Techniques involved are Selective Laser Sintering (SLS), Selective Laser Melting (SLM), Direct Metal Laser Sintering (DMLS) and Electron Beam Melting (EBM). SLS, DMLS and SLM utilize a laser beam whereas EBM utilizes a high energy electron beam.

Droplet-based printing: In this method, liquid droplets are jetted on to a substrate layer-by-layer. Techniques involved are MultiJet Modelling (MJM), Wax Deposition Modelling (WDM), Laser Induced Forward Transfer (LIFT) and Binder Jetting (BJ).

Extrusion-based printing: In this method, paste or filament is ejected from a hot nozzle or a syringe. Techniques involved are Fused Deposition Modelling (FDM) and Direct Ink Writing (DIW).

Usually a printing technique is favorable for one kind of printing material to obtain the best print quality. But new printing techniques are being investigated that can use any printing material depending on the object to be printed. The most common printing materials are polymers (polyamide, Poly Lactic Acid [PLA], nylon, Acrylonitrile Butadiene Styrene [ABS], Poly Ethylene Terephthalate [PET], et al.), metals or alloys (Ti6Al4V, IN625, IN718, etc.), ceramics (Alumina, Silica, ZrB_2, etc.) or composites made of these previously mentioned materials like polymer-metal and polymer-ceramic [33]. Sometimes concrete is also used for 3D printing in construction industry. Eatables like chocolate and sugar syrup are used for 3D printing food. Even organic materials like live cells have been used by researchers in bio-printing.

2 Applications of AM

Let's move onto the applications now where we shall see the various aspects of 3D printing in detail.

The applications have been divided into three categories which are biomedical, industrial and miscellaneous. The biomedical sector has been kept out of industrial applications as the medical industry alone has utilized a significant percentage of AM use in the recent years. So the industrial applications will mainly focus on aerospace, automotive and construction industries with some mention of the marine industry. Whereas the miscellaneous applications will focus on the ones left out and where 3D printing is still in the developing phase.

2.1 Medical Applications

The most prevalent use of additive manufacturing is found in the bio-medical sector. The process of 3D printing comes to rescue owing to the complex geometries involved. 3D printing has been used to print personalized medical devices and instruments. Another major use has been in dentistry and surgical planning. 3D printing has also been used to create artificial bone implants and orthotics that have proven to be successful. It is also used to design prosthetic limbs for amputees. Currently research is more focused towards bio printing and tissue engineering. This can prove to be a breakthrough in organ transplants and cancer research.

More and more medical devices are getting 3D printed because of the ongoing research in the field of additive manufacturing. The case of 3D printed hearing aids is a striking example. According to Phil Reeves, more than 10,000,000 hearing aids manufactured using 3D printing were in circulation in 2013. The number has only increased since then. Earlier hearing aids were produced with the help of manual labor, but with the advancement in technology the process has become fully automated. This has drastically shortened the time span of manufacturing a hearing aid from one week to one day [19]. The initiative of 3D printing applications was taken by a Belgian company, Materialize, along with a hearing aids manufacturer from Switzerland. They revolutionized the domain by developing RSM or Rapid Shell Modelling back in 2000. In 2005, EnvisionTec took the lead and developed its own process called Digital Shell Modelling (DSM). On the other hand, world's smallest aid was manufactured with CAMISHA (Computer Aided Manufacturing of Individual Shells for Hearing Aids) by a Danish company called Widex [42].

Another incredible 3D printed medical device is the cost efficient stethoscope which was developed to be used in Gaza Strip hospitals. Later a Polish company came up with the idea of Parsee glasses (see Fig. 3) that is designed to help blind people. The frame of the glass is 3D printed and is equipped with an IP camera, photo button and headphone. On clicking the button, a photo of the surroundings is captured, and the user hears information on text, shapes, colors and faces. 3D printing has also been used to manufacture medical instruments. Several surgical equipments have been fabricated this way and are being extensively used by surgeons across the globe [56]. Zortrax, a Polish company, 3D printed a 'winch' for Endo Venous

Fig. 3 A prototype of parsee glass [19]

Laser Therapy (EVLT) used in treatment of varicose veins. Recently, AM was used to create patient-specific surgical guide made from ABS using Fused Deposition Modelling during a mosaic-arthroplasty operation [53]. An SLS 3D printer was used to print resection guides from polyamide and it enabled the orthopedic surgeons for fast and precise procedures.

With the help of rapid tooling and rapid prototyping, additive manufacturing found its way into dentistry. Additive Manufacturing can create state of the art components thus making it a lucrative deal for orthodontists. 3D printing technology has changed drastically in the last five years. The research in biomaterials and developments in intraoral scanning led to successful restorations and orthodontic appliances [56].

Photo-polymerization and powder based printing are the most used techniques in dentistry. Photo-polymerization technology uses photosensitive resins reinforced with either ceramic fillers or metal to create physical models/surgical guides/orthodontic aligners/retainers/restorations. Photo-polymerization has various merits including quick manufacturing, good quality and polished texture. Though parts fabricated with this technology have weak mechanical properties and are temporary restorations [1]. Powder based technology includes SLS/SLM/DMLS/BJ and printing material like Stainless Steel, Co-Cr alloys and titanium alloys to make implants/crowns/denture frameworks. The polymeric material used in this technique is pigment filled polyamide powder which is used to create dental models [75].

Accuracy is the chief element in dentistry, which is difficult to achieve because of the reduced working area inside the patient's mouth and other physical constraints. The digital model and the printed construct should be very accurate given the construct fits into the patient's mouth as propositioned. After a series of tests and studies, the scientific community has started accepting 3D printed dental models [35].

It is difficult to foretell the future of AM in dentistry. We do not know whether 3D printing will replace its conventional counterparts or which technology will dominate the market. More clinical trials will be essential to certify the validity of dental devices.

Surgeries require planning and introducing 3D printing to it brings essential improvement. Imaging techniques like CT scan or MRI produce detailed images of internal organs. 3D printing is gaining popularity in anatomy with the advancement of AM technology. Due to handiness and cost effectiveness, 3D printing has become popular in craniomaxillofacial and cardiothoracic surgery. It is also being employed in spinal surgery, neurology, lung surgery, hepatobilary surgery, urology, vascular surgery, transplantation, tumor surgery, anesthesia and plastic surgery [56]. Fasotec, a Japanese company, developed a Bio- texture wet model that mimics organs on which surgeons can plan surgery and students can practice. Another example is of the 4 months old baby who got a kidney transplant. The size discrepancy between the child's abdomen and the adult donor's kidney was a huge challenge for the surgeons. Thus the child's abdomen and the donor kidney was 3D printed which allowed surgeons to be prepared for the surgery and locate the suturing site beforehand [9].

Several printing technologies are available to produce medical models. Different printing techniques offer different accuracy, stability, resolution and color. SLS [62,

Fig. 4 A 3D printed orthotic [19]

112] and SLA [12, 96] techniques generally produce single color models. FDM technique is less expensive but produces poor texture and resolution [17, 98]. Binder Jet technique produces multicolor prints which is helpful to highlight different regions of the model [43, 77]. MJM technique can incorporate variety of colors and texture to imitate soft/hard tissue [7, 20].

3D printing has escalated doctors' confidence as these 3D printed models have shown a very high success rate and also reduced the operating time. Also students experience better anatomical learning using AM models as compared to traditional models. However, there are many limitations associated with 3D printed anatomical models. Usually the models created are not suitable for dissection exercises as most bio-printable materials are brittle. Also the wall thickness and hole size for the models is constrained due to limitations caused by printing material and printing techniques, thus harming the accuracy of the model.

Orthotics are used for support & alignment whereas prosthetics are devices that restore the functions of missing limbs. In old times, people used to get heavy plaster casts which were dull and boring. Now people use 3D printed casts instead which are light and attractive as shown in Fig. 4. Many companies are producing 3D printed orthosis and several options are available in the market. The AM techniques employed are Selective Laser Sintering, Fused Deposition Modelling and Multi Jet Modelling and fabrication is done using polyamide, ABS, PP and PC [11]. Some examples include wrist splints, foot orthoses, robotic exoskeletons, prosthetic arms, hands and feet [56].

3D printed prosthetics are more cozy and take less time in manufacturing. 3D printed prosthetics are low cost which have led to a revolution in the prosthetics market. The hand prosthesis worth $80,000 was refined and repurposed to $500 by then high school student Easton LaChapelle [66] to help a poor little girl, who couldn't afford a prosthetic hand. The idea of inexpensive 3D printed prosthetics for landmine victims in Asia and Africa gave birth to the community of e-NABLE. The individuals of the community use AM for manufacturing free prosthetic limbs for amputees. Not Impossible Labs provides low cost 3D printing for war victims and poor amputees. Companies like Open Bionic have prosthetic limbs designed in Star Wars, Marvel and Disney Frozen theme for young amputees. 3D printed eye prosthetic is also a remarkable example. A heart touching case is the story of Eric

Monger, who recovered from face cancer and received a partly 3D printed prosthetic face [26].

Additive Manufacturing allows for inexpensive user-personalized implants. Implants like splints and fixators require proper surface properties and mechanical strength for optimal performance [87]. The benefit of 3D printing is that these implants can be made patient-specific concerning their size and shape as determined by the MRI and CT scans. 3D Slicer is an open-source software intended for 3D printing purposes. The software allows analyzing and visualizing medical images to carry out research.

Powder based 3D printing technology is the most favorable method as it offers high product quality. Thus SLS, SLM, EBM and BJ techniques are used with Co-Cr alloys, titanium alloys, ceramics, Polyether ether ketone (PEEK), and Ultra High Molecular Weight Poly Ethylene (UHMWPE) [18]. Lightweight implants with high mechanical strength are available from many companies.

In tracheobronchomalacia surgery, bioresorbable splints were printed by SLS technique to prevent tracheal collapse in three infants [69]. The splint allowed the airway to continue to grow and slowly disintegrated itself. In maxillo facial surgery, a BJ printer from ZCorp was used to create PEEK implants to rectify facial deformity [89]. In upper cervical reconstruction surgery, an axial vertebra was 3D printed from Titanium alloy by Electron Beam Melting [109]. A cranial implant was manufactured using 3D printing for a stroke patient [28]. It was made using biocompatible Titanium alloy and had a porosity of 95% which allowed fluids to pass through easily. Another application of 3D printed implants was in crippled animals. These implants gained more success than the human implants because of less stringent medical regulations for animals.

Bio-printing is a new trend in additive manufacturing. It means printing live tissue using cells as ink. This area aims at improving the current situation of organ transplantation. Before moving to bio-printing, we must understand tissue engineered scaffolds. Tissue engineering scaffolds lay out structural support to cells. Any scaffold should be biocompatible and mechanically strong with high porosity and permeability to allow diffusion of nutrients and wastes. It should also be biodegradable so that the scaffold is replaced with newly formed tissue [56].

Bio-printing is of two types: scaffold-based and scaffold-free. In scaffold-based method, cells are seeded into the scaffold and the main AM technologies used are Direct Ink Writing [5], Multi Jet Modelling [83, 110], vat polymerization [8, 67] and Laser Induced Forward Transfer [30, 83]. On the other hand, scaffold-free approach uses high density cell suspension and relies on cellular interchange for a period of maturation [63, 68].

Flat tissues such as skin, tubular structure like trachea or urethra [97] and hollow organs such as liver [103] have been 3D printed. Chinese researchers have reported the 3D bio printed kidneys, ears and livers [81] but they are not implantation ready. A Bio-pen which works like a bio-printer can be used directly to draw new cells into the bone to repair the damage in the middle of surgery. But bio-printing is still in its developing phase. 3D printed organs for implants are beyond our scope. They may come into existence after 20 years from now.

Tissue engineering majorly focuses on tissue development models and assessing drug toxicity. Engineered human tissue models have become popular for studying diseases and estimating the potency of new drugs [27, 41, 61, 76]. Traditional method requires extraction of diseased tissue from human body and engrafting into immunodeficient mice [86, 95]. This process is tedious and time consuming and above all requires mice for testing. Thus significant development has taken place to create animal-free in vitro models [22, 37].

The tumor microenvironment is extremely important to study tumor progression and metastasis. AM technologies like Laser Induced Forward Transfer [57, 84], droplet based [58, 79, 108], extrusion based [29, 117], vat photo-polymerization [40] can be used to create physiological models that mimic cancer microenvironment. Study showed that the structure and growth kinetics of micro-printed human ovarian cancer cells 'OVCAR-5' resembled that to the in body cancer cells [108]. Another hydrogel fiber model co-cultured with bio-printed 'MDA-MB 231' breast cancer cells and macrophages was developed to study interaction of cancer cells with the surroundings [29]. Despite the current efforts, the cancer microenvironment still needs multicellular systems including tumor cells, non-tumor cells, cells generated by immune response and vascular cells which are difficult to mimic using a 3D printer.

Liver is a highly sensitive organ and thus liver tissue engineering is a booming area in drug screening. In a study of drug metabolism, a liver micro organ model was bio-printed from hepatocytes encased in alignate [10]. There is great potential for evaluation of drug toxicity in simplified bio-printed liver tissue. Apart from these models, 3D printing is also used to develop skin tissue models. This led to the creation of 3D 'in vitro skin tissue' models [50, 55]. After the EU prohibited testing of cosmetics on animals in 2013, the cosmetic company L'Oreal is 3D printing skin models for cosmetic testing in collaboration with Organovo.

Over the past decade, additive manufacturing is being slowly accepted by the drug industry. 3D printed drugs require a sophisticated design for optimal performance [25]. Sprintam, a levetiracetam drug used against seizure disorder, produced and marketed by Aprecia Pharmaceuticals is the first 3D printed drug that has obtained FDA approval. The company's trademark 'ZipDose' technology creates solid yet highly porous tablets, resulting in superior disintegration characteristics of the tablets [65]. 3D printing allows tablets to be printed in complex shapes with tuned drug release kinetics. Also 3D printed drugs can be personalized based on patient's particulars and medical history as opposed to traditional drugs [80].

The various techniques used for drug manufacturing are Multi Jet Modelling, Binder Jet, Direct Ink Writing and Fused Deposition Modelling. In BJ process, the drug is contained in either the powder bed or the liquid binder. Complex designs like core–shell [104], layered [114], multi-compartment [85], porosity gradient [115] have been achieved on changing the printing parameters. But this approach has many limitations. The printed drug takes very long time to dry and the printing process might contaminate the drug or downgrade its performance. With FDM technique, we can achieve good quality and strength but the drug might get deteriorated due to

excess heat from printing. To avoid this, Direct Ink Writing technique can be used which uses pressure from a nozzle to extrude instead of heat [2].

On the other hand, 3D printing drugs from appropriate 3D printers using downloadable pharmaceutical recipes will lead to a disruption in the current pharmaceutical industry. Also availability of 3D printers will lead to the possibility of drug abuse. These are some serious legal problems 3D printing can cause [19].

2.2 Industrial Applications

Additive manufacturing has paved its way into the industry due to its fast fabrication, accuracy and precision. The two major industries that have abundantly accepted AM are the aerospace and automotive industries. The aerospace industry uses it for two purposes. First, for manufacturing components and second for repairing damaged components. The automotive industry mostly uses AM for fabrication of small parts for the gas engine assembly. Also a great amount of research is currently being invested upon the use of AM in the construction industry. Even 3D printed houses have been developed and new printing techniques are being inspected. AM has also found little use in the marine industry, but it is expected to grow in the coming years.

Additive manufacturing has started to gain acceptance in the aerospace industry. It has significant impact on the design, material and fabrication methods involved in the industry. Aerospace components have complex geometries and are difficult to manufacture. High performance alloys like Ti6Al4V, Inconel 625, and GRCorp-84 are used for aerospace applications. The 3D printed alloys have marginally better mechanical properties than standard material [111]. They are highly expensive and thus wastage has to be minimized. A way to measure the degree of wastage is the buy to fly ratio. It is defined as the ratio of the mass of material required to manufacture a part to the mass of the final product that flies. Using traditional subtractive manufacturing processes, this ratio can be as high as 20:1. With the help of tool less additive manufacturing, the buy to fly ratio approaches one [38]. AM can also be used to manufacture open cell foams (see Fig. 5) and porous mesh arrays with varying density and stiffness. Apart from metals and alloys, the aerospace industry also requires ceramics. Ultra High Temperature Ceramics (UHTC) like Zirconium Diboride and Zirconium Carbide can tolerate temperatures as high as 2000 °C. Because of the extremely brittle nature of UHTC materials, traditional methods like drilling and mining fail. Thus 3D printing is a promising technology in the aerospace industry.

Additive manufacturing finds its use in aircrafts, space, missiles, engine/turbine systems that require alloys. Optomec used the Laser Engineered Net Shaping process to fabricate a miniature model of a gas turbine exhaust. Arcam applied its Electron Beam Melting system to produce a titanium alloy compressor support case. Investment casting can be used for creating small, accurate castings in refractory alloys using mold formed around wax which can be melted. This was used for creating turbine blades using ceramic SLA [3] or by gel casting ceramic slurry into plastic molds [106]. Wind tunnel testing models of aircrafts, airfoils, etc. have also been

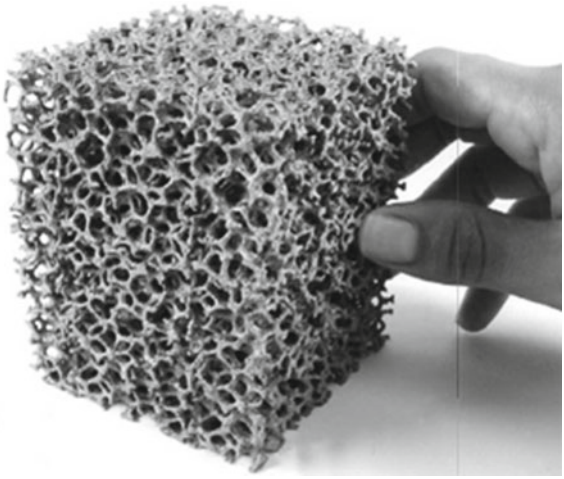

Fig. 5 Titanium alloy open cell foam [71]

fabricated using 3D printing. SLS technology was used to build a flight-model with glass-reinforced nylon to study aerodynamic characteristics [16]. UHTC material can be blended with a heat resistant metal and applied to Mach 5 jets or nose of aircrafts and missiles that undergo immense heat during operation. Also 3D printing has been used to produce plastic parts such as vents and ducts. Flame retardant polymers like PEEK are being developed to bring into use in the aerospace industry.

Besides fabrication, Additive Manufacturing is used in repairing aircraft engine parts to extend the life of the product and minimize the overall cost. A damaged IN738 blade was repaired using LMD technique [111]. Richter et al. [82] studied the physical/mechanical properties of a repaired Ti6-2–4-2 blade. Optomec has successfully used LENS technique to repair parts used in gas turbine engine like vanes, stators, seals and rotors and other complex geometries like airfoils, blisks, ducts and diffusers [36, 70].

However, AM development has been slow-paced in the aerospace industry because quality certification is necessary before commercial use. Understanding of fatigue and aging in AM alloys is really important as these parts will be subjected to harsh environment. A lot of testing and certification is carried out on 3D printed aircraft parts to build a certain level of confidence. Yet, they are not suited as load bearing structures and are restricted to nonstructural and non- critical use only.

One of the most prolific applications of additive manufacturing in the automotive world is rapid prototyping. It is used for prototyping as well as mass production. AM has proved to be an integral part of automotive industry. AM has brought wonders to the automotive industry by allowing lighter and intricate structures at best possible cost. Material wastage can be significantly reduced with the use of additive manufacturing. Also it makes possible to create internal complexities and precisely control microstructure. The engine compartment temperatures are extremely high thus the 3D printed parts should be able to withstand heat deflections. SLS nylon and some photo-cured polymers are suitable for high temperature applications. Automobile

components should be moisture resistant. With proper post processing, AM parts can be created to be water-tight and moisture resistant. Another advantage of AM in the automotive industry is part consolidation. With the help of part consolidation, smaller parts can be integrated into a big complex part thereby reducing the net weight of the assembly [88].

CRP Technology [21] has applied AM techniques including SLM, SLS and EBM to produce various components for motorsports. Optomec used LENS technique to produce suspension mounting brackets and drive shaft spider for a Red Bull Racing car. Arcam used EBM technique to produce Ti6Al4V components like gearboxes, suspension/engine parts. Concept Laser used SLM technique to produce steel and Aluminum car components. Prometal developed engine components using its own 3D printing technique called 'Prometal' process. Studies show that AM produced parts, in this case a water pump for motorsports car, have mechanical properties equivalent to traditionally manufactured parts. AM technology can be used to produce parts with properties that were previously unattainable. For instance, an open-cell structure will lessen the engine's weight as well boost its stiffness hence improving fuel efficiency and engine life. Additive manufacturing has greatly benefitted the automotive industry [32].

AM is not yet able to completely replace the traditional techniques. There are several limitations and challenges associated with the production techniques and materials used. The automotive industry relies on mass production. Thus for AM to expand, they have to overcome the challenge of limited production volume. Parts made with AM have voids or pores which weaken the overall strength. Sometimes the dimensional accuracy of the printed product is not on par with the CAD or STL file of the same. Constant research is being done to improve product quality and tackle the production problems. Another limitation of AM is the restricted build size. For creating large parts, individual small parts are created first and then assembled together. However, new methods like Big Area Additive Manufacturing (BAAM) and Wire Arc Additive Manufacturing (WAAM) are being investigated for greater build size of printers [88].

Additive manufacturing technology has been expanded into the construction industry. According to Wohler's report, architectural applications account for only 3% of AM applications [73] which shows that it is still in an infancy stage. Contour crafting is a new printing technique developed specifically for buildings. It is similar to inkjet printing except it uses large nozzles and pressure for extruding thick mortar. A trowel like apparatus is attached to the printer to obtain even and flat surfaces [47]. The use of AM for residential structures started in 2014. Automated building construction has gained increasing attention since then. 3D printing can be helpful in difficult conformations and structures with cavities. It has the potential to revolutionize the construction industry as it offers easier construction and reduced time and manpower [107].

Properties of fresh concrete greatly influence the printing process. A mix has to be designed which is workable before setting but also has sufficient early strength to hold up succeeding layers and resist shear. This can be achieved through well designed equipment and material. Gosselin et al. [24] developed a printing process that pumps

the accelerator and mortar in different tubes which are combined at the printhead before extrusion. A study found out that rheological properties of concrete like the time dependent shear thinning seriously affect the printing process [78]. A high performance polypropylene fiber reinforced mortar was developed using Ordinary Portland Concrete, aggregate, silica and flyash [54]. The advantage with 3D printed fiber reinforced concrete composite is that fibers can be oriented in a particular direction unlike the random positioning of fibers in traditional fiber reinforced concrete. Flexural strength can be increased by up to 30 MPa while printing fibers parallel to the XY-plane [34]. Another important parameter for concrete structures is the inter-layer adhesion. A study showed that smaller MSA and higher cement/aggregate ratio had better inter-layer bonding and thus greater strength [116]. Powder bed fusion method has also been investigated for additive manufacturing of concrete. OPC mixed with $CaAl_2O_4$ as the powder bed was used with Li_2CO_3 mixed with water as binder to obtain compression strength of nearly 8 MPa, porosity close to 0.5 and limited hydration [93].

Additive manufacturing has the ability to fabricate complex designs with high precision. It can be used for low income housing or in areas where construction is restricted due to geometric constraints. In 2014, the first house was fabricated using AM in Amsterdam by DUSArchitects using FDM technique. In the same year, a Chinese firm named WinSun manufactured residential structures in Shanghai in less than a day [107]. They used a large build 3D printer with dimensions (in m) $150 \times 10 \times 6.6$.

Contour crafting (CC) is the most feasible AM technique for building construction. It is capable of onsite printing enabling larger component manufacturing with no boundations. Another technique is the D-shape method which utilizes powder deposition process in which a chemical agent is used to bind the powder. It can be potentially used for in-situ space applications like building infrastructure on moon using lunar soil. Lough borough University came up with another developing technique called mesh molding which does not require short-term support. It utilizes thermoplastic polymers that act as reinforcement for concrete. There is also the option of varying the mesh-density as per load bearing requirements [73].

Challenges involved with 3D printing of wet concrete include controlling the fresh properties as well as structural properties. Shape-stability is another important parameter. The 3D printed shapes must resist settlement and deformation due to successive layers. One obstacle of using AM in construction is the inadequacy of support/scaffolding. Absence of formwork exposes the structure to open atmosphere which can cause shrinkage and cracking. Thus 3D printed structures should be inspected and provided with great care. Another hurdle is the lack of skilled workers who can handle AM technology in civil works. The construction industry consumes one-third of the earth's resources. Considering the environmental impact, efficient techniques and economic strategies are of primary importance. AM technology has a bright future in the construction industry as it has the potential to improve the traditional methods and with profound research it is expected to grow quickly.

The use of AM in marine industry is very limited. Marine environment offers harsh and corrosive conditions like salinity, alkalinity and exposure to air and water.

Marine industry requires the use of complex and large components that operate in this kind of environment. Also these parts are integrated along with other parts into a complex assembly and should be able to sustain dynamic loading profiles. US Navy has deployed 3D printers for afloat manufacturing of spare parts [46]. Some US Navy activities are underway to inspect the quality of parts and their effectiveness [64]. The marine industry is still new to AM and may take some time to accept the 3D printing technology like the aerospace and automotive industries.

Additive manufacturing has grown rapidly considering the relatively short period of time. However, applicability into marine industry has been limited. It still has a tremendous potential for discrete applications of the technology within the major subsystems of a ship/vessel. The most promising areas are in manufacturing of spare parts and agile tooling. All AM techniques rely on gravity to assist the printing process. Many improvements in the technology are needed given the non-static environment on a ship/vessel for hassle free offshore printing. In totality, mass acceptance and utilization of AM into the marine industry is still a long way ahead [99].

2.3 Miscellaneous Applications

3D printing has been used extensively these days for research purposes. Most research institutes usually own a 3D printer for creating prototypes. It makes fabrication of complex geometries easier. For example, it is practically impossible to create a hollow structure using subtractive manufacturing. But using additive manufacturing this can be achieved with ease. In 2012, University of Glassgow, UK used FDM process to print chemical reaction vessels and then used the printer to deposit reactants into them [101]. The 3D printed vessels need to be air and water-tight because they might develop reactive substances inside even when printed in an inert atmosphere. Also most research labs have adopted 3D printing as an alternative to manufacture components for use in experiments.

Apart from research, 3D printing has also entered the classrooms for better teaching experience. Global accessibility and user friendliness of 3D printers have led to a great demand in the market worldwide. Low cost and easy to assemble 3D printers are available on leading e-commerce websites like Amazon, etc. Unlike the expensive subtractive manufacturing techniques, 3D printing enables students to create their own prototypes at much lower cost. Teachers can use 3D printed prototypes to explain organs in human biology or show the chemical structure of molecules. It can also be used for teaching students about topographic maps [39].

3D printing has played a significant role in the field of research and education. Low cost and fast manufacturing are the most important benefits of using 3D printing in research. Specimens can be fabricated quickly and experimented upon to produce fast results. 3D printing is said to enhance the learning process in students and provide better understanding of concepts. However not many schools have adapted to this style of teaching as most schools don't usually have a 3D printer. But these limitations

are not long-term. With the current rate of growth, 3D printing is expected to boom in this area as well.

One of the most important socio-cultural applications of 3D printing is in the art and jewelry sector. 3D printing can be used for making molds for jewelry involving delicate work or when contact with the molding substance may harm the integrity of the artifact. However, with the advancement of 3D scanning technology, replication of real objects has become easier without involving molding techniques which are very expensive as well as invasive. In 2015, MIT developed a 3D printer that prints with glass [49].

Also 3D printing has changed clothing and fashion. The most common printing technique used is FDM and materials like ABS or TPU is preferred. Dresses, bikinis, shoes as well as complete outfits have been 3D printed. Dutch fashion designer Iris Van Herpen has even introduced 3D printing on fashion runways of Amsterdam Fashion Week and Paris Haute Couture Week [51]. Nike used 3D printing for commercial production of 2012 Vapor Laser Talon football shoes for American footballers. New Balance, an American sports footwear manufacturer, is 3D printing custom-fit shoes for athletes [105]. Some companies are also printing custom designed eyewear on demand of the customers. Frames, without glasses, have been 3D printed [15].

Despite so many applications, people have not completely accepted 3D printed apparel as an alternative for traditional clothing. 3D printed clothes are heavier than usual fabric material and may cause discomfort to the wearer. Also these clothes are very delicate and take up considerable time in putting on [48]. But 3D printed artistic items and jewelry have really won people's hearts. It is highly possibile that people will incline more and more towards 3D printing for clothing in the coming years.

Soft sensors are working software where several measurements are processed together. They are mostly based on control theory. They use interaction of signals to measure hundreds of quantities and filter out those which are not required. On the other hand, actuators are components that are responsible for movement in a machine or system. Actuators require a source of energy and a control signal. Once it receives a low energy control signal, it converts the energy from a high energy source into mechanical work thus causing movement.

The traditional soft-sensors and actuators are manufactured from less efficient processes. With 3D printing, customization and reproducibility is possible. Also the manual work can be eliminated to avoid lengthy and time-consuming process. The concept of 4D printing has led to the development of soft, lightweight and biocompatible soft sensors and actuators [74, 102]. This is largely used in robotics to mimic human gait (see Fig. 6). Shape Memory Polymer (SMP) actuators respond to the stimuli very similar to human muscles [113] due to which open-source robots are built using 3D printing. A 3D printed wheeled robot and a 3D printed humanoid are just a few examples.

3D printing firearms is strictly illegal as they must be licensed by the authorities before owning. This application portrays 3D printing as a liability instead of an asset as it gives people the freedom to print anything they want, be it a utility box or a small hand grenade.

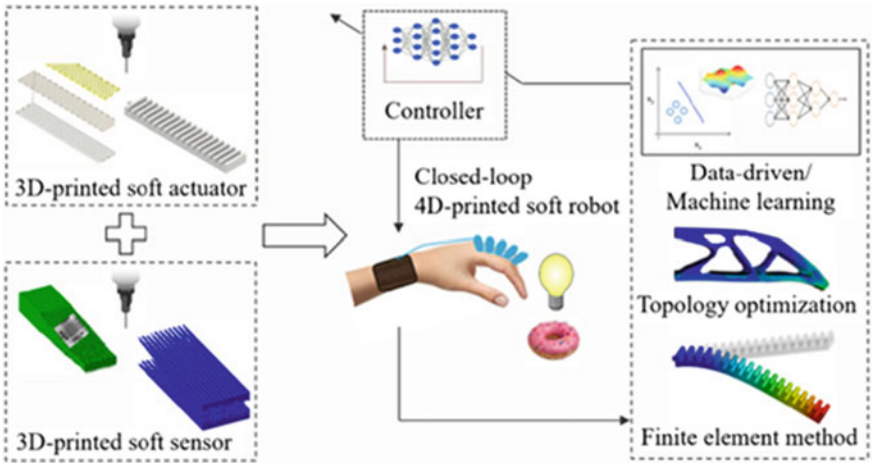

Fig. 6 Use of soft sensors and actuators in soft robotics [118]

In 2012, an American organization called Defense Distributed uploaded plans for a working gun. In 2013, they also released a blueprint for a gun "Liberator" which was later removed on orders of the United States Department of State. The gun was made completely with plastic except the metal firing pin. It was originally printed on a Stratasys uPrint SE FDM printer using ABS plastic. It was confirmed that the gun was a potentially lethal firearm and could also cause catastrophic failure injuring the user. In 2013, Solid Concepts Inc. 1911 used DMLS technology to print a Colt Government Model 1911 pistol. The grip panels were manufactured from carbon filled nylon powder using SLS [31]. Also 3D printing can be used to manufacture firearm components and accessories like the 3D printable AR-15 type rifle lower receiver designed by Defense Distributed [44].

The growth of AM in firearms is only possible with intervention from the concerned authorities. Firearms manufacturing should be regulated. Every 3D printed firearm must be marked and kept in government record for future tracing. This is supported by the fact that high end manufacturing particularly SLS and DMLS are very expensive for individuals. Therefore only authorized and legitimate manufacturers will be able to fabricate firearms. Also research is being carried out to develop materials that can endure the heat and pressure from the operation of a firearm [44].

The trend of selfies began in the last decade. With ever increasing popularity of 3D printing, a new aspect of selfie, called a 3D selfie, has been discovered. A 3D selfie is a 3D printed scale replica of a person. However, getting a 3D selfie is not as easy as a normal selfie. For printing a 3D selfie, a 3D model needs to be developed first. For this we use photogrammetry, i.e., making precise measurements from a photo or set of photos. One way is to click pictures from different heights and all the angles which can be used to reconstruct a 3D model with the help of a software [23]. Another way could be to use a vertical bar of cameras that rotate around the subject or special 3D scanning equipment [92] which will be able to capture more details.

To get sandstone like texture and look, gypsum based binder jetting techniques are used.

Cultural Heritage is one field where 3D printing has brought a paradigm shift. 3D printing is now being used for preservation, restoration and dissemination purposes of museum artifacts [91]. Rapid improvement in visualization technology has caused this change. 3D printed models are useful in studying artwork, documentation for onsite archaeology, restoration of fragmented artwork and virtual restoration of painted decorations. The famous and beautiful statue of Pietranico Madonna was damaged after the 2009 earthquake. With the help of digital reconstruction, the statue was reassembled by adding broken fragments to the fill components made using 3D printing [90]. In another case, with the help of scanning technology and 3D graphics, researchers were able to digitally reconstruct a king's head using only bones collected from a car park [6]. Also 3D printed models could be shown to visitors up close for getting a better view of what the actual artifact looks like. In fact, British Museum has started 3D printing souvenirs which can be bought by the visitors at the museum shop.

Innovation in improving the texture and print quality of 3D selfies or museum artifacts is of prime importance. This is possible with the development of advance photography techniques. One such technique is Tactile Photography which is based on photogrammetry and digital spectroscopy. With this technique, we can capture color as well as the plasticity and surface properties. This technique is even able to produce 3D models of non-stationary objects and produces superior quality prints [72]. More such techniques are being investigated to improve print quality.

Additive Manufacturing has entered the food industry with great potential. But it is restricted to limited applications. The first 3D printer was designed more than 10 years ago. 3D food printing allows users to design and fabricate food with customized color, shape, flavor and texture. Food printing can be divided on the basis of material used for printing. Natively printable materials can be extruded smoothly from a syringe. The examples would be cake frosting, cheese, special dough and chocolate [13]. Most food items printed this way can retain their shape or can be post processed [60] like steamed/baked/fried to retain their shape. Food like rice, meat, fruit and vegetables which are consumed daily are not printable in nature. Adding hydrocolloids can enhance their extrudability. Another solution could be to use a gastronomic trick by separating a group of ingredients that have a high degree of freedom on flavor and texture. These traditional foods usually require post-deposition cooking to retain their shape [100].

The 'Fab@Home I' 3D printer was launched in 2006. It was the first 3D printer capable of printing food like chocolate-frosting. Customization in bakery products is said to directly relate with consumer satisfaction and hence more inclination towards 3D printed products. PIQ chocolates sell chocolates custom designed for the customers. Another application in food printing is pizza replication (see Fig. 7). A customized pizza was printed using a 3D printer where each component (dough/sauce/cheese) was added in subsequent layers. Also additive manufacturing allows us to control food texture with voids inside. A dense dough was 3D printed

Fig. 7 A custom shaped pizza being 3D printed [59]

and its structure was highly porous. The added porosity helped it in complete frying both from outside as well as inside [59].

The future of 3D printing in food industry is very bright. It allows users to print food customized to their dietary needs. This can be used to monitor food intake in old people and expecting mothers. But personalized nutrition comes with additional cost. It will not be financially viable for individual users to personalize their daily food requirements. Seeing the growth of population, it is also an attractive option to produce food using 3D printing for a sustainable future [100]. Another possible use could be 3D printing food in space to minimize wastage and maximize resource usage. However, there are still a lot of challenges that need to be encountered. For example, the speed of printing is so slow that it is not fit for everyday cooking purposes. Also the food has to be ensured as 'safe to consume' because there shall be a chance of contamination during the printing process. These limitations will be resolved in the coming years as 3D printing will grow.

3 Additive Manufacturing—A New Approach for Composite Materials

Composite materials are formed by combining two or more different materials to obtain a new material with entirely different properties. Most composites are made up of only two materials. One component is called the matrix (usually the one in abundance) or the binder which holds together the fragments of the other component called the reinforcement. Some common examples of composite materials are reinforced concrete, polymer matrix composites (PMC), ceramic matrix composites (CMC), metal matrix composites (MMC). Composites are used excessively these days in aircrafts, automobile bodies, buildings and bridges.

Composites are preferred because they are light weight, inexpensive and have better mechanical properties. They can be manufactured using a variety of techniques which involve wetting/mixing/saturating the reinforcement with the matrix and then using heat or pressure to bind them together. The drawback of these techniques is that we cannot pre-set the reinforcement position and orientation. The reinforcement is bound arbitrarily with the matrix which often results in diminished properties than expected. But with Additive Manufacturing, this problem can be eliminated. 3D printers are capable to print using different materials at the same time and the user can define the material properties in the STL file so that the printer will know where to fill matrix and where to fill reinforcement.

Additive Manufacturing has the potential to completely transform and restructure the composites industry. However, only a few sectors have ventured into the idea of 3D printing composites. The majority uses of AM composites are in the aerospace and biomedical industry. Ceramic composites of the type C/C, C/SiC, SiC/SiC have high strength, heat resistance, low density and abrasion stability. Due to this, they are used for making gas turbines, diesel engines and heat exchangers for aviation industry [45]. In the biomedical industry, polymer-ceramic composites have been used to manufacture scaffolds and bone implants due to their biocompatible and bioresorbable nature [52]. Also Titanium Nickelide (TiNi) and Hydroxylapatite (HA) have been used to make a biocomposite material suitable for manufacturing bone implants [94].

Some minor applications are in the field of automotive and construction industry as well, but there the composites are manufactured using the traditional way mostly. With advancement in printing technologies and development of new composite materials, the applicability of AM composites is expected to grow fast.

4 Conclusions and Future Perspective

In this chapter, we learnt about the various applications of 3D printing in different sectors. In the recent years, 3D printing has become omnipresent. It has variety of remarkable applications ranging from manufacturing a life saving medical implant for a patient to designing 3D printed clothes for fashion models. Though 3D printing cannot be seen as a complete replacement for traditional methods yet it continues to grow because of its added benefits over subtractive manufacturing. Table 1 [73] summarizes the various AM applications, materials used and benefits.

Additive Manufacturing is a booming domain with a lot of scope and opportunities. With more and more research, 3D printing has been adopted more into the industry as well as the household. However, its applicability is restricted due to various limitations caused during the printing process.

Some of the most common challenges associated with 3D printing are mentioned below:

- Inability to produce large components due to size limitations

Table 1 Materials, applications and benefits of AM

Material	Applications	Benefits
Metals Alloys	Biomedical Aerospace Automotive	Mass customization Less wastage of material Fewer assembly components
Polymers Composites	Biomedical Aerospace Automotive Architecture Toys	Fast prototyping Complex structures Mass customization Cost effective
Ceramics	Aerospace Automotive Biomedical Chemical Industries	Porous lattice Reduced fabrication time Controlled composition and microstructure
Concrete	Infrastructure Construction	No formwork required Less labor

- Not suitable for bulk industrial production due to slow printing speed
- Limited choice of printing materials and high costs
- Lack of printers that can print objects using different materials
- Quality consistency issues due to heat involved in printing process.

All these limitations can be resolved with intensive multi-disciplinary research. A lot of work is being done to develop large build 3D printers. Also limited choice of materials can be expanded with advances in material science technology. Other researches are focused on increasing the efficiency and printing speed while dealing with heating issues. The most important aspect of 3D printing is the print quality. New techniques and methods are being developed that produce superior print quality, strength and resistance to heat and moisture.

The global impact of 3D printing has been largely positive due to which it has been dubbed as “the new industrial revolution”. According to Wohlers Associates, it is expected to hold a market share of $10.8 billion by the end of 2020 [14]. The future outlook of 3D printing is very appealing and successful. Since 3D printed objects are printed on specific demand, there would be no risk of having unsold products. Also with the venture of 3D printing in household, people shall be able to buy designs of parts and print them at home. This will lead to a decrease in price of those parts. The increasing use of 3D printing will also lead to a heightened number of CAD-CAM applications as 3D model designing is the first step of AM process. Overall, 3D printing is believed to skyrocket through the coming years for individuals as well as the industry [4].

References

1. Abdulmohsen B, Parker S, Braden M, Patel MP (2016) A study to investigate and compare the physicomechanical properties of experimental and commercial temporary crown and bridge materials. Dent Mater 32(2):200–210. https://doi.org/10.1016/j.dental.2015.11.025
2. Alhnan MA, Okwuosa TC, Sadia M, Wan K-W, Ahmed W, Arafat B (2016) Emergence of 3D printed dosage forms: opportunities and challenges. Pharm Res 33(8):1817–1832. https://doi.org/10.1007/s11095-016-1933-1
3. Bae CJ (2008) "Integrally cored ceramic investment casting mold fabricated by ceramic stereo lithography," p 228
4. Berman B (2012) 3-D printing: the new industrial revolution. Bus Horiz 55(2):155–162. https://doi.org/10.1016/j.bushor.2011.11.003
5. Billiet T, Gevaert E, De Schryver T, Cornelissen M, Dubruel P (2014) The 3D printing of gelatin methacrylamide cell-laden tissue-engineered constructs with high cell viability. Biomaterials 35(1):49–62. https://doi.org/10.1016/j.biomaterials.2013.09.078
6. Buckley R, Morris M, Appleby Jo, King T, O'Sullivan D, Foxhall L (2013) 'The king in the car park': new light on the death and burial of richard III in the Grey Friars Church, Leicester, in 1485. Antiquity 87(336):519–538. https://doi.org/10.1017/S0003598X00049103
7. Bustamante S, Bose S, Bishop P, Klatte R, Norris F (2014) Novel application of rapid prototyping for simulation of bronchoscopic anatomy. J Cardiothorac Vasc Anesth 28(4):1122–1125. https://doi.org/10.1053/j.jvca.2013.08.015
8. Chan V, Zorlutuna P, Jeong JH, Kong H, Bashir R (2010) Three-dimensional photopatterning of hydrogels using stereolithography for long-term cell encapsulation. Lab Chip 10(16):2062. https://doi.org/10.1039/c004285d
9. Chandak P (2017) "Using 3D printing for complex pediatric transplantation: an interview with Pankaj Chandak." J 3D Print Med 1(1): 9–12. https://doi.org/10.2217/3dp-2016-0012
10. Chang R, Nam J, Sun W (2008) Direct cell writing of 3D microorgan for *In Vitro* pharmacokinetic model. Tissue Eng Part C Methods 14(2):157–166. https://doi.org/10.1089/ten.tec.2007.0392
11. Chen RK, Jin Y-a, Wensman J, Shih A (2016) Additive manufacturing of custom orthoses and prostheses—a review. Addit Manuf 12(October):77–89. https://doi.org/10.1016/j.addma.2016.04.002
12. Cohen A, Laviv A, Berman P, Nashef R, Abu-Tair J (2009) Mandibular reconstruction using stereolithographic 3-dimensional printing modeling technology. Oral Surg Oral Med Oral Pathol Oral Radiol Endodontol 108(5):661–666. https://doi.org/10.1016/j.tripleo.2009.05.023
13. Cohen DL, Lipton JI, Cutler M, Coulter D, Vesco A, Lipson H (2016) Hydrocolloid printing: a novel platform for customized food production
14. Cotteleer, Mark J (2014) "3D opportunity: additive manufacturing paths to performance, innovation, and growth," 23
15. "Custom Eyewear: The Next Focal Point For 3D Printing?" (2016). Accessed 16 July 2020. https://www.forbes.com/sites/rakeshsharma/2013/09/10/custom-eyewear-the-next-focal-point-for-3d-printing/#39009f17ed79
16. Daneshmand S, Adelnia R, Aghanajafi S (2006) Design and production of wind tunnel testing models with selective laser sintering technology using glass-reinforced nylon. Mater Sci Forum 532–533(December):653–656. https://doi.org/10.4028/www.scientific.net/MSF.532-533.653
17. Dhakshyani R, Nukman Y, Abu Osman NA (2012) Rapid prototyping models for dysplastic hip surgeries in Malaysia. Eur J Orthop Surg Traumatol 22(1):41–46. https://doi.org/10.1007/s00590-011-0778-x
18. Dion NT, Bragdon C, Muratoglu O, Freiberg AA (2015) Durability of highly cross-linked polyethylene in total hip and total knee arthroplasty. Orthop Clin North Am 46(3):321–327. https://doi.org/10.1016/j.ocl.2015.02.001

19. Dodziuk H (2016) Applications of 3D printing in healthcare. Polish J Cardio-Thoracic Surg 3:283–293. https://doi.org/10.5114/kitp.2016.62625
20. Esses SJ, Berman P, Bloom AI, Sosna J (2011) Clinical applications of physical 3D models derived from mdct data and created by rapid prototyping. Am J Roentgenol 196(6):W683–W688. https://doi.org/10.2214/AJR.10.5681
21. Ferri JK (2016) "CRP Technology." 3D Printing Company. CRP Technology. Accessed 28 June 2020. https://www.crptechnology.com/
22. Fischbach C, Chen R, Matsumoto T, Schmelzle T, Brugge JS, Polverini PJ, Mooney DJ (2007) Engineering tumors with 3D scaffolds. Nat Methods 4(10):855–860. https://doi.org/10.1038/nmeth1085
23. Garsthagen R (2014) "An open source, low-cost, multi camera full-body 3D scanner." In Proceedings of the 5th international conference on 3D Body scanning technologies, Lugano, Switzerland, 21–22 October 2014, pp 174–83. Lugano, Switzerland: Hometrica Consulting—Dr. Nicola D'Apuzzo. https://doi.org/10.15221/14.174
24. Gosselin C, Duballet R, Roux Ph, Gaudillière N, Dirrenberger J, Morel Ph (2016) Large-scale 3D printing of ultra-high performance concrete—a new processing route for architects and builders. Mater Des 100(June):102–109. https://doi.org/10.1016/j.matdes.2016.03.097
25. Goyanes A, Martinez PR, Buanz A, Basit AW, Gaisford S (2015) Effect of Geometry on Drug Release from 3D Printed Tablets. Int J Pharm 494(2):657–663. https://doi.org/10.1016/j.ijpharm.2015.04.069
26. Gray R (2013) "How doctors printed my new face," March 31, 2013, sec. News. https://www.telegraph.co.uk/news/9962798/How-doctors-printed-my-new-face.html
27. Griffith LG, Swartz MA (2006) Capturing complex 3D tissue physiology in Vitro. Nat Rev Mol Cell Biol 7(3):211–224. https://doi.org/10.1038/nrm1858
28. Griffiths L (2015) "Stroke patient gets life back with 3D printed cranial implant from EOS." TCT Magazine. May 12, 2015. https://www.tctmagazine.com/api/content/b67e5ac8-f88c-11e4-82c9-22000b078648/
29. Grolman JM, Zhang D, Smith AM, Moore JS, Kilian KA (2015) Rapid 3D extrusion of synthetic tumor microenvironments. Adv Mater 27(37):5512–5517. https://doi.org/10.1002/adma.201501729
30. Guillemot F, Souquet A, Catros S, Guillotin B, Lopez J, Faucon M, Pippenger B et al (2010) High-throughput laser printing of cells and biomaterials for tissue engineering. Acta Biomater 6(7):2494–2500. https://doi.org/10.1016/j.actbio.2009.09.029
31. "Gun Review: Solid Concepts 1911 DMLS" (2013) The truth about guns. 10 Dec 2013. https://www.thetruthaboutguns.com/gun-review-solid-concepts-1911-dmls-direct-metal-laser-sintering/
32. Guo N, Leu MC (2013) Additive manufacturing: technology, applications and research needs. Front Mech Eng 8(3):215–243. https://doi.org/10.1007/s11465-013-0248-8
33. Gupta MK, Song Q, Liu Z, Sarikaya M, Jamil M, Mia M, Kushvaha V, Singla AK, Li Z (2020) Ecological, economical and technological perspectives based sustainability assessment in hybrid-cooling assisted machining of Ti-6Al-4 V alloy. Sustain Mater Technol 26:e00218
34. Hambach M, Volkmer D (2017) Properties of 3D-printed fiber-reinforced portland cement paste. Cement Concr Compos 79(May):62–70. https://doi.org/10.1016/j.cemconcomp.2017.02.001
35. Hazeveld A, Slater JJRH, Ren Y (2014) Accuracy and reproducibility of dental replica models reconstructed by different rapid prototyping techniques. Am J Orthod Dentofac Orthop 145(1):108–115. https://doi.org/10.1016/j.ajodo.2013.05.011
36. Hedges M, Calder NC (2006) "Near net shape rapid manufacture & repair by LENS (Registered Trademark)." In
37. Hickman JA, Graeser R, Hoogt de R, Vidic S, Brito C, Gutekunst M, Kuip van der H, IMI PREDECT consortium (2014) "Three-dimensional models of cancer for pharmacology and cancer cell biology: capturing tumor complexity in Vitro/Ex Vivo." Biotech J 9(9):1115–28. https://doi.org/10.1002/biot.201300492

38. Horn TJ, Harrysson OLA (2012) Overview of current additive manufacturing technologies and selected applications. Sci Prog 95(3):255–282. https://doi.org/10.3184/003685012X13420984463047
39. Horowitz SS, Schultz PH (2014) Printing space: using 3D printing of digital terrain models in geosciences education and research. J Geosci Educ 62(1):138–145. https://doi.org/10.5408/13-031.1
40. Huang TQ, Xin Qu, Liu J, Chen S (2014) 3D printing of biomimetic microstructures for cancer cell migration. Biomed Microdevice 16(1):127–132. https://doi.org/10.1007/s10544-013-9812-6
41. Hutmacher DW, Loessner D, Rizzi S, Kaplan DL, Mooney DJ, Clements JA (2010) Can tissue engineering concepts advance tumor biology research? Trends Biotechnol 28(3):125–133. https://doi.org/10.1016/j.tibtech.2009.12.001
42. "Invisible-in-Canal Hearing Aids (IIC)." 2016 Accessed 21 June 2020. http://webfiles.widex.com/en/products/hearingaidtypes/iic/
43. Jardini AL, Larosa MA, Maciel Filho R, de Carvalho Zavaglia CA, Bernardes LF, Lambert CS, Calderoni DR, Kharmandayan P (2014) "Cranial reconstruction: 3D biomodel and custom-built implant created using additive manufacturing." J Cranio-Maxillofac Surg 42(8):1877–84.https://doi.org/10.1016/j.jcms.2014.07.006
44. Jenzen-Jones NR (2015) "Small arms and additive manufacturing: an assessment of 3D-printed firearms, components, and accessories." Behind the Curve. Small Arms Survey. JSTOR. https://www.jstor.org/stable/resrep10742.10.
45. Katz-Demyanetz A, Popov VV, Kovalevsky A, Safranchik D, Koptyug A (2019) "Powder-bed additive manufacturing for aerospace application: techniques, metallic and metal/ceramic composite materials and trends." Piticescu R, Vlaicu I (ed) Manufacturing review 6:5. https://doi.org/10.1051/mfreview/2019003.
46. Kenney, Michael E (2013) "Cost reduction through the use of additive manufacturing (3D printing) and collaborative product life cycle management technologies to enhance the navy's maintenance programs." In
47. Khoshnevis B (2004) "Automated construction by contour crafting—related robotics and information technologies." Autom Constr, The best of ISARC 2002, 13(1):5–19. https://doi.org/10.1016/j.autcon.2003.08.012
48. Kim S, Seong H, Her Y, Chun J (2019) A study of the development and improvement of fashion products using a FDM type 3D printer. Fashion Textiles 6(1):9. https://doi.org/10.1186/s40691-018-0162-0
49. Klein J, Stern M, Franchin G, Kayser M, Inamura C, Dave S, Weaver JC et al (2015) "Additive manufacturing of optically transparent glass." 3D Printing Add Manuf, September. https://doi.org/10.1089/3dp.2015.0021
50. Koch L, Deiwick A, Schlie S, Michael S, Gruene M, Coger V, Zychlinski D et al (2012) Skin tissue generation by laser cell printing. Biotechnol Bioeng 109(7):1855–1863. https://doi.org/10.1002/bit.24455
51. Kuhn R (2015) "The 3D printing's panorama in fashion design," 12
52. Kumar S, Kruth J-P (2010) Composites by rapid prototyping technology. Mater Des 31(2):850–856. https://doi.org/10.1016/j.matdes.2009.07.045
53. Kunz M, Waldman SD, Rudan JF, Bardana DD, James Stewart A (2012) Computer-assisted mosaic arthroplasty using patient-specific instrument guides. Knee Surg Sports Traumatol Arthrosc 20(5):857–861. https://doi.org/10.1007/s00167-011-1638-2
54. Le TT, Austin SA, Lim S, Buswell RA, Gibb AGF, Thorpe T (2012) Mix design and fresh properties for high-performance printing concrete. Mater Struct 45(8):1221–1232. https://doi.org/10.1617/s11527-012-9828-z
55. Lee V, Singh G, Trasatti JP, Bjornsson C, Xiawei Xu, Tran TN, Yoo S-S, Dai G, Karande P (2014) Design and fabrication of human skin by three-dimensional bioprinting. Tissue Eng Part C Methods 20(6):473–484. https://doi.org/10.1089/ten.tec.2013.0335
56. Liaw C-Y, Guvendiren M (2017) Current and emerging applications of 3d printing in medicine. Biofabrication 9(2):024102. https://doi.org/10.1088/1758-5090/aa7279

57. Lin Y, Huang G, Huang Y, Jeremy Tzeng TR, Chrisey D (2010) "Effect of laser fluence in laser-assisted direct writing of human colon cancer cell." Bourell D (ed). Rapid Prototyping J 16(3):202–8. https://doi.org/10.1108/13552541011034870
58. Ling K, Huang G, Liu J, Zhang X, Ma Y, Lu T, Xu F (2015) "Bioprinting-based high-throughput fabrication of three-dimensional mcf-7 human breast cancer cellular spheroids." Engineering 1(2):269–74. https://doi.org/10.15302/J-ENG-2015062.
59. Lipton JI, Cutler M, Nigl F, Cohen D, Lipson H (2015) Additive manufacturing for the food industry. Trends Food Sci Technol 43(1):114–123. https://doi.org/10.1016/j.tifs.2015.02.004
60. Lipton J, Arnold D, Nigl F, Lopez N, Cohen D, Norén N, Lipson H (2010) "Multi-material food printing with complex internal structure suitable for conventional post-processing," January
61. Loessner D, Stok KS, Lutolf MP, Hutmacher DW, Clements JA, Rizzi SC (2010) Bioengineered 3D platform to explore cell–ecm interactions and drug resistance of epithelial ovarian cancer cells. Biomaterials 31(32):8494–8506. https://doi.org/10.1016/j.biomaterials.2010.07.064
62. Mao K, Wang Y, Xiao S, Liu Z, Zhang Y, Zhang X, Wang Z et al (2010) Clinical application of computer-designed polystyrene models in complex severe spinal deformities: a pilot study. Eur Spine J 19(5):797–802. https://doi.org/10.1007/s00586-010-1359-0
63. Marga F, Jakab K, Khatiwala C, Shepherd B, Dorfman S, Hubbard B, Colbert S, Gabor F (2012) Toward engineering functional organ modules by additive manufacturing. Biofabrication 4(2):022001. https://doi.org/10.1088/1758-5082/4/2/022001
64. McLeary P (2013) "Navy warship is taking 3D printer to sea; don't expect a revolution." Breaking Defense (blog). 2013. https://breakingdefense.com/2014/04/navy-carrier-is-taking-3d-printer-to-sea-dont-expect-a-revolution/
65. Mearian L (2016) "This is the first 3D-printed drug to win fda approval | computerworld.". https://www.computerworld.com/article/3048823/this-is-the-first-3d-printed-drug-to-win-fda-approval.html
66. "Meet Easton LaChappelle." (2015) Tonyrobbins.Com (blog). July 17, 2015. https://www.tonyrobbins.com/leadership-impact/easton-lachappelle/
67. Melchels FPW, Feijen J, Grijpma DW (2010) A review on stereolithography and its applications in biomedical engineering. Biomaterials 31(24):6121–6130. https://doi.org/10.1016/j.biomaterials.2010.04.050
68. Mironov V, Visconti RP, Kasyanov V, Forgacs G, Drake CJ, Markwald RR (2009) Organ printing: tissue spheroids as building blocks. Biomaterials 30(12):2164–2174. https://doi.org/10.1016/j.biomaterials.2008.12.084
69. Morrison RJ, Hollister SJ, Niedner MF, Mahani MG, Park AH, Mehta DK, Ohye RG, Green GE (2015) "Mitigation of tracheobronchomalacia with 3D-printed personalized medical devices in pediatric patients." Sci Transl Med 7(285):285ra64–285ra64. https://doi.org/10.1126/scitranslmed.3010825.
70. Mudge RP, Wald N (2007) "Laser engineered net shaping advances additive manufacturing and repair." In
71. Murr LE, Gaytan SM, Medina F, Martinez E, Martinez JL, Hernandez DH, Machado BI, Ramirez DA, Wicker RB (2010) Characterization of Ti–6Al–4V open cellular foams fabricated by additive manufacturing using electron beam melting. Mater Sci Eng, A 527(7):1861–1868. https://doi.org/10.1016/j.msea.2009.11.015
72. Neumüller M, Reichinger A, Rist F, Kern C (2014) "3D printing for cultural heritage: preservation, accessibility, research and education." In 3D research challenges in cultural heritage: a roadmap in digital heritage preservation Ioannides M, Quak E(eds). Lecture Notes in Computer Science. Berlin, Heidelberg, Springer, pp 119–34. https://doi.org/10.1007/978-3-662-44630-0_9
73. Ngo TD, Kashani A, Imbalzano G, Nguyen KTQ, Hui D (2018) Additive manufacturing (3D printing): a review of materials, methods, applications and challenges. Compos B Eng 143(June):172–196. https://doi.org/10.1016/j.compositesb.2018.02.012
74. Ni Y, Ji Ru, Long K, Ting Bu, Chen K, Zhuang S (2017) A review of 3D-printed sensors. Appl Spectrosc Rev 52(7):623–652. https://doi.org/10.1080/05704928.2017.1287082

75. van Noort R (2012) The future of dental devices is digital. Dent Mater 28(1):3–12. https://doi.org/10.1016/j.dental.2011.10.014
76. Nyga A, Cheema U, Loizidou M (2011) 3D tumour models: novel in vitro approaches to cancer studies. J Cell Commun Signaling 5(3):239–248. https://doi.org/10.1007/s12079-011-0132-4
77. O'Reilly MK, Reese S, Herlihy T, Geoghegan T, Cantwell CP, Feeney RNM, Jones JFX (2016) Fabrication and assessment of 3D printed anatomical models of the lower limb for anatomical teaching and femoral vessel access training in medicine: subject specific 3D-printed anatomy. Anat Sci Educ 9(1):71–79. https://doi.org/10.1002/ase.1538
78. Paul SC, Tay YWD, Panda B, Tan MJ (2018) Fresh and hardened properties of 3D printable cementitious materials for building and construction. Arch Civ Mech Eng 18(1):311–319. https://doi.org/10.1016/j.acme.2017.02.008
79. Pepper ME, Parzel CA, Burg T, Boland T, Burg KJL, Groff RE (2009) "Design and implementation of a two-dimensional inkjet bioprinter." In 2009 annual international conference of the IEEE engineering in medicine and biology society, Minneapolis, MN, IEEE, pp 6001–5. https://doi.org/10.1109/IEMBS.2009.5332513
80. Prasad LK, Smyth H (2016) 3D printing technologies for drug delivery: a review. Drug Dev Ind Pharm 42(7):1019–1031. https://doi.org/10.3109/03639045.2015.1120743
81. Quigley JT (2016) "Chinese scientists are 3D printing ears and livers—with living tissue." Accessed 24 June 2020. https://thediplomat.com/2013/08/chinese-scientists-are-3d-printing-ears-and-livers-with-living-tissue/
82. Richter KH, Orban S, Nowotny S (2004) "Laser cladding of the titanium alloy TI6242 to restore damaged blades." In International congress on applications of lasers & electro-optics, San Francisco, California, USA, Laser Institute of America, 1506p . https://doi.org/10.2351/1.5060222
83. Ringeisen BR, Othon CM, Barron JA, Young D, Spargo BJ (2006) Jet-based methods to print living cells. Biotechnol J 1(9):930–948. https://doi.org/10.1002/biot.200600058
84. Ringeisen BR, Kim H, Barron JA, Krizman DB, Chrisey DB, Jackman S, Auyeung RYC, Spargo BJ (2004) "Laser printing of pluripotent embryonal carcinoma cells." Tissue Eng 10(3–4):483–91. https://doi.org/10.1089/107632704323061843
85. Rowe CW, Katstra WE, Palazzolo RD, Giritlioglu B, Teung P, Cima MJ (2000) Multimechanism oral dosage forms fabricated by three dimensional printing^{TM}. J Control Release 66(1):11–17. https://doi.org/10.1016/S0168-3659(99)00224-2
86. Ruggeri BA, Camp F, Miknyoczki S (2014) Animal models of disease: pre-clinical animal models of cancer and their applications and utility in drug discovery. Biochem Pharmacol 87(1):150–161. https://doi.org/10.1016/j.bcp.2013.06.020
87. Saini M (2015) "Implant biomaterials: a comprehensive review." World J Clin Cases 3(1):52. https://doi.org/10.12998/wjcc.v3.i1.52
88. Sarvankar SG, Yewale SN (2019) "Additive manufacturing in automobile industry," 4:10
89. Scolozzi P (2012) Maxillofacial reconstruction using polyetheretherketone patient-specific implants by 'mirroring' computational planning. Aesthetic Plast Surg 36(3):660–665. https://doi.org/10.1007/s00266-011-9853-2
90. Scopigno R, Callieri M, Cignoni P, Corsini M, Dellepiane M, Ponchio F, Ranzuglia G (2011) 3D models for cultural heritage: beyond plain visualization. Computer 44(7):48–55. https://doi.org/10.1109/MC.2011.196
91. Scopigno R, Cignoni P, Pietroni N, Callieri M, Dellepiane M (2017) Digital fabrication techniques for cultural heritage: a survey. Computer Graphics Forum 36(1):6–21. https://doi.org/10.1111/cgf.12781
92. Se S, Stephen Y, Jasiobedzki P, Parry DO, Jakola RH (2010) 3D imaging system. United States US7860301B2, filed February 13, 2006, and issued December 28, 2010. https://patents.google.com/patent/US7860301/en
93. Shakor P, Sanjayan J, Nazari A, Nejadi S (2017) Modified 3D printed powder to cement-based material and mechanical properties of cement scaffold used in 3D printing. Constr Build Mater 138(May):398–409. https://doi.org/10.1016/j.conbuildmat.2017.02.037

94. Shishkovsky I, Tarasova E, Zhuravel' L, Petrov AL (2001) "The synthesis of a biocomposite based on nickel titanium and hydroxyapatite under selective laser sintering conditions." Tech Phys Lett 27(January):211–13https://doi.org/10.1134/1.1359830
95. Siolas D, Hannon GJ (2013) Patient-derived tumor xenografts: transforming clinical samples into mouse models. Can Res 73(17):5315–5319. https://doi.org/10.1158/0008-5472.CAN-13-1069
96. Sodian R, Weber S, Markert M, Rassoulian D, Kaczmarek I, Lueth TC, Reichart B, Daebritz S (2007) Stereolithographic models for surgical planning in congenital heart surgery. Ann Thorac Surg 83(5):1854–1857. https://doi.org/10.1016/j.athoracsur.2006.12.004
97. Soliman Y, Feibus AH, Baum N (2015) 3D printing and its urologic applications. Rev Urol 17(1):20–24
98. Soon DSC, Chae MP, Pilgrim CHC, Rozen WM, Spychal RT, Hunter-Smith DJ (2016) 3D haptic modelling for preoperative planning of hepatic resection: a systematic review. Ann Med Surg 10(September):1–7. https://doi.org/10.1016/j.amsu.2016.07.002
99. Strickland JD (2016) "Applications of additive manufacturing in the marine industry." https://doi.org/10.13140/RG.2.2.29930.31685
100. Sun J, Zhou W, Huang D, Fuh JYH, Hong GS (2015) An overview of 3D printing technologies for food fabrication. Food Bioprocess Technol 8(8):1605–1615. https://doi.org/10.1007/s11947-015-1528-6
101. Symes MD, Kitson PJ, Yan J, Richmond CJ, Cooper GJT, Bowman RW, Vilbrandt T, Cronin L (2012) Integrated 3D-printed reactionware for chemical synthesis and analysis. Nat Chem 4(5):349–354. https://doi.org/10.1038/nchem.1313
102. Tibbits S (2014) 4D printing: multi-material shape change. Archit Des 84(1):116–121. https://doi.org/10.1002/ad.1710
103. "University of California San Diego's 3D Printed Liver Tissue May Be the Closest We've Gotten to a Real Printed Liver—3DPrint.Com | The Voice of 3D Printing / Additive Manufacturing." 2016 Accessed June 24, 2020. https://3dprint.com/118932/uc-san-diego-3d-printed-liver/
104. Wang CC, Tejwani (Motwani) MR, Roach WJ, Kay JL, Yoo J, Surprenant HL, Monkhouse DC, Pryor TJ (2006) "Development of near zero-order release dosage forms using three-dimensional printing (3-DP^{TM}) technology." Drug Dev Ind Pharm 32(3):367–76https://doi.org/10.1080/03639040500519300
105. "With 3-D Printing, the Shoe Really Fits." 2013 (2013). https://sloanreview.mit.edu/article/with-3-d-printing-the-shoe-really-fits/
106. Wu H, Li D, Guo N (2009) Fabrication of integral ceramic mold for investment casting of hollow turbine blade based on stereolithography. Rapid Prototyping J 15(4):232–237. https://doi.org/10.1108/13552540910979749
107. Wu P, Wang J, Wang X (2016) A critical review of the use of 3-D printing in the construction industry. Autom Constr 68(August):21–31. https://doi.org/10.1016/j.autcon.2016.04.005
108. Xu F, Celli J, Rizvi I, Moon S, Hasan T, Demirci U (2011) A three-dimensional in vitro ovarian cancer coculture model using a high-throughput cell patterning platform. Biotechnol J 6(2):204–212. https://doi.org/10.1002/biot.201000340
109. Xu N, Wei F, Liu X, Jiang L, Cai H, Li Z, Miao Yu, Fengliang Wu, Liu Z (2016) Reconstruction of the upper cervical spine using a personalized 3D-printed vertebral body in an adolescent with ewing sarcoma. Spine 41(1):E50-54. https://doi.org/10.1097/BRS.0000000000001179
110. Xu T, Zhao W, Zhu J-M, Albanna MZ, Yoo JJ, Atala A (2013) Complex heterogeneous tissue constructs containing multiple cell types prepared by inkjet printing technology. Biomaterials 34(1):130–139. https://doi.org/10.1016/j.biomaterials.2012.09.035
111. Xue L, Islam MU (2006) "Laser consolidation—a novel one-step manufacturing process for making net-shape functional components." In
112. Yang M, Li C, Li Y, Zhao Y, Wei X, Zhang G, Fan J et al (2015) Application of 3D rapid prototyping technology in posterior corrective surgery for lenke 1 adolescent idiopathic scoliosis patients. Medicine 94(8):e582. https://doi.org/10.1097/MD.0000000000000582

113. Ying CY, Clarrisa SM, Eng H, Wei J, Pei-Chen Su (2017) 4D printing of high performance shape memory polymer using stereolithography. Mater Des 126(July):219–225. https://doi.org/10.1016/j.matdes.2017.04.049
114. Yu D-G, Branford-White C, Ma Z-H, Zhu L-M, Li X-Y, Yang X-L (2009) Novel drug delivery devices for providing linear release profiles fabricated by 3DP. Int J Pharm 370(1–2):160–166. https://doi.org/10.1016/j.ijpharm.2008.12.008
115. Yu DG, Yang XL, Huang WD, Liu J, Wang YG, Huibi Xu (2007) Tablets with material gradients fabricated by three-dimensional printing. J Pharm Sci 96(9):2446–2456. https://doi.org/10.1002/jps.20864
116. Zareiyan B, Khoshnevis B (2017) Interlayer adhesion and strength of structures in contour crafting—effects of aggregate size, extrusion rate, and layer thickness. Autom Constr 81(September):112–121. https://doi.org/10.1016/j.autcon.2017.06.013
117. Zhao Yu, Yao R, Ouyang L, Ding H, Zhang T, Zhang K, Cheng S, Sun W (2014) Three-dimensional printing of hela cells for cervical tumor model *in Vitro*. Biofabrication 6(3):035001. https://doi.org/10.1088/1758-5082/6/3/035001
118. Zolfagharian A, Kaynak A, Kouzani A (2020) Closed-loop 4D-printed soft robots. Mater Des 188(March):108411. https://doi.org/10.1016/j.matdes.2019.108411

Future Trends and Technologies in Additive and Substractive Manufacturing

Vineet Kumar, Bhargav Reddy Isanaka, Sristi Gupta, and Vinod Kushvaha

1 Introduction

Manufacturing is a process by which raw materials are converted into products by manual labor or machinery. This process is broadly divided into two broad categories: Additive Manufacturing (AM) and Subtractive Manufacturing (SM). Traditionally, manufacturing a fully finished and assembled product from a raw material requires several machining tools which can be eliminated by using advanced technologies like AM [2]. In recent years, AM evolved as a better and efficient alternative over subtractive manufacturing. In the last few decades, different types of additive processes [5] had been developed like photopolymer, deposition, lamination, powder-based techniques, and many more. Several types of research are proceeding already for the advancement in the processes to increase the efficiency of the AM. These researches are not only limited to deposition techniques but also spread in the field of materials [47]. Many industries like aerospace, automotive, and healthcare industries are using AM for the production of several engineering parts [18]. In the present chapter, the details like types and methods of additive and subtractive manufacturing are discussed. In available literature, there are limited number of resources available on future trends of SM. For this reason, the present chapter mainly focus on the global trends and future of AM with respect to global markets value in each segment i.e. hardware, software, materials, post processing and research.

V. Kumar · B. R. Isanaka · S. Gupta · V. Kushvaha (✉)
Department of Civil Engineering, IIT Jammu, Jammu, India
e-mail: vinod.kushvaha@iitjammu.ac.in

V. Kumar
e-mail: 2018uce0052@iitjammu.ac.in

S. Gupta
e-mail: sristi.gupta@iitjammu.ac.in

S. Mavinkere Rangappa et al. (eds.), *Additive and Subtractive Manufacturing of Composites*, Springer Series in Advanced Manufacturing,
https://doi.org/10.1007/978-981-16-3184-9_9

2 Additive and Subtractive Manufacturing

Additive manufacturing (AM) and Subtractive Manufacturing (SM) methods are being widely used for the assembling of different engineering, medical and architectural components. These methods generally comes under the Solid Freeform Fabrication (SFF) method. In the 1980s, AM was emerged to produce prototypes of complex objects using computer model data without specific part tooling. In the last few decades, this method was developed and its usage increased in numerous fields of engineering [24]. The term 'AM' and '3D printing' are used interchangeably. It is the technique where materials are compiled, usually layer by layer to make objects using 3D model data [14]. This method requires 3D models for printing, which makes the job easier and faster than Computer Numerical Control (CNC) machines. There are several types of additive techniques like Fused Deposition Modelling (FDM), Direct Metal Laser sintering (DMLS), PolyJet (3DP), Stereolithography (SLA), Selective Laser Sintering (SLS), etc. which are being mostly used for part manufacturing. Depending on the technology, the 3D printer melts at a specified location or deposits material according to the Computer-Aided Manufacturing (CAM) data. It is ideal for many engineering and manufacturing applications like mass customization, rapid prototyping, bio-printing, pharmaceuticals, industrial, art and jewelry and cultural heritage, etc. [39]. The most common materials that are being used in this type of manufacturing are plastics and metals. The present scenario in manufacturing depicts that AM has footprints in almost all major industries from aerospace, automotive to biomedical and fashion-designing. Among these industries, bio-medical is one of the major fields which has been popularly using AM on a large-scale basis. The major areas of bio-medical, where AM is being used are prosthetics, surgical implants, surgical guides, external aids, medical models, and bio-manufacturing.

The SM processes remove materials to create parts. It is an umbrella term that involves all the controlled machining, material removal processes and creates products from metals, solid blocks, rods of plastics, bars, and other materials by cutting, boring, grinding, and drilling. Subtractive manufacturing processes are either carried out manually or by using CNC. The CNC machine takes the input in the form of a virtual model which is designed by using Computer-Aided Design (CAD) software for the fabrication tool. These inputs instruct the machine on how to make channels, cuts, bores, holes, and other features that are required for final output. CNC tools require either little or no human interaction or assistance. The common materials that are used during CNC machining processes are soft metals, hard thermoplastics, hard metals (industrial machines), and thermoset plastics. In the Electrical discharge machining (EDM) process, the materials used are hard metals. Similarly, in Laser cutting (a technology that uses a laser source to slice materials), materials used are thermoplastics, wood, acrylic, fabrics, metals while in water jet cutting (a technology that uses a high-pressure jet of water to cut a wide variety of materials), materials used are plastics, hard and soft metals, stone, glass, composites [13].

3 Comparison Between Additive and Subtractive Manufacturing

3.1 Equipment Cost

The cost of professional desktop printers used in AM is more than that of small scale CNC machines which cost around $2000. The price for more advanced tools varies depending on the number of axes, part size, features, and tooling needed for specific materials [16].

3.2 Training

The human operators that are working on desktop printers which are being used in AM, require minor training on machine operation, maintenance, build setup, and finishing. In the case of SM, the small CNC machines need moderate training to operators for machine operation, maintenance, build setup, and finishing. However, both the systems used in industries require dedicated staff and extensive training for both manufacturing methods.

3.3 Facility Requirements

The desktop/benchtop systems used in AM are suitable for offices. However, industrial 3D printers require a dedicated space or room equipped with Heating, Ventilation, and Air Control (HVAC). It helps to maintain humidity, room temperature, and air condition in the specified space. On the other hand, SM requires a large and dedicated space for industrial systems and small CNC machines are only suitable for workshops.

3.4 Ancillary Equipment

The ancillary equipment used in AM are wet separator (vacuum cleaner that is used to safely vacuum the metal powders that cannot be cleaned by any other way), glove box (to deal mainly with reactive metals), powder sieve (to separate larger particle contaminants from the powder) and ultrasonic cleaner (to remove much-trapped powder). Contrarily, the tooling equipment required for subtractive manufacturing is completely based on the type of machinery used. If the system is more advanced it automates many processes such as chip clearing and handling, tool changing, and coolant management.

3.5 Wastes

Comparatively there is minimum wastage in AM method, there are material wastes in the form of vapor, dissolved ions, chips, scraps, etc.

3.6 Complexity of the Structure

Using AM, it is easier to fabricate complex structures and the structures containing completely closed internal hollow. Whereas, subtractive manufacturing has limited capability in the fabrication of complex structures and the structures which are fully closed internal hollow. AM does not constrain designers to solid parts like traditional mould and milling methods.

4 Types of Additive Processes Used in AM

The different types of additive processes that are being used widely in AM are discussed below.

4.1 Photopolymer

The photopolymer approach is layer-wise conversion of liquid photopolymer into solid or gel by selective exposure to light. This technique is further divided into two streams: Stereolithography (SLA) and Digital Light Processing (DLP) [53].

4.1.1 Stereolithography (SLA)

The SLA 3D printing is introduced by Chuck Hull in the year 1986. In this method, a movable photon source is used to activate photopolymerization of photocurable resin and print solid layers on top of the parent layer. Urethane dimethacrylate with a small fraction of acrylic acid, methyl ethyl hydroquinone, and benzophenone are the first photocurable materials that are used for SLA application [20]. SLA technique is used to fabricate 3D objects with inorganic–organic hybrid structures [10]. The application is also used to tissue engineering, fabricate high resolution and complex architecture like a human ear [36]. The SLA technique is mainly used in biological fields like for fabrication of aids for complex surgery, patient-specific models for mould-assisted implant fabrication, and tailor-made parts such as hearing aids [31].

4.1.2 Digital Light Processing (DLP)

This technique helps 3D fabrication feasible with less volume consumption of resins. It involves the photon source illumination from the bottom of the resin bath and then the building platform is dipped into the resin from the top. This technique is developed recently to reduce the printing time and it will also increase the fabrication accuracy [37]. DLP method is being widely used in a variety of contexts like inorganic hybrid networks, fabrication of luminescent 3D structures, reprocessable thermosets, engineered nerve guidance conduits, highly stretchable photopolymers, and other complex structures [3].

4.1.3 Continuous Liquid Interface Production (CLIP)

It is a new generation 3D printing method and apparatus. It is developed by DeSimone and his co-workers in the year 2015. This technique enables the continuous printing of monolithic and layer less polymeric objects [46]. In this process, an oxygen-containing interfacial layer is created using an oxygen-permeable window where free radical photopolymerization is inhibited. The free radical photopolymerization gets inhibited due to oxygen by (1) forming a peroxide upon interaction with a free radical of a propagating chain and (2) quenching the excited state photoinitiator [48]. As a result, it leaves a thin layer between the building platform and the window. This oxygen-inhibited dead zone helps in layer less part construction and fast printing speed simultaneously. Generally, an oxygen-permeable window contains an amorphous fluoropolymer window with high oxygen permeability, chemical inertness, and UV transparency [46].

4.2 Deposition

In deposition processes, a material stream is deposited without heating a point source, such that the motion of the material stream governs the selectivity [6]. This deposition method was divided into two parts: (1) Filament approach (2) Inkjet approach.

4.2.1 Filament Approach

In the filament approach (shown in Fig. 1), the polymer filament is fed to the preheated nozzle which melts the filament and flows it into the part position. The filament system contains a crucible that holds a reservoir of filament-forming material, a flow control apparatus that controls and deposits the flow of material filaments selectively on the substrate, and an orifice disposed of in the bottom of the crucible through which the forming material passes to form a flow of material filaments [45]. This method includes the following steps.

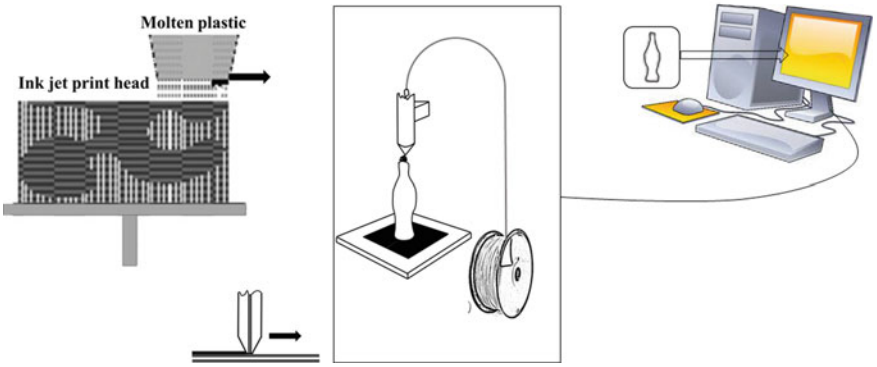

Fig. 1 (Right) Filament approach: extrusion of heated filament; (Left) Inkjet approach: inkjet with multiple print heads

1. The forming material is loaded in the reservoir (container) and heated to melt the forming material.
2. The molten forming material is ejected through an opening with adjusting the effective size to form a variable-size flow of molten forming material towards the substrate.
3. The flow is cooled to form variable-size material filaments flowing towards the substrate.
4. The substrate is positioned beneath the material filaments and it gets deposited in layers on the substrate to form the 3D objects

4.2.2 Inkjet Approach

Inkjet printing (shown in Fig. 1) can be used as an umbrella for a range of technologies like ceramic manufacturing technology, biomaterials manufacturing technology [11]. It is first commercialized in the early 1970s [8]. In this approach, the polymer is placed layer by layer, and the inkjet technology is used to selective spray an adhesive using a roller. For advancing the technology, high viscous inks which are 20 times more viscous than the regular inks are being used to produce biological materials, larger solid content, and jetting a catalyst into a ceramic powder bed [6].

4.3 Lamination

In the lamination processes, the material is applied in the form of the sheet and this process utilizes the detailed digital imaginary report created by a Computed Tomography (CT) scanner or by Magnetic Resonance Imaging (MRI) which provides detailed data to create a 3D electronic representation of an object [7]. The detailed

data of 3D representation is then electronically sectioned into thin parallel planar sections according to slices of the object. These sections are further used to create a 3D object that replicates the original object. The scale of the replicated object can be diminished, enlarged, or of the same size as the original object [7].

4.4 Powder-Based Techniques

The most important categories of powder-based techniques used in AM are selective laser sintering [15], electron beam melting, and selective laser melting [52].

4.4.1 Selective Laser Melting (SLM)

It is a powder-based AM which can produce parts layer-by-layer from a 3D CAD model [49]. The main operation in SLM is the laser beam scanning over the surface of a thin powder layer which is deposited previously on the substrate. The laser beam scanning is done along a specified direction according to the product requirement. This technique is widely being used in a large number of industries ranging from biomedical to aerospace [49]. In today's world, the use of the SLM technique has increased greatly in biomedical applications like in the fabrication of internal structure and engineered composition, implants, and prostheses with the desired shape. It is a suitable technique to create micro-objects [15, 50]. The properties of SLM manufactured material will depend mainly on laser-melted track, every single layer, and bonding between each deposited layer [49].

4.4.2 Selective Laser Sintering (SLS)

SLS is quite an energy-inefficient as compared to the traditional technique of manufacturing [5, 42]. From Table 1, it can be seen that all SLS machines do not consume

Table 1 Power consumption of different SLS based machines

Referencing	Machines	Total power consumed (in kW)	Laser unit power consumption (in kW)	Percentage of power consumed by laser unit (%)
Sreenivasan et al. [42]	SLS Vanguard HiQ Machine	19	3	16
Kellens et al. [22]	EOSINT P760 SLS machine	7	3.5	50
Nelson et al. [34]	SLS EOS EOSINT M250 Xtended machine	6	4	66

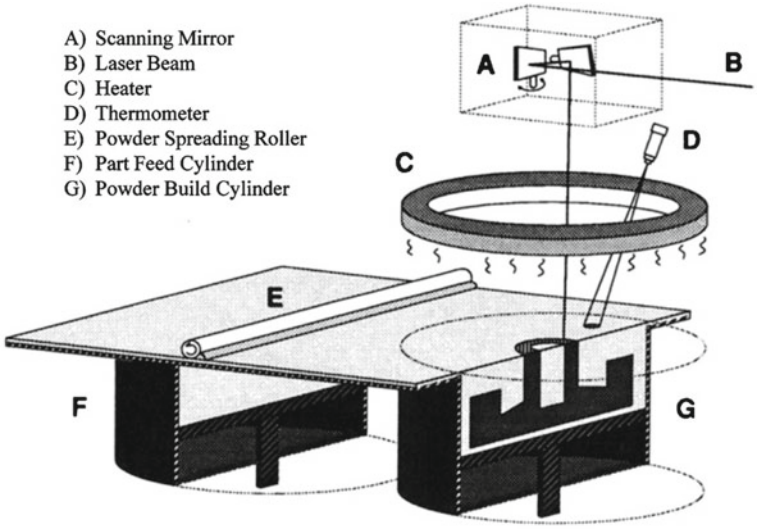

Fig. 2 Schematic of SLS process [34]

the same amount of power. The SLS process (as shown in Fig. 2) manufactures the parts by selectively sintering powder by the source of a powerful laser, generally a CO_2 laser [34]. The SLS technique received its attraction in the manufacturing industry due to its ability to produce complex geometry without using any supporting structures and special tooling.

4.4.3 Electron Beam Melting (EBM)

In the EBM system, the electrons which are generated using a gun are accelerated with a 60 kV potential. The generated electrons are focused using electromagnetic lenses and electronically scanned by an embedded CAD program. The focused electron beam is scanned with a high beam current (~30 mA) at a scan rate of ~104 mm/s in multiple passes to preheat the powder bed to approximately about 0.8 Tm (Tm is the melting temperature). Further, both the final melt scan and the beam current are reduced to ~102 mm/s and ~5 to 10 mA respectively. The beam scans *x*-*y*, and the final melt scan produces melt zones or pools related to the beam diameter and scan spacing. The melt scan melts only selected layer areas as prescribed in the CAD model [33].

Table 2 Market value share

Segments	Market share in percentage (%)
Hardware manufacturers	56.3
Software vendors	13.4
Material suppliers	20.3
Post-processing manufacturers	4.8
Research institutions	5.2

5 Trends

The innovation of AM started early at a fundamental level, later taken a shape of a revolution in the manufacturing industry, and is still growing exponentially in many fields of engineering. Even though the applications of AM are increasing day by day, the trends are not going to remain constant considering several restrictions like manufacturing and setup cost. In some fields, its applications have increased drastically whereas, in some fields, its applications are reduced. The challenges of materials used, applications, accuracy, and capabilities of technologies are going to affect the trends a lot. AM has experienced drastic growth during the last few decades from uncommercialized technologies in the 1980s to a market value of $4 billion in 2014 [12].

5.1 Global Market Trend

The present global market of AM products which consists of all the services is rising rapidly all over the world. The global AM market was estimated at around $10 billion by the end of 2019 [1]. However, it was estimated that about $1.1 billion investment was done by 77 early-stage AM companies in the year 2019. It was reported that 29% of AM companies have located their headquarters in the United States [43]. According to the report of AMFG 2020, the market value was not equally divided into each category [1, 44]. From Table 2, it can be observed that hardware manufacturing industries contribute more than half of the total market value, while other industries did not grow much.

5.1.1 Hardware

The available data shown in Fig. 3 depicts that hardware manufacturing industries contribute more than half of the total market value. Hardware industries are contributing mainly due to the start-up and up-gradation of existing technologies.

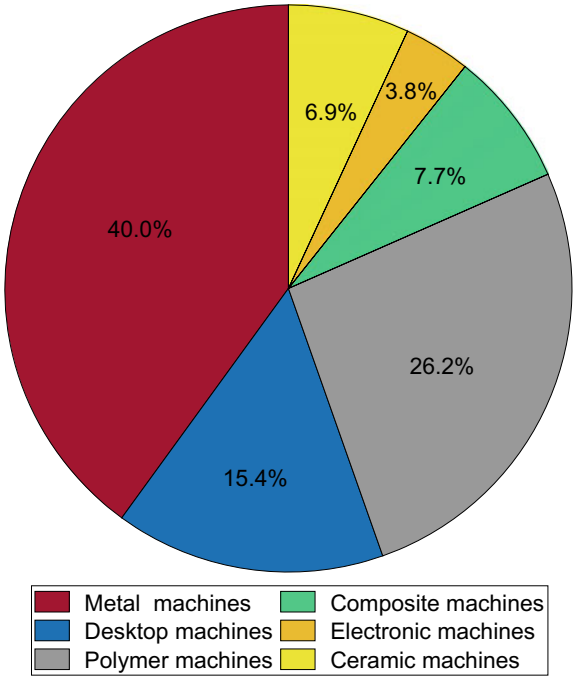

Fig. 3 Market value of machines [1]

Among all the materials, polymer 3D printers are more in use as compared to other materials due its high efficiency towards mechanical behaviour with low manufacturing cost and mouldability [17, 27]. It was reported that 72% of companies were using polymer AM systems whereas 49% are using metal AM systems by 2019 [43]. Considering the report by SmarTech Analysis 2020, Power Bed Fusion (PBF) technologies were in demand due to their potential for volume manufacturing and high productivity [35]. The metal extrusion techniques generated the highest revenue in professional environments. Desktop 3D printers played a significant role in manufacturing industries by reducing the AM cost. The rise in demand for desktop 3D printers is due to the demand for industrial systems that are smaller in size and requires a low cost as compared to their larger counterparts.

The metal 3D printer is growing at an average rate of over 30% in the last two years [1]. This is due to the increase in usage of AM based parts in the field of medical and aerospace. Among all, metal PBF variants remain the most widely used systems in terms of technologies. According to a report, 80% of the all-metal AM systems installations are of PBF in 2019 [30]. Ceramic 3D printing is still in the early stages of development not much developed as metal and polymer 3D printing technologies. It is estimated that in the next coming five to six years, ceramic 3D printing technology will reach maturity [41]. It is observed that like ceramic 3D printing, the electronics 3D printing market is also not like many other applications. There are very few companies that will provide hardware for electronics 3D printers. In the recent years, polymer based composites are playing major role in the field of

Table 3 Commercially available materials for AM of four consecutive years

Materials	Year			
	2017	2018	2019	2020
Ceramic	14	24	29	34
Composite	64	112	144	191
Metal	392	523	796	904
Polymer	385	524	802	1095
Sand	9	5	5	5
Wax	20	16	16	17

engineering research due to its high strength to weight ratio [26, 40]. To enhance the applications of these composites, 3D printing is a newly developed technique in AM and one of the main reasons behind the growth of this segment. It requires less cost than that of traditional composite manufacturing. Based on the available information, the market value of composite 3D printing is around $2.7 billion [41].

5.1.2 Materials

From Table 3, it can be seen that the materials being used for AM are growing steadily. According to Sculpteo's annual State of 3D printing report, polymers are being used by more than 80% of AM companies for 3D printing [32]. It is reported that there are 1095 types of polymer materials are available for 3D printing. According to Senvol Database, there are 2245 AM materials in 2020. However, it is just reported about 1700 in 2019 as shown in Fig. 4 [47].

The available literature shows that the number of metal-based AM materials is gradually increasing. According to Senvol Database, the leading AM materials in the market are nickel, steel, and titanium products. However, the use of aluminum products is also growing [47]. It can be seen from Table 4 that in 2017, commercially available aluminum products for AM are 43 and grown-up to 105 till March 2020 as shown in Fig. 5.

From Fig. 6, it can be observed that the companies supplying materials for AM have doubled from 2017 to 2019. But the growth in the number of suppliers has slightly lowered in 2020.

5.1.3 Software

The software segment has not developed like other 3D printing segments. However, it is slowly growing as the new demands to simplify the 3D printing workflow. The advancement of AM software ensures for part quality, a simultaneous increase in print success rates, and manage workflows more efficiently. Companies dealing with AM software development mainly focus on simulation software. The software either

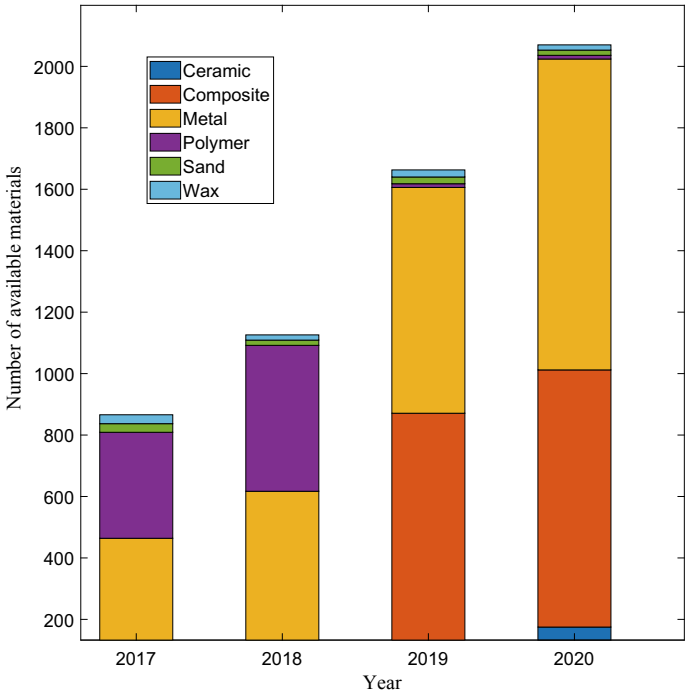

Fig. 4 Graphical representation for different types of commercially available materials for AM [47]

Table 4 Commercially available metals products for AM

Metals	Year			
	2017	2018	2019	2020
Aluminium	43	65	95	105
Cobalt	40	40	56	64
Copper	7	10	26	28
Nickel	92	113	168	197
Steel	90	136	210	240
Titanium	93	113	171	185
Other	27	46	70	85

eliminates or reduces the trial-and-error approach which helps to further save time consumption for model development. Today, 3D printing has become a manufacturing technology that is not only capable of small batch production but also capable of serial production. According to SmarTech Analysis, the software sector takes revenue of $458 million in 2020 as shown in Fig. 7 [25].

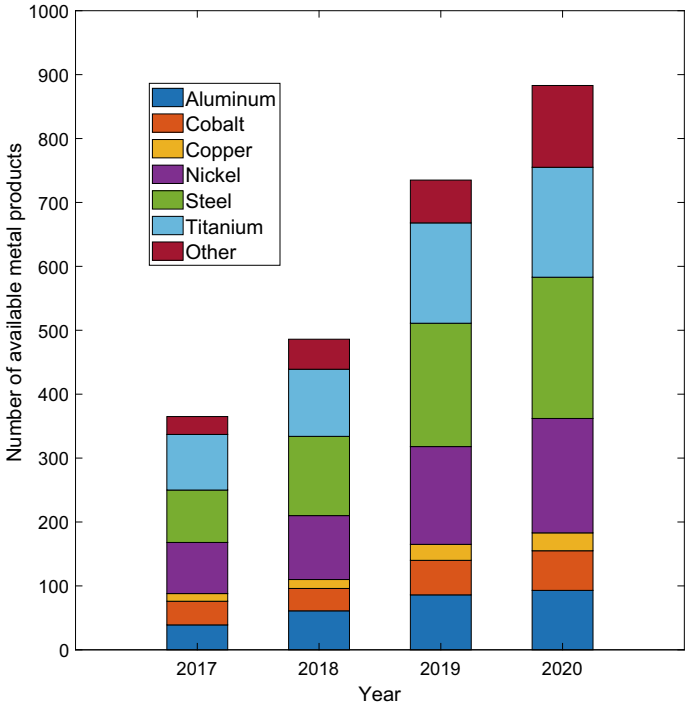

Fig. 5 Graphical representation of commercially available metal products for AM [47]

In the sector of security and Internet Protocol (IP), it is still a very handful of vendors that are providing security solutions to AM. One of the reasons behind it may be that many original equipment manufacturers (OEMs) are not investing in such solutions. The security solutions that are being used by manufacturing companies are either developed by companies outside of the AM industry or are developed in-house[1].

5.1.4 Post Processing

3D printing has emerged as a major manufacturing technique in industries, it is required to overcome the post-processing challenges. The major challenges in post-processing are an increase in lead-time and cost of 3D printing. Furthermore, the post-processed 3D parts make up to 60% of the total manufacturing cost according to their application [1]. There are several companies which are working to overcome the post-processing challenges by introducing automated solutions for dyeing, depowdering, surface-finishing and part-cleaning.

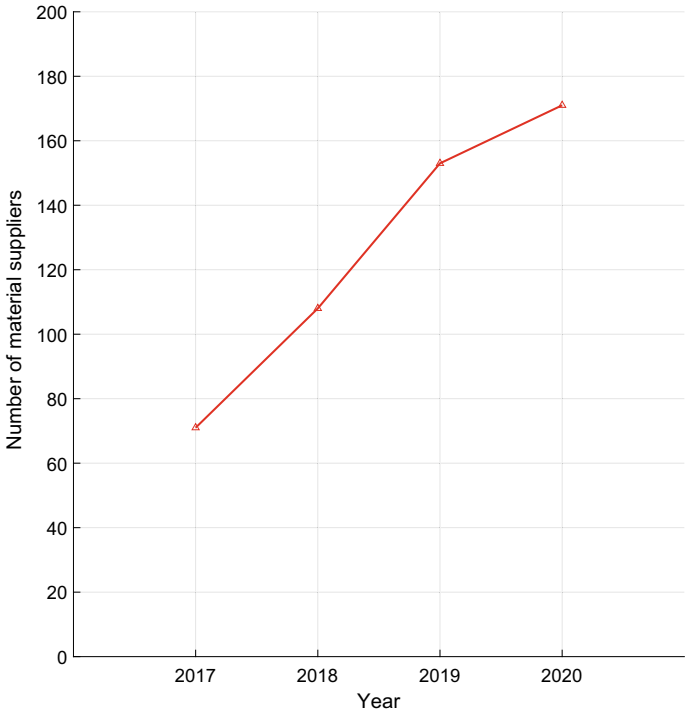

Fig. 6 Number of material suppliers for AM in four consecutive years [47]

5.1.5 Research Institutions

The immense research is carried out by the academicians to increase the efficiency of the AM. Research Institutions contribute only about 5.2% of the total market value of AM. Haleem and Javaid reported that the total number of research papers published on AM has increased drastically over the years [19]. The increase in the publication of research papers can be seen in Fig. 8.

There are several challenges that the researchers are facing in different technologies. Some of the research challenges with the respective technologies are discussed in Table 5.

6 Future of AM

The rapid growth in the AM-based industries like automotive, aerospace, sanitary beverages, production, and food industries areas are the main reasons for the overall growth of AM [9]. It is being expected that the global AM and materials market will register a Compound Annual Growth Rate (CAGR) of 25.7% over the forecast

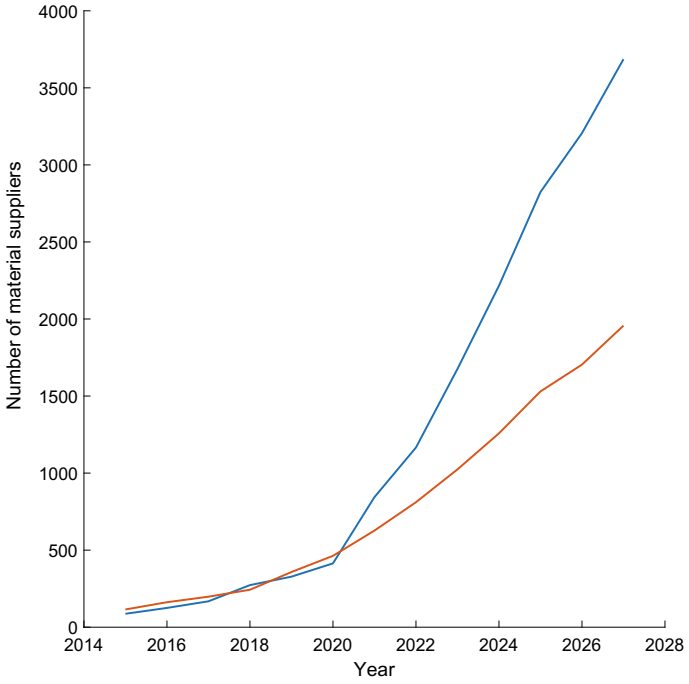

Fig. 7 Comparison of global AM software opportunity size- prior analysis versus current (2020) analysis [25]

period (2020–2025) [38]. It is also expected that in the forecast period, there might be a drop in prices of 3D printers which helps in improving the global market.

It is being expected that the overall growth of AM will not be the same and it may vary. Among all the sectors, the growth in the automotive sector will be expected as maximum. Figure 9 shows a comparison between the market value of AM in a different sector.

The underdeveloped and developing countries have limited resources to use AM whereas the countries with the developed economies are using AM on large scale. This limited usage of AM by underdeveloped and developing nations hinders the growth of global market value. Based on the available data, the largest regional market for AM in Europe, followed by North America and the Asia Pacific [41, 9]. According to SmarTech analysis, it is expected that the revenue from the global AM market will rise from $10,416.6 in 2019 to $53,843.5 in 2029 [41].

The use of AM will be slightly different from the current day's use. Day-by-day AM is expanding its roots in different industrial areas and its need is also increasing. As the human demand changes, the applications of AM will also change accordingly. Some of the future applications of AM are listed in Table 6.

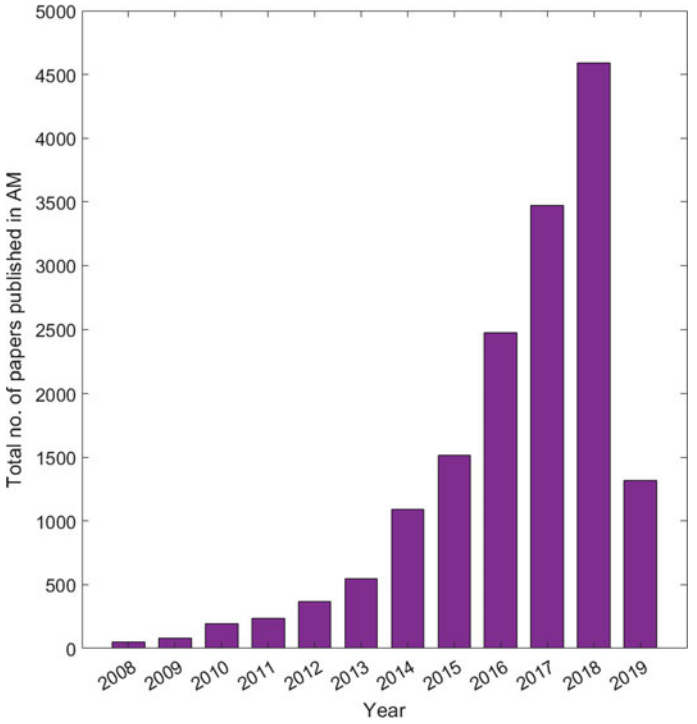

Fig. 8 Increase in publication of research papers on AM till march 2019 [19]

Table 5 Research challenges of some common technologies [29]

Technologies	Research challenges
Stereolithography (SLA) vat polymerisation	• After curing, the parts become photo-sensitive and treatment needs to be provided to overcome brittleness
Selective laser sintering (SLS) Powder bed fusion	• Post processing (powder removal) consumes a lot of time and also the recovery rate is not 100% • The cost of SLS technology is high as compared to SLA and FDM
Direct metal laser sintering (DMLS) Powder bed fusion	• The need of high-power lasers and an inert atmosphere makes the cost of DMLS technology high • Post-machining is required since the surface quality and dimensional accuracy is still limited
Continuous liquid interface production (CLIP) Vat photo-polymerisation	• Materials are limited for this technique and the cost of production is high

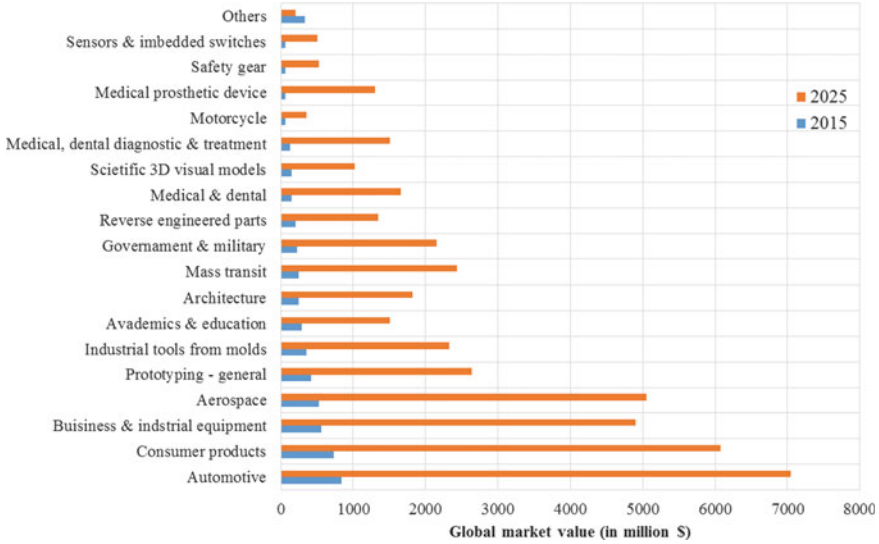

Fig. 9 Comparison of AM market value in 2015 and 2025 (expected) [4]

Table 6 Future applications (Bhattacharjya et al. 2014)

Industry	Future applications
Medical	Custom components specific to patent, orthodontics, rapid prototyping, surgical guides, splints, low volume manufacturing/prototyping, full and partial dentures
Aerospace	Complex parts with low volumes
Automotive	Replacement parts production for repair shops as well rapid prototype, spare parts, new products for trial and testing, low volume spares, and tooling
Tools for assembly purposes	Ease of manufacture of tooling
Consumer durables	Specific components required by a consumer e.g. household appliances, tools, photographic equipment, jewellery, etc.; the possibility of making parts as per the requirement

7 Conclusion and Future Perspective

The present paper is mainly focused to compile the future trends of additive and subtractive manufacturing. Using the available data from different survey reports, the future trends have been discussed. The data shows that AM has brought a third industrial revolution, where all companies are thinking to transform their traditional way of manufacturing [23]. Summary of the whole paper includes:

1. AM is being used in almost every aspect of industries.
2. More than half of the total market of AM is contributed by hardware segments.

3. The number of AM materials has increased from 1700 in 2019 to 2245 in 2020.
4. The software segments has grown much like other segments but it is estimated that it would grow rapidly in the future.
5. Several companies are working on post-processing challenges to reduce the total manufacturing cost. The total number of research papers published on AM has increased in the last few years.
6. AM will be more advance than today.
7. The research has increased in the sector of Additive Manufacturing in the past few years, the method will be highly useful in the automotive sector in the coming years.

There are still many limitations and challenges in emerging metal AM. Complex thermal stresses, process repeatability, and material microstructural implications of the process are the biggest challenges to AM applications in industries [51]. These challenges affect the density of the additive products, consequently all material characteristics and mechanical properties. Currently, industries are refining the quality of the additive parts through carefully controlled post-processing techniques to overcome these challenges [21, 28].

References

1. Akinsowon V (2020) The additive manufacturing landscape 2020 [Report]. https://amfg.ai/whitepapers/the-additive-manufacturing-landscape-2020-report/
2. Bhargav A, Sanjairaj V, Vinicius Rosa Lu, Feng W, Jerry Fuh Yh (2018) Applications of additive manufacturing in dentistry: a review. J Biomed Mater Res B Appl Biomater 106(5):2058–2064. https://doi.org/10.1002/jbm.b.33961
3. Bhattacharjya J, Tripathi S, Taylor A, Taylor M, Walters D (2014) Additive manufacturing: current status and future prospects. In: Working conference on virtual enterprises. Springer, pp 365–372
4. Blum H (2015) The future of 3D printing to 2025. Smithers Pira. http://www.smitherspira.com/news/2015/june/3d-print-market-expected-to-reach-%2449b-by-2025
5. Bourell DL, Leu MC, Rosen DW (2009) Roadmap for additive manufacturing: identifying the future of freeform processing. The University of Texas at Austin, Austin, TX, pp 11–15
6. Bourell DL, Beaman JJ (2004) Methodologies and processes. Additive/subtractive manufacturing techniques in Europe. https://apps.dtic.mil/sti/pdfs/ADA466756.pdf
7. Bynum DK (1992). Apparatus for forming a three-dimensional reproduction of an object from laminations. United States US5127037A, filed August 15, 1990, and issued June 30, 1992. https://patents.google.com/patent/US5127037A/en
8. Castrejon-Pita JR, Baxter WRS, Morgan J, Temple S, Martin GD, Hutchings IM (2013) Future, opportunities and challenges of inkjet technologies. Atom Sprays 23(6)
9. Cosmos Research (2019) Additive manufacturing market 2019–2025. Size & forecast. Research Cosmos. https://www.researchcosmos.com/reports/additive-manufacturing-market/1170635782
10. Credi C, Fiorese A, Tironi M, Bernasconi R, Magagnin L, Levi M, Turri S (2016) 3D printing of cantilever-type microstructures by stereolithography of ferromagnetic photopolymers. ACS Appl Mater Interfaces 8(39):26332–26342
11. Derby B (2015) additive manufacture of ceramics components by inkjet printing. Engineering 1(1):113–123

12. Domingues J, Marques T, Mateus A, Carreira P, Malça C (2017) An additive manufacturing solution to produce big green parts from tires and recycled plastics. Procedia Manuf 12:242–248
13. Donath S (2019) Water jet cutter. https://www.etmm-online.com/water-jet-cutting--function-methods-and-application-examples-a-834966/
14. Dudek P, Zagórski K (2017) Cost, resources, and energy efficiency of additive manufacturing. In: E3S web of conferences Jan 14, p 01040. https://doi.org/10.1051/e3sconf/20171401040
15. Exner Hv, Horn M, Streek A, Ullmann F, Hartwig L, Regenfuß P, Ebert R (2008) Laser micro sintering: a new method to generate metal and ceramic parts of high resolution with sub-micrometer powder. Virtual Phys Prototyping 3(1):3–11
16. Formlabs (2018). Additive versus subtractive manufacturing. Formlabs. https://formlabs.com/blog/additive-manufacturing-vs-subtractive-manufacturing/
17. Gowda Y, Vinod A, Madhu P, Kushvaha V, Sanjay MR, Siengchin S (2021) A new study on flax-basalt-carbon fiber reinforced epoxy/bio-epoxy hybrid composites. Polym Compos. https://doi.org/10.1002/pc.25944
18. Gupta MK, Song Q, Liu Z, Sarikaya M, Jamil M, Mia M, Kushvaha V, Singla AK, Li Z (2020) Ecological, economical and technological perspectives based sustainability assessment in hybrid-cooling assisted machining of Ti–6Al–4V alloy. Sustain Mater Technol 26(December):e00218. https://doi.org/10.1016/j.susmat.2020.e00218
19. Haleem A, Javaid M (2020) 3D printed medical parts with different materials using additive manufacturing. Clin Epidemiol Glob Health 8(1):215–223. https://doi.org/10.1016/j.cegh.2019.08.002
20. Hull CW, Spence ST, Albert DJ, Smalley DR, Harlow RA, Steinbaugh P, Tarnoff HL, Nguyen HD, Lewis CW, Vorgitch TJ (1991) Methods and apparatus for production of three-dimensional objects by stereolithography. issued 22 October 1991
21. Kasperovich G, Hausmann J (2015) Improvement of fatigue resistance and ductility of TiAl6V4 processed by selective laser melting. J Mater Process Technol 220:202–214
22. Kellens K, Yasa E, Dewulf W, Duflou J (2010) Environmental assessment of selective laser melting and selective laser sintering. In: Going green-care innovation: from legal compliance to energy-efficient products and services, Paper, no 2, pp 14–15
23. Kelly P (2017) Young people and the coming of the third industrial revolution. Routledge handbook of youth and young adulthood, pp 391–399
24. Kruth J-P, Leu M-C, Nakagawa T (1998) Progress in additive manufacturing and rapid prototyping. CIRP Ann Manuf Technol 47(2):525–540
25. Krycer G (2020) Opportunities in additive manufacturing software markets 2020. SmarTech Analysis. https://www.smartechanalysis.com/reports/opportunities-in-additive-manufacturing-software-markets-2020/
26. Kushvaha V, Anand Kumar S, Madhushri P, Sharma A (2020) Artificial neural network technique to predict dynamic fracture of particulate composite. J Compos Mater 54(22):3099–3108. https://doi.org/10.1177/0021998320911418
27. Kushvaha V, Branch A, Tippur H (2014) Effect of loading rate on dynamic fracture behavior of glass and carbon fiber modified epoxy. In: Song B, Casem D, Kimberley J (eds) Dynamic behavior of materials, vol 1. Conference proceedings of the society for experimental mechanics series. Springer, Cham, pp 169–76. https://doi.org/10.1007/978-3-319-00771-7_21
28. Leuders S, Thöne M, Andre Riemer T, Niendorf TT, Richard HA, Maier HJ (2013) On the mechanical behaviour of titanium alloy TiAl6V4 manufactured by selective laser melting: fatigue resistance and crack growth performance. Int J Fatigue 48:300–307
29. Li J, Wu B, Myant C (2016) The current landscape for additive manufacturing research. https://www.semanticscholar.org/paper/The-Current-Landscape-for-Additive-Manufacturing-Li-Wu/454eddc4e2e2707550bef3398e2dae42cc83620f#paper-header
30. McGeehin C (2019) Additive manufacturing with metal powders 2019. SmarTech Analysis. https://www.smartechanalysis.com/reports/additive-manufacturing-with-metal-powders-2019/
31. Melchels FPW, Feijen J, Grijpma DW (2010) A review on stereolithography and its applications in biomedical engineering. Biomaterials 31(24):6121–6130. https://doi.org/10.1016/j.biomaterials.2010.04.050

32. Moreau C (2019) The state of 3d printing report: 2019 by Sculpteo. https://www.sculpteo.com/media/ebook/State_of_3DP_2018.pdf
33. Murr LE, Gaytan SM, Ramirez DA, Martinez E, Hernandez J, Amato KN, Shindo PW, Medina FR, Wicker RB (2012) Metal fabrication by additive manufacturing using laser and electron beam melting technologies. J Mater Sci Technol 28(1):1–14
34. Nelson JC, Xue S, Barlow JW, Beaman JJ, Marcus HL, Bourell DL (1993) Model of the selective laser sintering of bisphenol—A polycarbonate. Ind Eng Chem Res 32(10):2305–2317
35. Nolan R (2020) SmarTech issues new report that projects polymer 3D printing to generate $11.7 Billion in 2020. GlobeNewswire News Room. 2 Ma 2020. http://www.globenewswire.com/news-release/2020/03/02/1993819/0/en/SmarTech-Issues-New-Report-That-Projects-Polymer-3D-Printing-to-Generate-11-7-billion-in-2020.html
36. Palaganas NB, Mangadlao JD, CC, de Leon ACC, Palaganas JO, Pangilinan KD, Lee YJ, Advincula RC (2017) 3D printing of photocurable cellulose nanocrystal composite for fabrication of complex architectures via stereolithography. ACS Appl Mater Interfaces 9(39):34314–34324
37. Pearlson MN (2018) Additive manufacturing using foaming radiation-curable resin. United States US20180162052A1, filed 6 Dec 2017, and issued 14 June 2018. https://patents.google.com/patent/US20180162052A1/en
38. Reddy B (2020) Global additive manufacturing & materials market. Growth, trends and forecasts (2020–2025). https://www.mordorintelligence.com/industry-reports/global-additive-manufacturing-and-material-market-industry
39. Shahrubudin N, Lee TC, Ramlan R (2019) An overview on 3D printing technology: technological, materials, and applications. In: Procedia manufacturing, the 2nd international conference on sustainable materials processing and manufacturing, SMPM 2019, 8–10 Mar 2019, Sun City, South Africa, 35 (January), pp 1286–1296. https://doi.org/10.1016/j.promfg.2019.06.089
40. Sharma A, Kushvaha V (2020) Predictive modelling of fracture behaviour in silica-filled polymer composite subjected to impact with varying loading rates using artificial neural network. Eng Fract Mech 239(November):107328. https://doi.org/10.1016/j.engfracmech.2020.107328
41. Sher D (2018) Final parts to drive composites additive manufacturing market to nearly $10 Billion by 2028—2018. SmarTech Analysis. https://www.3dprintingmedia.network/composites-additive-manufacturing-market-2028/
42. Sreenivasan et al (2010) Sustainability issues in laser-based additive manufacturing. Phys Procedia 5:81–90
43. Steinberg G (2019) Ey-3d-printing-game changer. https://assets.ey.com/content/dam/ey-sites/ey-com/en_gl/topics/advisory/ey-3d-printing-game-changer.pdf?download
44. The additive manufacturing landscape 2020 [Report]—AMFG. Accessed 19 July 2020. https://core.ac.uk/download/pdf/77018324.pdf
45. Tseng AA (2001) Adaptable filament deposition system and method for freeform fabrication of three-dimensional objects. Issued 26 June 2001
46. Tumbleston JR, Shirvanyants D, Ermoshkin N, Janusziewicz R, Johnson AR, Kelly D, Chen K, Pinschmidt R, Rolland JP, Ermoshkin A (2015) Continuous liquid interface production of 3D objects. Science 347(6228):1349–1352
47. Wohlers and Senvol Database (2020) Analysis of Additive Manufacturing materials. https://www.metal-am.com/analysis-of-additive-manufacturing-materials-from-wohlers-and-senvol-database/
48. Xu J, Jung K, Atme A, Shanmugam S, Boyer C (2014) A robust and versatile photoinduced living polymerization of conjugated and unconjugated monomers and its oxygen tolerance. J Am Chem Soc 136(14):5508–5519
49. Yadroitsev I, Smurov I (2011) Surface morphology in selective laser melting of metal powders. Phys Procedia 12:264–270
50. Yadroitsev I, Bertrand P (2010) Selective laser melting in micro manufacturing. In: Annals of DAAAM for 2010 & Proceedings of the 21st International DAAAM Symposium. https://www.daaam.info/Downloads/Pdfs/proceedings/proceedings_2010/19717_Annals_1_head.pdf

51. Yakout M, Elbestawi M, Veldhuis SC (2018) A review of metal additive manufacturing technologies. Solid State Phenom 278(July):1–14. https://doi.org/10.4028/www.scientific.net/SSP.278.1
52. Yuan S, Shen F, Chua CK, Zhou K (2019) Polymeric composites for powder-based additive manufacturing: materials and applications. Prog Polym Sci 91:141–168
53. Zorlutuna P, Jeong JH, Kong H, Bashir R (2011) Stereolithography-based hydrogel microenvironments to examine cellular interactions. Adv Func Mater 21(19):3642–3651